ISSN 0494-7304 0207-4508

ARTU ÜLIKOOLI

TOIMETISED

ACTA ET COMMENTATIONES UNIVERSITATIS TARTUENSIS

975

PUBLICATIONS ON CHEMISTRY

XXII

TARTU 1994

TARTU ÜLIKOOLI TOIMETISED
ACTA ET COMMENTATIONES UNIVERSITATIS TARTUENSIS
· ALUSTATUD 1893. a. VIHIK 975

PUBLICATIONS ON CHEMISTRY

XXII

Tartu 1994

Dedicated to the 75th Anniversary of the Estonian University

Tartu Ülikooli Kirjastuse trükikoda
Tiigi 78, EE2400 Tartu
Tellimus nr. 39, 1995.

CONTENTS

1. V. Past

75 AASTAT EESTI ÜLIKOOLI.
TARTU ÜLIKOOLI KEEMIAOSAKOND AASTATEL 1919-1936 7
75 YEARS OF THE ESTONIAN UNIVERSITY. DEPARTMENT OF
CHEMISTRY OF TARTU UNIVERSITY IN 1919-1936 14

2. I. Kahn, U. Maran, M. Karelson

QUANTUM-CHEMICAL MODELLING OF THE SOLVATOCHROMIC
SHIFTS IN ELECTRONIC SPECTRA 15
ELEKTRONSPEKTRITE SOLVATOKROOMSETE NIHETE KVANT-
KEEMILINE MODELLEERIMINE 27

3. T. Jürimäe, M. Strandberg, M. Karelson

A THEORETIC STUDY OF FIVE-MEMBERED HETEROCYCLE AND
METALLOCYCLE OLIGOMERS 29
VIIELÜLILISTE HETEROTSÜKLITE JA METALLOTSÜKLILISTE OLIGO-
MEERIDE TEOREETILINE UURIMINE 38

4. M. Väärtnõu

A STUDY OF THE CORRELATION BETWEEN GIBBS ADSORPTION
ENERGY OF IONS AND QUANTUM CHEMICAL INDECES OF REACTI-
VITY ON THE BISMUTH (001)/SOLUTION INTERFACE 39
IOONIDE ADSORPTSIOONI GIBBSI ENERGIA JA KVANTKEEMILISTE
REAKTSIOONIVÕIME INDEKSITE VAHELISE KORRELATSIOONI
UURIMINE PIIRPINNAL VISMUT (001)/LAHUS 43

5. E. Lust, K. Lust, A. Jänes

ELECTRICAL DOUBLE LAYER AND ADSORPTION OF POLYMET-
ACRYLIC ACID ON THE GLASSY CARBON ELECTRODES 45
ELEKTRILINE KAKSIKKIHT JA POLÜMETAKRÜÜLHAPPE ADSORPT-
SIOON KLAASSSÜSINIKELEKTROODIL 56

6. R. Salem

ELECTRON RESPONSE OF METAL/SOLUTION INTERFACE TO EX-
TERNAL ELECTRICAL FIELD 57
VÄLISE ELEKTRIVÄLJA MÕJU METALL/LAHUS PIIRPINNA ELEKT-
ROONSETELE KARAKTERISTIKUTELE 70

7. T. Tenno, A. Mashirin

THE DYNAMIC MODEL OF THE PRESSURE OF GAS 71
GAASI RÕHU DÜNAAMILINE MUDEL 77

8. T. Tenno, A. Mashirin

SOME ASPECTS OF APPLICATION OF THE LAW OF STATE OF IDEAL
GAS 79
IDEAALSE GAASI OLEKU VÕRRANDI MÕNINGAID ASPEKTE 88

9. T. Tenno, A. Mashirin

THE PHYSICAL CONTENT OF ENTROPY FOR IDEAL GAS SYSTEM 89
IDEAALSE GAASI ENTROOPIA FÜÜSIKALINE OLEMUS 96

10. K. Tammeveski, T. Tenno
ELECTROCHEMICAL STUDIES OF HYDROGEN PEROXIDE AT THIN FILMS OF GOLD AND PLATINUM IN NEUTRAL AND ALKALINE AQUEOUS SOLUTIONS 97
VESINIKPEROKSIIDI ELEKTROKEEMILISTE REAKTSIOONIDE UURIMINE KULLA JA PLAATINA ÕHUKESTEL KIHTIDEL NEUTRAALSES JA LEELISELISES LAHUSES 107

11. Ü. Piibar, H. Keis
POLAROGRAPHY AND STRIPPING VOLTAMMMETRY OF SOME METAL-POLYCARBOXYLATE COMPLEXES 109
MÕNEDE METALL-POLÜKARBOKSÜLAATKOMPLEKSIDE POLAROGRAAFILINE JA VOLTAMPEROMEETRILINE UURIMINE 117

12. H. Keis, Ü. Piibar
DETERMINATION OF HEAVY METALS IN SEA- AND FRESHWATERS BY ANODIC STRIPPING VOLTAMMETRY 119
RASKMETALLIDE MÄÄRAMISEST MERE- JA MAGEVETES INVERSIOONVOLTAMPEROMEETRILISEL MEETODIL 127

13. Taavo Tenno, Aleksei Mashirin, Toomas Tenno
MEASUREMENT OF OXYGEN CONSUMPTION 129
HAPNIKUTARBE MÄÄRAMINE 137

14. A. Tuulmets, P. Kullamaa, M. Mikk
TOLUENE SOLUTIONS OF N-BUTYLMAGNESIUM BROMIDE-DIETHYL ETHER COMPLEXES 139
N-BUTÜÜLMAGNEESIUMBROMIID-DIETÜÜLEETER KOMPLEKSIDE LAHUSED TOLUEENIS 144

15. A. Talvik
EFFECT OF STRUCTURE ON THE KINETIC AND EQUILIBRIUM ACIDITY OF CARBON ACIDS 145
STRUKTUURI MÕJU KARBOHAPETE KINEETILISELE JA TERMODÜNAAMILISELE HAPPELISUSELE 153

16. H. Timotheus
SYNTHESIS OF 1,3-DIOLS 155
1,3-DIOOLIDE SÜNTEES 191

17. T. Rodima, N. Lissov, M. Saar
SEX ATTRACTANTS FOR SOME FOREST LEPIDOPTEROUS SPECIES .. 193
MÕNINGATE METSA KAHJUSTAVATE LIBLIKATE SUGUATRAKTAKTIDEST 200

18. A. Pruks, T. Tenno
PHOSPHORUS REMOVAL IN SOME SEWAGE PLANTS IN ESTONIA 203
FOSFORI ÄRASTAMINE MÕNINGATES EESTI HEITVEEPUHASTITES ... 209

19. L. Saarinen, M. Reinik
RECOVERY OF SOME ORGANIC COMPOUNDS FROM VAPOUR SAMPLING CHARCOAL ADSORBENT 211
MÕNINGATE ORGAANILISTE ÜHENDITE DESORPTSIOON AKTIIVSÖELT 219

20. L. Piiri, L. Paama, T. Ilomets
ELEMENTAL COMPOSITION OF HISTORICAL GLAZES FROM ST. JOHN'S CHURCH OF TARTU 221

TARTU JAANI KIRIKU AJALOOLISTE GLASUURIDE ELEMENDILINE KOOSTIS 227

21. J. Ruut, V Past

CHRONOPOTENTIOMETRIC STRIPPING ANALYSIS FOR DETERMINATION OF HEAVY METALS IN FOODSTUFFS 229

RASKMETALLIDE MÄÄRAMINE TOIDUAINETES INVERSIOONKRONOPOTENTSIOMEETRILISELT 232

22. L. Reio

ANALYSIS OF NUTRIENTS 233

TOIDUAINETE ANALÜÜS 237

CHRONICLE

PROFESSOR LEMBITU REIO 70 239

KROONIKA

PROFESSOR LEMBITU REIO 70 242

75 AASTAT EESTI ÜLIKOOLI TARTU ÜLIKOOLI KEEMIAOSAKOND AASTATEL 1919-1936

V. Past
Tartu Riiklik Ülikooli füüsikalise keemia instituut

Tartu Ülikooli ajaloos on perioode, kus keemiaosakond on pidanud oma töökorraldust põhjalikult muutma või isegi alustama päris algusest. Nii oli see Eesti ülikooli avamisel 1919. a., samuti osakonna taasavamisel 1947. a. Ka praegusel ajal elab ülikool ümberkorralduste tähe all. Sellega seoses oleks õpetlik tutvustada lugejaskonda nende tulemustega, mis ilmestasid keemiaosakonna tegevust 75 aastat tagasi avatud ülikoolis.

Eesti ülikooli avamisega 1. detsembril 1919. a. algas uus ajajärk meie kultuuri- ja hariduselus. Esmakordselt hakkas ülikoolis täiseõiguslikuna kõlama eesti keel, arenema rahvuslik kultuur ja teadus. Ehkki ülikool ei tekkinud tühjal kohal, olid Eesti ülikooli eesmärgid ja töökorralduse põhimõtted oluliselt erinevad eelnenud perioodi omadest. Kardinaalselt muutus üliõpilaskonna sotsiaalne ning rahvuslik koosseis. Kui näiteks 1916. a. oli Tartu üliõpilaste seas eestlasi vaid 14,5%, siis 1920. a. oli eestlasi juba 81,1% [1]. Rahvusliku õppejõudude kaadri loomine nõudis ülikoolilt suuri pingutusi ja vajas aega. Professorite seas oli enne rahvusülikooli loomist paremal juhul ainult 1–2 eestlast, 1920. a. oli eestlasi umbes kolmandik professoritest ja 1930. a. juba üle kahe kolmandiku [1].

Tsaariajal andis Tartu Ülikooli keemiaosakond oma lõpetajatele hea ettevalmistuse teoreetilise ja eksperimentaalse keemia alal, mis võimaldas neil edukalt töötada Ida-Euroopa ja Venemaa ülikoolides, teadus- ja tööstuslaboratooriumides. Eesti ülikool ei saanud enam piirduda keemikute teadusliku koolitamisega, vaid pidi vabariigi huvides oma tegevusvälja laiendama. Esmakordselt tuli ülikoolis keemikute kõrval hakata ette valmistama ka keemiatehnolooge.

1919. a. augustis, veel enne ülikooli ametlikku avamist, valis Ajutine Nõukogu keemiaosakonna esimesteks professoriteks G. Landeseni anorgaanilise ja analüütilise keemia ning M. Wittlichi tehnilise keemia

alal [2]. Tehnilise keemia professuuri avamine näitas, et ka Vabariigi Valitsus pooldas sel ajal kõrgema tehnilise hariduse edendamist Tartus [3]. Kolmas osakonnale määratud professuur orgaanilise keemia alal jäi esialgu täitmata.

Baltisakslane Georg Rudolf Wilhelm Landesen (1866-1935) lõpetas Tartu Ülikooli keemiaosakonna 1892. a. Ta töötas samas tuntud füsikokeemiku Gustav Tammanni juhendamisel ja kaitses 1906. a. Peterburi Ülikoolis magistrikraadi. G. Landesen sai 1909. a. Tartus erakorraliseks ja 1917. a. korraliseks professoriks. Kuni pensionile siirdumiseni (1932) oli G. Landesen osakonna juhtiv õppejõud ja Keemiainstituudi direktor. Eesti ülikoolis oli G. Landesenil erandkorras lubatud pidada loenguid saksa keeles.

Üks vanemaid Eesti keemiatööstuse spetsialiste Michael Wittlich (Mihkel Vitsut) (1866-1933) on sündinud Kunda vallas, lõpetanud Tallinna Reaalkooli ja 1890. a. I järgu inseneridiplomiga Riia Polütehnikumi. Pärast praktiseerimist 15 aasta vältel Tallinna keemiatehases kutsuti M. Wittlich 1905. a. õppejõuks Riiga, kus ta 1909. a. sai keemilise tehnoloogia korraliseks professoriks. Tartu perioodil olid M. Wittlichi tähelepanu all kohaliku tööstuse, energeetika ja transpordi arengu probleemid. M. Wittlichi tegevus ülikooli õppejõuna aitas kaasa keemia- ja tehnoloogiaõpetuse lähendamisele praktikale [4]. Oma mitmekülgsete teadmiste põhjal kirjutas ta esimese eestikeelse keemilise tehnoloogia õpiku. 1920-1925 oli M. Wittlich ka matemaatika-loodusteaduskonna dekaan.

1920-ndate aastate algul oli ülikoolis lektoriks Johannes Narbut (1879-1937), kes õppeülesande korras luges orgaanilist keemiat, füüsikalist keemiat ja teisi distsipliine. Varssavi Polütehnilises Instituudis 1917. a. erakorraliseks professoriks valitud J. Narbut taotles Tartu Ülikoolis professuuri orgaanilise keemia alal, kuid talle öeldi ära. Leidmata ülikoolis vajalikku rakendust lahkus J. Narbut 1924. a. Tartust [5].

1921-1922. a. loodi keemiaosakonnas lisaks olemasolnud kolmele õppetoolile veel 2 professuuri – anorgaaniliste ainete tehnoloogia ja füüsikalise keemia alal [2]. 1922. a. tuli Tartusse tööle soomlane Yrjö Kauko (1886-1974), kes anorgaanilise tehnoloogia professorina asus energiliselt korraldama tehnoloogide ettevalmistamist. Y. Kauko rajas anorgaanilise tehnoloogia laboratooriumi, kus juhendas praktikume ja arvukalt tööstustemaatilisi uurimistöid. Suhteliselt lühikese aja jooksul valmis tema käe all 8 magistritööd ja üks doktoritöö [6].

Ajal, millal tehnoloogide ettevalmistamine ülikoolis oli saanud täishoo, otsustas vabariigi valitsus, et Eestis ei ole tehnolooge tarvis koolitada. Selle tulemusena suleti Tartus 1924. a. tehnoloogia haru; uusi üliõpilasi sellel alal enam vastu ei võetud, kuid nendel, kellel õppimine oli pooleli, lubati stuudium 1-2 aasta jooksul lõpetada. Seoses keemiatehnoloogia eriala kadumisega liideti anorgaanilise tehnoloogia professuur füüsikalise keemia omaga. Vakantsele füüsikalise keemia professori kohale kinnitati Y. Kauko, kes aga juba 1925. a. alguses lahkus omal soovil töölt Tartu Ülikoolis [6].

J. Narbuti ja Y. Kauko lahkumise tõttu tõusis keemiaosakonnas jälle teravalt päevakorda õppejõudude kaadri probleem. Selle probleemi lahendamine oli võimalik vaid noorte andekate eesti keemikute ettevalmistamise teel õppejõu kutseks. Juba 1919. a. saadeti aasta varem Tartu Ülikooli keemiaosakonna lõpetanud Paul Kogerman ülikooli stipendiaadina Londonisse, et ta ennast Kuninglikus Teaduse ja Tehnoloogia Kolledzis professori kutseks ette valmistaks. Kaheaastase kursuse ja uurimistöö eduka lõpetamise ning teadusliku kraadi (M.Sc.) kaitsmise järel valiti P. Kogerman 1922. a. Tartu Ülikooli orgaanilise keemia dotsendiks, 1924. a. erakorraliseks ja 1925.a. korraliseks professoriks [2]. P. Kogermani tegevus pani aluse orgaanilise keemia ja põlevkivikeemia uurimissuunale Tartu Ülikoolis. Pärast II Maailmasõda viljeldi nimetatud temaatikat peamiselt Eesti Teaduste Akadeemias.

1920-ndatel aastatel täienes keemiaosakonna õppejõudude pere veel teisegi eesti keemikuga. August Paris (1888-1944) lõpetas keemiaosakonna 1915. a. ja töötas seejärel Moskvas suures peenkeemia tehases. Ülikooli tööle tuli ta 1920. a. Teaduslik kraad (dr. phil. nat) omistati talle Tartu Ülikoolis 1924. a. 1925. a. määrati A. Paris füüsikalise keemia õppetooli dotsendi kohale. 1925-1926 töötas A. Paris komandeerituna Berliinis Keiser Wilhelmi nimelises Füüsikalise Keemia ja Elektrokeemia Instituudis. 1929. a. sai A. Paris esimeseks eestlasest füüsikalise keemia professoriks Tartu Ülikoolis [7]. 1933. a. asus A. Paris G. Landeseni järglasena keemiaosakonna kõige suurema - anorgaanilise keemia kateedri etteotsa. Füüsikalise keemia õppetooli hakkas dotsendina täitma Y. Kauko ja A. Parise õpilane A. Parts.

Adolf-Gustav Parts (sünd. 1904) sai hariduse juba Eesti ülikoolis. Keemiaosakonna tehnoloogiaharu lõpetas ta 1925. a. Tartu Ülikoolis omandas ta ka teaduslikud kraadid: magistrikraadi 1926. a. ja doktorikraadi 1929. a. A. Parts oli esimene eesti keemik, kes kogu aja tegeles aktiivselt uurimistööga füüsikalise keemia alal [8]. 1929-1931 määras ta

Tartu Ülikooli füüsikalise keemia laboratooriumis kokku 38 erineva orgaanilise ühendi dipoolmomendid ning avaldas tulemused artiklite seeriana tuntud rahvusvahelises ajakirjas "Zeitschrift für physikalische Chemie". A. Partsi ja hiljem seda tööd jätkanud Leonhard Tiganiku (1900-1962) uurimused äratasid tähelepanu teadlasringkondades, neid tsiteeriti ja dipoolmomentide väärtused leidsid koha tuntud käsiraamatutes. Noore keemiku A. Partsi töödele sai osaks suur tunnustus, kui Tartu Ülikool lähetas ta Rockefeller Foundation'i stipendiaadina aastaks teadustööle Saksamaale ja seejärel ka Hispaaniasse [8]. Väliskomandeeringute ajal tugevnes teoreetiline suund A. Partsi loomingus. Esimese eesti teadlasena hakkas ta juba 1932. aastast alates molekulide ehituse ja omaduste uurimisel rakendama kvantmehaanika põhimõtteid. A. Partsi loomingutee on ilmekaks näiteks sellest, kuidas andekatest eesti noortest võrsusid ülikoolis edukad teadlased ja tunnustatud õppejõud. Tuleb märkida, et teadlaskaadri loomisel kasutas Tartu Ülikool sellel ajal oskuslikult teaduslike stipendiumide süsteemi. Teaduslikeks stipendiaatiteks olid peale P. Kogermani ja A. Partsi veel mitmed teised keemikud, nagu J. Kranig, A. Laur, J. Kuusk [2].

1947. a. kujunes taasavatud keemiaosakonnas füüsikalise ja teoreetilise keemia uurimissuund jälle üheks edukamaks ülikooli keemikute tegevusvaldkonnaks.

Õppetöö korraldamisel olid Tartu Ülikoolil ja teaduskondadel vabad käed. Õppetöö toimus teaduskondades koostatud ja ülikooli nõukogus kinnitatud õppekavade alusel. 1922 ja 1923. a. trükis ilmunud matemaatika-loodusteaduskonna (kuhu kuulus ka keemiaosakond) õppekavades anti õpetatavate ainete nimistu loengu- ja harjutustundide äramärkimisega [9]. Ained olid küll jaotatud neljale õppeaastale, kuid õppimise aeg ülikoolis ei olnud fikseeritud. Seega puudus siin varasem kursusteks jaotamine. Eksamid sooritati ainerühmade kaupa 2 korda semestris. Lõpueksameid (keemiaosakonnas 7 eksamit) sai asuda sooritama pärast kõikide praktikumide lõpetamist. Need eksamid pidid olema tehtud kas korraga kõikides ainetes või kahes osas ühe semestri jooksul.

Keemiaosakonna õppekava oli küllalt mahukas, seda eriti keemiatehnoloogide osas. Peale keemia ainete õpetati keemikutele matemaatikat, füüsikat, mineraloogiat, petrograafiat, geoloogiat. Keemiatehnoloogidel tuli lisaks õppida mitmeid tööstuslikke ja tehnoloogilisi aineid, nagu mehaanikat ja masinaõpetust, keemiatööstuse aparatuuri, tööstuse projekteerimist, anorgaaniliste ja orgaaniliste ainete tehnoloogiat, ehitusteadust jm. Keemiliste ja tehnoloogiliste ainete õppejõududest oli juttu

eespool. Teiste ainete lektoriteks olid näiteks prof. J. Wilip (füüsika), prof. H. Scupin (mineraloogia), prof. kt. G. Rägo (kõrgem matemaatika ja teoreetiline mehaanika), dots. H. Perlitz (termodünaamika) [3]. Nõudmiste ulatuse ja aine mahu poolest oli tolleaegses Tartu Ülikoolis esikohal analüütiline keemia. Klassikalist keemilist analüüsi õpetas prof. G. Landesen, kes oma ranguse poolest oli tuntud kogu ülikoolis. Peale ulatuslikke praktikume kvalitatiivses analüüsis (kus keemiaüliõpilastel tuli teha 60 tööd) ning maht- ja kaalanalüüsis (12+15 tööd) olid õppekavas veel mitmed analüüsi valdkonna ained, nagu gaasianalüüs, elektroanalüüs, orgaaniline analüüs, spektraalanalüüs ja kolorimeetria.

Üleminek kursuste süsteemilt ainesüsteemile eeldas üliõpilaste iseseisvat tööd teadmiste omandamisel. Et virgutada üliõpilasi tööle, oli õppekavades rohkesti harjutusi, seminare, kollokviume. Stuudiumi teisel poolel nähti ette valikained keemias ja tehnoloogias. Ülikooli esimese 10 aasta tegevust käsitlevas ülevaates [10] märgiti positiivselt, et matemaatika-loodusteaduskonnas võeti esimesena aluseks uudne õppekorraldus ja koostati üliõpilastele suuremaid valikuvõimalusi andvad õppekavad. Hiljem veenduti, et üliõpilase liiga suur vabadus õppeainete valikul mõjub halvasti keemiku ettevalmistusele. Seetõttu kitsenesid 1928. a. õppekavade rakendamisel valikuvõimalused [11]. Valitavaks jäid vaid üksikud ained stuudiumi lõpuetapil. Samal ajal muutus rangemaks eksamite korraldus. Antud aines 3 korda eksamil läbi kukkunud või eksamile mitteilmunud üliõpilane kaotas õiguse valitud erialal edasi õppida.

Eesti ülikool alustas 1919. a. tagasihoidliku arvu üliõpilastega. Sisseastumiseksamite puudumisel suurenes üliõpilaste arv kiiresti. Andmed keemiaosakonna üliõpilaste arvu kohta on vastuolulised, sest üliõpilaskonna liikuvus oli väga suur. Ka andis ametlik statistika andmeid ainult teaduskondade kohta [10]. Keemiaosakonna suuruse iseloomustamiseks toome meie arvates kõige tõepärasema näitaja, mille järgi oli 1. dets. 1923. a. ülikoolis ametlikult 260 keemiaüliõpilast, kellest 132 olid tehnoloogid [2, 12]. Üliõpilaste suur arv oli ühelt poolt rõõmustav, kuid teiselt poolt tõi see kaasa ka muresid. Keemialaboratooriumides ei jätkunud enam töökohti kõikidele soovijatele, kellest osa oli ka teistest teaduskondadest. Et mitmetes laboratooriumides tekkisid töökohta ootavate üliõpilaste järjekorrad, pöördus keemiaosakond korduvalt juhtkonna poole palvega piirata üliõpilaste vastuvõttu. 1923. a. suleti matemaatika-loodusteaduskond vabakuulajatele ja 1927. a. hakati vastuvõttu järkjärgult piirama sisseastumiseksamitega ja kõrgema õppemaksuga [10].

Ülikoolis olid olemas keemikute ja keemiatehnoloogide koolitamiseks vajalikud laboratooriumid. 1924. a. oli üldse 7 õppelaboratooriumi, milles oli töökohti ligikaudu 200. Laboratooriumid paiknesid ülikooli peahoones ning Raekoja platsi ja Rüütli tänava nurgal asuvas ülikooli hoones. Tehnoloogiaosakonna likvideerimise järel kadus vajadus anorgaanilise tehnoloogia laboratooriumi järele, mille ruumid läksid füüsikalise keemia laboratooriumi laiendamiseks. Mitmed õppelaboratooriumid olid ebasobivates ruumides (näiteks peahoone keldris), kus polnud täidetud esmased töötervishoiu nõuded [3]. Seetõttu arutati ülikoolis juba 1920- ndate aastate algul keemiahoone ehitamist. Tegudeni jõuti siin aga mitu aastakümmet hiljem.

1920-ndate aastate esimesel poolel väljastati ülikooli lõpetanud isikule lõputunnistus (hiljem lõpudiplom). Kraadiga lõpetajad said vastava diplomi. Kuni 1921. aastani oli esimeseks teaduslikuks kraadiks kandidaadikraad, hiljem magistrikraad. Magistrikraad eeldas väga häid hindeid eriala ainete eksamitel ja magistritöö edukat kaitsmist [9]. Kõrgeim teaduslik kraad (dr. phil. nat) omistati doktoritöö kaitsmise põhjal.

Arhiiviandmete järgi lõpetas aastatel 1920–1927 keemiaosakonna 67 isikut. Magistrikraadiga lõpetanuid oli 39, neist 13 lõpetasid ülikooli tehnoloogiamagistrina [2]. Aastatel 1928–1936 lõpetas ülikooli 95 keemikut. Seega oli esimesel iseseisvusajal keemiaosakonnas ühtekokku 162 lõpetajat, kellest 68 said magistrikraadi [13]. Teaduslikku kraadi omavate keemikute kõrge erikaal osakonna lõpetajate seas (42%) näitab ülikooli lõpetanud keemikute ja keemiatehnoloogide head kvaliteeti. Oli ju valik ülikoolis väga range, sest ainult umbes 30% osakonda astunud üliõpilastest suutis ülikooli valitud erialal lõpetada.

Tartu Ülikooli keemiaosakonna tegevus keemikute koolitamisel, keemia ja tema rakenduste uurimisel, eestikeelse keemiaterminoloogia ja õppekirjanduse loomisel ning teistel aladel oli igati edukas. Osakonnna elujõudu ei tahtnud tunnistada Eesti poliitikud, kelle survel keemiaosakond 1936. a. likvideeriti. Tartu Ülikoolile ja paljudele keemikutele ei olnud arusaadav, miks oli vaja edukalt töötanud osakond sulgeda ja jätta arvestamata ülikooli seisukoht selles küsimuses [14].

KIRJANDUS

1. Tartu Ülikooli ajalugu, Tallinn, **1982**, K. III, lk. 52, 58.
2. Eesti Vabariigi Tartu Ülikool 1919–1929, Tartu, **1929**, lk. 209–212.
3. Aktid tehnilise keemia ja kõrgema tehnilise hariduse küsimuste lahendamise kohta Eestis, Tartu, **1924**, 96.
4. P. Kogerman, Prof. emer. Michael Wittlich (nekroloog), Keemia Teated, **1933**. K.1, Nr. 3, 81-83.
5. RAA. F. 2100. Nim. 2. S. 713, lk. 101–105.
6. RAA. F. 2100. Nim. 2. S. 310, lk. 78, 131, 160, 182, 183.
7. V. Past, Keemiaosakonna töö algus Tartu Ülikoolis. August Parise tegevus. Tartu Ülikooli ajaloo küsimusi, Tartu, **1989**, K. XXIII, lk. 36–45.
8. V. Past, M. Oopkaup, Väljapaistev eesti füsikokeemik Adolf Gustav Parts. Inseneerikultuur Eestis, Tallinn, **1992**, K.1., 116–125.
9. Tartu Ülikooli Matemaatika-loodusteaduskonna õppekavad ja eksamite korraldus, Tartu, **1922,** 33 lk.; **1923,** 35 lk.
10. P. Põld, Tartu Ülikool 1918–1929, Tartu, **1929,** 118 lk.
11. Eesti Vabariigi Tartu Ülikooli Matemaatika-loodusteaduskonnas maksvad õppekavad, eksamite ja muud korraldused, Tartu, **1928**, 16 lk.
12. H. Martinson, Keemia Eestis kodanliku võimu perioodil, Tallinn, **1987,** 177–180.
13. RAA. F. 2100. Nim. 11. S. 13, lk. 226–231, 241-249.
14. A. Paris, Kolm pööripäeva Tartu Ülikooli Keemiainstituudi ajaloos. Keemia Teated, **1937**, K. 2, Nr. 4.,161–163.

75 YEARS OF THE ESTONIAN UNIVERSITY THE DEPARTMENT OF CHEMISTRY OF THE UNIVERSITY OF TARTU IN 1919–1936

V. Past

Summary

In 1850, after the formation of the independent Chair of Chemistry as a department of the new Faculty of Physics and Mathematics, the University of Tartu was granted the right to give a chemist's diploma to graduates. During the second half of the 19th century, the Department of Chemistry had a high reputation as an outstanding research and training center of chemistry in Eastern Europe.

A new period in the activity of the Department started in 1919 when the Estonian University was opened. In the beginning, the staff of the Department included 2 professors, only one of them having previously worked in the University of Tartu. It is wonderful that after only a decade the Department became an efficient institution, with young Estonian professors on the staff. The Faculty of Mathematics and Natural Sciences and the Department of Chemistry were mostly independent in the organizing of research and instructional work, as well as in their economic activity. The Faculty chose an entirely new direction in the arrangement of studies, following the examples of Western countries. The curriculum provided a great deal of freedom in the choice of subjects of study. The role of seminars and independent work of students increased. From 1920 to 1936, the Department had 162 graduates (chemists and technologists), among the graduates were 68 persons with a scientific degree-master of chemistry or technology. In the field of scientific work and particularly in the establishment of new research trends the activity of young Estonian chemists Paul Kogerman and Adolf-Gustav Parts must be especially emphasized. The investigation of local oil-shale and phosphorite also gave promising results. Some research trends called forth in the Department of Chemistry were developed further after II World War in the Estonian Academy of Sciences and other institutions. The Department of Chemistry deserved well in the creating of chemical terminology and compiling textbooks for students in the Estonian language. The unexpected closure of the Department in 1936 was a result of the politics of the Estonian Government.

QUANTUM-CHEMICAL MODELLING OF THE SOLVATOCHROMIC SHIFTS IN ELECTRONIC SPECTRA

I. Kahn, U. Maran, M. Karelson
Department of Chemistry, University of Tartu

Abstract: The quantum-chemical calculations of the solvatochromic effects on the electronic transition spectra in solutions have been performed for five compounds – 4'-nitro[1,1']-biphenyl-4-amine, N,N-diethyl-4-nitroaniline, 1-nitro-2-(4'-dimethylamino-phenyl)ethene, mesityl oxide and N-methyl-4'-hydroxy-4-stilbazolium betaine. The configuration interaction technique was applied at the level of intermediate neglect of differential overlap parameterization for spectra (INDO/S CI) together with the self-consistent reaction field modified Hamiltonian to account for solvent polarizability effects. A good agreement between the calculated and experimentally observed UV/Visible spectral maxima was obtained for compounds with large bathochromic effects on spectra when transferred from low dielectric constant solvents to high polarity solvents. In the case of the N-methyl-4'-hydroxy-4-stilbazolium betaine which is characterized by a very polar ground state and has large solvatochromic blue shift when transferred to a high dielectric constant medium, much larger discrepancy between the calculated and experimental spectral maxima was obtained.

INTRODUCTION

Present understanding of solvent shifts of dye molecules is derived from generalizations about the expected effect of polarizable solvents on the difference in energy between the ground and excited state electronic structures of dye molecules [1]. Experts in a particular field of dye chemistry can make accurate predictions based upon previous experience, but this is of little use in understanding the response of new dyes or dyes in novel environments. In particular, cases where a change in solvent dielectric allows a new geometry or electronic structure to dominate the resonant absorption processes are not explained by present generalizations [2, 3]. A study of solvent shifts in dyestuffs offers a means for testing the predictions of reaction field theory in a precise, experimentally accessible manner. In general, semi-empirical methods such as intermediate neglect of differential overlap with configuration interaction

(INDO/S CI) can accurately predict absorption maxima in the UV/Visible region [3, 4]. Although differences between experimental and calculated wavelengths can be greater than 50 nm, trends are most often correctly reproduced. Absorption of organic colorants is often sensitive to environmental effects and this is usually neglected in the calculations. The introduction of the special techniques which account for the solvent perturbation to molecular Hamiltonian should to reproduce the important spectroscopic shifts that accompany solvation, and to use this in design of new dyestuffs.

In this paper, a test study has been made on the calculation of the solvent effects on the UV/Visible absorption spectra of several donor-acceptor dye molecules with significant solvatochromic shifts. The semiempirical INDO/S parameterization is used as the background throughout this study [4, 5]. In order to account for the solvent polarity effects, the selfconsistent reaction field (SCRF) method [6-10] is applied. The statistical treatment of interactions due to the local orientational and electronic polarization of the solvent in the electric field of the solute molecule (non-specific or macroscopic solvation) for energies less than kT may proceed by using the macroscopic dielectric properties of solvent to represent the observable polarizability of a randomly oriented assembly of solvent molecules in the vicinity of a solute molecule. A quantum-chemical reaction field model for the description of this effect can be based on the classical Kirkwood-Onsager theory of electrical polarization in liquids [11-14].

METHODOLOGY

According to Kirkwood and Onsager, the solvent is described as a polarizable dielectric continuum, characterized by its static dielectric constant ε. The solute molecule is represented by M point charges (e_i), situated at fixed points ($\mathbf{r}_i$) inside of sphere of radius a_o. By solving the appropriate electrostatic equations inside and outside the sphere and applying the boundary conditions that are needed, one can deduce the following equation for the potential at any point inside the sphere

$$V_1(\mathbf{r}) = \sum_{k=1}^{M} \frac{e_k}{|\mathbf{r}-\mathbf{r}_k|} + \sum_{k=1}^{M} \frac{e_k}{a_o} \sum_{m=0}^{\infty} \left[\frac{(m+1)(1-\varepsilon)}{\varepsilon(m+1)+1} \right] \frac{(\mathbf{r}\mathbf{r}_k)^m}{a_o^m} P_m(\cos\theta_k) \quad (1)$$

The total electrostatic energy due to the molecular charge distribution $\rho(\mathbf{r})$ interaction with the polarized medium is

$$U = -1/2\int\rho(\mathbf{r})V(\mathbf{r})d\mathbf{r} \qquad (2)$$

In the classical model of Kirkwood, the charge distribution is represented by a set of point charges

$$\rho(\mathbf{r}) = \sum_{j=1}^{M} e_i \delta(\mathbf{r} - \mathbf{r}_i) \qquad (3)$$

and the appropriate potential $V(\mathbf{r})$ is the second term in equation (1). Thus, for the additional energy of the system inside the sphere due to the effect of the medium on the charges contained in the sphere, the model gives

$$U = \sum_{k=1}^{M} -\frac{1}{2}\sum_{i,j}\frac{e_i e_j}{a_o}\sum_{m=0}^{\infty}\left[\frac{(m+1)(1-\varepsilon)}{\varepsilon(m+1)+1}\right]\frac{(r_i r_j)^m}{a_o^{2+m}} P_m(\cos\theta_k) \qquad (4)$$

where the summation extends over all charged particles in the system (molecule).

In a quantum chemical model this interaction energy can be represented by the corresponding additional terms in the molecular Hamiltonian which can be divided into nuclear-nuclear, nuclear-electronic and electron-electron terms [7, 8]. For most applications, the two first terms in the infinite expansion of equation (4) are most important, corresponding to the Born ionic solvation (m = 0), and the Onsager "dipolar" term (m = 1). Therefore the following modified Hamiltonian $\mathbf{H'}$ can be used in the Schrödinger equation for the polar solute molecules in a polarizable medium:

$$\mathbf{H'} = \mathbf{H_0} + \Gamma\boldsymbol{\mu}^2 \qquad (5)$$

where $\boldsymbol{\mu}$ is the dipole moment operator, and $\mathbf{H_0}$ is the Hamiltonian for the isolated molecule. The discussion below is easily generalized to higher moments. The multiplier Γ (the reaction field tensor) is a function of both the dielectric properties of the solvent and the size of the solute molecule. In general, every atomic nucleus and electron in the molecule may have its own Γ value. However, in the framework of the classical Kirkwood-

Onsager theory a common value of this variable is assumed for every charged particle in the molecule :

$$\Gamma = -\frac{\varepsilon - 1}{(2\varepsilon + 1)a_o^3} \tag{6}$$

where ε is the macroscopic dielectric constant of the pure solvent and a_o the cavity radius into which the solute molecule is embedded. The use of the macroscopic value of the dielectric constant of the solvent in this formula is justified only in the case of the time-averaged orientational polarization of the solvent molecules in the field of solute molecule. If the physical or chemical phenomenon investigated by this method is characterized by a lifetime shorter than the orientational relaxation time of the solvent, an alternative value of ε (and Γ) can be used. In the limit of the purely electronic polarization of the solvent the dielectric constant, ε has to be replaced in formula (1), with the value of the dielectric constant at the infinite frequency of external electromagnetic field. This constant is approximately equal to the square of the refraction index n_D^2 of the solvent. The electronic energy of the solute molecule in the dielectric medium E_{el} may then be found by the solution of the respective one-electron Fock equations using the self-consistent reaction field (SCRF) procedure. Two different versions, based on different definition of total energy variational functional, are applicable for proceeding this procedure (described as Model A and Model B in Ref. [15] , respectively).

We shall consider the absorption of the light as an instantaneous process. This means that during the absorption process there will be no solvent reorientation, but rather only the electronic polarization of the solvent will respond to the changed electron density of the molecule in its excited state. Considering the Hamiltonian of Equation (5), we have the following configuration interaction (CI) diagonal matrix elements for state $|\psi_I\rangle$

$$\mathbf{H}_{II} = \langle \psi_I | \mathbf{H}_o - \Gamma \langle \psi_o | \boldsymbol{\mu} | \psi_o \rangle \boldsymbol{\mu} | \psi_I \rangle \tag{7}$$

and the off-diagonal elements of the CI matrix are given by

$$\mathbf{H}_{IJ} = \langle \psi_I | \mathbf{H}_o - \Gamma \langle \psi_o | \boldsymbol{\mu} | \psi_o \rangle \boldsymbol{\mu} | \psi_J \rangle \tag{8}$$

The last two equations demonstrate that the solvent effects are included "directly" into CI. However, the expression $\langle \psi_o | \mu | \psi_o \rangle$ relates only to the ground-state dipole moment after CI. For CI singles (CIS) this is no concern because of Brillouin's theorem [16] which implies that CI does not change the calculated ground state dipole moment. It has been shown by us earlier that even at higher levels of excitation in CI, this effect is not large and can be estimated from the corresponding perturbation operator [15]. For closed-shell SCF reaction field corrections do not arise until third order and should be small.

The first order approximation to take into account the instantaneous electronic polarization of the solvent during the excitation of the solute molecule is given by the following formula [15]

$$\Delta E_{IJ} = \frac{1}{2}\left[\langle \psi_o|\mu|\psi_o\rangle\langle \psi_I|\mu|\psi_I\rangle - \left|\langle \psi_I|\mu|\psi_I\rangle^2\right|\right]\Gamma(\varepsilon_\infty) \qquad (9)$$

where $\Gamma(\varepsilon_\infty)$ corresponds to the reaction field tensor (Eq. (6)) at the infinite frequency of external electromagnetic field. Summarizing, the electronic transition energy of a solute molecule in a dielectric polarizable medium is calculated as

$$\begin{aligned}\Delta W_{0I} = {} & \langle \psi_I|H|\psi_I\rangle - \langle \psi_o|H|\psi_o\rangle + \\ & \frac{1}{2}\Gamma(\varepsilon)\langle \psi_o|\mu|\psi_o\rangle\left[\langle \psi_I|\mu|\psi_I\rangle - |\langle \psi_o|\mu|\psi_o\rangle|\right] - \\ & \frac{1}{2}\Gamma(\varepsilon_\infty)\langle \psi_I|\mu|\psi_I\rangle\left[\langle \psi_I|\mu|\psi_I\rangle - |\langle \psi_o|\mu|\psi_o\rangle|\right] \qquad (10)\end{aligned}$$

This equation corresponds to the full electronic relaxation of the solute in its reaction field in the ground state. It corresponds to theory B in Ref. [15] which gives reasonable solvation energies of ionic and electroneutral solutes [17, 18], and will be used throughout this paper.

For the cavity radius a_o (Eq. (6)) the values were derived from the mass densities ρ of solute compounds:

$$a_o = 0.7346\left(\frac{WM}{\rho}\right)^{1/3} \qquad (11)$$

where *WM* denotes the molecular mass of the solute.

RESULTS AND DISCUSSION

Compounds with large solvatochromic shifts are of substantial technological importance as prospective materials with large optical nonlinearities. Some classes of these compounds have been of considerable interest as clinical agents of photodynamic therapy of cancer and diseases caused by human immunodeficiency viruses [19, 20]. In the present work, several compounds with large bathochromic and hypsochromic solvent effects in their UV/Visible spectra were chosen as model compounds. Those include 4'-nitro[1,1']-biphenyl-4-amine (**1**), N,N - diethyl- 4 -nitroaniline (**2**), 1 -nitro -2-(4'-dimethylamino-phenyl)ethene (**3**), mesityl oxide (**4**) and N-methyl-4'-hydroxy-4-stilbazolium betaine (**5**)

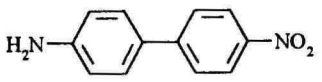

1

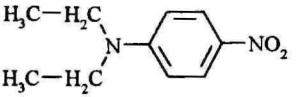

2

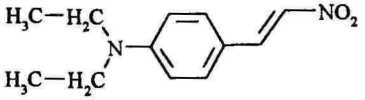

3

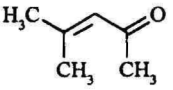

4

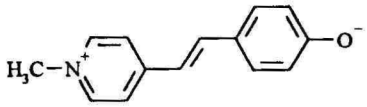

5

All spectra were calculated for model media which were described with the dielectric permittivity ε, index of refraction n_D and density ρ, corresponding to some real solvents. The list of these physical constants for media used in this work , are given in Table 1.

The molecular geometries were optimized in each medium using MOPAC 6.0 program package [21]. The initial geometries were found by MMX molecular mechanics technique [22] using graphical program PCMODEL [23]. In the quantum-chemical optimization, AM1 paramete-

rization was applied [24]. Optimized molecular geometries were input for the spectroscopic calculations to the ZINDO program package [25].

In the CI calculations, 200 most significant configurations in the space of 10 highest occupied molecular orbitals and 10 lowest unoccupied molecular orbitals were used in each calculation. INDO/S parameterization [4, 5] was applied in the molecular Hamiltonian.

Table 1. Physical Constants of the Solvents Corresponding to the Model Media Used Throughout the Calculations.

Solvent	ε	n_D	ρ (g/cm^3)
isooctane	1.95	1.3949	0.6980
cyclohexane	2.02	1.4262	0.7786
tetrachloromethane	2.23	1.4602	1.5940
benzene	2.27	1.5011	0.8787
diethyl amine	3.78	1.3846	0.7056
diethyl ether	4.20	1.3524	0.7138
chloroform	4.81	1.4459	1.4832
ethanol	24.55	1.3614	0.7893
DMSO	46.45	1.4793	1.1014
water	78.50	1.3330	1.0000

(a) ***4'-nitro[1,1']-biphenyl-4-amine*** **(1)**

The lowest maximum of the electronic absorption spectrum of 4'-nitro[1,1']-biphenyl-4-amine is in the blue part of spectra. The transfer of this compound from tetrachloromethane to DMSO is accompanied by a solvatochromic red shift of 3860 cm^{-1} (56 nm). In the hydroxylic solvents, the amino- and nitrogroup may be bound to the solvent through hydrogen bonds. Therefore a combined supermolecule-continuum approach was used in the case of these solvents, i.e. each of the hydrogen-bonding acceptor groups was solvated explicitly by one water molecule. The respective effect to the spectra appears to be small (86 cm^{-1}), as expected in the case of the $\pi \rightarrow \pi^*$ transition, which corresponds to the lowest electronic transition in the spectrum of this compound. The results of the INDO/S CI calculations of the solvatochromic shifts and their comparison with the experimental data [26, 27] are given in Table 2.

It should be noticed that the INDO/S CI calculated maxima are in good accordance with the experimentally observed maxima (in average, the difference in absolute values does not exceed 2000-2500 cm^{-1}). The solvatochromic shifts are described almost quantitatively. The respective linear regression equation between the calculated and observed solvatochromic shifts is as follows:

$$\Delta\nu(\text{calc}) = (-61\pm337) + (1.132\pm0.155)\Delta\nu(\text{exp})$$
$$R = 0.964 \qquad s = 471$$

where R is the correlation coefficient an s is the standard deviation of the regression.

Table 2. The INDO/S CI Calculated Lowest Electronic Transitions (cm^{-1}) and Experimental UV/Visible Spectral Maxima of 4'-Nitro[1,1']-biphenyl-4-amine in Different Solvents.

Solvent	ν(exp)	ν(calc)	Δν(exp)	Δν(calc)
gas phase		33 808		
CCl_4	28 248	26 214	0	0
benzene	27 397	25 934	851	280
diethyl ether	26 810	24 434	1438	1780
ethanol	26 316	23 454	1932	2760
diethyl amine	25 641	23 404	2607	2810
DMSO	24 390	22 111	3858	4103

(b) ***N,N-diethyl-4-nitroaniline*** **(2)**

The electronic absorption spectrum of the N,N-diethyl-4-nitroaniline is positioned also in the blue region and it is characterized by a large red shift (4170 cm^{-1} or 65 nm) when transferred from the cyclohexane to water. This is characteristic for the $\pi\rightarrow\pi^*$ transitions, which follow large increase in the dipole moment of the molecule during the spectral excitation of the molecule. The effect of calculated hydrogen bonding effects was again small (77 cm^{-1}). The INDO/S CI calculated and experimental [28] maxima for N,N-diethyl-4-nitroaniline in five different media are presented in Table 3.

Table 3. The INDO/S CI Calculated Lowest Electronic Transitions (cm^{-1}) and Experimental UV/Visible Spectral Maxima of N,N-Diethyl-4-nitroaniline in Different Solvents.

Solvent	ν(exp)	ν(calc)	Δν(exp)	Δν(calc)
gas phase		34 489		
C_6H_{12}	27 400	30 655	0	0
ethanol	25 480	29 013	1920	1642
DMSO	24 300	28 333	3100	2322
water	23 230	27 635	4170	3020

Notably, the absolute values of the calculated spectral transition energies are somewhat higher than experimental. However, the relative trend of the solvatochromic red shift over a wide polarity change of the medium is presented correctly.

(c) ***1-nitro-2-(4'-dimethylaminophenyl)ethene*** **(3)**

The electronic absorption spectrum of 1-nitro-2-(4'-dimethylamino-phenyl)ethene is also characterized by a large red shift (3100 cm^{-1} or 57 nm) when transferred from the cyclohexane to DMSO. The calculated hydrogen bonding effect on the $\pi \rightarrow \pi^*$ transition in ethanol was significant in the case of this compound (1443 cm^{-1}). The INDO/S CI calculated and experimental [29] maxima for N,N-diethyl-4-nitroaniline in six different media are presented in Table 4.

Table 4. The INDO/S CI Calculated Lowest Electronic Transitions (cm^{-1}) and Experimental UV/Visible Spectral Maxima of 1-Nitro-2-(4-dimethylaminophenyl)ethene in Different Solvents.

Solvent	ν(exp)	ν(calc)	Δν(exp)	Δν(calc)
gas phase		31 047		
C_6H_{12}	25 000	25 016	0	0
CCl_4	24 510	24 626	490	390
ethanol	23 150	23 230	1850	1786
chloroform	22 160	22 341	2380	2675
DMSO	21 900	21 410	3100	3606

Remarkably, there is an excellent agreement between the absolute values of the experimental and calculated UV/Visible spectral maxima for this compound. Also, the spectroscopic red shift in higher polarity media is presented quantitatively. The respective linear regression line was obtained:

$$\Delta\nu(\text{calc}) = (-131\pm133) + (1.165\pm0.068)\Delta\nu(\text{exp})$$
$$R = 0.995 \qquad s = 176$$

Notably, the inclusion of the hydrogen bonding is imperative for the correct prediction of the solvatochromic shift in ethanol (hydrogen bonding solvent).

(d) *mesityl oxide* (4)

The lowest electronic transition of the mesityl oxide is positioned in the ultraviolet part of the spectrum. Again, this compound is characterized by a solvatochromic red shift when transferred from isooctane to water (2150 cm^{-1} or 12 nm). The INDO/S CI calculated and experimental [30] maxima for mesityl oxide in five different media are given in Table 5.

Table 5. The INDO/S CI Calculated Lowest Electronic Transitions (cm^{-1}) and Experimental UV/Visible Spectral Maxima of Mesityl Oxide in Different Solvents.

Solvent	ν(exp)	ν(calc)	$\Delta\nu$(exp)	$\Delta\nu$(calc)
gas phase		47 404		
isooctane	43 370	45 022	0	0
ethanol	42 301	43 887	1069	1135
chloroform	42 087	44 082	1283	940
water	41 120	43 103	2150	1919

The agreement between the calculated and experimental absolute values of the spectroscopic transition energies is satisfactory. In general, the trend of the solvatochromic red shift is also given correctly, except of

the reversal in the maxima in ethanol and water. For water, the predicted red shift is correct as compared to the isooctane.

(e) *N-methyl-4'-hydroxy-4-stilbazolium betaine* (5)

The electronic absorption spectrum of N-methyl-4'-hydroxy-4-stilbazolium betaine is mostly in the long-wave part of the visible spectra. However, this compound is characterized by a very large solvatochromic blue shift (−6490 cm^{-1} or −178 nm) when transferred from a low dielectric constant medium (chloroform) to the high polarity solvent (water). This is due to the additional electrostatic stabilization of the highly polar (zwitterionic) ground state of this molecule in high dielectric constant media. The excited state of the $\pi \rightarrow \pi^*$ transition has much lower dipole moment and thus it is relatively less stabilized in these media as compared to the ground state. INDO/S CI calculated and experimental [31, 32] maxima for N-methyl-4'-hydroxy-4-stilbazolium betaine in four different media are given in Table 6.

Table 6. The INDO/S CI Calculated Lowest Electronic Transitions (cm^{-1}) and Experimental UV/Visible Spectral Maxima of N-methyl-4'-hydroxy-4-stilbazolium betaine in Different Solvents.

Solvent	ν(exp)	ν(calc)	Δν(exp)	Δν(calc)
gas phase		22 631		
chloroform	16 129	30 508	0	0
DMSO	17 482	31 834	−1353	−1326
water	22 620	34 315	−6491	−3807

It should be noted that the predicted INDO/S CI spectral maxima for this compound are at much higher energies than experimentally observable absorption maxima. This is an interesting observation and calls for more detailed analysis of the spectroscopic parameterization for the compounds with highly polar ground states. The solvatochromic shift is predicted qualitatively correctly but for water there is a large deviation from the experimental value. Thus, it would be of special interest to investigate such compounds in further studies.

CONCLUSIONS

The solvatochromic shifts accompanying the transfer of the compounds from the low dielectric constant media to the high dielectric constant and hydrogen bonding media were calculated for five compounds using SCRF INDO/S CI theory. For the compounds with large solvatochromic red shifts a good agreement between the calculated lowest electron transition energies and experimental UV/Visible spectral maxima was observed. In the case of the N-methyl-4'-hydroxy-4-stilbazolium betaine which is characterized by a very polar ground state and has large solvatochromic blue shift when transferred to a high dielectric constant medium, the discrepancy between the calculated and experimental spectral maxima is much larger. Further, more extensive investigation on the spectra modelling of analogous compounds are therefore needed.

REFERENCES

1. J. Fabian, H. Hartmann, *Light Absorption of Organic Colorants; Theoretical Treatment and Empirical Rules*, Springer-Verlag, Berlin, 1980.
2. T. Kobayashi, P. M. Rentzepis, *J. Chem. Phys.*, **1979**, *70*, 886.
3. A. Corval, H. P. Trommsdorff, *J. Phys. Chem.*, **1987**, *91*, 1317.
4. J. E. Ridley, M. C. Zerner, *Theoret. Chim. Acta*, **1973**, *32*, 111.
5. A. D. Bacon. M. C. Zerner, *Theoret. Chim. Acta*, **1979**, *53*, 21.
6. J. Hylton, R. E. Christoffersen, G. G. Hall, *Chem. Phys. Lett.*, **1974**, *26*, 501.
7. O. Tapia, O. Goscinski, *Mol. Phys.*, **1976**, 29, 1653.
8. M. M. Karelson, *Organic Reactivity (Tartu)*, **1980**, *17*, 357.
9. M. M. Karelson, *Organic Reactivity (Tartu)*, **1980**, *17*, 366.
10. R. Constanciel, O. Tapia, *Theoret. Chim. Acta*, **1980**, *55*, 177.
11. J. G. Kirkwood, *J. Chem. Phys.*, **1934**, *2*, 351.
12. L. Onsager, *J. Am. Chem. Soc.*, **1936**, *58*, 1486.
13. C. J. F. Böttcher, P. Bordewijk, *Theory of Electric Polarization, 2nd ed., vol. II*, Elsevier Co, Amsterdam, 1978.
14. O. Tapia, in: *Molecular Interactions*, H. Ratajczak, W. J. Orville–Thomas, Eds., J. Wiley & Sons, Chichester, **1983**, vol. 3, p. 183.
15. M. M. Karelson, M. C. Zerner, *J. Phys. Chem.*, **1992**, *92*, 6949.

16. A. Szabo, N. Ostlund, *Modern Quantum Chemistry*, Macmillan Publ. Co, New York, 1982.
17. M. M. Karelson, *Organic Reactivity (Tartu)*, **1983**, *20*, 127.
18. M. Karelson, T. Tamm, M. C. Zerner, *J. Phys. Chem.*, **1993**, *97*, 11901.
19. T. J. Dougherty, *Photochem. Photobiol*, **1987**, *45*, 879.
20. B. Roeder, D. Naether, T. Lewald, M. Braune, C. Nowak, W. Freyer, *Biophysical Chemistry*, **1990**, *35*, 303.
21. J. J. P. Stewart, *MOPAC 6.0*, Frank J. Seiler Research Laboratory, U.S.Air Force Academy, CO 80840,1990.
22. U. Burkert, N. L. Allinger, *Molecular Mechanics*. - ASC Monograph 177, American Chemical Society, Washington, 1982.
23. *PCMODEL 4.0*, Molecular Modeling Software for the IBM PC. Serena Softwate, 1990.
24. M. J. S. Dewar, E. G. Zoebisch, E. F. Healy, J. J. P. Stewart, *J. Am. Chem. Soc.*, **1985**, *107*, 3902.
25. M. C. Zerner, *ZINDO - A Comprehensive Semi-Empirical SCF/CI Package*, University of Florida, 1994.
26. A. E. Lutskii, V. V. Bocharova, Z. Kanevskaja, *Zh. Obsch. Khim.*, **1975**, *45*, 2731.
27. K. A. Al-Hassan, M. A. El-Bayoumi, *Chem. Phys. Lett.*, **1987**, *138*, 594.
28. M. J. Kamlet, R. W. Taft, *J. Am. Chem. Soc.*, **1976**, *98*, 377.
29. D. J. Cowley, *J. Chem. Soc. Perkin Trans. II*, **1975**, *4*, 287.
30. E. M. Kosower, *J. Am. Chem. Soc.*, **1985**, ***80***, 3261.
31. M. J. Minch, S. S. Sadic, *J. Chem. Educ.*, **1977**, ***54***, 704.
32. S. Hünig, O. Rosenthal, *Liebigs Ann. Chem.*, **1955**, *592*, 161.

ELEKTRONSPEKTRITE SOLVATOKROOMSETE NIHETE KVANTKEEMILINE MODELLEERIMINE

I. Kahn, U. Maran, M. Karelson

Resümee

Viie ühendi (4'-nitro-[1,1']-bifenüül-4-amiini, N,N-dietüül-4-nitroaniliini, 1-nitro-2-(4'-dimetüülaminofenüül)eteeni, mesitüüloksiidi ja

N-metüül-4'-hüdroksü-4-stilbasooliumbetaiini) solvatokroomsed nihked mitmesugustes keskkondades arvutati kvantkeemiliselt, kasutades INDO/S parametrisatsiooni konfiguratsioonilise interaktsiooni meetodi raames. Solvendi efekti kirjeldati reaktsioonivälja häiritusena molekuli hamiltoniaanis. Ühendite korral, mida iseloomustab solvatokroomne batokroomne nihe üleminekul kõrgema dielektrilise konstandiga keskkonda, saavutati hea kooskõla arvutatud ning eksperimentaalsete solvatokroomsete nihete vahel. N-metüül-4'-hüdroksü-4-stilbasooliumbetaiini korral, mida iseloomustab suur solvatokroomne sininihe üleminekul kõrgema dielektrilise konstandiga keskkonda, oli saadud kooskõla tunduvalt halvem.

A THEORETICAL STUDY OF FIVE-MEMBERED HETEROCYCLE AND METALLOCYCLE OLIGOMERS

T. Jürimäe, M. Strandberg, M. Karelson
Department of Chemistry, University of Tartu

Abstract: The results of the semiempirical PM3 calculations of phosphole, arsole, stibole and bismole and their oligomers with the chain length of 2, 4, 6, and 10 units are presented. As a comparison the data for pyrrole are also given. Oligomers of the parent heterocycles and those with the homolytically dissociated X-H (X = heteroatom) bond have been studied. Predictions on the conductive properties of the respective heterocyclic polymers are made by using the extrapolation from the bandgap data of oligomers.

INTRODUCTION

Organic heterocyclic polymers have been of considerable interest as potentially effective electrically conductive materials [1-4] and compounds with large nonlinear optical responses [5-7]. A large number of theoretical studies on these polymers have been published (for a review, cf. [8]). Apart of the calculations of polymers themselves the experimental [9-17] and theoretical [15-33] investigation of respective oligomers is widespread. From these results the extrapolated prediction of the electronic properties of polymer chains has proven to be a feasible procedure.

For instance, the electrical conductivity and optical properties of intrinsically conducting polymers would be directly related to the bandgap between the valence and empty zone as well to the bandwidth of these zones. In the framework of LCAO MO formalism, the polymer bandgap corresponds to the energy gap between the highest occupied molecular orbital (HOMO) and the lowest unoccupied molecular orbital (LUMO) in oligomers. The bandwidth is often related to the symmetry, degeneracy and relative position of active occupied and virtual orbitals. An almost linear relationship between the orbital energies ε_{HOMO},

ε_{LUMO} and their difference $\Delta\varepsilon = \varepsilon_{HOMO} - \varepsilon_{LUMO}$ on one hand and the reciprocal of the oligomer chain length in monomer units (1/n), on the other hand, has been established proceeding from quantum-chemical theories of different complexity (Valence Effective Hamiltonian, various ZDO models, *ab initio* calculations).

The aim of the present work is to study the influence of the oxidative modification (analogous to n-doping in polymers) on the electronic structure and properties of heterocycle oligomers. The objects of study consist five-membered heterocycles pyrrole, phosphole, arsole, stibole and bismole and their oligomers with chain length of 2, 4, 6 and 10 units. Also the modified oligomers consisting the units with homolytically dissociated X-H bond have been studied.

METHODOLOGY

In the present work we have made a comparative study of the oligomers of the heterocycles with isoelectronic fifth group atoms - pyrrole (**1**), phosphole (**2**), arsole (**3**), stibole (**4**) and bismole (**5**):

1 **2** **3** **4** **5**

Two chemical modifications of the heterocycle oligomer (polymer) chains were studied. The first of them has 2,2'-connected monomer subunits of the parent heterocycles (a). In the second form, (b), the heterocycles have been oxidatively modified by the homolytical cleavage of the X-H bond (X = heteroatom). This leads, with the inclusion of the heteroatom, to the formation of a 4n+2 π-electron unit system in the polymer chain.

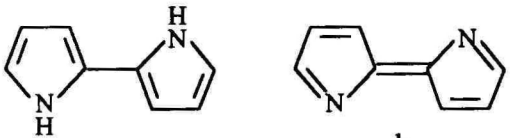

a b

In the case of the original heterocycle (a), the π-conjugation along the carbon chain is considered the origin of the intrinsic conductivity of the polymer [8]. In this case the carbon chain resembles the polyacetylene chain, slightly perturbed by the heteroatom included in the heterocycle. However, in the oligomers of form (b) the frontier orbitals include a significant contribution from the heteroatom p_z-orbitals. Therefore, in the case of this form, one may expect a much larger dependence of the electronic properties of the heterocycle polymer on the chemical nature of the heteroatom involved. In this work we have studied the trends in the change of the conductivity-related properties of the heterocyclic oligomers by the isoelectronic substitution of the heteroatom and by the above-discussed modifications of the monomer chemical structure.

The geometry of all oligomers in forms (a) and (b) and with the chain length of 2, 4, 6 and 10 monomer units were fully optimized by using the semiempirical PM3-MNDO [36] method. In general, the optimized geometry of oligomers corresponds to the planar structure of monomer subunits. Only in the case of the parent phosphole (a) the planar geometric structure of monomer is distorted. Namely, the phosphorus atom is turned out of the plane defined by four dienic carbons of the heterocycle (≈ 7–9 deg), and the hydrogen atoms deviate from the ring plane (30–45 deg).

The PM3-MNDO heats of formation ΔH°_f, HOMO and LUMO energies, and the difference between frontier orbital energies

$$\Delta\varepsilon = \varepsilon_{LUMO} - \varepsilon_{HOMO} \qquad (1)$$

were calculated for each oligomer. In the limit of the infinite oligomer length, the Δε presumably corresponds to the bandgap between valence and empty zones in the polymer chain.

In the case of pyrrole and phosphole oligomers, the calculations were proceeded also using INDO/S CI method [37]. The PM3-MNDO optimized geometry was assumed in these calculations for oligomer structures. The CI space included 2 HOMO's and 2 LUMO's per monomer unit. Therefore, for instance, in the dimers 4 HOMO's and 4 LUMO's were accounted for in CI whereas in decamers 20 HOMO's and 20 LUMO's were considered. This scaling of the CI space should correct somewhat for the size-extensivity error of the CI. Furthermore, the results, obtained by using larger CI for smaller oligomers expose little dependence of the result on the size of CI.

RESULTS AND DISCUSSION

The MNDO-PM3 calculated heats of formation ΔH°_{f}, energies of highest occupied molecular orbital ε_{HOMO} and lowest unoccupied molecular orbital ε_{LUMO}, and the corresponding bandgap energies $\Delta\varepsilon$ are given in Table 1. The calculations of the pyrrole and phosphole monomers were performed using also AM1 parameterization. In the case of pyrrole the resulting energies and geometries are close to the corresponding PM3 results and experimental data (cf. [34]). However, the results obtained for the phosphole are considerably different for two methods employed. The PM3 bond lengths are close to the experimental values for various substituted phospholes whereas C-P bond lengths obtained by the AM1 method are much shorter than experimental. Therefore, only PM3 parameterization was chosen for oligomer calculations.

In the case of dimers, the anti-conformation (**I**) was found to be favored over the syn-conformation (**II**) for some heterocycles whereas for others the syn-conformation was predicted to be more stable (Table 2).

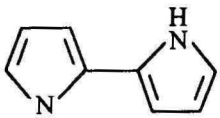

(**I**)

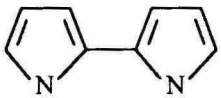

(**II**)

However, starting from the tetramers the all-anti forms have been more favored over other possible conformations and therefore we have limited ourselves in the following discussion only to the regular anti-conformations of the oligomer (polymer) chains. Notably, the data given in Table 1 correspond to this structure.

The frontier orbital energies difference $\Delta\varepsilon = \varepsilon_{HOMO} - \varepsilon_{LUMO}$ for a set of a oligomers of a given heterocycle were plotted according to the following linear relationship

$$\Delta\varepsilon = \alpha + \beta n^{-1} \qquad (2)$$

where n is the number of the monomeric units in the oligomer. The results of the linear regression treatment of the PM3 calculated data according to the Equation (2) are given in Table 3. In the case of all heterocycles, this equation describes satisfactorily the data, therefore permitting to extrapolate for the infinite chain length ($n^{-1} \rightarrow 0$).

Table 1. PM3 SCF Calculated Enthalpies of Formation ΔH°_{f} (kcal/mol), HOMO and LUMO Energies (eV) and Bandgap Energy $\Delta\varepsilon$ (eV) of Pyrrole, Phosphole, Arsole, Stibole and Bismole, and Respective Oxidatively Modified Heterocycle Oligomers (n = 2, 4, 6, 10).

Heterocycle	n	ΔH°_{f}	ε(LUMO)	ε(HOMO)	Δε
1. Pyrrole	2	50.87	0.28	-8.09	8.37
	4	98.64	-0.20	-7.62	7.42
	6	146.42	-0.36	-7.48	7.12
	10	192.77	-0.68	-7.13	6.45
2. Phosphole	2	76.83	-0.36	-8.68	8.32
	4	158.07	-1.12	-8.47	7.35
	6	249.60	-1.18	-8.06	6.88
	10	419.59	-1.29	-7.96	6.69
3. Arsole	2	113.49	-0.93	-8.81	7.88
	4	235.97	-1.27	-8.36	7.09
	6	359.23	-1.49	-8.09	6.60
	10	471.55	-1.71	-7.77	6.08
4. Stibole	2	142.95	-0.80	-8.68	7.88
	4	281.63	-1.27	-8.14	6.87
	6	420.18	-1.39	-7.95	6.66
	10	697.62	-1.53	-7.87	6.34
5.Bismole	2	172.15	0.02	-7.68	7.70
	4	339.57	-0.25	-7.02	6.77
	6	506.85	-0.31	-6.81	6.50
	10	841.35	-0.35	-6.64	6.29
6. 1-Dehydro-pyrrole	2	107.88	-1.92	-9.84	7.92
	4	210.55	-2.37	-9.51	7.14
	6	325.16	-2.57	-9.38	6.81
	10	542.65	-2.72	-9.30	6.58
7. 1-Dehydro-phosphole	2	117.87	-2.08	-8.69	6.61
	4	243.40	-1.95	-8.09	6.14
	6	368.93	-2.66	-8.09	5.43
	10	620.18	-2.76	-8.09	5.33
8. 1-Dehydro-arsole	2	158.14	-2.54	-8.93	6.39
	4	323.54	-3.21	-8.45	5.24
	6	489.04	-3.42	-8.41	4.99
	10	820.00	-3.56	-8.39	4.83
9. 1-Dehydro-stibole	2	161.37	-2.77	-8.19	5.42
	4	309.10	-3.46	-7.63	4.27
	6	456.98	-3.61	-7.59	3.99
	10	752.55	-3.70	-7.56	3.86
10. 1-Dehydro-bismole	2	215.24	-2.16	-7.42	5.26
	4	415.65	-2.57	-7.19	4.62
	6	797.03	-2.88	-6.16	3.28
	10	988.07	-3.04	-5.35	2.31

Table 2. PM3 SCF Calculated Enthalpies of Formation ΔH°_{f} (kcal/mol), HOMO and LUMO Energies (eV) and Bandgap Energy $\Delta\varepsilon$ (eV) of Pyrrole and Phosphole Dimers in Two Conformations.

Heterocycle	Conf	$\Delta H^{\bullet}_{f}$	ε_{LUMO}	ε_{HOMO}	$\Delta\varepsilon$
1. Pyrrole	anti	50.90	0.28	-8.09	8.37
	syn	54.22	0.27	-8.08	8.35
2. Phosphole	anti	78.06	-0.72	-8.59	7.87
	syn	75.46	-0.56	-8.59	8.03
3. 1-Dehydro-	anti	107.88	-1.92	-9.85	7.93
pyrrole	syn	110.49	-1.94	-9.88	7.94
4. 1-Dehydro-	anti	117.87	-2.08	-8.69	6.61
phosphole	syn	115.60	-2.05	-8.71	6.66

The dependence of the orbital energies difference $\Delta\varepsilon$ on the reciprocal of the chain length is quite similar for all parent heterocycle oligomers. The slope, β, of the relationship (2) shows a small regular diminishing in the row from pyrrole to bismole. The extrapolated bandgaps (intercept,α) of the polymer are close for different heterocycles. In comparison with the absolute values of experimental bandgaps in the polymers, the PM3 SCF values are higher by about 3–4 eV, probably because of the neglect of the electron correlation effects. Notably, PM3 extrapolated bandgap for the polypyrrole (6.47 eV) is lower than those calculated from the extrapolated HOMO-LUMO energy differences for oligomers using *ab initio* SCF theory (7.54 eV [37]) or using *ab initio* Hartree-Fock crystal orbital theory (9.10 eV [38, 39]). A comparison of the present data with those calculated using INDO/CI method for pyrrole and phosphole systems [34] suggests that the correlation effects result only in an almost constant shift of the electronic levels whereas the slope of the relationship (2) is essentially unaffected. It should be noted that the INDO/CI extrapolated bandgaps for polythiophene and polypyrrole are in good agreement with the respective experimental estimates [34].

In the case of most oxidatively modified oligomers, the slope of the linear relationship (2) is close to that observed in the case of unmodified polymers. For the (1-dehydro)bismole, the calculated slope is significantly

more steep, leading therefore to substantially lower values of the extrapolated polymer bandgap.

Table 3. Results of the Linear Regression Treatment of the Dependence of the PM3 SCF Calculated $\Delta\varepsilon$ on the Reciprocal Value of the Chain Length for Different Heterocyclic Oligomers According to the Equation (2).

Heterocycle	Form[a]	$\alpha \pm \Delta\alpha$	$\beta \pm \Delta\beta$	R[b]	s[c]
1. Pyrrole	A	6.21 ± 0.20	4.46 ± 0.68	0.978	0.205
2. Phosphole	A	6.23 ± 0.06	4.20 ± 0.20	0.998	0.061
3. Arsole	A	5.97 ± 0.12	3.92 ± 0.39	0.990	0.118
4. Stibole	A	5.98 ± 0.05	3.74 ± 0.17	0.998	0.053
5. Bismole	A	5.91 ± 0.03	3.55 ± 0.09	0.999	0.028
6. Pyrrole	Q	6.26 ± 0.03	3.34 ± 0.11	0.999	0.034
7. Phosphole	Q	5.04 ± 0.23	3.29 ± 0.77	0.949	0.234
8 Arsole	Q	4.35 ± 0.10	4.00 ± 0.33	0.993	0.102
9. Stibole	Q	3.36 ± 0.10	4.03 ± 0.35	0.993	0.106
10. Bismole	Q	1.50 ± 0.16	7.67 ± 0.53	0.995	0.160

[a] – A denotes the "aromatic" form, Q denotes the "quinoid" form.
[b] – Correlation coefficient.
[c] – Standard deviation.

However, the variation of the bandgaps for different oxidized heterocycles is much larger than for the parent systems (Table 2). Assuming the overestimation of the bandgaps by SCF method by about 3–4 eV, the predicted bandgaps for oxidatively modified poly(1-dehydrophosphole), poly(1-dehydroarsole) and poly(1-dehydrostibole) are less than 2 eV, which is the conventional limit for the bandgap of semiconductors. Therefore, these systems can be expected to have, along with the dopant-chain electron-phonon induced electrical conductivity, a part that is relevant to intrinsic chain excitations (intrinsic conductivity). For poly(1-dehydrobismole) the extrapolated intercept from the Equation (2), after accounting for the electron correlation, should be negative. Consequently, this hypothetical polymer should have zero bandgap and thus it would be a good example of a quasi-one-dimensional polymer with the metallic conductivity.

REFERENCES

1. T. A. Skotheim, (Ed.), *Handbook of Conducting Polymers*, Vol. 1. and 2., New York, Marcel Dekker, Inc.,1986-88.
2. C. C. Ku, R. Liepins, *Electrical Properties of Polymers.* Chemical Principles, Munich, Hanser Publishers, 1987.
3. M. R. Bryce, *Chem. Brit.*, **1988**, 781.
4. H. Naarmann, *Adv. Mater.*, **1990**, *2*, 345.
5. D. S. Chemla, J. Zyss, (Eds.), *Nonlinear Optical Properties of Organic Molecules and Crystals*, Academic Press, New York, 1987.
6. A. J. Heeger, J. Orenstein, D. R. Ulrich, (Eds.), *Nonlinear Optical Properties of Polymers*, Materials Research Society Symposium Proceedings, vol. 109, Boston, MA, 1988.
7. J. L. Brédas, R. R. Chance, (Eds.), *Conjugated Polymeric Materials,: Opportunities in Electronics, Optoelectronics, and Molecular Electronics*, NATO-ARW Series E, vol.182, Kluwer, Dordrecht, 1990.
8. J. M. André, J. Delhalle, J. L. Brédas, *Quantum Chemistry Aided Design of Organic Polymers for Molecular Electronics*, World Scientific, 1991.
9. J. Kagan, S. K. Arora, *Heterocycles*, **1983**, *20*, 1937.
10. G. B. Street, S. E. Lindsey, A. I. Nazzal, K. J. Wynne, *Mol. Cryst. Liq. Cryst.*, **1985**, *118*, 137.
11. A. I. Nazzal, G. B. Street, K. J. Wynne, *Mol. Cryst. Liq. Cryst.*, **1985**, *125*, 303.
12. J. T. Arnason, B. J. Philogene, C. Berg, A. Macearchen, J. Kaminski, L. C. Leitch, P. Morand, J. Lam, *Phytochemistry*, **1986**, *25*, 1609.
13. Y. Furukawa, S. Tazawa, Y. Fujii, I. Harada, *Synth. Met.*, **1988**, *24*, 329.
14. J. V. Caspar, V. Ramamurthy, D. R. Corbin, *J. Am. Chem. Soc.*, **1991**, *113*, 600.
15. D. Birnbaum, D. Fichou, B. E. Kohler, *J. Chem. Phys.*, **1992**, *96*, 165.
16. D. Birnbaum, B. E. Kohler, *J. Phys. Chem.*, **1991**, *95*, 4783.
17. G. Distefano, D. Jones, M. Guerra, L. Favaretto, A. Modelli, G. Mengoli, *J. Phys. Chem.*, **1991**, *95*, 9746.
18. C. B. Duke, *Int. J. Quant. Chem. Symp.*, **1979**, *13*, 267.
19. J. L. Brédas, R. R. Chance, R. Silbey, *Phys. Rev. B.*, **1982**, *26* 5843.
20. W. K. Ford, C. B. Duke, A. Paton, *J. Chem. Phys.*, **1982**, *77*, 4564.

21. J. L. Brédas, R. Silbey, D. S. Boudreaux, R. R. Chance, *J. Am. Chem. Soc.*, **1983**, *105*, 6555.
22. J. L. Brédas, B. Thémans, J. G. Fripiat, J. M. André, R. R. Chance, *Phys. Rev. B*, **1985**, *29*, 6761.
23. R. H. Abu-Eittah, F. A. Al-Sageir, *Bull. Chem. Soc. Japan*, **1985**, *58*, 2126.
24. E. Orti, J. Sanchez-Marin, F. Tomas, *Theoret. Chim. Acta*, **1986**, *69*, 41.
25. Y. S. Lee, M. Kertesz, *Int. J. Quant. Chem. Symp.*, **1987**, *21*, 163.
26. B. Tian, G. Zerbi, *J. Chem. Phys.*, **1990**, *92*, 3886.
27. B. Tian, G. Zerbi, *J. Chem. Phys.*, **1990**, *92*, 3892.
28. D. Jones, L. Guerra, L. Favaretto, A. Modelli, M. Fabrizio, G. Distefano, *J. Phys. Chem.*, **1990**, *94*, 5761.
29. H. Fujimoto, U. Nagashima, H. Inokuchi, K. Seki, H. Cao, H. Nakahara, J. Nakayama, M. Hoshino, K. Fukuda, *J. Chem. Phys.*, **1990**, *92*, 4077.
30. G. Zerbi, B. Chierichetti, O. Inganas, *J. Chem. Phys.*, **1991**, *94*, 4637.
31. D. Birnbaum, B. E. Kohler, *J. Chem. Phys.*, **1991**, *95*, 4783.
32. A. Karpfen, M. Kertesz, *J. Phys. Chem.*, **1991**, *95*, 7680.
33. M. Kofranek, T. Kovar, A. Karpfen, H. Lischka, *J. Chem. Phys.*, **1992**, *96*, 4464.
34. M. Karelson, M. C. Zerner, *Chem. Phys. Lett.*, **1994**, *224*, 213.
35. M. J. S. Dewar, E. G. Zoebisch, E. F. Healy, J. J. P. Stewart, *J. Am. Chem. Soc.*, **1985**, *107*, 3902.
36. J. J. P. Stewart, *J. Comput. Chem.*, **1989**, 10, 209.
37. H. O. Villar, P. Otto, M. Dupuis, J. Ladik, *Synth. Met.*, **1993**, 59, 97.
38. A. K. Bakshi, J. Ladik, M. Seel, *Phys Rev.*, B35, **1987**, 704.
39. A. K. Bakshi, *J. Chem. Phys.*,**1992**, *96*, 2339.

VIIELÜLILISTE HETEROTSÜKLITE JA METALLOTSÜKLILISTE OLIGOMEERIDE TEOREETILINE UURIMINE

T. Jürimäe, M. Strandberg, M. Karelson

Resümee

Pürrooli, fosfooli, arsooli, stibooli ja vismooli oligomeeride (n = 2, 4, 6, 10) elektroonsed omadused arvutati kvantkeemilise poolempiirilise meetodi PM3 abil. Arvutused teostati ka oksüdatiivselt modifitseeritud oligomeeride korral. Vastavate polümeeride elektrijuhtivuslikud omadused saadi ekstrapolatsiooni teel oligomeeride andmetest. Leiti, et oksüdatiivselt modifitseeritud polüvismool võib osutuda metallilise juhtivusega kvaasi-ühedimensionaalseks elektrijuhiks.

A STUDY OF THE CORRELATION BETWEEN GIBBS ADSORPTION ENERGY OF IONS AND QUANTUM CHEMICAL INDICES OF REACTIVITY ON THE BISMUTH(001) / SOLUTION INTERFACE

M. Väärtnõu
Institute of Physical Chemistry, University of Tartu

Abstract: Quantum chemical indices of reactivity have been used to find a correlation between experimental Gibbs adsorption energy and various interactions involved in the adsorption process of ions. It has been found that good correlation exists for Bi(001)/protic solvents interface, but number of systems studied is not sufficient to obtain physically reasonable coefficient values by multilinear regression analysis.

INTRODUCTION

In our previous work [1] we have studied the correlation between standard Gibbs adsorption energy ΔG^A obtained from experimental results of ion adsorption on the drop-like bismuth electrode from solutions in water and 5 different aliphatic alcohols, and quantum chemical indices of reactivity, calculated according to the AM1 method [2]. The correlation was found to be satisfactory. Therefore, it is of interest to carry out a similar analysis for bismuth single crystal faces. In the present paper, the results for Bi(001) face will be examined.

THEORY

The quantum chemical indices of reactivity, commonly used for the description of reactions between organic compounds [3], are combinations of molecular orbital (MO) energy values and electron location coefficients on these orbitals. As was stated in [3], the best form for such an index S is

$$S = \sum_i c_i / \left(E_a - E_e\right) \qquad (1)$$

where E_a and E_e are respectively the energies of the lowest unoccupied MO (LUMO) of the acceptor of electrons and of the highest occupied MO (HOMO) for the donor of electrons. Σc_i characterizes the degree of the localization of electrons on HOMO and i denotes the orbital (for a detailed explanation see [1]). The value of this coefficient is usually in good correlation with the reaction speed when we compare reactions of one certain compound with various others [3].

The adsorption process on electrodes can be considered as a combination of various interactions: ion-metal (i-m), ion-solvent (i-s), metal-solvent (m-s) and solvent-solvent (s-s). Therefore, the adsorption energy can be expressed as follows [4]

$$\Delta G^A = \Delta G_{i\text{-}m} - \Delta G_{i\text{-}s} - \Delta G_{m\text{-}s} + \Delta G_{s\text{-}s} \qquad (2)$$

and each interaction can be described with the appropriate quantum chemical index. So, in our work [1] we calculated, using the semiempirical AM1 method, the energies of HOMO and LUMO and electron localization coefficients for ions and solvents, most commonly used in adsorption studies on Bi. Next, according to Eq.1, the quantum chemical indices for each interaction were calculated. Then, proceeding from Eq. 2, the following equation for multilinear correlation analysis was developed

$$\Delta G^A = S_o + k_1 S_{i\text{-}m} + k_2 S_{i\text{-}s} + k_3 S_{m\text{-}s} + k_4 S_{s\text{-}s} \qquad (3)$$

Using the least-square method, the coefficients S_o and k_1-k_4 were estimated. However, as was shown in [1], reasonable results could be obtained only when $k_4 = 0$ was suggested. Experimental ΔG^A values for 20 different ionic systems in water and various alcohols were used. As a result, the following equation was obtained [1]

$$\Delta G^A = 101{,}5 + 0{,}9 S_{i\text{-}m} - 1{,}9 S_{i\text{-}s} - 1{,}1 S_{m\text{-}s} \qquad (4)$$

with the correlation coefficient 0.95 and the mean deviation 1.8 kJ mol^{-1}. It must be noted that because we were not able to calculate the energy levels for metal surface, different surfaces cannot be joined into one analysis. Therefore, only the results gathered on the Bi(001) plane are included in the present study.

Table 1.

System	E_e^i	E_a^s	E_e^s	S_{i-m}	S_{i-s}	S_{m-s}	G^A_{exp}
H_2O / Cl^-	-3.629	4.418	-12.464	22.297	11.995	7.333	90.3
H_2O /Br^-	-2.786	4.418	-12.464	27.689	13.399	7.333	95.8
H_2O / I^-	-1.384	4.418	-12.464	46.317	16.637	7.333	104.3
EtOH / Cl^-	-3.629	3.549	-10.874	22.297	13.447	3.936	89.9
EtOH /I^-	-1.384	3.549	-10.874	46.317	19.567	3.936	105.8
i-PrOH / Cl^-	-3.629	3.575	-11.122	22.297	13.399	4.393	91.3
i-PrOH /Br^-	-2.786	3.575	-11.122	27.689	15.165	4.393	97.4

COMPUTATIONS AND RESULTS

No additional quantum chemical computations were necessary because no new ions and solvents were used when studying the adsorption on Bi(001) face. The virial isotherm parameter lnß values were obtained from papers [5-8], and the corresponding ΔG^A were calculated. The quantum chemical characteristics together with the experimental ΔG^A values are presented in Table 1.

According to Eq. 3, the regression analysis was carried out. As follows from Fig. 1, the correlation is good (correlation coefficient 0.988), and when we put the constants into Eq. 3, we got the following formula

$$\Delta G^A = 52.6 + 1.1S_{i\text{-}m} + 1.6S_{i\text{-}s} + 0.9S_{m\text{-}s} \qquad (5)$$

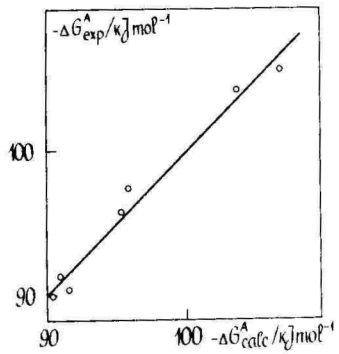

Figure 1. Plot of experimental ΔG^A values against the calculated ΔG^A. Calculations were made according to Eq. 3.

As follows from Eq. 5, the coefficients are rather different from those obtained for polycrystal. However, we found that there must be many more systems for the analysis to get correct coefficient values. If we select 6 systems from those for polycrystal several times, we get very different coefficients for each selection. Analysis showed that there must be at least 12 systems to get constant values, not depending on the selection.

CONCLUSION

Results of the present analysis demonstrate that the standard Gibbs energy of adsorption is in good correlation with combination of appropriate quantum chemical indices. However, the realistic coefficients can be obtained only if there are at least 12–15 different experimentally studied systems.

REFERENCES

1. M. Väärtnõu, M. Karelson, Elektrokhimiya, **1991**, *27*, 1366.
2. M. J. S. Dewar, E. G. Zoebisch, E. F. Healy, J. J. P. Sterwart, J. Amer. Chem. Soc., **1985**, *107*, 3902.
3. K. Fukui, Theory of Orientation and Stereoselection. Berlin: Springer Verlag, **1975**.
4. B. E. Conway, J. Sol. Chem., **1978**, *7*, 721.
5. K. Lust, M. Salve, E. Lust, Proc. 9th Symp. on Double Layer and Adsorption at Solid Electrodes. Tartu, **1991**, p.116.
6. K. Anni, M. Väärtnõu, U. Palm, Elektrokhimiya, **1988**, *24*, 846.
7. K. Anni, M. Väärtnõu, U. Palm, Elektrokhimiya, **1988**, *24*, 858.
8. M. Väärtnõu, P. Pärsimägi. E. Lust, J. Electroanal. Chem., in press.

IOONIDE ADSORPTSIOONI GIBBSI ENERGIA JA KVANTKEEMILISTE REAKTSIOONIVÕIMEINDEKSITE VAHELISE KORRELATSIOONI UURIMINE PIIRPINNAL VISMUT(001)/LAHUS

M. Väärtnõu

Resümee

Kasutades adsorptsiooniprotsessis sisalduvate erinevate interaktsioonide kirjeldamiseks kvantkeemilisi reaktsioonivõimeindekseid, uuriti korrelatsiooni ioonide eksperimentaalse Gibbsi adsorptsioonienergia ja nimetatud interaktsioone iseloomustavate arvutatud suuruste vahel. Leiti, et esineb küllalt hea korrelatsioon. Ühtlasi selgus, et multilineaarse regressioonanalüüsi abil leitud kordajate väärtused on uuritud süsteemide väikese arvu tõttu väga ebatäpsed.

ELECTRICAL DOUBLE LAYER AND ADSORPTION OF POLYMETACRYLIC ACID ON THE GLASSY CARBON ELECTRODES

E. Lust, K. Lust, A. Jänes
Institute of Physical Chemistry, University of Tartu

Abstract: The electrical double layer structure on surface inactive electrolytes and adsorption of polymetacrylic acid on the glassy carbon electrodes have been investigated by using the cyclic voltammetry and impedance measurement techniques. The limits of ideal polarizability, values of zero charge potential, surface roughness factor and other fundamental parameters have been established. The adsorption characteristics of polymetacrylic acid on the glassy carbon electrodes have been obtained.

INTRODUCTION

It is commonly accepted that the electrochemical properties of solid electrodes significantly depend not only on the chemical composition but also on the surface structure of the electrode studied [1]. In the electrochemical literature there are a lot of experimental data indicating that the electrochemical activity of the glassy carbon electrode depends to a considerable degree on the previous treatment of the surface [2]. But there is little quantitative information about the structure of the electrical double layer (edl) and adsorption of organic compounds on the glassy carbon electrodes (GCE) [3].

This paper concentrates on a comprehensive study of the influence of the previous surface treatment (surface structure) of glassy carbon electrodes on the electrical double layer (edl) and adsorption characteristics of polymetacrylic acid (PMA) from aqueous solutions of surface inactive electrolyte solutions.

EXPERIMENTAL

The glassy carbon electrodes (GCE-I and GCE-II) are discs of 4.1± 0.05 mm diameter and 4 mm thickness which were prepared from the glassy carbon rod CY-2000. The GCE-III electrodes were prepared from

the glassy carbon plate CY-2000 and they are discs of 3.6 ± 0.05 mm diameter and 5 mm thickness. The isolation of the electrodes was carried out by a thin polystyrene film (dissolved in toluene), covering the lateral surface of no interest, and then the samples were placed into a Teflon holder.

In order to obtain information about the influence of the surface structure (surface treatment) of glassy carbon electrodes to their electrochemical properties, the surface of investigated GCE was prepared by three different methods.

At first the surface (tip) of GCE-I was mechanically polished with thin emery paper and then with aluminum oxide to achieve a mirror finish. Thereafter the working surface was additionally cleared with an adhesive diamond shaver ("Buhlermet"). After the last stage of surface preparation, GCE-I was treated with concentrated NaOH and H_2SO_4, very well rinsed with ultra purified water and submerged into the deaerated working solution under the cathodic polarization (E = –0.5 V).

Secondly, the working surface of GCE-II was prepared by cleaving at the temperature of liquid nitrogen and submerged into the working solution without any mechanical or chemical treatment of cut surface under cathodic potential E = –0.5 V.

In the case of GCE-III, the working surface served as a pressed, shiny mirror finish surface of the glassy carbon plate, annealed at 1500 °C before constructing of electrode. Before each measurement, GCE-III was treated with concentrated NaOH and H_2SO_4, very well rinsed with ultra purified H_2O, and submerged into the working solution under cathodic polarization (E = –0.5 V). Before each measuring cycle, the working electrodes were scanned between –0.1 to –1.0 V to obtain reproducible results.

The cyclic voltammograms were measured using the polarographic analyzer PA-2. The differential capacity–potential curves (*C*,*E*-curves) were obtained by the a.c. impedance bridge P-568. All the solutions were prepared from triple-destilled water (the quartz system was used at the last) and purified additionally by using the special method described in [4]. Solutions were prepared volumetrically, using either $LiClO_4$, $NaNO_3$ or NaF purified by triple recrystallization from water followed by vacuum heating to dryness. NaF was calcined at 700°C immediately prior to the measurements. Electrolytic hydrogen was previously bubbled for 1–2 hrs through the electrolyte in the cell and was bubbled for the whole

time of the experiment. The temperature was kept at 293 K, and the reference electrode was an aqueous saturated calomel electrode.

RESULTS

The edl differential admittance was measured from 110 to 11000 Hz (Fig. 1). Differently from the electrochemically polished metal electrodes [1, 5, 6], a large variation of capacity C as a function of frequency ν has been observed for the GCE electrodes. The established values of $f_\nu = C_{\nu=210}/C_{\nu=2100\text{Hz}}$ at the potential of zero charged $E_{\sigma=0}$ were presented in Table 1.

Table 1. The electrical double layer parameters for GCE.

Electrode	f_υ	$E_{\sigma=0}$, V NaF	$f_{P\text{-}Z}$	D	$C_H^{\sigma<<0}$, μF·cm^{-2}	$C_H^{\sigma=0}$, μF·cm^{-2}	C_m, μF·cm^{-2}
GCE-I	2.6	–0.40	0.57	2.53	16.6	20.5	25.0
GCE-II	2.4	–0.23	0.95	2.51	20.6	22.2	29.1
GCE-III	1.9	–0.21	1.75	2.30	20.2	23.2	31.5

In the range of $-1.5 < E < +0.2$V, the value of f_ν is practically independent of the electrode potential and concentration of an electrolyte. According to the theoretical conception of Frumkin, Leikis and coworkers [7], it may be assumed that the considerable dependence of C on υ is mainly evoked by the geometrical roughness of the GCE surface. Therefore the investigated electrodes are ideally polarizable in the range of $-1.5 < E < +0.2$V and surface roughness factor $R = f_\upsilon$ can be estimated to be equal to R = 1.95 for GCE-III and R = 2.4 –2.6 for GCE-I and GCE-II.

For a long time the dependence of C on ν in the case of ideally polarizable electrodes was left unexplained and was only described in a phenomenological way. The phenomenological description of the frequency dependence of impedance Z_{CPE} (CPE – constant phase element) is given as [8, 9].

$$Z_{CPE} \approx (i\omega)^{-\alpha} \qquad (0 < \alpha < 1) \qquad (1)$$

The CPE angle φ is related to α by

$$\varphi = \frac{\pi}{2}(1-\alpha) \tag{2}$$

Obviously $\alpha = 1$ corresponds to normal capacitive behavior. Recently new ideas have been put forward in order to explain the constant phase element CPE, so-called because it affects the frequency-independent phase-shift between the applied a.c. voltage and its current response, in a satisfactory way [8, 9]. The central idea is that the deviations from ideal behavior are caused by surface roughness of a special kind, namely roughness showing scaling properties over a wide range of length scales behavior, nowadays commonly denoted by the therm "fractal" [8, 9]. The so-called fractal dimension D is a formal quantity introduced by Mandelbrot [9], which attains a value between 2 and 3 for a fractal structure and reduces to 2 when the surface is flat. D is related to α by

$$\alpha = 1/(D-1) \tag{3}$$

The established values of D, represented in Table 1, show that the surface of the GCE is geometrically (energetically) nonhomogenious.

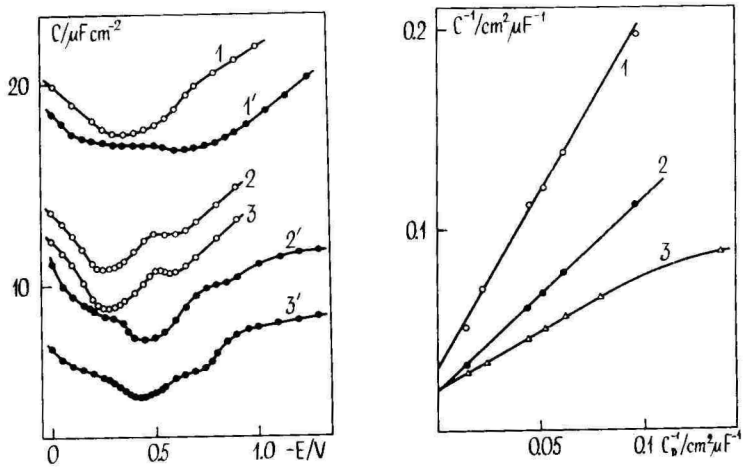

Figure 1. *C, E*- curves at υ = 210Hz for GCE-II (1-3) and GCE-I (1'-3') in aqueous solutions of NaF, M: 1,1' - 0.1; 2,2' - 0.005; 3,3' - 0.001.

Figure 2. Parsons - Zobel plots at σ=0 for GCE-I (1), GCE-II (2) and GCE-III (3).

The $C(E)$ curves in Fig.1 show that the influence of the diffuse layer is visible for concentration $c \leq 0.01$ M. The potential of the capacity minimum E_{min} is practically independent of the concentration of anions with a relative accuracy of ±10 mV. As for the single crystal Bi-, Sb-, Cd-electrodes [10], it may be assumed that no significant specific adsorption of ClO_4^- or F^- anions occurs at E_{min}, and for the most dilute solution the value of E_{min} may be identified with $E_{\sigma=0}$ for the GCE. It follows from Table 1 that the dispersion of $E_{\sigma=0}$ for the various GCE is noticeable. Accordingly, the previous surface treatment (i. e. the surface structure) of electrodes has a very important role for the edl parameters in the case of the GCE.

The applicability of the Gouy–Chapman–Stern–Grahame theory [7] has been tested by various methods. The so called theoretical differential capacity potential C, E -, the capacity charge density C,σ-curves and the Parsons–Zobel plots (the C^{-1}, C_D^{-1} curves, where C_D is the diffuse layer capacity, obtained by the Gouy – Chapman theory) were calculated for the GCE. According to Fig. 2, the Parsons–Zobel plots [11] for the GCE in the aqueous NaF and $LiClO_4$ solutions can be considered linear, when c_{el} decreases from 10^{-1} to $3 \cdot 10^{-3}$ M. The values for the fitting (roughness) coefficient, reflecting surface geometrical roughness and crystallographic heterogeneity an as shown before in [6, 10], the accuracy of the determination of the "true" surface area and solution concentration are given in Table 1. In the absence of the last two components of the mistakes, the fitting coefficient f_{P-Z} would correspond to $R \cdot f$, where f represents the crystalline heterogeneity and R the geometrical roughness of the surface, respectively. According to the data of Table 1, for GCE–III the value of f_{P-Z} is in good agreement with that of f_ν, obtained from the capacity dispersion with ν. The very low values of f_{P-Z} for GCE-I and GCE-II is a very surprising result (for the ideally flat surface $f_{P-Z} = 1.0$) and can be mainly explained by the very impressive deviations from the GCSG-theory.

The inner layer capacity charge density C_H, σ-curves were calculated according to the Grahame model (concerning the existence of the compact layer with concentration-independent properties) and by the Valette–Hamelin method [12] from the well-known equation, applicable to the edl model in the absence of specific adsorption of ions [7].

$$\frac{1}{C} = \frac{1}{FC_H} + \frac{1}{FC_D} \qquad (4)$$

where F is the fitting coefficient. The monotonic C_H, σ - curves were obtained for the values of fitting coefficient F, which varied from 1.95 to 2.2 for GCE-III, from 2.4 to 2.7 for GCE-I when c_{el} decreases from 10^{-1} to $5 \cdot 10^{-2}$ M. These values are in good agreement with the values of f_ν, obtained from the capacity dispersion (with ν) measurements. The higher values of F, observed for GCE, indicated that the surface of the GCE - electrodes is geometrically very inhomogenious.

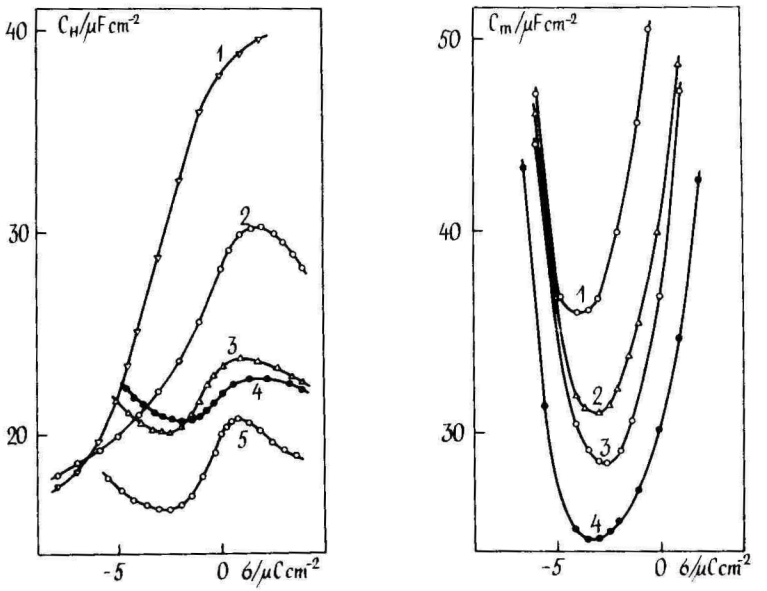

Figure 3. C_H, σ - curves in 0.1M aqueous solution of NaF for 1 – Cd(0001); 2 – Bi(001); 3 – GCE-III; 4 – GCE-II; 5 – GCE-I.

Figure 4. C_m, σ - curves in 0.1M aqueous solution of NaF for 1 – Bi(001); 2 – GCE-III; 3 – GCE-II and 4 – GCE-I.

The established values of C_H for 0.1M NaF solutions corrected by the fitting (roughness) coefficient F are presented in Table 1 and the established C_H, σ - curves in Fig. 3. According to the data of Table 1 and Fig. 3, the hydrophility of electrodes increases in the sequence of electrodes GCE-I ≤ GCE-II < GCE-III <Sb < Bi < Hg < Cd < Zn. Differently from the Cd-, Bi- and Sb- electrodes, the dependence of C_H on σ for GCE is very small (Fig. 3) and at the first approximation it may by assumed that the reorientation of solvent molecules at the surface of GCE with σ is negligible. But as for the Bi-, Sb- [10] and Hg- electrodes [13], a considerable concentration dependence of C and C_H (Fig. 1 and 3) was observed for the GCE. This effect was typically interpreted as a result of non uniform electrode polarization or analogous reasons. On the basis of the data of works [10] and experimental results in Table 1 and Fig. 1 and 3, the concentration dependence of C (or C_H) increases in the sequence of electrodes Cd < Hg < Bi < Sb < GCE, e.c. as the metallic nature of the electrodes decreases. In our opinion, these deviations from the GCSG theory, observed far from $E_{\sigma=0}$, must be connected with some secondary process on the compact layer properties, in view of the expected smallness of the diffuse layer contribution. The retarded relaxation of the compact layer as a reason for this deviation from the theoretical predictions, as well as the roughness of the GCE surface may be suggested [14-16].

The differential capacities of the "metal", e.c. the capacities of the thin surface layer of the GCE were calculated according to the Amokrane – Badiali model [16] from the equation

$$\frac{1}{C_H} = \frac{1}{C_m} + \frac{1}{C_s} \qquad (5)$$

where C_s is a "true " capacity of the solvent monolayer. The established C_m, σ - curves are presented in Fig. 4. As shown in Fig. 4 and Table 1, the values of C_m for GCE are somewhat lower than for Cd-, Bi- and Sb-electrodes. Accordingly, the lower values of C_H for GCE than for the Cd-, Bi- and Hg- electrodes can be explained by a higher contribution of the surface layer to the differential capacity of GCE / surface inactive electrolyte interface than to the semimetal (Bi, Sb) / electrolyte interface.

Adsorption of polymetacrylic acid on GCE- surface

Polymetacrylic acid adsorption from the 0.1M NaF aqueous surface-inactive electrolyte solution at GCE-I and GCE-II was studied by impedance measurement technique at T = 293 K. The concentration of PMA varied from $1.2 \cdot 10^{-4}$ to $2.27 \cdot 10^{-1}$M. According to the experimental results (Fig. 5.), the capacity depression in the very wide range of potentials $-1.6\ \text{V} < E < +0.1\ \text{V}$ can be observed. Therefore the surface of the GCE has a very low hydrophility. In the case of more concentrated PMA solutions ($c_{\text{PMA}} \geq 1.135 \cdot 10^{-1}$ M) the adsorption-desorption maxima at $E < -1.6$ V can be observed. But as we can see in Fig. 5, the most important feature of the C, E - curves is the presence of hysteresis of C with the direction of E in the region of maximum adsorption e.c. in the vicinity of $E_{\sigma=0}$. According to the conception of the Frumkin—Damaskin theory [7, 17], the diffusion of organic molecules to the electrode surface is a limiting stadium in the case of adsorption of PMA on GCE.

For the more concentrated PMA solutions ($c_{\text{PMA}} \geq 1.2 \cdot 10^{-2}$ M) in the region of $-1.2\ \text{V} < E < -0.8$ V, a supplementary low wide intermediate adsorption maximum can be observed. According to the Frumkin - Damaskin adsorption theory [7, 17], the intermediate maximum on the C, E - plot is probably due to the effect of reorientation of adsorbed molecules of PMA on the GCE surface and formation of the polymolecular adsoption layer (polylayer) of PMA on the GCE surface.

The main adsorption parameters of PMA calculated by the Frumkin - Damaskin theory are given in Table 2, where the symbols have their usual meanings. The adsorption isotherms for PMA on GCE-I and GCE-II were calculated from the C vs. E curves via the equation

$$\theta = \frac{C_o - C}{C_o - C'}, \tag{6}$$

where C_o and C' are the double layer capacity at $\theta = 0$ and $\theta = 1$, respectively. The quantity C' was found by extrapolating quantities $1/C$ to $1/C = 0$ for E_m = const. For determining the adsorption characteristics at E_m, the Frumkin adsorption isotherm was used

$$Bc = \frac{\theta}{(1-\theta)} \exp(-2a\theta). \tag{7}$$

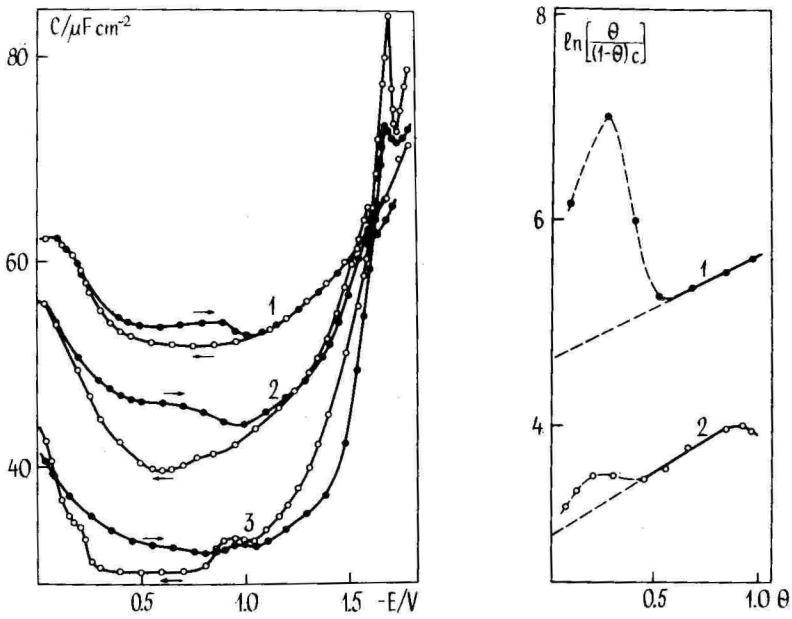

Figure 5. *C, E* - curves in 0.1M aqueous solution of NaF (1) and with additions of PMA in concentration, M: 2 – 0.0227; 3 – 0.227.

Figure 6. Adsorption isotherms of PMA on GCE-II (1) and on GCE-I (2).

Table 2. Adsorption parameters of PMA on GCE.

Electrode	a_m	B_m dm³/mol	C' μF·cm⁻²	E_N V	Γ_m mol/cm²	$-\Delta G_A^\circ$ kJ/mol
GCE-I	0.58	21.8	11.5	0.15	2.3	17.0
GCE-II	0.61	103.5	9.7	0.18	2.6	21.2

As shown in [18, 19], the most suitable form for the analysis of the experimental isotherm for polycrystalline surface is its representation in the linearizing Frumkin isotherm coordinates $\ln[\theta/(1-\theta)c]$ vs. θ.

One can see from Fig. 6, in contrast to the adsorption isotherm for homogeneous surfaces [18-19], that the adsorption isotherms for PMA on GCE-I and GCE-II at $\theta \leq 0.25$ and $\theta \leq 0.4$, respectively, are nonlinear. The bend for GCE-II is noticeably higher and wider than that for GCE-I. As shown in [19], the increasing of the adsorption heterogeneity of the two-plane model surface characterized by the ratio of adsorption equilibrium constants B_1°/B_2° increases the length and height of the bend in the experimental isotherm. Accordingly, the surface energetic heterogeneity of GCE-II is noticeably higher than that of GCE-I. At higher values of θ ($\theta \geq 0.4$), the adsorption isotherm of PMA on a cut glassy carbon electrode (GCE-II) is practically linear and the effective parameters of the linear section of the isotherm are represented in Table 2. The adsorption isotherm of PMA on GCE-II was simulated on a surface consisting of two regions under the assumption that the adsorption in each region obeys the Frumkin isotherm. As found, the attractive constant on the more active surface region a_1' (at the first approximation we observe this surface region as homogeneous or uniformly heterogeneous surface with effective parameters a_1' and B_1') was chosen greater than that on the less active surface region. As shown in [18, 19], the adsorption isotherms of this form are characteristic of the macro-polycrystalline surfaces.

The adsorption isotherm of PMA on GCE-I at $\theta \geq 0.25$ is to some degree convex (Fig. 6), and according to the results of [18, 20], the surface of GCE-I is uniformly heterogeneous (micro - polycrystalline surface).

The adsorption parameters listed in Table 2 indicate that the adsorption characteristics sufficiently depend on the previous surface treatment of GCE. The adsorption activity of PMA on GCE-II is noticeably higher than for GCE-I. But it must be noted, that the other calculated parameters (E_N, C', a_m, Γ_m) for GCE-II and GCE-I are probably (to some degree) apparent and only in the very rough approximation characterize the adsorption process at glassy-carbon electrodes.

REFERENCES

1. A. Hamelin, T. Vitanov, E. Sevastyanov, A. Popov, J. Electroanal. Chem., **1983**, *145*, 225.
2. M. R. Tarasevich, A. Sadkovski, E. B. Yeager, in B. E. Conway, J. O' M. Bockris, S. U. M. Khan and R. E. White (Eds.). Comprehensive Treatise of Electrochemistry. New York: Plenum Press, **1983**, Vol. *7*, p. 301.
3. L. A. Hanova, M. R. Tarasevich, in Electrokhimiya (Itogi Nauki i Tekhniki). Vol. 27. Ed. by Polukarov Yu. M., VINITI, Moscow. **1988**, p. 158.
4. N. P. Berezina, N. V. Nikolayeva-Fedorovich, Elektrokhimiya. **1967**, *3*, 3.
5. E. J. Lust, U. V. Palm, Soviet Electrochemistry. Engl. Tr. 21, **1985**, *9*, 1185.
6. E. J. Lust, A. A.-J. Jänes, K. K. Lust, Soviet Electrochemistry. Engl. Tr. 26, **1990**, *12*, 1448.
7. A. N. Frumkin, Potentsialy nulevogo zaryada. Moskva: Nauka. **1979**, 297 p.
8. L. Nuikos, T. Pajkossy, Electrochim. Acta, **1985**, *30*, 1533.
9. B. B. Mandelbrot, The fractal geometry of nature. San Francisko: Freeman, 1982.
10. E. Lust, A. Jänes, K. Lust, M. Salve, Acta et Comm. Univ. Tartuensis 996. Tartu, **1993**, 63.
11. R. Parsons, F. Zobel, J. Electroanal. Chem., **1965**, *9*, 333.
12. G. Valette, A. Hamelin, J. Electroanal. Chem., **1973**, *45*, 301.
13. A. Hamelin, L. Stoicoviciu, J. Electroanal. Chem., **1989**, *271*, 15.
14. M. A.Vorotyntsev, A. A. Kornyshev, Elektrokhimiya, **1984**, *20*, 3.
15. E. Leiva, W. Schmickler, J. Electroanal. Chem., **1986**, *205*, 323; **1987**, *229*, 39.
16. S. Amokrane, J. P. Badiali, J. Electroanal. Chem., 1989, 266, 21; **1991**, *297*, 377.
17. B. B. Damaskin, O. A. Petrii, V. V. Batrakov, Adsorption of organic compounds on electrodes. New York - London: Plenum Press. **1971**, 499 p.
18. A. R. Alumaa, E. I. Lust, N. A. Paltusova, U. V. Palm, Soviet Electrochemistry. Engl. Tr. 19, **1983**, *11*, 1420.
19. E. Lust, U. Palm, Acta et Comm. Univ. Tartuensis. 757.Tartu, **1986**, 105.

20. V. V. Batrakov, B. B. Damaskin, J. Electroanal. Chem., 1975, *65*, 361.

ELEKTRILINE KAKSIKKIHT JA POLÜMETAKRÜÜLHAPPE ADSORPTSIOON KLAASSÜSINIKELEKTROODIL

E. Lust, K. Lust, A. Jänes

Resümee

Voltamperomeetria- ja elektrokeemilise impedantsi mõõtmise meetodit kasutades uuriti elektrilise kaksikkihi ehituse seaduspärasusi erineva pinnatöötlusega klaassüsinikelektroodidel. Määrati kindlaks ideaalse polariseeritavuse ala ulatus, pinna karedusfaktori, null-laengu-potentsiaalide, elektrilise kaksikkihi tiheda osa diferentsiaalmahtuvuse ning klaassüsinikelektroodi pindkihis moodustuva elektroonse kondensaatori mahtuvuse väärtused. Tehti kindlaks, et eelpool nimetatud parameetrid sõltuvad oluliselt pinnatöötluse metoodikast. Leiti, et kõige väiksema karedusega on kõrge rõhu ja temperatuuri tingimustes pressitud sile pind. Tunduvalt suurema karedusega on klaassüsinikelektroodi mehhaaniliselt poleeritud ning vedela lämmastiku temperatuuril lõhestamise teel saadud pind. Leiti, et poleeritud pinnaga klaassüsinikelektroodi null-laengu-potentsiaali väärtus on tunduvalt (200 mV) negatiivsem, kui lõhestamise teel saadud pinna $E_{\sigma=0}$ väärtus. Leiti, et mehhaaniliselt poleeritud pinna tiheda kihi ning klaassüsinikelektroodi pindmises kihis moodustuva elektroonse kondensaatori mahtuvused omavad tunduvalt väiksemaid väärtusi, võrreldes teiste klaassüsinikelektroodidega. Tehti kindlaks, et klaassüsinikelektroodide mittemetallilised omadused on väljendunud tunduvalt tugevamini, kui tüüpiliste poolmetallide Sb ja Bi korral.

Uuriti ka polümetakrüülhappe (PMA) adsorptsiooni seaduspärasusi erineva pinnatöötlusega klaassüsinikelektroodidel. Leiti, et suuremate PMA kontsentratsioonide korral on võimalik polükihi moodustumine. Tehti kindlaks, et lõhestatud klaassüsinikelektroodi pind on energeetiliselt ebaühtlaselt ebaühtlane (pinnal esinevad praktiliselt kaht küllaltki erinevat adsorptsioonilist aktiivsust omavad adsorptsioonitsentrid), mehhaaniliselt poleeritud klaassüsinikelektroodi pind on aga vaadeldav ühtlaselt ebaühtlase pinnana.

ELECTRON RESPONSE OF METAL/SOLUTION INTERFACE TO THE EXTERNAL ELECTRIC FIELD

R. Salem
Moscow Commercial High School

Abstract: Influence of the external electric field to the electron-density distribution of metal and to the value of solvent molecules in contact with metal is investigated. The potential profile inside and beyond the metal has been established. The electrocapillary curve, total potential-charge density and differential capacity-charge density curves for electronic and dense part of electrical double layer at the mercury aqueous surface-inactive electrolyte solution interface were calculated theoretically and compared with experimental ones.

The present-day uncertainty in our ideas about the structure of the dense part of the electrical double layer (EDL) constrains the further development of the theory and of experimental studies. In spite of a considerable increase in the number investigations of the metal/vacuum interface and their obvious advance [1-5], the overall theory is far from being completed even for this interface, not to mention surface phenomena on the metal in contact with the liquid phase.

The present study is aimed at the further development of the ideas about the metal/electrolyte solution (*M/S*) phase boundary discussed in [6-9]. A complete explanation of the behaviour of metal at its interface with liquid cannot be made in terms of alternative models [5, 10, 11], to allow for the opposite sign of some properties such as, for example, the EDL capacity versus potential [12, 13]. Therefore, it is believed that the study of basic *M/S*-boundary parameters determining fundamental characteristics of this interface is required in order not so much to detail the *M/S*-interface structure but rather to choose the simplest models which have already been proposed for description of the surface of the metal in vacuum.

The simplest model (Smith's model) [14] might probably be exten-

ded for the case of the *M/S* interface were it not for the variation treatment this model requires and arbitrariness of electron-density-distribution functions used which, in principle, do not follow from anything.

Timashov S. F. [15] and the authors of [16, 17] have shown that the functions which fit the Scrödinger equation are the well-known Airy functions having a series of features: the Airy function goes exponentially down for the positive argument and performs oscillations for a negative one [18, 19]. Note that the electron-density oscillations (Friedel's oscillations) are associated with perturbation produced by the potential barrier of a square well and are quite general if we deal with perturbation in degenerated Fermi-gas [20]. With this perturbation being strong enough, the oscillations exhibit a change in their character on account of an additional phase component i.e.the phase shift. The account of a periodic electron-density distribution and of its modulations can result in a significant change in surface energy [21].

The validity of expressions, which describe the electron-density distribution in [14-17], being more or less evident, a model has been proposed in [7-9] for the basic characteristics of the non-charged *M/S* interface to be determined. However, it is the behavior of the *M/S* interface in the presence of the external field (electrocapillary phenomena, dependence of EDL capacity and metal potential of the charge, and so on) that is, most frequently, the researcher's concern.

On leaving the model adopted in [7-9] in force, consideration should be given to the physics of phenomena which happen at the *M/S* interface with the external electrical field. Supposing a flat metallic sample occupies the half-space $Z < 0$, the electron-density distribution on its boundary may be written as [7-9]

$$n(Z) = (n_+ - n_e)\exp\left(\frac{Z}{R_M}\right)\frac{\cos(2K_F Z + \delta)}{\cos\delta} \qquad Z < 0 \quad (1)$$

$$n(Z) = n_e \exp\left(-\frac{Z}{R_S}\right) \qquad Z > 0 \quad (2)$$

where n_+ is the density of free electrons in metal (i.e. under $Z = -\infty$), $R_M = (\pi\hbar^2/4me^2K_F)^{1/2} = (\pi a_o/4K_F)^{1/2}$ is the conventional distribution parameter used in the Thomas-Fermi model, it represents the characteristic distance at which the field inside metal is screened ($a_o = \hbar/2me^2$ is

the Bohr radius, K_F is the Fermi wave-vector). Interference of the incident and reflected waves results in the Friedel oscillations with frequency $2K_FZ$ and phase shift δ, and

$$R_S = \hbar(2mW_o)^{-1/2} = R_{So} \qquad (3)$$

is the metal-to-vacuum "outgoing" distance for a particle with mass m which moves inside the square well with barrier potential W [18]. Bringing *M/S* into the external electrical field with strength E_e, normal to the *M/S* interface, shifts the system of metal electrons against the field. A bulk of excessive charge is generated at the *M/S* interface. Designating the total electron shift in the external field by Z_e, the field made by excessive charge may be considered as that of a plane capacitor with a charge density on its plates of about $\sigma_e = \pm en_+Z_e$ [2]. This is the case when electron distribution in the external field is similar to the usual one biased by Z_e i.e. to distribution (1) or (2). Then we can write as follows

$$n(Z) = n_+ - (n_+ - n_e)\exp\left(\frac{Z+Z_e}{R_M}\right)\frac{\cos\left[2K_F(Z+Z_e)+\delta\right]}{\cos\delta} \qquad Z<0 \qquad (4)$$

$$n(Z) = n_e\exp\left[-\frac{Z+Z_e}{R_S}\right] \qquad Z>0 \qquad (5)$$

Here $n_e = n(0)$ is the electron density at the metal surface $Z = 0$, the other designations being the same. The system being affected by the external field, barrier potential W is changed by value $e\varphi$ i.e. $W = W_o \pm e\varphi$ (where W_o is related to the case of the absence of this field); then $R_S = R_{So}(1 \pm e\varphi/W_o)$, (where R_{So} is defined by eq. (3)). Values $n(Z)$ should be joined under $Z = 0$ to fit the continuity condition

$$n(-0) = n(+0)\,; \quad \frac{\partial n(-0)}{\partial Z} = \frac{\partial n(+0)}{\partial Z} \qquad (6)$$

Besides, one should fit the electroneutrality condition

$$e\int_{-\infty}^{o} dZ(n_+ - n_e)\exp\left(\frac{Z+Z_e}{R_M}\right)\frac{\cos\left[2K_F(Z+Z_e)+\delta\right]}{\cos\delta} -$$

$$-e\int_{o}^{\infty} dZn_e \exp\left(-\frac{Z+Z_e}{R_S}\right) = en_+Z_e \qquad (7)$$

where $en_+Z_e = \sigma_e$ is the excessive charge. From conditions (6) and (7) we get

$$n_e = \frac{\exp(Z_e/R_M)(\lambda-\alpha\cdot x)n_+}{\exp(Z_e/R_M)(\lambda-\alpha\cdot x)+\exp\left[-(Z_e/R_S)\right]\beta} \qquad (8)$$

$$\frac{n_+-n_e}{1+\alpha^2}\exp\left(\frac{Z_e}{R_M}\right)(\lambda+\alpha\cdot x)-n_e\exp\left(-\frac{Z_e}{R_S}\right) = n_+\beta\left[\exp\left(-\frac{Z_e}{R_S}\right)-1\right] \qquad (9)$$

where $\alpha = 2K_F R_M$; $\beta = R_M/R_S$; $\lambda = \cos 2K_F Z - \sin 2K_F Z \mathrm{tg}\delta$; $x = \sin 2K_F Z + \cos 2K_F Z \mathrm{tg}\delta$.

Matched solution of two transcendental equations (8) and (9) enables us to determine distribution parameters n_e and tgδ whose values at Z_e=0 are respectively equal to

$$n_e = 2n_+\beta\cdot\left[\alpha^2+(1+\beta)^2\right]^{-1} \qquad (10)$$

$$\alpha\mathrm{tg}\delta = (1+\alpha^2-\beta^2)(1+\alpha^2+\beta^2)^{-1}. \qquad (11)$$

Table.

Z_e, Å	n_e/n_+	tgδ	R_S, Å	$-\varphi(\infty)$ V	$\Delta\gamma$ erg/cm^2	Z_σ, Å	c_M μF·cm^2
–0.08	0.168	0.938	1.058	2.038	17.9	0.097	162
–0.06	0.179	0.836	1.072	2.107	10.7	0.138	114
–0.04	0.192	0.736	1.085	2.189	4.8	0.182	86
–0.02	0.205	0.635	1.100	2.300	2.2	0.224	70
0.00	0.219	0.574	1.118	2.390	0.0	0.263	63
+0.02	0.234	0.499	1.135	2.598	3.4	0.303	52
+0.04	0.250	0.429	1.155	2.817	12.4	0.343	46
+0.06	0.266	0.363	1.176	2.910	23.8	0.361	44
+0.08	0.282	0.302	1.210	3.135	42.8	0.422	37
+0.10	0.296	0.230	1.226	3.334	66.5	0.422	34
+0.12	0.312	0.182	1.256	3.667	107.2	0.501	31

In the table n_e/n_+ and tgδ for the Hg/water solution of a surface-inactive electrolyte for a wide range of charges are represented in columns 2 and 3, respectively. Poisson's equations for distributions (8) and (9) may be written as

$$\frac{d^2\varphi}{dZ^2} = -\frac{4\pi e}{\varepsilon_M}\left\{ n_+ - (n_+ - n_e)\exp\left(\frac{Z+Z_e}{R_M}\right)\frac{\cos\left[2K_F(Z+Z_e)+\delta\right]}{\cos\delta}\right\} \qquad Z<0 \qquad (12)$$

$$\frac{d^2\varphi}{dZ^2} = -4\pi\left[en_e\exp\left(-\frac{Z+Z_e}{R_S}\right)+\rho^{\text{bound}}\right] \qquad (13)$$

where ε_M is the dielectrical constant of the metal and according to [22], it may be written as $\varepsilon_M \approx 1+(K_F/R_M)^2 \approx 2$. Comparison between equation (13) and the conventional form of the Poisson equation shows the former to be endowed with one special feature. Here ρ^{bound} is a density of electricity bound in the dielectric and determined by polarization; it depends on field strength E [23].

$$\rho^{\text{bound}} = -div\vec{P} = -N_S div\left(\alpha\vec{E_e}\right) \qquad (14)$$

where α is the unit volume polarizability of solvent molecules in contact with metal. The number of solvent molecules in dilute solution being much bigger than that of the ions surrounded, in their turn, by solvation shells made of the same solvent molecules, the solvent molecules in the free or solvated state are in the direct contact with the metal surface. The field strength of the non-uniform distributions of electrons adjacent to metal is so high ($10^8 \div 10^9$ V/cm [3]), that the orientational polarization of the solvent molecules is degenerated (quasi-elastic dipoles). This is the case when only the induced dipole momentum arising on account of the electron polarization should be regarded. As the actual field differs from the average, $\alpha = 1+\alpha_o N_S(1-4/3\pi N_S\alpha_o)^{-1}$ (where α_o is the electron polarizability of every molecule and N_S is the number of solvent molecules in the unit volume) and bound-charge density ρ^{bound} may be written [23]

$$\rho^{\text{bound}} = -\alpha\cdot div\vec{E_e} = \alpha_o N_S\left(1-\frac{4}{3}\pi N_S\alpha_o\right)^{-1}\frac{d^2\varphi}{dZ^2} \qquad (15)$$

After introducing (15) into (13) and modification, we get

$$\frac{d^2\varphi}{dZ^2} = -\frac{4\pi e}{n_D^2} n_e \exp\left(-\frac{Z+Z_e}{R_S}\right) \qquad Z>0 \qquad (16)$$

as $1+4\pi\alpha = 1+4\pi\alpha_o N_S(1-4/3\pi N_S\alpha_o)^{-1} \approx n_D^2$ (where n_D is refractivity). So, in (16) consideration is given to the effect on the field on the value of electron polarization of solvent molecules in contact with metal.

Using conventional boundary conditions

$$\varphi(+0) = \varphi(-0)$$

$$\varphi_{M/S} = \varphi(-\infty)\ ;\ \varphi(+\infty) = 0 \qquad (17)$$

$$\varphi'(+0) = \varphi'(-0)$$

we can obtain the potential profile inside and beyond the metal

$$\varphi(Z) = -4\pi e \frac{n_+ - n_e}{\varepsilon_M (1+\alpha^2)^2} \exp\left(\frac{Z+Z_e}{R_M}\right) R_M^2 F(E) + \varphi(-\infty) \qquad Z<0 \quad (18)$$

$$\varphi(Z) = \frac{4\pi e}{n_D^2} n_e \exp\left(-\frac{Z+Z_e}{R_S}\right) R_S^2 + E_e(Z+Z_e) \qquad Z<0 \quad (19)$$

Here $F(E) = \cos 2K_F Z\left(\lambda + 2\alpha x - \alpha^2\lambda\right) + \sin 2K_F Z\left(2\alpha\lambda + \alpha^2 x - x\right)$ and E_e is the external field. The continuity of the potential at $Z = 0$ requires the expression for the potential drop to be $\varphi(-\infty) = \varphi_{M/S}$ as $\varphi(\infty) = 0$ (according to (17) the metal potential is counted from the adopted zero potential in the solution bulk)

$$\varphi_{M/S} = \varphi(-\infty) = \frac{4\pi e(n_+ - n_e) R_M^2 \exp(Z_e / R_M)}{\varepsilon_M (1+\alpha^2)^2} \alpha(E) +$$

$$+ \frac{4\pi e n_e \exp(-Z_e / R_S) R_S^2}{n_D^2} + E_e Z_e \qquad (20)$$

where $\alpha(E) = \lambda + 2\alpha x - \alpha^2\lambda$.

The expression for the total electrostatic potential arising from both the non-uniform electron distribution near the *M/S* boundary and the external electrical field on this distribution is provided in eq. (18) and (19). The general form of this external potential may be represented as [24]

$$\varphi_E(Z) = E_e\left[\frac{R_S}{2}\exp\left(-\frac{Z_e}{R_S}\right)+Z\theta(Z)\right] \qquad (21)$$

where $\theta(Z)$ is a step function (at $Z > 0$ $\theta(Z) = 1$, at $Z < 0$ $\theta(Z) = 0$). Then for fixed $Z = 0$ the total (measurable) potential is

$$\phi = \varphi(-\infty)+\varphi_E(0) \qquad (22)$$

or for this given distribution

$$\phi = -\frac{4\pi e(n_+ - n_e)\exp(Z_e / R_M)R_M^2}{\varepsilon_M(1+\alpha^2)^2}\alpha(E)+\frac{4\pi e n_e \exp(-Z_e / R_S)R_S^2}{n_D^2}+$$

$$+\frac{E_e R_S}{2} \qquad (23)$$

Relationship (23) can experimentally be verified. Fig.1 shows potential profiles, both calculated via (20) and (23) and experimental (based on the data of [25]), for the mercury electrode in water medium (adopted $\alpha_o = 1.48\cdot10^{-24}$ cm^{-3}, $n_+ = 8.64\cdot10^{22}$ cm^{-3} [26], the work function for the metal-to-water exit of an electron $\omega_o = 3.05$ eV [27].

From Fig.1 one can see the coincidence be qualitative with the experimental data [25], especially in areas of negative charges. In areas of positive charges, the matter is worse. This is apparently associated with the fact that for positive charges the electron "tail" hides deep inside metal, its intrinsic field increases and surface dipoles exhibit an appropriate increase in rigidity [28], thereof more accurate calculations of the screening effect inside the under-surface bulk of the metal should be made.

It is extremely significant to compare, at the point of zero charge, the potential values of $\varphi_{M/S} = \varphi(-\infty)$ calculated by virtue of (20) to those evaluated according to the data published in [29] for mercury as recommended. In [29] the potential of the mercury electrode with the respect to vacuum is –4.25 V. Calculations via (20) for the same metal

in the water solution result in the value $\varphi(-\infty) = -2.39$ V with respect to the water bulk. Metal electrons and those solvated in water (even for an infinitely small concentration [30]) being in thermodynamic equilibrium, the mercury potential may be supposedly measured with respect to hydrated electrons in water. Hydration energy is equal to (−1.57 ÷1.62 eV [31, 32]). Then the absolute mercury potential in water solution is −2.39+(−1.57÷ −1.62) = −3.96 ÷ −4.01 V.

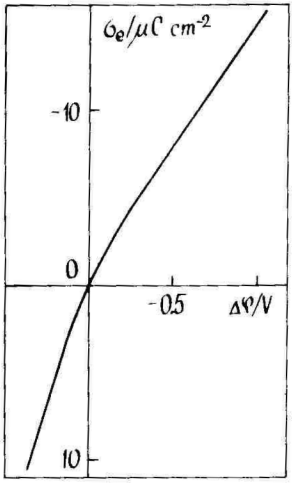

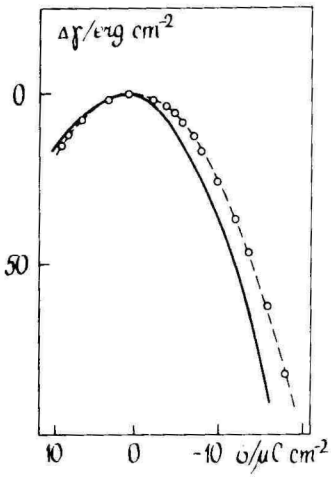

Figure 1. Total potential φ plotted versus external charge σ_e.
Figure 2. Electrocapillary curve. Dashed curve refers to the theory, points refer to the experiment [35, 36].

Surface tension of liquid metals γ may be described in terms of electrostatic and non-electrostatic (kinetic, exchange, correlation) energy [33]. Conventional consideration is based on the method of electron density functional [34], $n(Z)$, allowing for all forms of energy. An experience of calculations of the surface energy of metal at its interface with vacuum shows that the "jelly" model yields negative surface-energy parameters γ for metal with high electron density (this is the case for metals to be spontaneously broken). What may cause such a paradox ? For the present [1], we have no clear agreement on whether it is the

"jelly" model or the local density for exchange and correlation being introduced, however, it results from the calculations that the exchange and correlation energies make no change in the values of exponential distribution parameters R_M and R_S in the external field (see, for example, [2]). In [2] an effect of external field on variation parameter β which takes the sense of screening radii R_M and R_S has been analyzed. There we can see that it is only the electrostatic component of surface energy which may be affected by the external electric field. It may be written as

$$\gamma = \frac{1}{2}\int_{-\infty}^{\infty} \varphi(Z)\left[n(Z) - n_+(Z)\right]dZ \qquad (24)$$

For the above-adopted distribution, the electrostatic component of the surface tension is expressed by

$$\gamma = \frac{2\pi e^2 (n_+ - n_e)^2 \exp(2Z_e / R_M) R_M^3 \left(\lambda + 2\alpha x - \alpha^2 \lambda\right)}{\varepsilon_M (1+\alpha^2)^3} \cdot \frac{\alpha^2\lambda - \alpha\lambda + 4\alpha x}{2} +$$

$$+ \frac{\pi e^2 n_e^2 \exp(-2Z_e / R_S) R_S^3}{n_D^2} +$$

$$+ \frac{2\pi e^2 n_e (n_+ - n_e) \exp(Z_e / R_M) \exp(-Z_e / R_S) R_S^2 R_M (\lambda - \alpha x)}{n_D^2 \left(1+\alpha^2\right)} \qquad (25)$$

Calculations of the surface tension for mercury in water medium at the point of zero charge by virtue of (25) yield the value γ =406 erg/cm^2 (experiment gives 425 erg/cm^2). However, the result shows this coincidence with the experiment to be probably accidental, as, for this case, it is likely to be feasible that the change in the kinetic energy of the electron gas near the surface (whose contribution into γ is negative) is compensated by the positive contribution of exchange and correlation energies into the surface tension.

As it is only the Coulomb component that may be affected by the external field, a change in the surface tension for liquid metal affected by the external field may be described in terms of a change in the electrical energy of a capacitor with concentrated plates:

$$\Delta\gamma = \frac{1}{2}\varphi(-\infty)\sigma_e \tag{26}$$

where $\sigma_e = en_+ Z_e$ is an external charge located at distance Z_e from the "background" boundary ($Z = 0$) whose surface electron density is equal n_e (see eq. (8)). Then, on account of eq. (20), it may be written for the surface tension

$$\Delta\gamma = -\frac{1}{n_D^2}\left\{2\pi e^2 n_e^2 \exp\left(-\frac{Z_e}{R_S}\right)\left[1-\exp\left(-\frac{Z_e}{R_S}\right)\right]R_S^3\right\} - \frac{1}{\varepsilon_M(1+\alpha^2)^2} \cdot$$

$$\cdot\left\{2\pi e^2(n_+ - n_e)n_e \exp\left(\frac{Z_e}{R_M}\right)\left[1-\exp\left(-\frac{Z_e}{R_S}\right)\right]R_M^2 R_S\left(\lambda + 2\alpha x - \alpha^2\lambda\right)\right\} \tag{27}$$

From equation (27) one can see that change $\Delta\gamma$ obeys the parabolic law (non-symmetric parabole) and for liquid metal represents, in principle, the electrocapillary curve. This is illustrated by Fig.2. Fig.2 also represents the experimental data of [35, 36], their correlation calculated via (27) being rather good (in the table $\Delta\gamma$ are listed for a wide range of charges). This is coordinate Z_σ referred to the centre of mass of the additional electron density induced by the field $n_\sigma(Z)$ [3, 27, 28, 37]

$$Z_\sigma = -\frac{e}{\sigma_e}\int_{-\infty}^{\infty} Z\left[n_\sigma(Z) - n_o(Z)\right]dZ \tag{28}$$

that appears to be the key parameter characterizing electron response of the surface to the uniform electrical field, here $n_\sigma(Z)$ and $n_o(Z)$ are electron densities for the metal with and without the field, respectively, σ_e is external charge supplied to the metal. Using (12), (13) and (18), (19) and by virtue of (28), we obtain the centre-of-mass coordinate of the electron charge

$$Z_\sigma = \frac{(n_+ - n_e)e}{\sigma_e(1+\alpha^2)^2}R_M^2\left[\exp\left(\frac{Z_e}{R_M}\right)\left(\lambda + 2\alpha x - \alpha^2\lambda\right) + \left(\alpha^2 - 1 - 2\alpha\,\mathrm{tg}\delta\right)\right] -$$

$$\frac{n_e\left(e^{-Z_\sigma/R_S}-1\right)R_S^2 e}{\sigma_e} \tag{29}$$

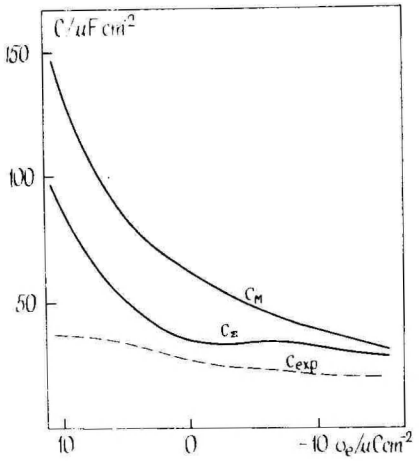

Figure 3. Electron (C_M), dense-part $C_\Sigma \cong d\sigma_S/d[\varphi(Z_\sigma) - \varphi(-\infty)]$ capacity and experimental data C_{exp} [38] of the electrical double layer at the mercury/water-solution of surface-inactiveelectrolyte interface.

Results of calculations of Z_σ are listed in the table. Parameter Z_σ possesses significance of the electron boundary of the metal with the field [3, 4] and depends strongly on the field strength and sign.

As both Z_σ referred to the (electron) boundary of the metal and the barrier potential and $\varphi(Z_\sigma) - \varphi(-\infty)$ may be approximated by the electron contribution to the total measured capacity including two consecutive capacities: geometric capacity of a gap located between the layer of the solution and the electric metal boundary Z_σ and a surface (electron) metal capacity made by plane Z_σ coupled with the flat of positive metal ions, it is interest to compare these values to experimentally measured for a dense part of the EDL. Fig.3 compares values $n_D^2/4\pi Z_\sigma$

with the results of graphic differentiation $d\sigma/d[\varphi(Z_\sigma)-\varphi(-\infty)]$ and experimental data for the EDL-dense-part capacity calculated on the basis of the experiment [38].

The present results show that we rely on the electron EDL model with emphasis shifted towards consideration of electron "tail" properties at the *M/S* interface, it appears to be possible to describe reasonably a wide range of experimental phenomena. And if till now special properties of the dense EDL part have been supposed to arise from both the adsorption and solvent-molecule orientation, model presented above draws our attention to parameters deforming the potential profile. They include R_S which is the function of the external field (see the table) and the work function for the electron exit to the given medium. Phase shift, ρ, of the Friedel oscillations, being also dependent on the field and the work function (see this dependence for mercury in different solutions [39]) is of great importance. Electron properties of the liquid in contact with the metal play their part as they affect not only high-frequency polarization of the liquid but also, to a great extent, the electron work function.

REFERENCES

1. Theory of the Inhomogeneous Electron Gas. Ed. S. Lundguist, N.H. March. Plenum Press, N.-Y., London, **1983**.
2. V. F. Uhov, R. M. Kobeleva, G. V. Detkov, A. I. Temrokov, Electron static theory of metals and ion crystals. Nauka, M., **1982**.
3. M. B. Partenskiy, UFN, **1979**, v.*128*, part I, p. 69-102.
4. M. B. Partenskiy, Poverhnost, **1982**, *10*, p. 15-32.
5. M. L. Rosinbeig, These de doctorat d'etat L'universite Pierre et Marie Curie, Paris, **1983**.
6. S. S. Salem, J.F.H., **1980**, *46*, p. 191-195.
7. G. A. Martynov, R. R. Salem, Elektrohimiya, **1983**, *19*, p. 1060-1070.
8. G. A. Martynov, R. R. Salem, Can. J. Chem., **1984**, *62*, p. 1145-1158.
9. G. A. Martynov, R. R. Salem, Electrical Double Layer at a Metal-dilute Electrolyte Solution Interface, Springen-Verlag, Berlin, N.-Y., **1983**, 170 p.
10. V. J. Feldman, M. V. Partenskiy, Solid St. Commun., **1985**, *55*, 2, p. 157-164.

11. M. A. Vorotyncev, A. A. Kornishev, Elektrohimiya, **1984**, *20*, part 1, p. 3-47.
12. M. B. Partenskiy, M. M. Vorobiev, DAN SSSR, **1984**, *27*, 2, p. 343-347.
13. J.-P. Badiali, M.-L. Rosinberg, J. Goodisman, J. Electroanal. Chem., **1983**, *143*, p. 73.
14. J. R. Smith, Phys. Rev., **1965**, *181*, p. 512-523.
15. S. F. Timashev, Electrohimiya, **1979**, *15*, 5, p. 730-732.
16. G. H. Gräf, Nuclear Physics, **1980**, *A349*, p. 349-358.
17. B. G. Euglert, J. Schwinger, Phys. Rev., **1984**, *29A*, 5, p. 2239-2352.
18. L. D. Landau, E. M. Lifshice, Quantum mechanics. Ed. fiz.-mat. lit., M., **1969**, 524 p.
19. F. Bassani, J. P. Parravichini, Electron states and optical transitions in solida, M., Nauka, **1982**, 391 p.
20. N. March, N. Parinello, Collective effects in solids and liquids, Mir, M., **1986**.
21. S. N. Burmistrov, L. B. Dubovskiy, FTT, **1981**, *23*, 10, p. 304-309.
22. Ch. Kittel Introduction to physics of solids, M., Nauka, 1977, *791* p.
23. I. E. Tamm, Principles of the theory of electricity, M., Nauka, **1976**, 616 p.
24. J. R. Smith, Phys. Rev. Lett., **1970**, *25*, 15, p. 1023-1025.
25. C. D. Russel, J. Electroanal. Chem., **1963**, *6*, p. 485-490.
26. P. G. Dzhavakidze, A. A. Kornyshev, G. A. Thsitsushvili, Solid St. Commun., **1984**, *52*, 4, p. 401-405.
27. Ya. M. Zolotovnitskiy, V. A. Benderskiy, S. A. Babenko, L. I. Korshunov, T. S. Rudenko, Double layer and adsorbtion on solid electrodes, III, Tartu, **1972**, p. 119-123.
28. A. K. Theophilou, A. Modinos, Phys. Rev., **1972**, *B6*, p. 801-807.
29. Recommendations 1986, J. Electroanal. Chem., **1986**, *209*, 2, p. 418-428.
30. B. B. Damaskin, O. A. Petriy, Electrohimiya, Visshaya Shkola, M., **1987**, 225 p.
31. E. Hart, M. Anbar, Hydrated electron, Atomizdat, M., **1971**, 271 p.
32. A. K. Pikaev, Solvated electron in radiation chemistry, Nauka, M., **1969**, 457 p.
33. G. Paash, H. Wohn, Phys. St. Sol., **1975**, *70*, p. 555-561.
34. P. Hohenberg, W. Kohn, Phys. Rev., **1964**, *136*, 864 and W. Kohn, L. J. Sham, Phys. Rev., **1965**, *A140*, 1333.
35. D. C. Grahame, J. Am. Chem. Soc., **1958**, *80*, p. 4201-4207.

36. R. G. Barradas, F. H. Kimerle, Can. J. Chem., **1967**, *45*, p. 109-116.
37. M. B. Partenskiy, V. E. Kuzema, V. I. Feldman, Izv. Vuzov, ser. phys., **1981**, *11*, p. 10-14.
38. D. C. Grahame, J. Am. Chem. Soc., **1954**, *76*, p. 4821-4829.
39. R. R. Salem, J. Electroanal. Chem., **1988**, *245*, p. 307-312.

VÄLISE ELEKTRIVÄLJA MÕJU METALL/LAHUS PIIRPINNA ELEKTROONSETELE KARAKTERISTIKUTELE

R. Salem

Resümee

Analüüsitakse välise elektrivälja mõju metallide üliõhukeses pindkihis moodustuva elektroonse kondensaatori ja lahusti molekulide elektrilistele omadustele (pindseisundile) faasidevahelisel piirpinnal Hg/pindinaktiivse elektrolüüdi vesilahus. Tuletatakse võrrandid potentsiaalilanguse kirjeldamiseks metalli pindkihis ning elektrilise kaksikkihi tihedas osas ning võrrandid elektroonse kondensaatori ja kaksikkihi tiheda osa diferentsiaalmahtuvuse arvutamiseks. Samuti tuletatakse võrrandid teoreetilise elektrokapillaarkõvera leidmiseks.

Saadud seoseid kasutades arvutatakse teoreetiliselt elektroonse kondensaatori ning elektrilise kaksikkihi tiheda osa diferentsiaalmahtuvuse ja summaarse potentsiaalilanguse sõltuvused elektrilaengu pindtihedusest. Samuti leitakse teoreetiline elektrokapillaarkõver piirpinna Hg/pindinaktiivse elektrolüüdi vesilahus jaoks. Arvutatud kõveraid võrreldakse eksperimentaalsete tulemustega ning täheldatakse rahuldavat kooskõla teooria ning eksperimendi vahel väikeste pinnalaengute alas.

THE DYNAMIC MODEL OF THE PRESSURE OF GAS

T. Tenno, A. Mashirin

Institute of Physical Chemistry, University of Tartu

Abstract: Definition of the pressure of the ideal (perfect) mono-atomic gas as a factor of dynamic effect of the gas phase on the interfacial surface is considered. The model of that effect is described on the basis of the kinetic theory of the ideal gas. The expression of Boltzmann's constant is discussed.

The gas factor affecting the interfacial surface is the component of the momentum of its atoms i_n, normal for the surface.

$$i_n = m\, v_n \tag{1}$$

where m – mass of the gas atom; v_n – the component of the velocity of the gas atoms in the direction normal for the interfacial surface.

The force that gas exerts on the interfacial surface is determined by the change of the normal component of the average momentum of atoms at the surface of the gas phase according to Newton's law of motion. The dynamic effect of gas per unit of interfacial surface, the so-called pressure P can be expressed as a derivative from I_n with respect to time t[1]:

$$\mathrm{P} = -\frac{\mathrm{d}I_n}{\mathrm{d}t} \tag{2}$$

where I_n – the normal component of the average momentum of the atoms of gas per unit of surface.

The differential of the average momentum of the atoms of gas $\mathrm{d}I_n$ is determined as a sum of the differentials of the average momentum $\mathrm{d}I_{ni}$ of the i th fraction of the atoms of gas. The atoms of i th fraction have the velocity in a narrow range v_{ni} to $v_{ni} + \Delta v_n$.[2]

$$\mathrm{d}I_n = \sum_i \mathrm{d}I_{ni} \tag{3}$$

The number of collisions of the atoms of i th fraction $d\omega_i$ per unit of surface during time dt is $d\omega_i = n_i^* v_{ni} dt$, and we can express the normal component of the change of momentum per time dt:

$$dI_{ni} = n_i^* v_{ni} \Delta i_{ni} dt \qquad (4)$$

where n_i^* – number of atoms N_i of the i th fraction in the unit of volume ($n_i^* = N_i / V$); $\Delta i_{ni} = -2mv_{ni}$, the change of the average momentum of atoms of the i th fraction upon its collision with the interfacial surface; v_{ni} – the average value of the velocity v_n of gas atoms of the i th fraction.

Here, via determination of the number of collisions $d\omega_i$ an assumption is made, that all atoms of gas of the i th fraction in the layer being against the surface and having thickness $dX_i = v_{ni} dt$, can reach the interfacial surface during time dt (Fig. 1), where v_{ni} is characterizing the component of the average velocity in the direction normal to interfacial surface [1]. The number of collisions is $d\Omega_i$ i.e. the number of atoms which collide with surface S from volume dV during time dt is $d\Omega_i = n_i^* dV_i$, and we can be express $d\omega_i$ as:

$$d\omega_i = d\Omega_i / S \qquad (5)$$

where $dV_i = S dX_i$

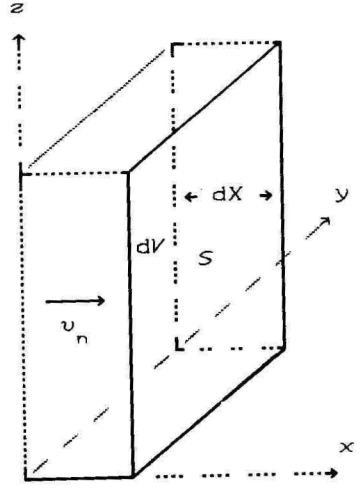

Figure 1. Element of the volume of gas bearing against the interfacial surface.

Replacing dI_{ni} from equation (4) into equation (3) we get the expression for the differential of the normal component of the average momentum of the atoms of gas per unit of surface:

$$dI_n = \sum_i n_i^* v_{ni} \Delta i_{ni} dt \tag{6}$$

From equations (2 and 6), replacing variables, we can express pressure as a macroquantity characterizing the dynamic action of gas on the interfacial surface through the average microquantities, characterizing the state of the atoms of gas:

$$P = -\sum_i n_i^* v_{ni} \Delta i_{ni} = -\sum \frac{v_{ni} \Delta i_{ni}}{V_{oi}} \tag{7}$$

where $V_{oi} = V/N_i$ – specific volume of the space for one atom of the i th fraction.

The concentration of atoms of the i th fraction can be expressed:

$$n_i^* = n^* \frac{N_i}{N} \tag{8}$$

where $n^* = N/V$ is the number of atoms of gas (atoms per unit of volume V).

The equation (7) can be rearranged using the expression for the change of the average momentum of atoms of the i th fraction:

$$P = 2n^* m \sum_i \frac{N_i}{N} v_{ni}^2 \tag{9}$$

By conditions $\Delta v_n \to dv_n$ and $N_i \to dN$ we get:

$$P = 2n^* m \int_0^\infty \frac{dN}{N} v_n^2 \tag{10}$$

where dN/N is the distribution function of speed v_n and can be expressed by following:

$$\frac{dN}{N} = \left[\frac{m}{2\pi kT}\right]^{1/2} \exp\left[-\frac{mv_n^2}{2kT}\right] dv_n \tag{11}$$

where k is Boltzmann's constant. Therefore

$$P = 2n^{*}m\left[\frac{m}{2\pi kT}\right]^{1/2}\int_{0}^{\infty}\exp\left[-\frac{mv_n^2}{2kT}\right]v_n^2 dv_n \qquad (12)$$

By integrating we get the expression for pressure:

$$P = 2n^{*}m\left[\frac{m}{2\pi kT}\right]^{1/2}\frac{\pi^{1/2}}{4}\left[\frac{2kT}{m}\right]^{3/2} = 2n^{*}mu_n^2 \qquad (13)$$

where $u_n^2 = (kT/2m)^{1/2}$ root mean square speed in direction normal to the interfacial surface.

The pressure can be expressed as following:

$$P = -f_n\Delta i_n \qquad (14)$$

where $f_n = n^{*}u_n$ is the mean square frequency of collisions per the unit of the interfacial surface, $\Delta i_n = -2mu_n$ is the mean square change of momentum of an atom at its collision with the interfacial surface.

The expression of the pressure through the mean square quantities the frequence of collisions of the atoms f_n and the change of the momentum Δi_n is describing the physical meaning of the action of gas to the interfacial surface as a result of action on the microscopic level. The mean square quantities f_n and Δi_n take into account the quadratic dependence of the action of the atoms by the collisions on their velocity. This quantities differ from the mean arithmetic quantity which describe separately the frequency of collisions of the atoms and the change of their momentum.

The mean arithmetic frequence of collisions of atoms with interfacial surface is determined by the expression:

$$f_n^{*} = n^{*}w_n \qquad (15)$$

where $w_n = (kT/2\pi m)^{1/2}$ is the component of the mean velocity of the atoms normal to the interfacial surface. The average change of the momentum of the atoms of gas taking into consideration the above given quadratic dependence is determined by following:

$$\Delta i_n^* = \frac{dI_n / dt}{f_n^*} = -\sqrt{2\pi mkT} \qquad (16)$$

where $dI_n/dt = -n^*kT$ is the velocity of summarized change of momentum of atoms of gas by their collisions with the unit of surface.

The expression (16) Δi_n^* can be given:

$$\Delta i_n^* = -2mw_n \qquad (17)$$

where $w_n = (\pi kT/2m)^{1/2}$ is equivalent value of the mean velocity of gas which are taking into account quadratic dependence upon the velocity of change of momentum.

The values of the mean arithmetic and mean square frequency of the collisions and change of momentum of the atoms are described as following:

$$f_n^* = f_n/\pi^{1/2} \qquad \Delta i_n^* = \pi^{1/2}\Delta i_n \qquad (18)$$

From the equation (13) the pressure P can be written:

$$P = nkT \qquad (19)$$

The given expression is statistical as it is got on the basis of the equation (11) describing statistical distribution function dN/N of atoms by the normal component of the velocity. This function is got from the Boltzmann's distribution law, where multiplier $\mu = 1/kT$ normalizes the energy of particles of the system as an argument of the distribution function.

By the derivation of the Boltzmann's distribution law correspondence of the multiplier μ to the quantity $1/kT$ is determined through the energy E of the particles and entropy from the following equations [1]:

$$\left[\frac{dE}{dS}\right]_V = \frac{1}{k\mu} \qquad (20)$$

where $[dE/dS]_V = T_S$ – statistical determination of the temperature through E and S. From the equation (20) the multiplier μ is determined:

$$\mu = 1/kT_S \qquad (21)$$

Therefore in the equation (19) the pressure P contains statistical definition of the product of Boltzmann's consatant k and temperature T (T_S).

Let us note that the comparision of the equation (19) with the equation of the state of ideal gas (22) leads to well-know definition of the absolute value of the Boltzmann's constant (23).

$$P = cRT \tag{22}$$

where $c = n/N_A V$ – the concentration of gas in mole in the volume V:

$$k = R/N_A \tag{23}$$

Thus the well-know equation (23) for determination of Boltzmann's constant is true if the determination of temperature as by the statistical Boltzmann's law and as by the equation of the ideal gas is identical.

The initial definition of Boltzmann's constant is obtained by the derivation of the Boltzmann's law on the basis of statistical modelling of the thermodynamic system [1]:

$$k = \mathrm{d}S/\mathrm{d}(\ln W) \tag{24}$$

where S is the entropy of the system, W is the weight of the most probable configuration of the system i e. thermodynamic probability.

Therefore the determination the Boltzmann's constant is also statistical and its absolute value is not possible to determine.

On the basis of the Boltzmann's law the statistical definition of the average energy $\bar{\varepsilon}$ of the atoms of the ideal gas through the statistical Boltzmann's constant and the statistical temperature T by the motion of the gas atoms with three degree of freedom is given:

$$\bar{\varepsilon} = 3/2kT \tag{25}$$

This equation allows to determine the value of the constant k through the average energy of one degree of freedom of atoms $\bar{\varepsilon}/3$:

$$\frac{k}{2} = \frac{1}{T}\frac{\bar{\varepsilon}}{3} \tag{26}$$

From equation (26) it follows that the quantity $k/2$ has the physical meaning (the derivative of the energy by one degree of freedom with respect to the temperature):

$$k/2 = \mathrm{d}(\bar{\varepsilon}/3)/\mathrm{d}T \qquad (27)$$

If the quantity $k/2$ expresses the physical meaning in some degree, then equation (19) for the pressure P may be re-arranged:

$$P = 2n(k/2)T \qquad (28)$$

The comparision of the equation (28) with the initial equation (13) allows to assume that this form of equation (28) expresses the change of the momentum of the atoms of gas through its double momentum (before and after the collision).

The offered definition of the pressure can be used at the analysis of the contents of the thermodynamic functions containing pressure.

REFERENCES

1. E. A. Moelwin-Hughes, Physical Chemistry, M.: Izd. inostr. lit., **1962**, pp. 16-92.
2. L. Bolzmann, Lektsii po teorii gazov, M., Izd. teh. teor. lit., **1956**, p. 31.

GAASI RÕHU DÜNAAMILINE MUDEL

T. Tenno, A. Mashirin

R e s ü m e e

Ideaalse gaasi rõhk on esitatav Newtoni teise seaduse järgi gaasi molekulide keskmise liikumishulga pinna normaali suunalise muutumise kiirusena. Töös toodud mudeli alusel on rõhk määratud faasidevahelise piirpinna ühikule vastava gaasi molekulide põrgete sageduse ja pinna normaali suunalise liikumishulga muutuse korrutisega. Kuna mõlemad suurused sõltuvad piirpinna normaali suunalisest keskmisest kiirusest, siis ideaalse gaasi rõhk on ruutfunktsioon gaasi aatomite ruut-

keskmisest kiirusest antud suunas. Gaasi rõhku saab iseloomustada energia kahekordse muundumise kaudu ühe vabadusastme järgi. Boltzmanni konstandi füüsikaline sisu on väljendatav osakeste liikumise ühe vabadusastme energia kaudu.

SOME ASPECTS OF APPLICATION OF THE LAW OF STATE OF IDEAL GAS

T. Tenno, A. Mashirin
Institute of Physical Chemistry, University of Tartu

Abstract:The physical content of the equation of the state of perfect gas is considered. The function of the state of gas is determined on the base of Newton's second law through the rate of the change of the momentum of the atoms of gas. The structure of the total differential d(PV) is represented on the microscopic and macroscopic levels. For describing the state of gas on the microscopic level, the normal component of the average velocity of the atoms and the change of the average momentum of atoms at their collisions with the interfacial surface is used.

Let us take under examination the monoatomic perfect (or ideal) gas, which is an idealized model of the gaseous state of matter in which the pressure is related to the volume, temperature, and amount of substance by the relation [1]:

$$PV=nRT \tag{1}$$

Let us recall that the equation of state is based on experimental facts concerning the macroscopic behaviour of gases. The physical properties used in the equation of state for defining the physical state of pure gas were determined by the measurement possibilities of the parameters of the time when the equation was derived. Real gases under normal conditions satisfy quite accurately the ideal gas equation.

Now let us examine the equation of state from the energetic point of view. The dimensions of terms PV and RT congruent with the energy dimension [E] are taken as a basis at the genesis of the ordinary energetic conception:

$$[PV] = [nRT] = [(\mathrm{N/m^2})\ \mathrm{m^3}] = [(\mathrm{mol})(\mathrm{J/mol\ K})\ \mathrm{K}]=[\mathrm{J}].$$

The energy of the monoatomic perfect gas is translational kinetic energy. To charactherize the energy of n moles of the monoatomic perfect gas from the quantitative side, we can write:

$$E = nN_A\bar{\varepsilon} \tag{2}$$

where: N_A – number of Avogadro; $\bar{\varepsilon} = (3/2)\ kT$ – average translational kinetic energy per gas atom; k – Bolzmann's constant.

The total kinetic energy of n moles of a perfect monoatomic gas is given by:

$$E = (3/2)\ nRT \tag{3}$$

Comparision of the equation of state (1) of perfect gas with the latter is shown by:

$$PV = (2/3)\ E \tag{4}$$

The term PV in the equation of state is not equal to the energy of gas. According to the equation of state, the pressure of perfect gas can be exspressed by:

$$P = (n/V)\ RT = c\ RT \tag{5}$$

where c is the concentration of gas (moles per unit of volume).

Appreciable difference of the last equation from expression (1) is that the state of perfect gas is expressed using the intensive quantities directly describing the state of gas, i.e. equation (5) is characterizing the state of the unit volume of gas. At that, the state of gas is given as an intensive characteristic of gas, not depending on its quantity and equally characterizing the whole gas and its average statistic molecule. At the same time, the main form of the equation of the state of gas (1) through the combination of extensive and intensive quantities is describing the state of gas.

From the definition of pressure we can write [2, 3]:

$$P = -f_n\Delta i_n = -n^*v_n\Delta i_n \tag{6}$$

where: n^* – number of atoms per unit of volume ($n^* = N/V$);

v_n – normal component of the average velocity;

$\Delta\ i_n$ – average change of momentum of an atom at its collision with the interfacial surface;

f_n – number of collisions per unit of time and per unit of surface; i.e. frequency of collisions.

The term $n^* v_n$ can be observed as the density of the flow of gas atoms (specific flow) in the direction perpendicular (normal) to the surface.

The pressure can be expressed as the specific flow of the average change of momentum of gas atoms in the normal direction to the interfacial surface.

Taking into account equation (6), we get for product PV:

$$PV = -n^* v_n \Delta i_n V \tag{7}$$

From equation (7) the dimension of the term PV is:

$$[PV] = [n^*]\ [v_n]\ [\Delta i_n]\ [V] = [1/m^3]\ [m/s]\ [kg\ m/s]\ [m^3].$$

Comparing the dimension of PV with the one derived from the energetic point of view where the energy can be expressed through force F, required to move an object to a distance L ($[E] = [F]\ [L] = [kg\ (m/s^2)]$ [m]) one can mention that they are equivalent to each other and have different structure. The latter of them does not include the dimension of momentum in a revealed form.

Differentiating the equation of the state of perfect gas in the case when all the variables P, V and T change during the process, we get:

$$d(PV) = \frac{\partial}{\partial P}(PV)dP + \frac{\partial}{\partial V}(PV)dV = nRdT \tag{8}$$

The partial differential $\partial_P (PV)$ at V = const and P = var can be expressed:

$$\partial_P(PV) = VdP = nR\partial_P T$$

where: $\partial_P T$ is the change of temperature when the pressure is changing by dP. The partial differential $\partial_V(PV)$ at P = const and V = var can be expressed:

$$\partial_V(PV) = PdV = nR\partial_V T$$

where: $\partial_V T$ is the change of temperature when the volume is changing by dV. Replacing the partial differentials into equation (8) we get:

$$\mathrm{d}(PV) = V\mathrm{d}P + P\mathrm{d}V = nR(\partial_P T + \partial_V T), \tag{9}$$

where $\mathrm{d}T = \partial_P T + \partial_V T$. The total differential d(PV) is describing the change of the state of perfect gas from the initial conditions P, V, T to the final conditions P+dP, V+dV, T+dT. The total change consists of two partial changes from the state P, V, T to the conditions P+dP(dP < 0), V, $T+\partial_P T$, expressed by the term VdP and another from the state P, V, T up to the conditions having parameters P, V+dV, $T+\partial_V T$, expressed by the term PdV (Fig.1).

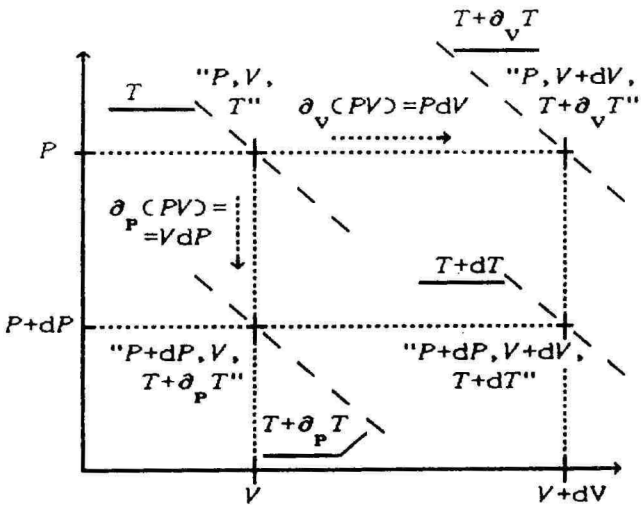

Figure 1. Differentiation of the function of the state of perfect gas.
- - - Isoterms for perfect gas at various temperatures T; $T+\partial_P T$; $T+\partial_V T$; T+dT.

Partial differentials in general are not equal $\partial_P T + \partial_V T \neq 0$. Thereby in the case when $|\partial_V T| > |\partial_P T|$, the process of expansion is accompanied by an increase of temperature.

By an isochoric process (V = const and P = var), the partial change of temperature can be calculated from the relation $\partial_P T = (V/nR)\,dP$ and the partial change of the energy of gas by $\partial_P E = (3/2)\,nR\partial_P T$.

At an isobaric process (V = var and P = const), the partial change of temperature for the monoatomic gas can be calculated by $\partial_V T = (P/nR)\cdot dV$ and the partial change of energy by $\partial_V E = (3/2)\,nR\partial_V T$.

At an isotermal process $\partial_P T + \partial_V T = 0$ and also the total differential $d(PV) = 0$. In this case the pressure and volume are related by PV = const. The relative change of volume $|dV/V|$ in the case of isothermic process is equal to the relative change of pressure $|dP/P|$.

In the case of adiabatic exspansion, the relative change of volume $|dV/V|$ is less than the relative change of pressure $|dP/P|$ ($5dV/V = -3dP/P$). Therefore the PV diagram for adiabatic expansion is steeper than that for isothermal expansion (Fig. 2). As gas expands adiabatically, no heat is transferred into the system or out of it and gas cools during adibatic expansion ($dT < 0$).

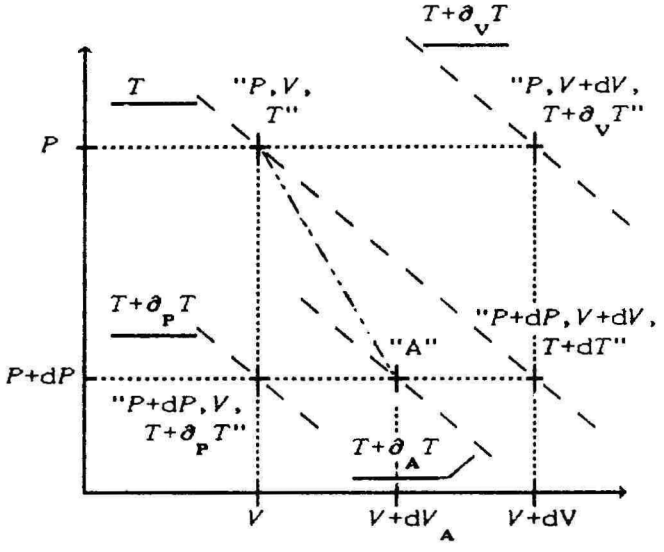

Figure 2. Differentiation of the function of perfect gas in the case of isothermal and adiabatic processes. – – – Isoterms for perfect gas at various temperatures T, $T+\partial_P T$, $T+\partial_V T$, $T+\partial_A T$. – – – – Adiabatic expansion of gas.

By differentiating equation (6), the total differential dP can be expressed as the sum of partial differentials:

$$dP = (\partial P/\partial f_n)\, df_n + (\partial P/\partial \Delta i_n)\, d(\Delta i_n) \qquad (10)$$

where $\partial P/\partial f_n = -\Delta i = -2mv_n$; $df_n = n^* dv_n$ at V= const; $\partial P/\partial \Delta i_n = -f_n$. Rearranging equation (10), we get the expression for dP:

$$dP = -n^*[\Delta i_n dv_n + v_n d(\Delta i_n)] \qquad (11)$$

where: $n^*\Delta i_n dv_n$ is the partial change of the specific flow of the average change of the momentum of atoms, that is caused by the change of the frequency of collissions per unit of surface, $n^* v_n d(\Delta i_n)$ is the partial change of the specific flow of the average change of the momentum of atoms, that is caused by the change of its average change of momentum Δi_n.

Partial differential $V dP$ is the change of the state at the macroscopic level can be expressed through quantities on the microlevel in the following way:

$$V dP = N[\Delta i_n dv_n + v_n d(\Delta i_n)] \qquad (12)$$

The term $V dP$ is connected with the change of the flow of the average change of the momentum due to the change of the frequency of collisions and the average change of the momentum of atoms. The concentration of atoms is not changing. Thereby the normal component of the average velocity of atoms v_n and kinetic energy of atoms E_k are changing. The partial differential of the kinetic energy $\partial_P E$ (proportional to the change of the flow of the change of momentum, but not equal) can be expressed for the monoatomic gas:

$$\partial_P E = (3/2)\, V dP$$

The decrease of pressure is determined by the decrease in temperature by $\partial_P T$. The amount of heat $\partial_P q$, that had to be taken from the gas to decrease the average velocity of atoms, is determined only by the change of kinetic energy. Kinetic energy will include the all components of the motion of atoms. Partial differential VdP is characterizing only the change of the normal component of motion, and from the energetic

point of view this component is included in the differential $\partial_P E$. The term $V\mathrm{d}P$ is characterizing the ordered component of the motion of atoms through the change of momentum and is not connected with the exchange of energy between gas and environment.

$$\partial_P q = \partial_P E = (3/2)\, nR\partial_P T$$

where (3/2) R is specific heat capacity C_V of gas when V = const.
If P = const. and V = var the total differential of pressure $\mathrm{d}P = 0$, and we can write:

$$\mathrm{d}P = (\partial P/\partial n^*)\, \mathrm{d}n^* + (\partial P/\partial v_n)\, \mathrm{d}v_n + (\partial P/\partial \Delta i_n)\, \mathrm{d}(\Delta i_n) = 0 \qquad (13)$$

where $\partial P/\partial n^* = -\Delta i_n v_n$, $\partial P/\partial v_n = -n^* \Delta i_n$, and $\partial P/\partial \Delta i_n = n^* v_n$. Rearranging equation (13), we get:

$$\mathrm{d}P = -\Delta i_n v_n \mathrm{d}n^* - \Delta i_n n^* \mathrm{d}v_n - n^* v_n \mathrm{d}(\Delta i_n) = 0$$
$$\mathrm{d}P = -\Delta i_n (v_n \mathrm{d}n^* + n^* \mathrm{d}v_n) - n^* v_n \mathrm{d}(\Delta i_n) = 0 \qquad (14)$$

In expression (14), the term Δi_n $(v_n \mathrm{d}n^* + n^* \mathrm{d}v_n)$ is determning the partial change of pressure caused by the change of collision frequency, meaning that the specific flow of the change of momentum is reduced due to the decrease of concentration ($\mathrm{d}n^* < 0$) and is partially compensated by the increase of the normal component of the average velocity of atoms.

The term $n^* v_n \mathrm{d}(\Delta i_n)$ is the partial change of pressure, caused by the increase of the change of the average momentum of atoms. At the isobaric expansion process, the decrease of the specific flow of the change of momentum caused by the decrease of the concentration of atoms has to be compensated by the increase of the average velocity of atoms, owing to what the system has to get an additional amount of heat $\partial_V q$ which can provide the increase of temperature $\partial_V T$. Thereby the total specific flow of the change of the momentum of atoms will be constant, what will guarantee the constancy of pressure during isobaric expansion ($\mathrm{d}P = 0$).

The term $P\mathrm{d}V$ if P = const and V = var can be expressed in the form:

$$P\mathrm{d}V = -N v_n \Delta i_n\, (\mathrm{d}V/V) \qquad (15)$$

Partial differential $P\mathrm{d}V$ is characterising the change of the concentration of atoms on the macrolevel which is determined by the relative change of volume $\mathrm{d}V/V$, thereby the specific flow of the average change of the momentum of atoms will be constant at the microlevel, i.e. the pressure will be constant.The number of atoms in the system will be constant, but their concentration is decreasing. The descending of the concentration of atoms will decrease the frequency of collision on the interfacial surface. The decrease of the frequency of collisions caused by the decrease of concentration will be compensated by the increase of temperature $\partial_V T$ (i.e. the increase of the average velocity of atoms). The increase of kinetic energy E by $\partial_V E$ caused by the increase of velocity is accompanied also by the increase of the normal component of the velocity of atoms. The normal component of the average velocity in one's turn will enter into terms of the frequency of collisions and the average change of momentum and through the change of both of them will compensate the effect of the decrease of the frequency of collosions on the interfacial surface to pressure (i.e. the effect caused by the decrease of concentracion). For the monoatomic gas we get:

$$\partial_V E = (3/2)\, P\mathrm{d}V = (3/2)\, nR\, \partial_V T$$

The amount of heat needed to be given to the system for the preservation the constancy of the density of the flow of the change of momentum is determined by the sum of the change of kinetic energy and the work done by gas against the surrounding enviroment, while the change of the flow of the change of momentum $P\mathrm{d}V$ is accompanied by the equivalent exchange of energy $\mathrm{d}w$ between gas and environment:

$$\partial_V q = \partial_V E + \mathrm{d}w = (5/2)\, nR\partial_V T \qquad (16)$$

where $\mathrm{d}w = P\mathrm{d}V = nR\partial_V T$.

The heat received by the system at the constant pressure that has caused the change of the temperature of the system by $\partial_V T$, can be divided into two components: one part of it is determined by the amount of gas and its heat capacity C_V, i.e.is connected with the change of translational kinetic of gas. The second part of the heat is used for doing work, and therefore the capacity of heat at the constant pressure is determined both by the properties of gas and by heat received by gas and used for the work done by the gas.The work done at the expansion of

gas dw is equivalent to the energy change between gas and surrounding environment.

The total change of the state of gas d(PV) is connected with the change of the total flow of the change of the momentum of atoms:

$$\mathrm{d}(PV) = V\mathrm{d}P+P\mathrm{d}V = -N[\Delta i_n \mathrm{d}v_n + v_n \mathrm{d}(\Delta i_n)] - Nv_n\Delta i_n \mathrm{d}V/V \qquad (17)$$

The change of the total flow of the change of the momentum of atoms of gas (consisting of N atoms) has two parts: the first term corresponds to the constant volume and the second is characterizing the change of the total flow of the change of momentum caused by the relative change of volume dV/V at P = const. The change of kinetic energy that can be expressed through partial changes corresponds to the total change of the state of the monoatomic gas:

$$\mathrm{d}E = \partial_P E+\partial_V E = (3/2)\, nR(\partial_P T+\partial_V T)$$

The total amount of heat, that gas has exchanged with the surrounding enviroment can also be expressed through the partial changes of heat:

$$\mathrm{d}q = \partial_P q+\partial_V q = \mathrm{d}E+P\mathrm{d}V$$

where $\mathrm{d}E = nc_V\mathrm{d}T$ is the total change of the kinetic energy of the gas atoms which corresponds to the total change of temperature and $P\mathrm{d}V = -Nv_n\Delta i_n$ (dV/V) is the change of the total flow of the change of momentum of atoms of gas (gas, containing N atoms in it) which is compensating the relative change of volume dV/V to preserve the constancy of pressure. Partial differential $P\mathrm{d}V$ (quantitatively equal to the work done by gas) is characterizing the ordered transfer of momentum of the atoms of gas to the surrounding environment. At that, the ordered change of the momentum of the atoms of gas is converted into the ordered change of the momentum of the particles of the environment on the interfacial surface and in the case of gas environment through the process of interchange of speed among the particles, the corresponding energy gained by environment will be distributed to the other particles.

REFERENCES

1. P. W. Atkins, Physical Chemistry, 4th Ed., **1994,** p. 2.
2. E. A. Moelwyn-Hughes, Physical Chemistry, **1961**, p. 51.
3. T. Tenno, A. Mashirin, Acta et Comm. Univ. Tartuensis, *975*, **1994**, 71.

IDEAALSE GAASI OLEKU VÕRRANDI MÕNINGAID ASPEKTE

T. Tenno, A. Mashirin

Resümee

Ideaalse gaasi olekut kirjeldavat P,V-funktsiooni saab esitada Newtoni II seaduse alusel gaasi molekulide liikumishulga muutuse voona. Molekulide liikumishulga muutus on faaside kokkupuutepinna suhtes suunatud suurus. Ideaalse gaasi P,V-funktsioon erineb nii kvalitatiivselt kui kvantitatiivselt gaasi energiast. P,V-funktsioon ja diferentsiaal d(PV) kirjeldavad gaasi molekulide korrastatud liikumist, energia E ja diferentsiaal dE aga korrapäratut kaootilist soojusliikumist. Diferentsiaali d(PV) füüsikalise olemuse kaudu nii mikro- kui makrotasandil saab avada ideaalse gaasi termodünaamiliste funktsioonide füüsikalise sisu.

PHYSICAL CONTENT OF ENTROPY FOR IDEAL GAS SYSTEM

T. Tenno, A. Mashirin
Institute of Physical Chemistry, University of Tartu

Abstract: The definition of entropy on the basis of the second law of thermodynamics for the ideal gas is observed. The macroquantities of the definition of entropy are expressed on the microlevel. The chaotic and ordered forms of the motion of gas molecules in the determination of entropy are discussed. To express the entropy the dynamic model of the pressure of the ideal gas and the time of the change of the state of the gas are used.

Entropy as a function of the state of a system in differential form dS defined on the basis of the second law of thermodynamics as a ratio of heat dq transferred to the system and temperature T (on the Kelvin scale) at which the transfer of heat takes place:

$$dS = dq/T \tag{1}$$

In the case when the volume of the gas changes heat dq can be expressed on the basis of the first law of thermodynamics [1]:

$$dq = dE + PdV \tag{2}$$

where E is the internal energy of the system, P is the pressure of the gas, V is the volume of the gas.

From equations (1) and (2) we get the following expression for differential dS:

$$dS = dE/T + PdV/T \tag{3}$$

The physical content of differential dE is connected with the total change of kinetic energy of the chaotic motion of the gas moleculs. The differential of the macroquantity E can be defined through the microquantity of the average energy $\bar{\varepsilon}$:

$$E = nf_d\,(R/2)\,T = Nf_d(k/2)\,T = N\bar{\varepsilon} \tag{4}$$

$$\mathrm{d}E = N\mathrm{d}\bar{\varepsilon} = Nf_d(k/2)\,\mathrm{d}T \tag{5}$$

where n is the number of moles, N is the number of molecules in volume V, f_d is degree of freedom of the motion of the gas moleculs, R is the universal gas constant and k is Boltzmann's constant. The term $P\mathrm{d}V$ is a partial differential from the product PV of the equation of the state of the ideal gas ($PV = nRT$) at constant pressure:

$$P\mathrm{d}V = nR\mathrm{d}T = Nk\mathrm{d}T \tag{6}$$

The physical content of the term $P\mathrm{d}V$ is the ordered change of the total flow of the change of the momentum of the gas moleculs at their collisions with the inerfacial surface [2]. The partial differential $P\mathrm{d}V$ is expressed through the average value of the parameters of the motion of molecules on the microlevel [2]:

$$P\mathrm{d}V = -Nv_n\Delta i_n\,(\mathrm{d}V/V) = -Nv_n\Delta i_n\,(\mathrm{d}V_o/V_o) \tag{7}$$

where v_n is the normal component of the average velocity of the gas moleculs, $\Delta i_n = -2mv_n$ is the average change of the momentum of the gas molecule in its collision with the interfacial surface, m is mass of the gas molecule, $V_o = V/N$ is the specific volume of the space for one molecule. Thus the differential of energy is describing the thermal chaotic motion of molecules, but partial differential $P\mathrm{d}V$ – the ordered component of motion, normal to the intefacial surface.

Temperature T of the system in equation (1) is ordinarily not defined but only postulated. The definition of the physical content of the differential of entropy $\mathrm{d}S$ considered here needs an additional definition of temperature T of the system, being in this case the ideal gas. From equation (4) we get the energetic definition of temperature T for the first term $\mathrm{d}E/T$ of equation (3) through microquantities $\bar{\varepsilon}$ and k:

$$T = (\bar{\varepsilon}/f_d)/(k/2) \tag{8}$$

where $\bar{\varepsilon}/f_d$ is the average energy of the motion of gas molecules to one degree of freedom.

From the second term (PdV/T) of expression (3) temperature is defined on the basis of the equation of the state of the ideal gas, i.e. macroquantity T is defined on the basis of the state of the gas through microquantities:

$$T = PV/nR = P\,(V_o/k) = -\,v_n \Delta i_n/k \qquad (9)$$

where macroquantity pressure ($P = v_n \Delta i_n/V_o$) is expressed through the quantities on the microlevel [3].

The physical content of the energetic definition of temperature on the microlevel can be expressed as a relation of the average energy for one degree of freedom of the molecules and constant $k/2$. The corresponding definition of temperature by the state of gas on the microlevel can be expressed as a relation of the average velocity of the change of the momentum of gas molecules and constant k.

Definitions (8) and (9) for temperature T through the average parameters of the gas molecules $\bar{\varepsilon}$, v_n, Δi_n correspond to the definitions of differentials dE (5) and PdV (7) through these parameters. By putting terms (5, 7, 8, 9,) into equation (3), we can get the definition of the differential of entropy using microquantities $\bar{\varepsilon}$, V_o and their differentials that is describing the state of the molecules of gas:

$$dS = Nk\,[\,(f_d/2)\,(d\bar{\varepsilon}/\bar{\varepsilon}) + dV_o/V_o\,] \qquad (10)$$

The physical content of the first term on the right side of equation (10) is connected to the relative change of the average energy of the thermal motion of molecules $d\bar{\varepsilon}/\bar{\varepsilon}$. The second term of equation (10) is formally connected with the relative change of the specific volume dV_o/V_o. We can show that the change dV_o/V_o is also connected with the relative change of the average velocity of the change of the momentum of gas molecules at their collisions with the interfacial surface

Let us examine the volume of gas dV_{st} that is bearing against the element of the interfacial surface $\Delta\Omega$ (Fig. 1).

Thickness dX_{st} of the gas layer from which molecules can reach the surface of the gaseous phase with the time dt is determined through the average velocity of the molecules in the direction normal for the interfacial surface:

$$dX_{st} = v_n dt \qquad (11)$$

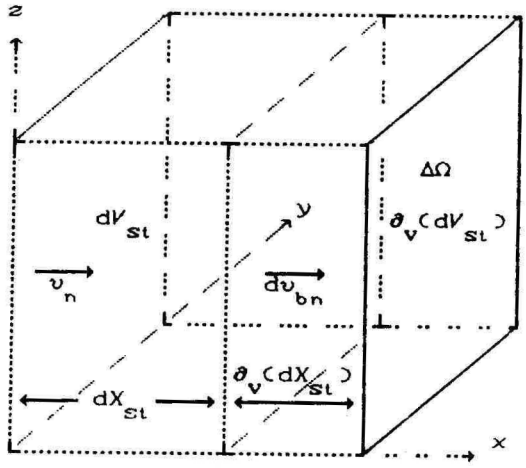

Figure 1. Element of the layer of gas bearing against the interfacal surface, dV_{st} – volume of the gas layer bearing against surface $\Delta\Omega$, dX_{st} – thickness of the layer from which the molecules can reach immobile surface $\Delta\Omega$ with time dt, $\partial_v(dV_{st})$ – change of dV_{st} at the displacing $\Delta\Omega$ for $\partial_v(dX_{st})$, $\partial_v(dX_{st})$ – displacement $\Delta\Omega$ at the change of volume V by dV.

The velocity of the average change of the momentum of gas molecules at the collision with the immobile element of surface $\Delta\Omega$ is determined as follows:

$$(dI_n/dt)\,\Delta\Omega = -\,(v_n/V_o)\Delta i_n\,\Delta\Omega \qquad (12)$$

where $dI_n/dt = -f_n\Delta i_n$ is the rate of of change of the momentum of gas molecules at the collision with the unit of the surface, $f_n = n^*v_n = v_n/V_o$ frequency of the collisions of gas molecules with the unit of the interfacial surface, $n^* = N/V$ number of gas molecules in the unit of volume. In equation (12) the minus sign shows that the rate $(dI_n/dt) > 0$ is directed from the surface to the gaseous phase. By changing the volume of gas V by dV, specific volume V_o changes by dV_o, and elementary volume dV_{st} is portionally changing by $d_v(dV_{st})$:

$$dV/V = dV_o/V_o = \partial_v(dV_{st})/dV_{st} \qquad (13)$$

By $\Delta\Omega$ = const to change $\partial_v(dV_{st})$ of elementary volume dV_{st} is corresponding to proportional displacement $\partial_v(dX_{st})$of the inerfacial surface $\Delta\Omega$ to the direction which is normal to it:

$$\partial_v(dX_{st})/dX_{st} = \partial_v(dV_{st})/dV_{st} \tag{14}$$

From the system of equations (11, 13, 14), displacement $\partial_v(dX_{st})$ is determined as a function of the relative change of the specific volume of the gas phase dV_o/V_o:

$$\partial_v(dX_{st}) = v_n dt\ (dV_o/V_o) \tag{15}$$

Usully in thermodynamics time t at the desrcibing of the transition process of the system from the initial state to the final one is not observed. In this case we try to describe the transition of the gas from the volume V up to $V+dV$. This transition is proceeding by the finite interval of time Δt_b. By the time of the transition of gas from state (P, V) to state (P, $V+dV$), the element of surface $\Delta\Omega$ is moving with velocity dv_{bn} in the direction normal to the interfacial surface:

$$dv_{bn} = \partial_v(dX_{st})/\Delta t_b \tag{16}$$

Inserting equation (15) into (16) we get dv_{bn} as a function of the relative change of volume:

$$dv_{bn} = (dt/\Delta t_b)\ v_n\ (dV_o/V_o) \tag{17}$$

One can show that if the surface of the gaseous phase is moving with velocity dv_{bn} , the average velocity of gas molecules in the direction, normal for the intefacial surface, after a collision with it has the value:

$$v_n' = v_n - 2dv_{bn} \tag{18}$$

where: v_n' – average velocity of gas molecules in the normal direction after the collision, v_n – average velocity of gas molecules in the normal direction before the collision. After the collision with the moving interfacial surface, the molecule will return with the changed momentum:

$$\partial_v \, |\Delta i_n| \, = - 2m \, \mathrm{d}v_{bn} \qquad (19)$$

where $\partial_v \, |\Delta i_n|$ – differential of the average change of the momentum of gas molecules at the moving surface $\Delta\Omega$. Inserting the equation (17) into equation (19), we can get the definition of the differential of the average change of the momentum of a gas molecule as a function from the change of specific volume $\mathrm{d}V_o/V_o$:

$$\partial_v \, |\Delta i_n| \, = - 2m(\mathrm{d}t/\Delta t_b)v_n(\mathrm{d}V_o/V_o) = (\mathrm{d}t/\Delta t_b)\Delta i_n(\mathrm{d}V_o/V_o) \qquad (20)$$

Frequency of the collisions of gas molecules with the moving element of surface $\Delta\Omega$ is:

$$f_b = f_n' \, \Delta\Omega \qquad (21)$$

where $f_n' = f_n(1 - \mathrm{d}V_{bn}/V_n)$ – frequency of collisions with the unit of the moving surface (eq.12). One can determine the differential of the change of the average momentum of gas molecules as a result of their collisions with the mobile element of the interfacial surface $\Delta\Omega$ at time Δt_b as follows:

$$\partial_v(\mathrm{d}I_n) \, \Delta\Omega = f_b \Delta t_b \partial_v \, |\Delta i_n| \qquad (22)$$

Replacing the terms in equation (22) correspondingly, we can get the equation of the differential $\partial_v(\mathrm{d}I_n) \, \Delta\Omega$ as a function of the change of specific volume $\mathrm{d}V_o/V_o$:

$$\partial_v(\mathrm{d}I_n) \, \Delta\Omega = 2(\Delta\Omega/V_o)v_n\Delta i_n(\mathrm{d}V_o/V_o)\mathrm{d}t \qquad (23)$$

where $(v_n/V_o)\Delta i_n = -\mathrm{d}I_n/\mathrm{d}t$ is velocity of the change of the average momentum of gas molecules at the collision with the unit of the immobile interfacial surface (eq.12). It is also important to add that the differential of the velocity of the change of the average of the momentum of gas molecules (23) which is caused by the movement of the interfacial surface, at the relative change of the volume of gas $\mathrm{d}V/V$ does not depend on time Δt_b for that change. We can rearrange equation (23) according to the next formula:

$$[\partial_v(f_n \, \Delta i_n)]/(f_n \, \Delta i_n) = -2(\mathrm{d}V_o/V_o) \qquad (24)$$

From equation (24) we can see that the relative change of the average change of the momentum corresponds to the relative change of the gas volume, it only has the opposite sign. Re-placing term dV_o/V_o (24) into the equation (10), we can get the formula for the differential of entropy:

$$dS = N(k/2)\{f_d\,(d\varepsilon/\varepsilon) - \partial_v(f_n\Delta i_n)/(f_n\Delta i_n)\} \qquad (25)$$

where $d\varepsilon/\varepsilon = d\{\ln(\varepsilon)\}$ and $\partial_v(f_n\,\Delta i_n)/(f_n\,\Delta i_n) = \partial_v\{\ln(f_n\,\Delta i_n)\}$.

As a result the formula for the differential of entropy at P = const gets the form:

$$dS = N(k/2)\partial_v\{\ln[\varepsilon^{f_d}/(f_n\,\Delta i_n)]\} \qquad (26)$$

The obtained equation (26) defines the entropy of the gas in the differential form as a function of the relation of average energy of the motion of molecules and the average change of momentum of the molecuIs at their collisions with the interfacial surface. This equation can be presented as follows:

$$dS = N\,dS^{o} \qquad (27)$$

where $dS^{o} = (k/2)\partial_v\{\ln[\varepsilon^{f_d}/(f_n\,\Delta i_n)]\}$ – average differential of the entropy of gas molecules.

As the average kinetic energy of gas molecules quantitatively characterises the chaotic, irregular motion of molecules and the average velocity of the change of momentum is a measure of the ordered motion, so equation (27) determines the entropy of the ideal gas as a function of the relation of chaotic and ordered motion of gas molecules. On the ground of the presented transformations, we can assume that in the well known interpretation of the definition of the differential of entropy, the relative change of temperature consists of the relative change of energy of the thermal chaotic motion of gas molecules. The relative change of the volume of the gas consists of a relative change of the velocity of the ordered change of the momentum of gas molecules at their collisions with the interfacial surface. When the chaotic form of the motion of molecules in the constant ordered form is increasing, entropy increases correspondingly, and vice versa, when the ordered form of motion is increasing, in the constant chaotic motion, entropy is correspondingly

decreasing. This conception corresponds to the general meaning of entropy which is a measure of the degree of the disorder of the state of a system.

REFERENCES

1. E. A. Moelvin-Hughes, Physical Chemistry, p. 51-235
2. T. Tenno, A. Mashirin, Acta et Comm. Univ. Tartuensis, 975, **1994**, 79.
3. T. Tenno, A. Mashirin, Acta et Comm. Univ. Tartuensis, 975, **1994**, 71.

IDEAALSE GAASI ENTROOPIA FÜÜSIKALINE OLEMUS

T. Tenno, A. Mashirin

Resümee

Ideaalse gaasi entroopia määratlus sisaldab eneses nii gaasi molekulide korrapäratu kui korrastatud liikumise vorme. Ideaalse gaasi temperatuuri saab defineerida kahel viisil–kui gaasi molekulide korrapäratu liikumise energia mõõtu nende liikumise ühe vabadusastme järgi ja kui molekulide korrastatud liikumishulga kiiruse muutuse mõõtu nende põrkumisel faasidevahelise piirpinnaga. Temperatuuri suhteline muutus üldtuntud entroopia määratluses on gaasi molekulide kaootilise soojusliikumise energia suhtelise muutuse lühendatud vorm. Gaasi ruumala suhteline muutus entroopia avaldises iseloomustab gaasi molekulide korrastatud liikumishulga muutuse kiiruse suhtelist muutust.

Ideaalse gaasi entroopia on funktsioon gaasi molekulide korrapäratu kaootilise liikumisvormi energia ja molekulide pinnaga põrkumisel kaasneva korrastatud liikumishulga muutuse suhtest.

ELECTROCHEMICAL STUDIES OF HYDROGEN PEROXIDE AT THIN FILMS OF GOLD AND PLATINUM IN NEUTRAL AND ALKALINE AQUEOUS SOLUTIONS

K. Tammeveski, T. Tenno
Institute of Physical Chemistry, University of Tartu

Abstract: The electrochemical reduction and oxidation of hydrogen peroxide at thin films of platinum and gold have been studied. The pH dependences of the mixed potential and the half-wave potential of the reduction and oxidation of hydrogen peroxide were linear for the thin film of Pt, with the slope values of –60, –68 and –51 mV/pH, respectively. A linear calibration graph was obtained for the electro-oxidation of H_2O_2 at the thin film of platinum in the peroxide concentration range from 10^{-5} to $5 \cdot 10^{-3}$ M in phosphate buffer at pH 7. Thin film of gold shows a remarkable activity towards H_2O_2 oxidation in the pH range of 12–14, but the reduction of hydrogen peroxide is kinetically controlled in a wide range of potentials. At pH<10 both processes proceed at a high overpotential at the gold film.

INTRODUCTION

The investigation of the electrochemical reactions of hydrogen peroxide has received much attention because of the importance of H_2O_2 in various electrochemical and biological systems [1-7]. Hydrogen peroxide is formed as a relatively stable intermediate of the oxygen reduction reaction. H_2O_2 can undergo either further electroreduction or catalytic decomposition. In neutral and slightly alkaline solution these reactions are

$$H_2O_2 + 2e^- \rightarrow 2OH^- \quad (1)$$

$$2H_2O_2 \rightarrow O_2 + 2H_2O \quad (2)$$

Pt electrode has been known to show a high catalytic activity towards hydrogen peroxide oxidation and reduction in a wide pH range [1, 2, 5, 6]. The kinetics of these processes is strongly influenced by the electrode surface conditions. At a gold electrode the $2e^-$ reduction of oxygen to

hydrogen peroxide is the main pathway in various media [7–9]. Therefore, the further behaviour of hydrogen peroxide is crucial in determining the overall process of oxygen reduction on gold.

The purpose of this work is to study the electrochemical reactions of hydrogen peroxide at the thin film of gold and platinum in neutral and alkaline aqueous solutions.

EXPERIMENTAL

Electrochemical measurements were carried out on voltammetric system SVA-1, employing the rotating disc electrode technique. Cyclic voltammetry was used to characterize the surface state and to determine the roughness factor. The glassy carbon (GC) electrodes SU-2000 (0.41 cm in diam.) were cut from rods and embedded into a teflon holder. The electrode was polished to a mirror finish with 1.0 and 0.3 μm alumina (BDH), followed by ultrasonication in bidistilled water. The details of film fabrication were described in the previous report [10].

The 0.066 M phosphate buffer solutions were prepared from reagent grade KH_2PO_4 and Na_2HPO_4. In some experiments 0.1 M NaCl was added as supporting electrolyte. The pH value of solutions was checked by laboratory pH-meter EV-74. 0.01-1.0 M solutions of KOH were prepared from p.a. quality KOH (Merck). All solutions were prepared with deionized 18 MΩ cm Milli-Q water (Millipore Inc.). 1 M stock solution of H_2O_2 was used to prepare the test solutions of desired concentrations. The concentration of stock solution was determined by titration with potassium permanganate. Measurements were conducted in the three-electrode three-compartment electrochemical cell. Pt-foil was used as a counter electrode. A saturated calomel electrode served as a referene electrode and all potentials are given with respect to SCE. The solutions were deaerated by bubbling with argon gas. All measurements were performed at room temperature, 23 ± 1 °C.

RESULTS AND DISCUSSION

A typical cyclic voltammogram for the thin platinum film on GC is shown in Fig.1. The roughness factor f_r was calculated from the amount of charge associated with hydrogen desorption, assuming that 1 cm^2 of polycrystalline Pt can adsorb hydrogen equivalent to 210 μC [11]. An average value of f_r was found to be 5.5 ± 0.5.

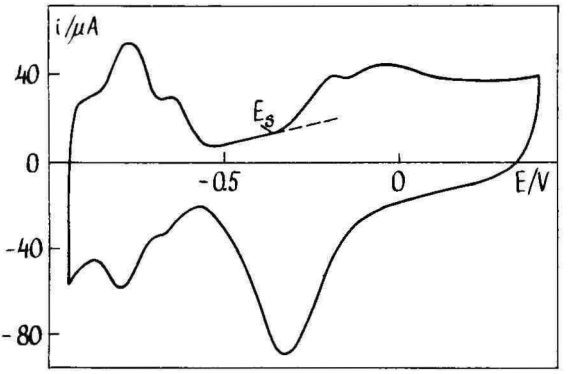

Figure 1. Cyclic voltammogram of thin Pt film in Ar-saturated 0.1 M KOH solution at sweep rate of 100 mVs^{-1}.

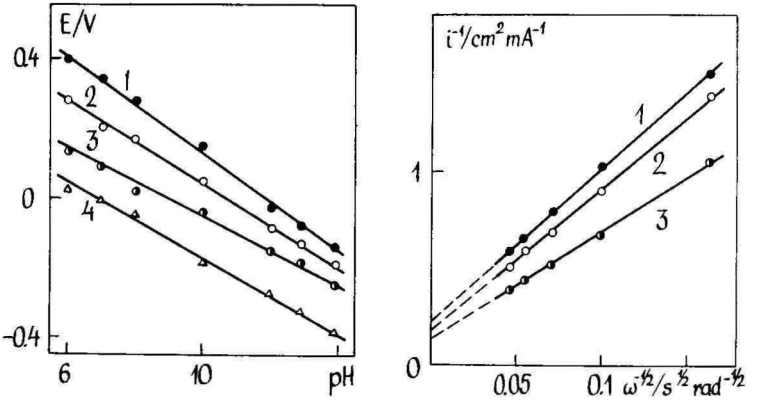

Figure 2. The pH dependences of mixed potential (2), onset potential of Pt oxidation (4) and $E_{1/2}$ for H_2O_2 oxidation (1) and reduction(3) at thin Pt film.
Figure 3. Koutecky-Levich plots for H_2O_2 oxidation in 1.0 M KOH (1); 0.1 M KOH (2) and 0.066 M phosphate buffer, pH 7 (3) at thin Pt film.

Approximate values of the onset potential of Pt oxidation (E_s) were determined from the intersects of extrapolated curves in the double layer and oxide region. The E_s values at different pH's are presented in Fig.2. The plot of E_s vs. pH is a straight line with the slope of −55 mV/pH which is assigned to reaction

$$Pt + OH^- \rightarrow PtOH + e^- \quad (3)$$

Experimental data of hydrogen peroxide reduction and oxidation at thin film Pt indicate that these processes are strongly affected by solution pH and electrode pretreatment. The voltammetry curves of H_2O_2 oxidation were obtained by anodic scan commencing from the potential of zero current. The currents of reverse scan were somewhat smaller. Hysteresis is decreasing at higher pH. If the electrode does not reach the cathodic region, one can assume that the electrode surface is in an oxidized state. This is also evident from Fig. 2, where the mixed potential E_m is about 150 mV more positive than the onset potential of Pt surface oxidation. It should be mentioned that due to the irreversible nature of surface reduction, even more positive potential than E is required for the complete reduction of surface oxides. Well-defined diffusion-limiting current plateaus for the oxidation of H_2O_2 are formed in the pH range of 6-14. The Koutecky-Levich method of analysis was used to differentiate between kinetic (i_k) and diffusion (i_d) currents

$$1/i = 1/i_k + 1/i_d \quad (4)$$

Even at high anodic potentials there still remains some kinetic component of the current as can be seen from K-L plots in Fig.3. The curves extrapolated to $\omega^{-1/2} = 0$ do not cross the origin. The experimental values of Levich slope B obtained from the plot of $1/i$ vs. $\omega^{-1/2}$ are in good agreement with the theoretical ones calculated by the equation

$$i_d = B\omega^{1/2} = 0.62nFD^{2/3}\nu^{-1/6}c\omega^{1/2} \quad (5)$$

where D is the diffusion coefficient, ν is the kinematic viscosity, c is the concentration and ω the rotation speed. The following values were used for the H_2O_2 diffusion coefficient: $0.86 \cdot 10^{-5}$ cm^2/s in 1.0 M KOH [12]; $1.2 \cdot 10^{-5}$ cm^2/s in 0.1 M KOH [13] and $1.6 \cdot 10^{-5}$ cm^2/s at neutral pH [6].

The electrochemical reduction of H_2O_2 at Pt is also dependent on surface conditioning. Starting cathodic scan from the zero current potential, the reduction currents of H_2O_2 were lower than when the initial potential was held 400-600 mV more anodic than E_m. In the latter case, electrode activity was higher and more reproducible data were obtained. In the return sweep, high hysteresis was observed and the zero current is achieved at more positive potentials (see Fig. 4).

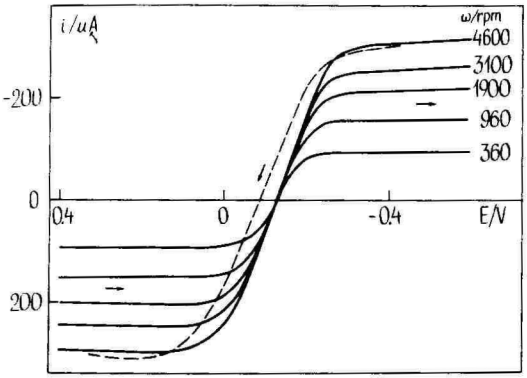

Figure 4. Polarization curves for hydrogen peroxide at thin Pt film in Ar-saturated 0.1 M KOH containing 1 mM HO_2^- at $v = 10$ mVs^{-1}.

The general tendency is that at higher pH both the anodic oxidation and cathodic reduction of H_2O_2 proceed at lower overpotentials. This is evident from the plots of $E_{1/2}$ vs. pH for both processes given in Fig.2. The slopes of $dE_{1/2}/dpH$ are –68 mV/pH and –51 mV/pH for anodic and cathodic process, respectively. The plot of E_m vs. pH is also given in Fig. 2, with the slope $dE_m/dpH = -60$ mV/pH. The plots of $1/i$ vs. $1/\omega^{1/2}$ have non-zero intercepts by extrapolating to $\omega^{-1/2} = 0$ in the whole region of cathodic potentials. Unfortunately, the kinetic currents obtained from the intercepts are not reproducible enough in order to construct Tafel plots. The plot of $\lg i/(i_d - i)$ vs. E was used to obtain Tafel slope values. The rate constants k_s were obtained by extrapolation the Tafel lines to the reversible potential of O_2/H_2O_2 and H_2O_2/H_2O couple. However, the method used is formal for the given process: the back reaction and the catalytic decomposition of H_2O_2 are not taken into account. The values of kinetic parameters are listed in Table 1. k_s is calculated per true surface area.

Table 1. Kinetic parameters for hydrogen peroxide reduction and oxidation at thin platinum film.

pH	Tafel slope (mV/dec) (oxidation)	k_s^a (cm/s)	Tafel slope (mV/dec) (reduction)	k_s^c (cm/s)
7.0	157	$9.1 \cdot 10^{-5}$	–146	$1.6 \cdot 10^{-10}$
10.0	128	$6.8 \cdot 10^{-5}$	–125	$9.2 \cdot 10^{-11}$
13.0	104	$5.4 \cdot 10^{-5}$	–98	$4.3 \cdot 10^{-13}$

The presence of chloride ions in the solution influences the shape of voltammograms. In the anodic region no remarkable change of voltammogram was observed. On the contrary, the cathodic reaction was strongly affected by chloride ions. As a result, the half-wave potential shifted in the negative direction and the current plateau was ill-defined. The influence of Cl^- on the activity of Pt towards H_2O_2 reduction was more essential in neutral than in alkaline solutions.

The detection of hydrogen peroxide by anodic oxidation is utilized in oxidase-based biosensors. H_2O_2 is formed by enzyme catalysis

$$substrate + O_2 \xrightarrow{oxidase} product + H_2O_2 \qquad (6)$$

The production rate of H_2O_2 which is a linear function of substrate concentration is measured amperometrically by applying a sufficiently high anodic potential [1].

$$H_2O_2 \rightarrow O_2 + 2H^+ + 2e^- \qquad (7)$$

Pt was found to be a suitable material for the working electrode of the given type of biosensors. For the purpose of miniaturizing the sensor's dimensions and to produce a single use sensor, it is possible to use thin metal film electrodes in the biosensor design. In order to study the applicability of thin film Pt on GC, measurements were provided at constant pH at various H_2O_2 concentrations over the range 10^{-5} – $2 \cdot 10^{-2}$ M. As was stated above, there is only a slight influence of chloride anions on the anodic oxidation of H_2O_2. Therefore buffer solutions containing Cl^- were used. The latter is also an electrolyte in practical devices. Measurements were provided by poising the electrode at a constant potential of +0.6 V. The electrode surface was allowed to stabilize in a H_2O_2-free solution at the same potential for half an hour. The current was then registered as a function of ω, changing the concentration of H_2O_2 successively. The currents of H_2O_2 oxidation show a decrease in comparison with the data obtained by potential cycling. As the surface of Pt is partially covered by oxygen-containing species, it can be assumed that the decrease in electrocatalytic activity is connected with the formation of more strongly bound oxide layers on the electrode surface during the time of stabilization. On the other hand, the stabilization of the surface is an advantage for analytical purposes which leads to a stable signal. The application of a constant potential is also neces-

sary to reduce the background current. At very low H_2O_2 concentrations, it is complicated to obtain the correct data for H_2O_2 oxidation by potential cycling, as the currents of the process of interest are lower than the currents of Pt surface oxidation. The values of i_k and B for H_2O_2 oxidation were obtained from K-L plots by extrapolating to infinite rotation rate.

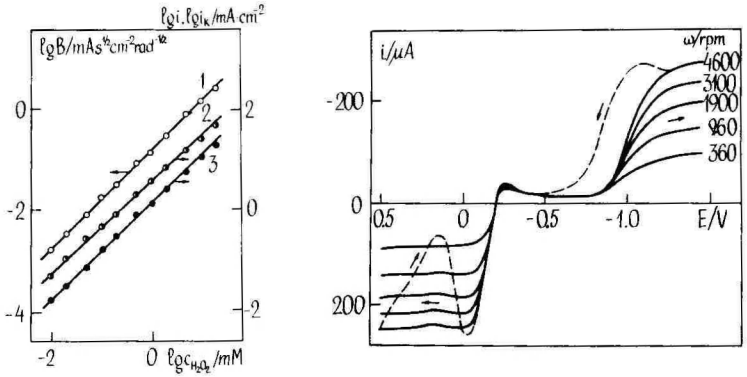

Figure 5. The dependences of 1 – lg$B$; 2 – lgi_k and 3 – lg$i$ (ω = 1900 rpm) on H_2O_2 concentration for H_2O_2 oxidation at thin Pt film in 0.066 M phosphate buffer, pH 7, containing 0.1 M NaCl. E = +0.6 V.

Figure 6. Polarization curves for hydrogen peroxide at thin Au film in Ar-saturated 1.0 M KOH containing 1 mM HO_2^- at v = 10 mVs^{-1}.

Fig. 5 presents the dependences of lg$B$, lg$i$ and lgi_k on H_2O_2 concentration. The slopes of these plots obtained by least square method are 0.98, 0.97 and 0.94 respectively. Deviation of the slope value from unity indicates that the rate constant of H_2O_2 oxidation depends slightly on concentration. Rate constant k was determined using the expression

$$i_k = nFkc \qquad (8)$$

The average rate constant at +0.6 V calculated per true surface area was found to be $k = 4 \cdot 10^{-3}$ cm/s. It should be noted that the thin film Pt electrode can be used as anode in H_2O_2-based biosensors.

Polarization curves for thin film Au on GC are completely different to that for thin film Pt on GC. Typical *i,E* - curves in alkaline solutions are shown in Fig. 6. A characteristic feature of H_2O_2 reduction at gold in the solution of high pH is a current peak, that appears at ca 100 mV more cathodic than the mixed potential. Such current maximum has been observed in many reports dealing with the problem of H_2O_2 reduction on bulk gold in alkaline media [8, 9]. However, the values of the current maximum obtained vary to a large extent in different papers. The shape of the reduction curve is strongly dependent on the face index of single crystal gold [13]. Therefore, the electrocatalytic properties of polycrystalline gold depend on the relative contribution of different planes. Preferential orientation of surfaces caused by special electrode pretreatment was also found to be essential on gold [8]. At some particular electrode surfaces of thin film gold electrodes, rather high peak currents were obtained, showing the dependence on rotation speed. The K-L plots were linear and parallel to those found at high cathodic potentials. The current maximum is followed by a potential region $-0.8\ V < E < -0.4\ V$, where the current is nearly constant and independent on rotation speed. This is probably caused by the recycling of oxygen which is released by the heterogeneous decomposition of hydrogen peroxide. At $E < -0.8\ V$ the electrochemical reduction of H_2O_2 occurs. Considerable hysteresis was observed between positive and negative sweep directions, indicating that the reduced surface is more active towards hydrogen peroxide reduction. Similar current increase was also observed for O_2 reduction at the thin film of gold using the positive potential scan [10]. The change of surface properties is responsible for such behaviour.

Well-defined diffusion-limiting current plateaus were observed for H_2O_2 oxidation in a wide range of potentials at high pH using the anodic potential scan. K-L analysis shows that the curves extrapolated to infinite rotation rate do not cross the origin and some kinetic component still remains. The *i,E*-curves registered on return sweep exhibit a considerable current drop in the anodic region. At the potentials of minimum, the currents are only slightly dependent on ω. Going to lower anodic overpotentials the electrode activity is restored, and the currents gain their limiting values. This behaviour is rather different as compared to that of thin film Pt on GC. The depth of minimum is a function of the potential at which the scan was reversed. If a sufficiently low anodic potential was applied, no hysteresis was observed. Such

behaviour can be caused by the influence of surface oxides on electrocatalytic properties. At low overpotentials the surface oxides catalyze the process of HO_2^- oxidation, whereas at high overpotentials the formation of oxide leads to the inhibition of catalytic activity. Further studies are required to elucidate the effect of holding time at constant potential on electrocatalytic properties in the anodic region of potentials. Fig.7 presents the pH dependences of E_m and $E_{1/2}$ for H_2O_2 oxidation. In the pH range of 12-14 the slope values of dE_m/dpH and $dE_{1/2}$/dpH are –60 mV/pH and –85 mV/pH, respectively. It is interesting to note that the slopes of dE_m/dpH are equal for both thin film gold and platinum electrodes in the given range of pH.

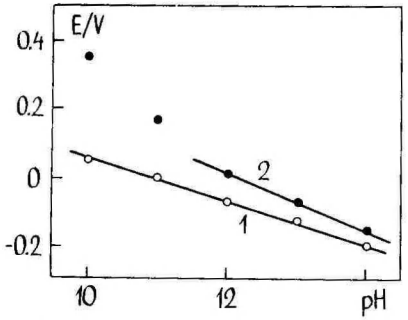

Figure 7. The pH dependences of mixed potential (1) and $E_{1/2}$ for H_2O_2 oxidation (2) at thin Au film.

At neutral pH the voltammetry curves of H_2O_2 reduction and oxidation at the thin film of gold were completely different to that in alkaline solution. It is interesting to note that the application of anodic potentials higher than +1.0 V led to the deterioration of the thin film gold electrode in chloride containing solution. At lower overpotentials the oxidation of H_2O_2 was negligible. It follows that gold is not a suitable material for the H_2O_2-based biosensor anode. However, gold has been used as a composite material in the Au/Pd codeposited catalyst for electrochemical detection of H_2O_2 [14, 15].

Some differences were also found for the reduction of H_2O_2. In the neutral pH range, the catalytic peak at the beginning of the cathodic wave was not present. At pH 6 the current was risen gradually, prior the potentials of cathodic hydrogen evolution. The formation of poorly defined current plateau was observed at pH 7–8. From the K-L plots, the value of B was found to be close to the theoretical one.

Acknowledgement: Dr. A. Rosental (Institute of Physics, Estonian Academy of Sciences, Tartu) is gratefully acknowledged for his help in preparing thin metal films.

REFERENCES

1. Y. Zhang, G. S. Wilson, J. Electroanal. Chem., **1993**, *345*, 253.
2. S. Sh. Leites, V. S. Bagotskii, V. I. Lukyanycheva, V. F. Konanykina, Elektrokhimiya,**1973**, *9*, 1166.
3. M. Honda, T. Kodera, H. Kita, Electrochim. Acta, **1983**, *28*, 727.
4. M. V. Vazquez, S. R. de Sanches, E. J. Calvo, D. J. Schiffrin, J. Electroanal. Chem., **1994**, *374*, 179.
5. M. R. Tarasevich, K.A. Radyushkina, Elektrokhimiya, **1970**, *6*, 376.
6. V. G. Prabhu, L. R. Zarapkar, R. G. Dhaneshvar, Electrochim. Acta. **1981**, *26*, 725.
7. R. Buvet, P. Sechaud, J. Darolles, L. Leport, F. Sechaud, Bioelectrochem. Bioergetics, **1987**, *18*, 13.
8. C. Paliteiro, Electrochim. Acta, **1994**, *39*, 1633.
9. R. W. Zurilla, R. K. Sen, E. Yeager, J. Electrochem. Soc., **1978**, *125*, 1103.
10. K. Tammeveski, T. Tenno, Acta et Comment. Univ. Tartuensis. **1993,** *966*, 92.
11. S. Trasatti, O. A. Petrii, J. Electroanal. Chem., **1992**, *327*, 353.
12. F. van den Brink, W. Visscher, E. Barendrecht, J. Electroanal. Chem. **1984**, *172*, 301.
13. R. R. Adzic, N. M. Markovic, V. B. Vesovic, J. Electroanal. Chem., **1984**, *165*, 105, 121.
14. L. Gorton, T. Svensson, J. Molec. Catal., **1986**, *38*, 49.
15. L. Gorton, Anal. Chim. Acta, **1985**, *198*, 247.

VESINIKPEROKSIIDI ELEKTROKEEMILISTE REAKTSIOONIDE UURIMINE KULLA JA PLAATINA ÕHUKESTEL KIHTIDEL NEUTRAALSES JA LEELISELISES LAHUSES

K. Tammeveski, T. Tenno

Resümee

Töös uuriti vesinikperoksiidi elektrokeemilist oksüdeerumist ja redutseerumist kulla ja plaatina õhukestel kihtidel pH väärtustel 6–14. Metallilised katted valmistati aurustamisel vaakumis, kusjuures alusmaterjalina kasutati klaassüsinikku. Mõõtmised viidi läbi pöörleva ketaselektroodi meetodil.

Vesinikperoksiidi oksüdeerumise ja redutseerumise poollainepotentsiaalid ning statsionaarne potentsiaal õhukesel Pt-kihil sõltuvad lineaarselt pH-st, millele vastavad graafiku tõusud −68; −51 ja −60 mV/pH. Määrati reaktsioonide kineetilised parameetrid. Õhukesekihiline kuld on aktiivne katalüsaator vesinikperoksiidi oksüdeerumisel pH vahemikus 12–14, kuid vesinikperoksiidi redutseerumine on kineetiliselt kontrollitud laias potentsiaalide vahemikus. Mõlemad reaktsioonid toimuvad õhukesel Au-kihil kõrge ülepingega, kui pH < 10.

POLAROGRAPHY AND STRIPPING VOLTAMMETRY OF SOME METAL - POLYCARBOXYLATE COMPLEXES

Ü. Piibar, H. Keis
Institute of Physical Chemistry, University of Tartu

Abstract: Complex formation of Zn(II) and Cu(II) with polymethacrylic acid (PMA) and polyacrylic acid (PAA) is studied by differential pulse anodic stripping voltammetry (DPASV) and direct current polarography (DCP). The effects of solution composition, supporting electrolyte concentration and pH of solution on the complexation measurements are examined. From experimental results lg K values for Me/polycarboxylate systems in different conditions are calculated.

INTRODUCTION

Voltammetric techniques have become an important tool in environmental speciation studies. In principle, they are suitable for the determination of the distribution of metal ions among the "free" and "complexed" forms [1]. The application of such techniques to the study of metal-polyelectrolyte systems is particularly interesting, since large numbers of natural ligands are of a polyelectrolytic nature [2].

Several classes of natural macromolecular ligands (humic and fulvic acid) contain a variety of metal binding groups and, as a consequence, their complexes with metal ions exhibit not only polyelectrolyte but also polyfunctional effects. That leads to additional difficulties in the interpretation on experimental results. Homofunctional polycarboxylic acids, such as polyacrylic acid (PAA) or polymethacrylic acids (PMA) are widely used as model ligands in methodological studies concerning macromolecular ligands [3].

The simplest complexation scheme in which an electroactive metal ion (denoted as M) associates with a ligand (L) to form an electroinactive complex (ML) can be presented as:

$$ML \underset{k_a}{\overset{k_d}{\rightleftarrows}} L + M \xrightarrow{ne} M^o$$

In this complexation scheme, M^0 denotes the metal atom and k_a and k_d are the association and dissociation rate constants, respectively.

The complexation equilibrium is expressed by the stability K:

$$K = \frac{c^*_{ML}}{c^*_M \cdot c^*_L} \tag{1}$$

where c_M^*, c_L^* and c_{ML}^* denote the bulk concentrations of M, L and ML, respectively.

The stability can only be obtained from the complexation curve under certain conditions [4]. First, the system must be voltammetrically labile and secondly, there must be a large excess of the complexing agent over the metal. In the presence of a large excess of a ligand, the association can be described as quasi-monomolekular with rate constant

$$k'_a = k_a \cdot c_L \tag{2}$$

and stability constant K'

$$K' = \frac{k_a}{k_d} = \frac{c^*_{ML}}{c^*_M} \tag{3}$$

The lability criterion depends on the used voltammetric technique. For the steady-state situation which corresponds to the anodic stripping analysis must be fullfilled [7]

$$\frac{k_d^{1/2}\delta}{D_M^{1/2}K'^{1/2}} >> 1 \tag{4}$$

In case of the rotating disk electrode (RDE) and under conditions $(D_{ML}/D_M)\,K' > 1$,

$$\delta = 1.61\, D_{ML}^{1/3}\, w^{-1/2}\, \nu^{1/6} \tag{5}$$

where w is the rotation frequency of the electrode and ν the kinematic viscosity of the solution. That is why RDE is preferable to mercury drop electrodes (MDE), due to the known hydrodynamic conditions. On the other hand, using MDE is better reproducibility of experimental results. Pre-electrolysis current (I_e) for a labile metal complex system can be written as

$$I_e - \overline{D}^p c_T^* \tag{6}$$

with $$\overline{D} = \frac{c_M^*}{c_T^*} D_M + \frac{c_{ML}^*}{c_T^*} D_{ML} \tag{7}$$

and $c_T^* = c_M^* + c_{ML}^*$.

Parameter p is related to the nature of mass transport during the preelectrolysis step and may be expected to lie between 1/2 (semi-infinite linear diffusion) and 2/3 (laminar convective diffusion, rotating disk electrode).

For the case of a labile system, the normalized limiting current ϕ is defined as

$$\phi = \frac{I(\ with\ ligand)}{I(without \cdot ligand)} \tag{8}$$

Combination of Eqns. 1, 6, 7 and 8 gives :

$$\phi = \frac{\left(\overline{D}\right)^p}{\left(D_M\right)^p} = \frac{\left(1 + aKc_L\right)^p}{\left(1 + Kc_L\right)^p}$$

where $a = D_{ML}/D_M$ and $a = 0.019$ for PAA systems and $a = 0.023$ for PMA systems.

EXPERIMENTAL

Voltammetric measurements were carried out with the Tacussell Polaropulse PR G5 analyser. Measurements were performed under potentiostatic control with a three-electrode system, consisting of a platinum plate as a counter electrode and a reference saturated calomel electrode. A glassy carbon CY-2000 rotating disc (for Zn system) or dropping mercury electrode (for Cu system) was used as a working electrode. A mercury film was previously plated onto the glassy carbon electrode from the solution of $1 \cdot 10^{-4}$ M Hg^{2+}.

The amount of the studied trace metal was determined by DPASV (Zn system) or direct current polarography (Cu system). For DPASV measurements, pulse heights of 25 mV and deposition potential of −1.5 V were employed. The scan rate in the stripping step was 10 mV/s.

All the solutions were prepared from three-distilled water, the reagents used were Merck Suprapur. Nitrogen was used for the deaeration of sample solutions, nitrogen flowed over the solution surface during the voltammetric measurements.

The total number of the carboxylic group of PMA and PAA was determined by conductometric and potentiometric titration.

Metal ion solution, with fixed pH, was placed in the voltammetric cell and voltammogramms were recorded in order obtain the current value without a ligand (I_o). Aliquots of solutions of the ligand were added to the cell and the voltammograms were recorded to obtain the current value in the presence of the ligand (I). Experiments were continued until a very large excesses of the ligand over the metal ion.

RESULTS

The voltammetric behaviour of Zn^{2+} and Cu^{2+} ions from PMA and PAA solutions was studied by DPASV and DCP. The DCP titration of $1 \cdot 10^{-4}$ M Cu^{2+} and $1 \cdot 10^{-4}$ M Zn^{2+} solutions with partially neutralized PMA and PAA yields to the plots of ϕ versus polyacid concentration (Figure 1). Complexes formed between Zn and PMA or Cu and PAA, are not electroactive in the potential range of the Zn_{ionic} or Cu_{ionic} peak. Therefore, after ligand addition, the concentration of Me_{ionic} will decrease and the decrease of the Me_{ionic} current will occur. In contrast to inert complexes, the current will not disappear altogether, a part of the current will always persist in the case of a labile complex. The previous observation [5, 6] confirm the essentially labile nature of both Zn^{2+} and Cu^{2+} complexes i.e. that the complex dissociation is sufficiently rapid for the equilibrium between Me^{2+} and ML to be maintained at all distances from the electrode, in spite of the consumption of Me^{2+}. The lg K values, calculated for figure 1 give a formation constant for the Cu-PMA complex of lg $K = 4.9$ and for the Zn-PAA complex of lg $K = 3.4$ at pH = 6.5 and 6.8, respectively.

Calculations were provided using power of D, indicated by the p value in eqn. (9) of 1/2 in direct current and differential pulse polarography measurements on the dropping mercury electrode of 2/3 for DPASV on the rotating electrode.

Figure 2 typifies the curve shapes obtained by DCP during titration of the solution with Zn^{2+} in the presence (curve 2) and without (curve 1) PAA. It is characteristic for the labile system that in the presence of

ligand, the calibration curves consist of two linear segments and it is the change in slope that reflects ligand saturation.

We investigated the influence of 3 factors that affect the results over complexation measurements – the supporting electrolyte, concentration of the supporting electrolyte and pH of the solution.

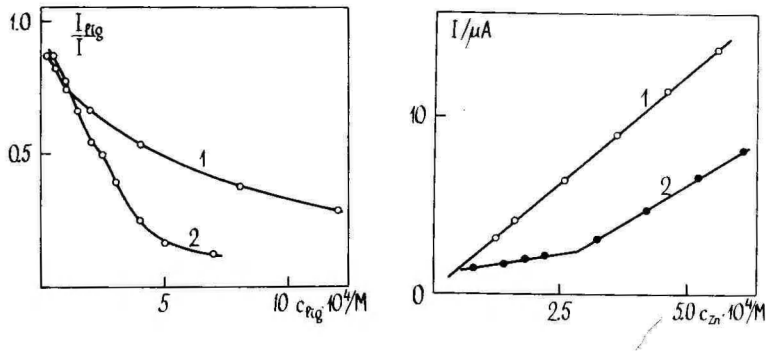

Figure 1. Normalized limiting current (I_{lig}/I) as a function of the concentration of carboxylate groups (C_{lig}) obtained for the Zn-PAA (1) and Cu-PMA (2) systems. 1 – pH = 6.8, MFE; 2 – pH = 6.5, DME.

Figure 2. Plots of reduction current of Zn^{2+} versus of Zn^{2+}concentration in the presence (2) and without (1) PAA.

Influence of the supporting electrolyte

Figure 3 shows the plots of normalized peak currents, obtained by DPASV titration at $4 \cdot 10^{-7}$ M Zn^{2+} with partially neutralized PMA solutions in different media. The influence of PMA on the peak height is much stronger in KNO_3 media than in CH_3COONa media. Calculated lg *K* values (Zn - PMA) for CH_3COONa and KNO_3 media appeared to be 2.3±0.1 and 4.1±0.2, respectively. The difference between lg *K* (1.8± 0.2) is in agreement with lg K value for Zn-Et complex(1.57). This agreement will disappear, when pH of the solution increases because of the dependence of the formation constant Zn-PMA on pH.

The formation of Zn-Et complex does not affect the peak height because of condition $D_{Zn} \cong D_{ZnEt}$, but CH_3COO^- may compete with polyions and it decreases the weight of Zn_{ionic} that could be bound by PAA. It seems to be undesirable to carry out complexation measure-

ments in buffered media. On the other hand, the buffered solution is much more suitable for such kind of experiments because of strong dependence of the peak height on pH of the solution.

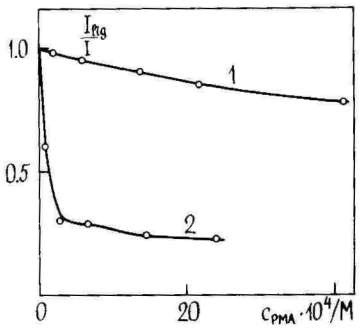

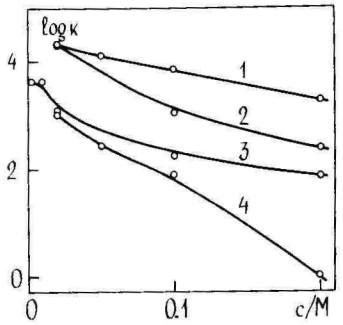

Figure 3. DPASV peak currents as a function of the concentration of PMA obtained in 0.02 M CH_3COONa (1) and 0.02 M KNO_3 (2). pH = 6.2, 4.10^{-7} M Zn^{2+}.

Figure 4. lg K values as a function of supporting electrolyte concentration. pH = 6.2, MFE, 1 – Zn-PAA, NH_4NO_3, 2 – Zn-PMA, KNO_3, 3 – Zn-PMA, CH_3COONa, 4 – Zn-PAA, $Ca(NO_3)_2$.

Influence of the supporting electrolyte concentration

Typically the proportion of ions by complexation measurements can be represented as follows: $c_{supp.electrolyte} >> c_{ligand} >> c_{metal}$.

For the present approach, there must be a large excess of the complexing agent over the metal. To avoid conductive effects, a large excess of the supporting electrolyte should be added to the system.

Figure 4 shows lg K versus the supporting electrolyte concentration plots obtained for Zn-polycarboxylate system in different media. As it appears on the graphs, lg K values decrease when the supporting electrolyte concentrations increase. Due to the electrostatic interaction of monovalent counterions (K^+) with polyions, they may compete with divalent counterions (Zn^{2+}) and affect the values of lg K (Zn-PMA).

lg K values for the Zn - PAA system at different concentrations of $Ca(NO_3)_2$, KNO_3 and NH_4NO_3 were investigated. The results are presented in Table 1.

As the table shows, the influence of the supporting electrolyte is much stronger using bivalent Ca^{2+} ions as counterions than in the case of monovalent K^+ or NH_4^+ ions. The ratio $c_{PAA(add.to\ the\ system)}/c_{PAA(binding\ Zn)}$ depend on the concentration of the Ca^{2+} ions. For example, in the solution of 0.1M $Ca(NO_3)_2$ the ratio = 88.1, in 0.05 M 44.9 and in 0.02 M 17.9.

Hence, the decreasing of the Ca^{2+} ion concentration twice, will also increase twice the polyion concentration binding Zn^{2+} ions.

Influence of pH *on the complexation reaction*

pH dependencies of Zn^{2+} and Cu^{2+} complexation with polycarboxylate ligands are shown in Figure 5. As it appears on the graphs, lg$K$ values increase when the pH of the solution increases. Increasing pH of the solution, the degree of the neutralization of the –COOH sites (f=[–COO^-]/[–COOH]+[–COO^-]) increases. The polymer electric charge and, therefore, the energy of electrostatic attraction for Zn^{2+} or Cu^{2+} increase with f. This results in an increase in both the fractions of Me^{2+} complexed and the equilibrium constant K = [–COOMe]/[Me^{2+}] [–COO^-].

The slope plot of lg K versus pH is stronger for the Cu-polycarboxylate system than for the Zn-polycarboxylate system.

Table 1. Formation constant of the Zn/PAA complex obtained at different levels of supporting electrolyte (pH = 6.2).

c (M)	$Ca(NO_3)_2$	KNO_3	NH_4NO_3
0.02	3.0	4.3	4.35
0.05	2.4	4.0	4.1
0.1	1.9	3.5	3.8

Table 2. Formation constant of the Zn-polycarboxylate complex obtained at different pH values by DPASV (0.1 M KNO_3).

pH	Zn/PMA	Zn/PAA
6.3	3.0	3.4
6.8	3.1	3.7
7.5	3.3	4.2

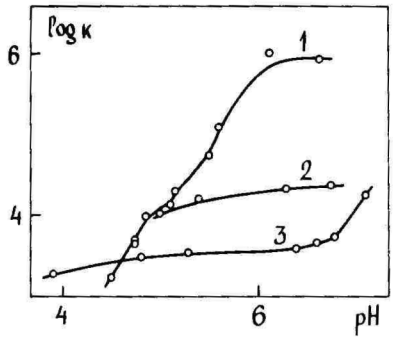

Figure 5. lg K values for Me^{2+}-polycarboxylate system as a function of pH of solution. 1 – Cu-PMA, 0.01 M KNO_3, 2 – Zn-PMA, 0.02 M KNO_3, 3 – Zn-PAA, 0.1 M KNO_3.

Table 2 compares lg *K* values evaluated for the Zn-PMA and Zn-PAA systems. These results indicate that PAA has a stronger binding ability for Me^{2+} than PMA. According to what was said previously, PAA is a stronger acid than PMA, the dissociation constant of PAA and PMA appeared to be $2 \cdot 10^{-5}$ M l^{-1} and $1.2 \cdot 10^{-5}$ M l^{-1}, respectively.

CONCLUSIONS

According to experimental results and also some previous studies [5, 6], the Cu(II)- and Zn(II)-polycarboxylate complexes appeared to be voltammetrically labile systems. The stability constant values for Zn-PMA, Zn-PAA and Cu- PAA systems were calculated using power of D, indicated by the *p* value in eqn. (9) of 1/2 in DCP and DPP and 2/3 in DPASV measurements. The influences of the supporting electrolyte and pH of the solution on the complexation measurements were investigated. The increases of pH of the solution increase the fractions of Me^{2+} complexed. In the complexation measurements it seems to be undesirable to carry out experiments in buffered media or use high levels of the supporting electrolyte.

Acknowledgments. The authors would like to thank the Estonian Science Foundation for the financial support to this work.

REFERENCES

1. J. M. Díaz-Cruz, C. Ariño, J. Electroanal. Chem., **1992**, *333*, 33.
2. J. Buffle, Complexation reactions in aquatic systems: an analytical approach, Horwood, Chichester, 1988.
3. M. Esteban, J. M. Díaz-Cruz, C. Ariño and E. Casassas, Biophysical Chemistry, **1992**, *45*, 109.
4. M. A. G. T. van den Hoop and H. P. van Leeuwen, Anal. Chim. Acta, **1993**, *273*, 275.
5. J. M. Díaz-Cruz, C. Ariño, M. Esteban, E. Casassas, Elektroanalysis, **1991**, *3*, 1.
6. J. M. Díaz-Cruz, C. Ariño, M. Esteban, E. Casassas, Electroanalysis, **1993**, *5*, 677.
7. H. P. van Leeuwen, Sci. Total Environ., **1987**, *60*, 45.
8. R. F. M. J. Cleven, H. G. De Jong, H. P. Van Leeuwen, J. Electroanal. Chem., **1987**, *202*, 57.

MÕNEDE METALL-POLÜKARBOKSÜLAATKOMPLEKSIDE POLAROGRAAFILINE JA VOLTAMPEROMEETRILINE UURIMINE

Ü. Piibar, H. Keis

Resümee

Antud töö eesmärgiks oli metalli ja polükarboksüülhappe vahelise kompleksimoodustumistasakaalu uurimine voltamperomeetrilisel meetodil.

Vaatluse all olid polüakrüül- ja polümetakrüülhape (PAA ja PMA), kuna neid võib vaadelda kui mitmete loodulikes vetes esinevate kompleksimoodustajate (humiin- ja fulvohapped) lihtsustatud mudeleid. Zn/PMA, Zn/PAA ja Cu/PMA süsteeme uuriti DPASV ja DCP meetodil, vastavad kompleksid leiti olevat labiilsed kompleksid ning arvutati püsivuskonstantide väärtused erinevatel tingimustel.

Uuriti foonilahuse koostise ja kontsentratsiooni ning lahuse pH mõju lg *K* väärtusele. Leiti, et foonilahuse valik mõjutab kompleksimoodustu-

misreaktsioonide uurimist nii anioonide kui katioonide kaudu. Foonilahuse katioonid (K^+) võivad konkureerida metalliioonidega polümeeri sidumises, mistõttu foonilahuse kontsentratsiooni suurendamisel lg *K* (Me^{2+}/PMA) väärtused näiliselt vähenevad. Puhverdatud keskkonda (näit. CH_3COONa) tuleb vaadelda kui kahe ligandiga (CH_3COO^-; PMA) keskkonda ja arvestada metalli sidumist kummagi ligandi poolt. Lahuse pH suurendamisel suureneb polümeeri neutralisatsiooniaste ja seega väheneb lahuses vaba metalli (Me^{2+}) osakaal, vastavalt suureneb lg *K* väärtus.

DETERMINATION OF HEAVY METALS IN SEA- AND FRESHWATERS BY ANODIC STRIPPING VOLTAMMETRY

H. Keis, Ü. Piibar

Institute of Physical Chemistry, University of Tartu

Abstract: Copper, lead, cadmium, zinc and mercury in the Baltic Sea waters and freshwaters of Estonia has been determined using hanging mercury drop, plated on the glassy carbon thin film and gold electrodes. Because of the presence of complexing agents, peak current-added metal concentration calibration curves in natural seawater for investigated copper, lead and cadmium are nonlinear and care must be taken in using spiked results in the calculation of the metal content. Using acidified to pH < 2 and UV irradiated samples, this problem disappears. The thin film electrode is more suitable than the hanging mercury electrode because of the best resolution of lead and cadmium peaks and less background current in the region of potentials of copper peak. At high concentration of copper (about mg/l), results of zinc determination are distorted, especially if the thin film electrode is used, and 10^{-6} mol/l Ga^{3+} must be added to the sample to overcome interferences.

INTRODUCTION

One of the most important problems in sea chemistry and water resources science is effect of the concentration on the water system. Toxic metals enter the marine food chain, ultimately reaching man. Therefore, accurate determination of trace metal levels in various water systems is becoming important. As a result of its high sensitivity, stripping analysis is one of the techniques, that is sufficiently sensitive to determine trace elements directly in natural waters in lots of cases without previous concentration, using, for example extraction or ion-exchange chromatography. It is important to minimize contamination possibilities and changes in the physicochemical nature of species prior to separation and preconcentration procedures that are associated with errors caused by the problems of contamination or losses.

Over the last 30 years, stripping analysis has been widely used in all fields of aquatic trace metal analysis. The technique has been used for measuring normal and pollution levels of more than 20 trace metals in different types of natural waters. Most of these are known as important toxic or micronutrient elements.

Very important is the chemical form in which a metal exist in water. It has been shown that trace elements exist in natural waters in different forms. They may be complexed with low-molecular inorganic and organic ligands, or with high-molecular organic ligands such as humic and fulvic acids and polysacharides, or they may be adsorbed on inorganic or organic colloids. Knowledge of the form of metals in samples is important for understanding their toxicity and transport. Usually, the samples are filtered through 450 nm filters to determine the "dissolved" trace metal fraction. Matter retained by the filter can be analysed after digestion to measure "colloidal" fraction. Another possibility is to provide analysis of non-filtered water and to calculate the content of metals bound to the particulate matter by the difference to the data of the filtered sample.

Because of the complicated composition of natural waters (metals, ligands, surfactants, ect.) and low levels of the measured metals, stripping analysis in natural waters presents several problems to the analyst. Two types of interferences, the adsorption of organic compounds and the formation of intermetallic compounds, are the main ones. A large number of organic compounds are able to adsorb onto the electrode. In addition to their effect on the stripping peaks due to their influence on the kinetics of the charge transfer process, they may cause adsorption-desorption peaks, especially if the pulse stripping mode is used [1]. This may present serious problems in the interpretation of the results in organic-rich waters. In seawater analysis the problem is more important for the analysis of near-shore waters. For destruction of the organic matter, UV-irradiation of the sample, acidified previously to prevent adsorption of the metal ions on the walls of the sample container, is usually used.

Intermetallic interferences cause the decreasing of the stripping peak of a more electronegative metal [2]. That is why care must be taken, to remain within the linear range of the response, i.e., to avoid the saturation of mercury because of low solubility of metal in mercury and the formation of intermetallic compounds (especially when the thin film electrode is used for measurements, for example, zinc in the presence of

nickel and copper). When the levels of the two interfering metals are on the sub-ppb level and the concentration of the more electropositive element is less, the standard addition method can correct intermetallic interferences [3].The best way to overcome this problem is by adding "the third metal" to the sample, for example, Ga^{3+} to exclude interferences in the system Cu-Zn or Ni-Zn. In practical water analysis, however, the last one is rarely a problem because of low Ni concentrations and exessive Zn presence.

Speciation information about free and complexed metal in labile or inert complexes from direct electrochemical analysis can be got after various preliminary treatments of the sample. For example, if the sample is irradiated at natural pH, only the metal associated with organic matter will be liberated, and the increase in labile metal concentration compared with the unirradiated sample represents the metal bound in inert organic complexes or in organic colloids [4, 5]. It was shown that for Cu, Pb and Cd the predominant form is labile organic colloids or complexes, measurable directly by A.S.V. at pH = 4.8 [6]. When the sample is acidified before irradiation, all forms of metal are converted into labile species and total metal can be measured.

EXPERIMENTAL

Collection and preservation of water samples

Seawater samples were collected during expeditions of research vessels Aranda and Livonia on the Baltic Sea. Because of different sampling systems on vessel Aranda teflon bottles were used for collection, and immediately after sampling, water was filtered through 450 nm filter in Marine Clean Room, storaged in initially acid cleaned polyethylene bottles and part of the filtered water was acidified with Suprapur HNO_3. After that 0.5 ml of Suprapur 30% H_2O_2 per liter was added to both acidified and natural pH water, and samples were irradiated with 800 W UV-lamp for 4 hours, storaged in polyethylene bottles and analysed.

Samples collected on board the Livonia were storaged in acid cleaned polyethylene bottles and retained at 4 °C. Analyses were provided of acidified and UV irradiated, non-acidified and UV irradiated water at natural pH, and water without any pretreatment. Freshwater samples were acidified and irradiated to determine "total" metal.

Apparatus and reagents

Voltammetric measurements were provided with a Metrohm 646 VA Processor/663 VA Stand and a Tacussell Polaropulse PRG5 analyser in the differential pulse mode. The hanging mercury drop electrode (HMDE) and thin film glassy carbon rotating disc electrode (RDE) were employed for the determination of Cu, Pb, Cd and Zn, gold RDE for the analysis of mercury. A platinum counter electrode and a saturated calomel electrode, connected with the cell using salt bridge were used in the electrode system. The sample in a 50 ml teflon or quarz cell was purged with argon, pH measurements in the cell were made using a solid contact glass electrode coupled to a UT-8806 pH-meter. Reagents were Suprapure grade and previously checked on the content of heavy metals.

The thin film electrode was prepared by adding $2 \cdot 10^{-5}$ M $Hg(NO_3)_2$ to the sample in the cell, and the first stripping scan was not registered. For measurements at natural pH, the pre-formed film electrode was used. After polishing a gold electrode was storaged in 6 M HNO_3, washed and activated in 0.1 M $HClO_4$ at 0.0 V. During the measurement, the potential was not scanned to a more positive value than +0.7 V, especially in seawater analysis.

RESULTS AND DISCUSSION

The method of pseudo-polarograms was used for the detection of deposition potential for measurement of copper, lead and cadmium. It was shown that $E_d = -1.0$ V was sufficient to obtain the maximum peak height in both acidified and irradiated samples (pH < 2) and after adjusting of pH with sodium acetate to value 4.7. If the deposition potential was more negative than −1.25 V, a smaller copper peak current was obtained on the TFE. This effect is similar to the one noted in [7] and can be explained with the deposition of zinc in this region of potentials and intermetallic interferences between copper and zinc. Peak current-metal concentration plots were linear with sensitivity for $1 \cdot 10^{-9}$ M Me^{2+} and deposition time of 10 min. (TFE): Cu^{2+} 1.6 μA, Pb^{2+} 5.0 μA and Cd^{2+} 4.5 μA. In the case of natural seawater, the calibration curves consist of two straight line parts (Fig. 1.) with the intersection point corresponding to copper concentrations of $2.5 \cdot 10^{-8}$ M, $3.5 \cdot 10^{-9}$ M Pb^{2+} and $2.6 \cdot 10^{-9}$ M Cd^{2+} . The slope of the second straight line part is near

the slope observed in acidified and irradiated samples. At pH = 4.7, depression of lead and cadmium peaks in irradiated water disappears, a nonlinear curve was again obtained fror copper, but the change in the slope was at $1.1 \cdot 10^{-9}$ M.

After the irradiation of the sample at natural pH value (pH = 7.7) the nonlinearity of calibration curves for copper and lead stayed, but after the addition of acetate buffer, the height of the lead corresponds to normal sensitivity. These seem to be the differences between copper and lead bounding in seawater. It seems part of the total ionic copper may be adsorbed on inorganic colloids and can be detected only after the acidifying of the sample [7], lead gets free from partially A.S.V. labile carbonato and hydroxy complexes [8] at pH = 4.7.

For the determination of zinc, the deposition potential of −1.5 V was used for the TFE and −1.4 V for the HMDE and analysis was provided at pH = 4.7 to minimize the background current. Some schemes of analysis were compared for the determination of all four metals from the same bulk of solution:

1. Cu, Pb and Cd were determined from the acidified sample, then pH was adjusted to 4.7 and Zn was determined.

2. pH of the sample was adjusted to 4.7 and analysis of all four metals was provided with deposition potential −1.0 V (10 min) and −1.5 V (2 min).

3. At pH = 4.7 Cu, Pb, Cd and after this Zn were determined.

4. At pH = 4.7 Zn was measured and then the other metals.

The problems with intermetallic Cu-Zn interferences were usually not serious on the HMDE in all cases, using short deposition time, though copper concentration arose 2–3 times with standard additions. On TFE, the fourth method appears to be the best and in samples with high copper concentration (mg/l level or more), the only possibility seems to be adding 10^{-6} mol/l of Ga^{3+} to the sample and to use the first or the third scheme. In general, TFE is more suitable than the HMDE because of the best resolution of lead and cadmium DPASV peaks and less background current in the region of copper peak potentials.

In Table 1, some results of seawater analyse are presented. Samples were filtered, acidified, irradiated and analysed on a Metrohm-analyser, using scheme 1. Cu, Pb and Cd were determined on the TFE, Zn on the HMDE.

Results of the determination of Cu, Pb, Cd, Zn and Hg in unfiltered but acidified and irradiated seawater samples are shown in Table 2. For

the analysis on the TFE, scheme 3 with Ga^{+3} addition for zinc measurement and scheme 4 were employed with a good agreement between them. Mercury from acidified and irradiated water was deposited onto the gold RDE at the deposition potential of +0.1 V and the stripping peak of Hg occurs between +0.45 and +0.50 V depending on salinity.

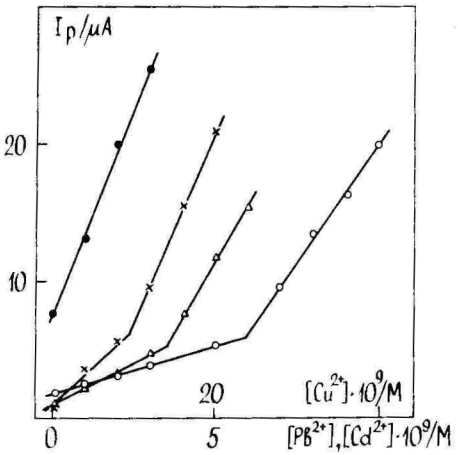

Figure 1. Stripping peak height - concentration plots for copper, lead and cadmium added to seawater (sampling point BY 28, 1 m). Natural pH = 7.7, previously deposited mercury film electrode, deposition potential −1.0V, deposition time 12 min for lead and cadmium, 6 min for copper. o – for Cu, Δ – Pb, + – Cd, • – Pb at pH = 4.7.

Freshwater samples were taken from several parts of East Estonia. For example, we will present some results of the analysis of the oil-shale region and the waters of the river Emajõgi before (Vorbuse) and after Tartu (Ihaste tee). Samples *A* and *B* in Table 3 are phreatic waters, pumped out of two different parts of the Ahtme Mine. The stream Jõuga and river Rannapungerja reach Lake Peipsi contaminated by oil - shale region waters. All samples were unfiltered, but acidified and irradiated. Analyse scheme is the same as for Table 2.

Table 1. Results of analysis of filtered Baltic Sea waters (ng/l).

Sampling point	Depht,m	Cu	Pb	Cd	Zn
Arkona 1	10	410	160	13	5900
Lithuanian Coast	10	1850	430	23	7320
	40	540	380	50	7900
Gdansk Bay	10	1300	94	21	2260
	90	1430	190	20	9900
Riga Bay - 1	10	1100	250	39	2000
West Gotland Deep	10	410	160	19	3400
	120	1070	160	21	5900
GF -4	10	760	50	20	3700
GF -3	10	1040	290	15	4000

Table 2. Results of analyse of unfiltered Baltic Sea waters (ng/l).

Sampling point	Depht,m	Hg	Cu	Pb	Cd	Zn
K -1	1	24	1200	260	55	8500
BY -15	1	16	800	360	35	3400
2	1	30	480	200	35	3600
8	1	35	1200	320	50	5900
LL - 7	1	40	1200	540	65	5800

Table 3. Results of analysis of freshwaters (ng/l). Dec. - December 1989; Apr. - April 1990.

Sampling point		Hg	Cu	Pb	Cd	Zn
A	Dec.		2000	800	100	2200
	Apr.		1700	300	100	1800
B	Dec.		700	600	50	300
	Apr.		570	600	45	390
Jõuga	Dec.		700	200	70	1100
	Apr		760	200	55	1300
Rannapungerja	Dec.		2000	1600	150	1700
	Apr.		1525	400	145	1300
Emajõgi	Vorbuse	40	100	370	30	
	Ihaste tee	40	300	720	150	

CONCLUSIONS

In the present paper, some results of heavy metal analyses in the Baltic Sea and freshwaters of Estonia are presented. It has been shown that the thin film glassy carbon electrode is more suitable than hanging mercury drop for the determination of copper, lead and cadmium because of the best resolution of lead and cadmium peaks and less background current in the region of copper peak potentials, but to be sure of the absence of copper-zinc interferences, Ga^{3+} must be added, especially at the mg/l level of copper. Some experiments are described to investigate speciation of copper, lead and cadmium in seawater. When nonacidified UV irradiated samples were analysed, calibration curves were nonlinear, but the curve for lead linearized at pH = 4.7, unlike the one for copper. It seems part of the copper may be adsorbed on inorganic colloids and can be detected only after the acidifying of the sample, lead gets free from partially A.S.V. labile carbonato and hydroxy complexes in the acetate buffer.

REFERENCES

1. G. E. Batley, T. M. Florence, J. Electroanal. Chem.,**1976**, *72*, 21. E. Jacobsen, H. Lindseth, Anal. Chim. Acta, **1976**, *86*, 123.
2. T. M. Florence, G. E. Batley, Anal. Chem., **1980**, *9*, 219.
3. A. Zirino, In "Marine Electrochemistry" , Eds. J. Wiley and Sons, New York, **1981**, 421.
4. T. M. Florence, G. E. Batley, Anal. Chem.,**1980**, *52*, 1962.
5. T. M. Florence, Anal. Chim. Acta, **1982**, *141*, 73.
6. G. E. Batley, T. M. Florence, Anal. Lett., **1976**, *9*, 379.
7. T. M. Florence, G. E. Batley, J. Electroanal. Chem., **1977**, *75*, 791.
8. P. Valenta, In Leppard G. G., (Ed.) "Trace element Speciation in Surface Waters", Plenum Press, New York, **1983**, 49.

RASKMETALLIDE MÄÄRAMISEST MERE- JA MAGEVETES INVERSIOONVOLTAMPEROMEETRILISEL MEETODIL

H. Keis, Ü. Piibar

Resümee

Töös on esitatud vase, plii, kaadmiumi, tsingi ja elavhõbeda kontsentratsiooni määramise tulemused Läänemeres ja mõnedes Ida-Eesti looduslikes vetes, kasutades anoodset inversioonvoltamperomeetriat statsionaarsel elavhõbetilkelektroodil, elavhõbedaga kaetud klaas-süsinikelektroodil ja kuldelektroodil. Kompleksimooodustajate tõttu analüütilise signaali suuruse sõltuvus lisatud vase, plii ja kaadmiumi kontsentratsioonist merevees lineaarne, vaid labiilsete kompleksi-moodustajate juuresolekule iseloomuliku murdekohaga. Seda tuleb arvestada tulemuste interpreteerimisel voolupiigi kõrguse alusel ka standardlisandite meetodi kasutamisel, rääkimata kalibratsioonigraafiku kasutamisest. Kui proov on hapustatud (pH < 2) ja orgaanilised ühendid lagundatud ultravioletkiirgusega, need probleemid kaovad. On väidetud, et õhukesekihiline elavhõbekileelektrood omab eeliseid statsionaarse elavhõbetilkelektroodi ees vase, plii ja kaadmiumi määramisel, kuna plii ja kaadmiumi lahutusvõime on parem ja foonivool vase piigile vastavas potentsiaalide vahemikus madalam. Kõrgete vasesisalduste korral tuleb aga tsingi määramisel kasutada Ga^{3+} lisamist, et vältida intermetalliidi Cu-Zn tekkest tulenevat viga. Elavhõbetilk-elektrood on sellise toime suhtes vähem tundlik.

MEASUREMENT OF OXYGEN CONSUMPTION

Taavo Tenno, Aleksei Mashirin, Toomas Tenno
Institute of Physical Chemistry, University of Tartu

Abstract: Equations of the transient process of the system containing constant gas volume, a gas permeable membrane and an oxygen consuming object have been described. The concept of the effective concentration of the gaseous component has been used. Transformation of the dynamic error of the oxygen sensor into the change of time is represented. The obtained equations can be used by mathematical processing of experimental data upon the determination of oxygen demand by the studied object and also by the determination of the parameters of the external diffusional layer of the object.

Possibility of the determination of oxygen flow through the diffusional membrane of the oxygen consuming object and oxygen concentration behind the membrane is observed. The device used for the measurement of oxygen concentration has the constant volume of gaseous mixture V with the fixed gaseous component. The gaseous mixture is in contact with external surface S of the gas permeable layer of the object (membrane, biological tissue).

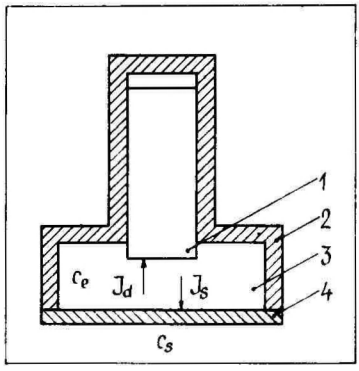

Figure 1. Schematic representation of device of oxygen consumption: 1 – oxygen sensor, 2 – frame, 3 – volume of gas V, 4 – gas permeable film of the object.

The effective oxygen concentration in volume V is the following [1,2]:

$$c_e = mRT/V \tag{1}$$

where m – number of moles of oxygen in volume V; R – universal gas constant; T – temperature.

In the exceptional case of the gas phase, the effective concentration of oxygen c_e is equal to partial pressure p. If the gaseous phase is on either side of the membrane, oxygen flow between volume V and the object is proportional to the difference in partial pressures:

$$J_s = k_s(p - p_s) \tag{2}$$

where k_s – coefficient of the diffusional conductivity of the membrane; p_s – partial pressure of oxygen on the external side of the membrane.

In general, on the other side of the membrane there might also be the liquid or solid phase, where partial pressure of the gaseous component does not have physical meaning. In this case the effective concentration of oxygen c_{es} can be expressed:

$$c_{es} = k_h c_s \tag{3}$$

where k_h – coefficient describing the state of oxygen in liquid or solid phase, compared with the standard gaseous phase; c_s - analytical concentration of oxygen on the external side of the membrane.

In the observed system, oxygen flow J_s is proportional to the difference of effective concentrations:

$$J_s = k_s(c_e - c_{es}) \tag{4}$$

In the studied device (Fig. 1) oxygen is consumed also by the amperometric sensor. Oxygen flow consumed by the sensor is proportional to effective concentration c_e:

$$J_d = k_d c_e \tag{5}$$

where k_d – coefficient of the diffusional conductivity of the sensor membrane. The total oxygen flow J in volume V is the following:

$$J = k_s(c_e - c_{es}) + k_d c_e \tag{6}$$

Velocity of the change of the amount of oxygen, amount m in volume V is determined by the total flow J:

$$\frac{dm}{dt} = -J \tag{7}$$

Taking into account equations (1) and (6), equation (7) may be rewritten:

$$\frac{dm}{dt} = -\frac{RT}{V}(k_s + k_d)\cdot\left(m - \frac{k_s c_{es}}{k_s + k_d}\cdot\frac{V}{RT}\right) \tag{8}$$

By the integration of this equation in the paths from $[t_o, m_o]$ to $[t, m]$, we can write:

$$ln\left(\frac{m - m_\infty}{m_o - m_\infty}\right) = -\frac{t - t_o}{\tau_s} \tag{9}$$

where $m_\infty = (k_s \cdot c_{es})/(k_s + k_d)\cdot V/RT$ is the value of m at $t \to \infty$ and $\tau_s = 1(k_d + k_s)\, V/RT$ is the time constant by oxygen permeation through the membrane. The time function $m(t)$ is :

$$m = (m_o - m_\infty)\cdot\exp\left(-\frac{t - t_o}{\tau_s}\right) + m_\infty \tag{10}$$

As volume V is known, the oxygen concentration is proportional to the quantity of gas m according to equation (1). Hereby the dependence of c_e upon the time is analogous to equation (10):

$$c_e = (c_{eo} - c_{e\infty})\cdot\exp\left(-\frac{t - t_o}{\tau_s}\right) + c_{e\infty} \tag{11}$$

where c_{eo} and $c_{e\infty}$ are the values of c_e at time moments t_o and t_∞.

The change of the oxygen concentration by time in volume V is measured by the oxygen sensor. If the inertia of the sensor is small, the output signal of the sensor is proportional to the effective concentration of oxygen c_e:

$$I = nFk_d c_e \tag{12}$$

where n – number of electrons, F – Faraday constant.

The dependence of output signal I on time t, analogically to equation (10), may be written as:

$$I = (I_o - I_\infty) \cdot \exp\left(-\frac{t - t_o}{\tau_s} \right) + I_\infty \qquad (13)$$

where I_o and I_α are the values of currents I at t_o and t_∞. Thus the output current dependence on the time is describing the change of the amount of oxygen in the volume on the time and oxygen flow J_s between volume V and the studied object. The function describing transient process $h(t)$ in volume V is the following:

$$h(t) = \left[1 - h(t)_\infty\right] \cdot \exp(-\frac{t - t_o}{\tau_s}) + h(t)_\infty \qquad (14)$$

where $h(t) = I / I_o$ – unit step function and $h(t)_\infty = I_\infty / I_o$ – value $h(t)$ at $t \to \infty$. The inertia of the oxygen sensor of the studied device causes dynamic error Δh of unit step function $h(t)$. The influence of inertia of the sensor at the exponential change of the oxygen quantity in volume V can be expressed as [3]:

$$h(t)^* = \left[1 - h(t)_\infty\right] \cdot \left[\exp(-\frac{t - t_o}{\tau_s}) + \Delta h \right] + h(t)_\infty \qquad (15)$$

where $h(t)^* = I / I_o$ is the unit step function of the output current of the sensor, taking into account its inertia;

$$\Delta h = -2 \sum_{n=1}^{\infty} (-1)^n \frac{\tau_d}{n^2 \tau_s - \tau_d} \left[\exp(\frac{t - t_o}{\tau_s}) - \exp(-n^2 \frac{t - t_o}{\tau_d}) \right]$$

$\tau_d = l_d^2 / \pi^2 D$ is time constant for the sensor; l_d is thickness of diffusional layer of sensor and D is diffusion coefficient.

The description of the dynamic error in the form of amplitude change Δh is very complicated [3]. Unit step function $h(t)$ will be simplified by transforming Δh through derivative dh/dt to the equivalent change of time Δt:

$$h(t)^* \cong \left[1 - h(t)_\infty\right] \cdot \exp(-\frac{t - t_o - \Delta t}{\tau_s}) + h(t)_\infty \qquad (16)$$

where $\Delta t \cong \tau_d \pi^2 / 6$ at $t >> \tau_d$ and $\tau_d << \tau_s$. This transformation replies to time lay Δt of the output signal of sensor Δt with regard to the measured parameter in volume V. Such a description of the dynamic error by time lay Δt, proximity to the constant value at given conditions has some advantages in practice. For instance, by treatment of the experimental data and by the determination of total inertia of the device including many sequence inertial elements and also by the determination of the standards for inertia of the oxygen sensor. Given a description of the transient process presents the main dependence between parameters of the gaseous component (oxygen) in volume V of the measuring device and parameters of the consumption of the gaseous component by the examined object.

These relationships can be used for the experimental measuring of the flow of consumption of gas J_s by the object, the coefficient of diffusional conductivity k_s of the membrane, as well as the effective concentration of the gaseous component c_{es} in the object.

Parameters τ_s and $h(t)_\infty$ can be calculated from equation (15) using the measured experimental values of function $h(t)^*$. Obtained values allow to estimate parameters of the studied object k_s, c_{es}, and J_s:

$$k_s = \frac{V}{\tau_s RT} - k_d \tag{17}$$

$$c_{es} = \left[\frac{k_d}{k_s} + 1 \right] \cdot h(t)_\infty \cdot c_{eo} \tag{18}$$

$$J_s = k_s (c_{eo} - c_{es}) \tag{19}$$

If membrane area S and its thickness l_s are known, permeability of the membrane can be determined:

$$P_s = \frac{l_s}{S} \cdot k_s \tag{20}$$

The above given method was checked on the basis mathematical model of the transient process at several ratios of duration of study t_m and time constant τ_s The dependence of parameter's τ_s and $h(t)_\infty$ on measuring error Δh was studied at various time durations of the measurement of function $h(t)$ (Table 1). As it is seen from the results, the

measurement error of parameters τ_s and $h(t)_\infty$ increases with the relative decrease of t_m. Thus it should be assumed that in practice the measurement tolerance at $t_m \geq 5\tau_m$ is about 1%, and at $t_m \geq \tau_m$ it is 0,1%.

Table 1.

$\Delta h(t)$	$t_m / \tau_s = 1.2$		$t_m / \tau_s = 6.0$	
	$\delta\tau_s$,%	$\Delta h(h)_\infty$	$\delta\tau_s$,%	$\Delta h(t)_\infty$
0.001	0.8	0.005	0.0	0.000
0.002	1.6	0.010	0.1	0.000
0.005	3.9	0.023	0.4	0.001
0.010	7.6	0.045	0.8	0.002
0.015	10.9	0.067	1.2	0.003
0.020	14.1	0.084	1.6	0.005

The method was checked by using the polymer membrane "MDK-3" – microporous teflon. The measurements were performed at t_m = 60, 270, 480 sec and τ_s = 20 – 90 sec. The measurement error of τ_s was estimated by comparing it with the data at $t_m/\tau_s \cong 6$ and $t_m/\tau_s \cong 1$.

The relative error was about 10% by the root-mean square error of experimental measurements 0.01 – 0.02. Error of determination of $h(t)_\infty$ was estimated by the measuring of oxygen concentration c_{es} in gaseous mixture of the studied object. The results are given in the table 2.

Table 2.

t_m / τ_∞	$h(t)_\infty$	$\delta h(t)_\infty$*	$\delta h(t)_\infty$,%	σ
0.85	0.598	0.519	+7.9	0.005
0.88	0.088	0.014	+7.4	0.015
1.61	0.020	0.016	+0.4	0.008
1.84	0.242	0.236	+0.6	0.005
2.78	0.000	0.017	–1.7	0.014
3.25	0.296	0.293	+0.3	0.008

* obtained by measuring experimentally

By the method given above, oxygen consumption by the human skin was estimated. Besides the contact method [4], where the oxygen sensor is placed immediately on the surface of the membrane, in this case the sensor is enclosed in the device, with constant volume of gas. There is immediate contact between the sensor and the surface of the examined object. The period of study lasted for 30 minutes. The ratio t_m/τ_s was within the limits from 0.1 to 0.5 , which was connected with the need of the decrease of the measurement error of oxygen concentration c_e to limit $\sigma \cong 0.0005 - 0.0010$. The experimental accuracy in the performed measurements was $\sigma \cong 0.0005 - 0.0025$. In order to diminish the experimental error, results of measurements with $\Delta h(t) \geq 2\sigma$ were rejected. The exclusion of these results reduced the measurement error to limit $\sigma \cong 0.0005 - 0.0015$ (Table 3).

From these results we can see quite good reproducibility of parameter $\Delta h(t)_\infty$, characterized oxygen concentration c_{es} in tissue under the human skin. The discrepancy of obtained values of τ_s may be caused by various states of the skin. Some information about this discrepancy can be got by the comparison of the average values of oxygen flow J_s, calculated by equation (19), with the average value of the flow of oxygen duration of the measurement of t_m, calculated by the following equation (Table 4):

Table 3.

t_m / τ_s	τ_s, min	$h(t)_\infty$	σ
0.11	106.7	0.340	0.0004
0.16	166.2	0.601	0.0007
0.18	171.6	0.582	0.0005
0.19	104.1	0.600	0.0005
0.40	70.9	0.639	0.0016
0.47	63.9	0.712	0.0002

As follows from data (Table 4), the values of J_s calculated from equation (19) correlate with the mean values of J_s. Consequently, the most plausible reason for the discrepancy of values τ_s is indeed connected with various states of the human skin. Relative error of δJ_s of

values J_s and $J_{s'}$ calculated from different equations (19 and 21) is:

$$\delta J_s = (J_s / \overline{J_s} - 1) \cdot 100\% \qquad (22)$$

Table 4.

t_m / τ_s	τ_s, min	J_s, mol/s	$J_{s'}$, mol/s	δJ_s, %
0.11	106.7	4.1×10^{-10}	3.8×10^{-10}	+7
0.16	166.2	1.6×10^{-10}	1.5×10^{-10}	+10
0.18	171.6	1.6×10^{-10}	1.5×10^{-10}	+10
0.19	104.1	2.6×10^{-10}	2.3×10^{-10}	+10
0.40	70.9	3.4×10^{-10}	2.7×10^{-10}	+24
0.47	63.9	3.0×10^{-10}	2.4×10^{-10}	+26

In all measurements $J_s > J_{s'}$. This is caused to some degree, by methodological error of the determination of $J_{s'}$. It is also the cause of the increasing of δJ_s by the decreasing of τ_s. Relation t_m/τ_s affects the deviation of relationship $h(t)$ from the linear, taken as a basis for the determination of the average value of the flow of oxygen $J_{s'}$.

The results of this paper show possibilities of using this method for the determination of oxygen demand of the studied object and also for the determination of the parameters of the external diffusional membrane of the object.

REFERENCES

1. T. T. Tenno, V. E. Past, Proc. 6th Symp. on Double Layer and Adsorption at Solid Electrodes. Tartu, **1981**. p. 328.
2. V. E. Past, T. T. Tenno, K. I. Bergmann, Elektrokhimiya, **1981,** *17*, 1094.
3. A. A. Benedek, W. J. Heideger, Water Research, **1970,** *4*, 9, 627.
4. N. J. Evans, M.R.C.P., N. Rutter M. D., M.R.C.P, The Journal of Pediatrics, **1986**, *108*, 282.

HAPNIKUTARBE MÄÄRAMINE

Taavo Tenno, Aleksei Mashirin, Toomas Tenno

Resümee

Töös on toodud hapnikutarbe määramiseks süsteem, mis koosneb uuritavast hapnikku tarbivast objektist, gaasi läbilaskvast membraanist ning mõõtekambrist, kus hapniku sisalduse muutust registreeritakse elektrokeemilise hapnikuanduriga. On esitatud membraani gaasi läbilaskvust kirjaldavad võrrandid. Gaasi sisaldus süsteemis on väljendatud efektiivse kontsentratsiooni kaudu, mis võimaldab mõõtesüsteemi matemaatilise modelleerimise lihtsustamist. On toodud eksperimendi dünaamilise vea muutus ajas. Esitatud võrrandeid võib kasutada uuritava objekti hapnikutarbe eksperimentaalandmete matemaatiliseks töötlemiseks ning objekti ja mõõtekambri vahelise difusioonilise kihi parameetrite määramiseks.

Toodud matemaatilise mudeli alusel saab määrata membraani ja objekti iseloomustavad parameetrid dünaamilise üleminekuprotsessi algmuutusest, mis vastab 5-10 % kogu protsessi toimumise ajale.

TOLUENE SOLUTIONS OF N-BUTYL-MAGNESIUM BROMIDE - DIETHYL ETHER COMPLEXES

A. Tuulmets, P. Kullamaa, M. Mikk
Institute of Organic Chemistry, University of Tartu

Abstract: Toluene solutions of n-butylmagnesium bromide partially solvated with diethyl ether were investigated. Concentration of the saturated solution of the mono-solvated complex was 3.68M at 20° C. A decrease in the ether content of the solution caused a disproportion of the reagent and the precipitation of a certain part of it with a higher content of magnesium bromide. Solutions of di- n-butylmagnesium in toluene with reduced contents of magnesium bromide and diethyl ether were obtained.

INTRODUCTION

Organomagnesium compounds can be prepared not only in conventional ethers but also in hydrocarbon media, or without any solvent at all [1-4]. For many purposes the replacement of ethers by hydrocarbons of higher boiling point is expedient. The process in hydrocarbons is preferable, since the reaction medium is cheap, nonhygroscopic, and fire hazards are low.

Insolubility of the unsolvated organomagnesium halides in hydrocarbons sets some limits to their use. In the presence of small admixtures of solvating agents, organomagnesium compounds form easily and exhibit high solubilities at least in aromatic hydrocarbons [1-7]. As the solvating agent is firmly bound to the Grignard reagent, such solutions have almost all the advantages of unsolvated organomagnesium halides in non-solvating media.

Because the Grignard reagents in donor solvents are complexed at least with two solvent molecules per atom of magnesium, the reagents obtained in the presence of catalytic amounts of donors should be considered as partially solvated ones. Although such Grignard reagents have been exploited also in big-scale industrial processes [8], their chemical and physical properties have been insufficiently investigated.

We found that the formation of Grignard reagents in toluene in the presence of catalytic amounts of organic bases (less than one mole per a mole of the organic halide) proceeds in two stages [9] (for a review see Ref. [7]). First, a rapid reaction takes place with the formation of a monosolvated organomagnesium halide. After the organic base added in a deficiency is consumed for the production of the monosolvated Grignard reagent, a slow process occurs until the organic halide is completely converted into an organomagnesium compound. This stage of the reaction is catalyzed by the monosolvated Grignard reagent formed in the first step of the reaction. The final product of the reaction is little solvated, however its solubility in toluene is remarkable.

Here we report some results of the investigation of a partially solvated Grignard reagent in toluene, n-butylmagnesium bromide complexed with small amounts of diethyl ether.

EXPERIMENTAL

All reagents were carefully purified. The reagents and solutions were operated under dry argon, and their transportation was carried out by cannulation or using hypodermic syringes.

The Grignard solutions were prepared in a 50 ml three-neck flask equipped with a mechanical stirrer. The reaction flask was loaded with 4 g of magnesium shavings, and appropriate amounts of toluene and diethyl ether (altogether 20 ml in an ordinary run). Then a calculated portion of n-butyl bromide was introduced, and the process started. Usually the first portion of the alkyl halide was such as required to obtain the monosolvated Grignard reagent. The excess of the halide was added in parts, usually by 5 ml portions, after the previous addition had completely reacted. The completeness of the reaction was checked by means of g.l.c. Before the next addition of butylbromide, a 2 ml aliquot was drawn from the reaction mixture, centrifuged, and the supernatant solution was analyzed for the content of basic magnesium acidimetrically, and that of bromide ion by the Mohr method. During the Grignard reagent synthesis, the temperature of the reaction mixture was kept at 30° C or a little higher, the analyses were carried out at ambient temperature that was permanently 20°±1 °C.

RESULTS AND DISCUSSION

Solutions of different concentration of the monosolvated n- butylmagnesium bromide were prepared in order to estimate the solubility of the reagent in toluene. As it is seen from Table 1, the concentration of a saturated toluene solution of the complex, $nBuMgBr \cdot Et_2O$, is 3.68 M at 20° C. It is also seen from the data in Table 1 that the Wurtz reaction is more pronounced at lower concentrations of diethyl ether.

Table 1. Solutions of monosolvated n-butylmagnesium bromide.

C_o [a]	R-Mg [b]	Mg-X [c]	Mg-X / R-Mg
1.60	1.33	1.65	1.24
2.21	1.93	2.20	1.14
2.75	2.56	2.72	1.06
3.59	3.38	3.50	1.04
3.94	3.65 [d]	3.71	1.02
4.10	3.68 [d]	3.62	0.98
4.25	3.68 [d]	3.69	1.00

[a] – intial concentration of n-butylbromide and dietyl ether
[b] – concentration of basic magnesium in the solution
[c] – determined as the concentration of bromide ion
[d] – saturated solution

The preparation of less solvated Grignard reagents was carried out at initial concentrations of diethyl ether from 1.25 M up to 3.96 M. Lower concentrations were not used because (1) they are less important for the preparative scale work (2): the rate of the reaction dramatically decreases with a decrease in ether content [9], and (3) the relative extent of the Wurtz reaction increases considerably with the decreasing ether concentration [9].

The results of some representative experiments are shown in the Figure. A decrease in the ether content of the solution causes a disproportion of the Grignard reagent according to the Schlenk equilibrium

$$2\ RMgX = R_2Mg + MgX_2\ ,$$

also the precipitation of a certain part of the reagent with a higher content of magnesium bromide occurs. The lower the relative content of the ether in the mixture, the higher is the excess of dibutylmagnesium

over magnesium bromide in the solution. The limit of solubility of di-n-butyl-magnesium in these conditions seems to be 1.1 M (about 2.2 molar for basic magnesium, Mg-R). Most likely it is complexed with magnesium bromide and diethyl ether. Preliminary estimation of the ether concentration by means of g.l.c. indicated that the ether content in the solution decreases with the decrease in the magnesium bromide concentration. Thus, because ether is preferably complexed with the magnesium halide, it is distributed in favour of the precipitate.

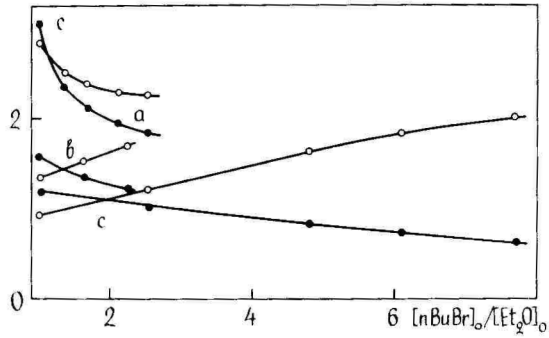

Figure. Concentrations of the basic magnesium R-Mg (circles) and Mg-X units (squares) in toluene solutions of "nBuMgBr" prepared at various initial concentrations of n-butyl bromide and diethyl ether (a – 2.97 M, b – 1.60 M, c – 1.25 M).

Table 2. Some partially solvated Grignard reagents.

$[Et_2O]_o$	$\frac{[nBuBr]}{[Et_2O]_o}$	[nBuMgBr][a]	R-Mg conc/% in soln.[b]	Mg-X conc/% in soln.[b]	$\frac{R\text{-}Mg}{Mg\text{-}X}$ in soln.
3.0	2.5	7.5	2.2 30	1.8 24	1.24
1.60	2.5	4.0	1.7 42	1.2 30	1.41
1.25	2.5	3.1	1.2 39	1.0 32	1.20
1.25	6.0	7.5	1.8 24	0.74 10	2.43

[a] – the concentration of the reagent if all the n-butylmagnesium bromide formed was dissolved

[b] – the part of the moiety in solution, relative to its total amount in the mixture

For a better comprehension of the dependences shown in the Figure see also the data in Table 2. The numbers in this table have been obtained with neglection of the Wurtz reaction. Actually, the yield of dibutylmagnesium is lower and that of magnesium bromide is higher than expected. Therefore, the dissolved part of dibutylmagnesium is higher than calculated in Table 2. Nevertheless, the dominant part of dibutylmagnesium contains in the precipitate. A deficiency of ether disfavours the dissolution of magnesium bromide and so enhances the relative content of dialkylmagnesium in the solution. The yield of the active Grignard reagent can be improved by the addition of appropriate amounts of toluene after the reaction is completed. So we were able to obtain di-n-butylmagnesium solutions with the reduced content of magnesium bromide, and diethyl ether with reasonable yields.

This work was partly supported by the Estonian Science Foundation, Grant Nr. 216-94.

REFERENCES

1. M. S. Kharash, O. Reinmuth, Grignard Reactions of Nonmetallic Subtances, London: Constable, **1954**.
2. D. Bryce-Smith, Bull. Soc. Chim. Fr., **1963**, 1418.
3. B. J. Wakefield, Organometal. Chem. Rev., **1966**, *1*, 131.
4. W. N. Smith, J. Organometal. Chem., **1974**, *64*, 25.
5. E. C. Ashby, R. Reed, J. Org. Chem., **1966**, *31*, 985.
6. T. Leigh, Chem. and Ind., **1965**, 426.
7. A. Tuulmets, Acta et Comment. Univ. Tartuensis, **1993**, *966*, 175.
8. Oligoorganosiloksany: Svoistva, Poluchenie, Primenenie. M. V. Sobolevskii (Ed.). Moscow: Khimiya, **1985**.
9. A. Tuulmets, M. Hõrak, E. Pill, A. Riikoja, Organic Reactivity, Tartu, **1985**, *22*, 93.

N-BUTÜÜLMAGNEESIUMBROMIID - DIETÜÜLEETER KOMPLEKSIDE LAHUSED TOLUEENIS

A. Tuulmets, P. Kullamaa, M. Mikk

Resümee

Töös uuriti dietüüleetriga osaliselt solvateeritud n-butüülmagneesiumbromiidi lahuseid tolueenis. Monosolvateeritud kompleksi küllastatud tolueenilahuse kontsentratsioon 20°C juures on 3,68 M. Eetri hulga vähendamine põhjustab Grignardi reagendi disproportsioneerumise ja osalise sadenemise. Sademes on magneesiumbromiidi sisaldus suurem kui lahuses. Niiviisi valmistati di-n-butüülmagneesiumi lahused tolueenis, mis sisaldavad ekvivalentsest väiksemaid hulki magneesiumbromiidi ja dietüüleetrit.

EFFECT OF STRUCTURE ON THE KINETIC AND EQUILIBRIUM ACIDITY OF CARBON ACIDS

A. Talvik
Institute of Organic Chemistry, University of Tartu

Abstract: Initial position in the correlation analysis of aliphatic compounds is usually the relationship $Y = f\,[\sigma^*, E_s]$. But the E_s scale defined from the hydrolysis of carbonic acid esters is not sufficiently universal as the scale of the total steric influence. Our treatment of steric influence (compare with the contemporary additive scheme of formation enthalpy) divides the total effect into several components. The most precise description of the kinetic and thermodynamic acidity of alkylsubstituted carbon acids gives the relationship $Y=f_s\,[\varphi_\alpha, E_s, E_{s\beta}]$, where all parameters take steric influence into account. The specific influence of electronegative substituents $Y_e=Y - f_s\,[\varphi_\alpha, E_{s\alpha}, E_{s\beta}]$ is also multiparametric: $Y_e=f_e\,[\sigma^*, R, E_{e\alpha}, E_{e\beta}]$. In addition to inductive and conjugative influence usually taken into account (σ^* and R scales), electrostatic repulsion is also essential ($E_{e\alpha}$ and $E_{e\beta}$ scales). The agreement in the results for the dissociation and recombination rate and for equilibrium acidity indicates the functional nature of the relationships obtained.

It is questionable if the scales of influence and the correlation equations given can be considered as final, yet, our results show for certain that in the analysis of kinetic and thermodynamic acidity we can not be limited with the traditional structural influences used in correlation analysis.

Carbon acids are hydrocarbons or their derivatives which form carbanion on ionization

$$RH \rightleftharpoons R^- + H^+$$

The rate of ionization measures kinetic acidity and the equilibrium intrinsic acidity.

The acidities of carbon acids depend greatly on activating groups due to resonance stabilization in the anion. The effect of substituents on the acidities of monosubstituted methanes XCH_3 is consistent with charge delocalization on vacant p- and d-orbitals mainly, in $X^1X^2CH_2$ and $X^1X^2X^3CH$ derivatives the sterical properties of substituents are important to the same degree. Therefore, the addition of extra activating groups increases acidity, the size of the effect substantially decreases for

hindered ones. Any set of activating groups gives anions with specific charge density distribution, and with specific sensitivity to polar and steric effects. Substitution effects vary in nature and in size, their detailed analysis has proved to be labor-consuming and difficult.

Data for several reaction series have been correlated over the years with various types of linear free-energy relationships [1-5] at the Chair of Organic Chemistry of the University of Tartu. Acidities for series XCH_2NO_2 [6-9], $XCH(NO_2)COOC_2H_5$ [2, 10, 11] and $XCH(CN)_2$ [12] have been investigated experimentally. All values available for carbon acid acidities up to 1990 have been compiled [13, 14].

Nitroalkanes are monofunctional carbon acids, which are acidic enough for equilibrium measurements in aqueous media. The effect of structure is quite contrary to that of carboxylic acids, since the substitution of R for H increases equilibrium acidity. It was suggested that the most likely explanation for this phenomenon should be the existence of a specific effect in the dissociation reaction of nitroalkanes, depending on the substituent at the carbon atom whose hybridization state has been changed

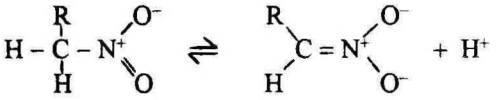

Therefore, an analogy between the dissociation of nitroalkanes and the dehydrogenation of alkanes exists.

The relationship between pK_a values for nitroalkanes and ΔH (or ΔG) for the dehydrogenation of the corresponding alkanes was investigated [4]. For compounds lacking in ß-branching alkyl, aromatic or heteroatomic substituents, pK_a values are indeed adequately correlated with the thermochemical parameters of the dehydrogenation process.

On the other hand, the notion "φ-interaction", connected with interactions between carbon atoms and the hydrogen strain, was introduced. This model seems to describe the alkyl substitution effects on dehydrogenation more authentically than the hyperconjugation model. Therefore, the φ-interaction was elected as the main parameter in the correlation analysis of the acidities of nitroalkanes.

Some possible ways of the separation of the gross substituent effects for series RCH_2NO_2, $RCHClNO_2$, and $RCH(NO_2)_2$were tested. In all cases the most reliable relationship proved to be the relationship

$$Y = a_o + a_1\varphi + a_2E_s' + a_3\Delta E_s^\circ \qquad (1)$$

where $Y = pK_a - lgn_H$, $E_s' = E_s - 1.24$, and ΔE_s° represents the difference between the E_s° value for the given substituent which is possible for 1,7-interaction and the E_s° value for a substituent with a similar α-branching but not possible for 1,7-interaction. Therefore, such a reference substituent for primary alkyls is CH_3CH_2, for secondary alkyls $(CH_3)_2CH$, and for tertiary alkyls $(CH_3)_3C$.

A model was suggested according to which (a) the term $a_1\varphi$ is related to the decrease in the relative free energy of the change $C_{sp}^{\ 3} \rightarrow C_{sp}^{\ 2}$ caused by the increase of the intensity of the φ-interaction, (b) the term a_2E_s reflects the increase in the relative free energy of anions caused by the steric inhibition of resonance, and (c) the term $a_3E_s^\circ$ reflects the decrease in the relative free energy of dissociation caused by the increase in 1,7-interactions. This approach was extended to the equilibrium ($Y_e = pK_a - lgn_H$) and kinetic ($Y_k = lgk - lgn_H$) acidities of other carbon acids [12, 15]. As the most reliable and representative, the following series were considered: RCH_2NO_2 (A), $RCH(NO_2)_2$ (B), $RCH(C_6H_5)COC_6H_5$ (C), $RCH(NO_2)COOC_2H_5$, RCH_2COCH_3, $RCH(CN)_2$.

On the basis of the results represented in Table 1, one can conclude that the application of Eq. (1) to the proton removal quite satisfactorily desribes the respective substituent effects. In case of the compounds with α- or β-branched substituents, anomalous in usual σ*-treatment, pK_a and lgk values are adequately correlated with this equation. Signs and absolute values of the terms proportional to the E_s constant and ΔE_s° value seem to confirm the assignments suggested, so far as the effect of the steric inhibition of resonance is expected to be acid weakening and the effect of the 1,7-interaction acid strengthening. The sign of the φ-interaction depends on the reaction considered.

In this way, possibility of the description of the acidity of alkyl-substituted carbon acids as functions of the φ-interaction and two types of steric effects $Y = f[\varphi, E_s, E_{s(1,7)}]$ was shown. However, following the interpretation of the φ-interaction via atom-atom interactions separated into contributions 1,2-, 1,3-, 1,4- and 1,5-interaction (φ_0) and that of 1,6- and 1,7-interaction ($\varphi - \varphi_0 = f[E_s]$), it seems to be more logical to search the dependence $Y = f[\varphi_0, E_{s(1,6)}, E_{s(1,7)}]$ where all contributions could possess the property of complementary. For this purpose, the scale

of the φ-interaction (φ_α) taking into account 1,2- and 1,3-interactions only, and the scales of steric interactions ($E_{s\alpha}$, $E_{s\beta}$) taking into account 1,6- and more distant interactions were suggested [16]. φ_α and $E_{s\alpha}$ substituent constants get the following numerical values: 3.94 and 1.24 for methyl, 3.25 and 1.31 for primary alkyls, 3.40 and 1.71 for secondary alkyls, 2.36 and 2.78 for tertiary alkyls, respectively. $E_{s\beta}$ constant can be determined as the difference $1.24-E_s-E_{s\alpha}$. Some examples of heats of the formation of sterically hindered compounds testify that these scales are indeed mutually complementary.

Table 1. Values of Regression Coefficients of Eq.(1) for Reactions A, B and C.

Parameter	A(Y_e)	A(Y_k)	B(Y_e)	C(Y_k)
a_0	10.72±0.09	−3.92±0.07	3.96±0.17	−3.12±0.70
a_1	−0.46±0.03	0.06±0.04	−0.21±0.07	0.75±0.16
a_2	–	0.45±0.10	−1.78±0.10	1.22±0.15
a_3	0.34±0.06	−0.53±0.10	2.09±0.14	−0.45±0.12
n	7	7	9	9
R	0.994	0.999	0.999	0.999
s_0	0.10	0.07	0.18	0.11

The three-parameter regression analysis has been carried out for the equilibrium acidity of 9-substituted fluorenes [5], for acidities and excitation energies of mono- and dinitroalkanes [16, 17]. In all cases the relationship $Y = f[\varphi_\alpha, E_{s\alpha}, E_{s\beta}]$ has given a satisfactory quantitative description of the alkyl substituent effect and is comparable with the relationship $Y = f[\varphi, E_s, E_{s(1,7)}]$. The correlations embrace the extreme points for all substituent constants, and broadening the set of data demands the interpolation procedure only. The most expressive example of this treatment is applying the equation

$$Y = a_0 + a_1\varphi_\alpha + a_2E_{s\alpha} + a_3E_{s\beta} \qquad (2)$$

to the acidities in series RCH_2NO_2 (A) and $RCH(NO_2)_2$ (B). See Table 2.

The parameters of Eq. (1) or (2) are characteristic of alkyl and polar substituents to the same degree, and the effect of the latter ones can be formally described by broadening both of them. Nevertheless, Eq. (2) where the contributions are connected with separate pair interaction mechanisms must be preferred.

Five interaction mechanisms are assumed to be operable for polar substituents of the XCH_2 type [16, 17]. These are 1,2- and 1,3-interactions (φ_α scale), 1,6-interaction ($E_{s\alpha}$ scale), 1,7-interaction ($E_{s\beta}$ scale), inductive interaction (σ^* scale), and an additional (mainly by the field effect mechanism) electron interaction. The latter one is assumed to be connected to the difference $1.24 - E_s - E_s^e = E_{e\beta}$, where E_s^e represents the pure steric effect of the polar substituent. Proceeding from this, differences between experimental values and values calculated by Eq. (2) for substituents XCH_2 were treated by the equation

$$Y - Y(\varphi_\alpha, E_{s\alpha}, E_{s\beta}) = a_4\sigma^* + a_5E_{e\beta} \qquad (3)$$

For all the processes considered, the accuracy of Eq. (3) is not less than that of Eq. (2). The $E_{e\beta}$ contribution is significant enough to admit, in principle, an additional perturbation besides the inductive one.

Table 2. The values of Regression Coefficients of Eq. (2) for Reactions A and B.

Parameter	$A(Y_e)$	$A(Y_k)$	$B(Y_e)$	$B(Y_k)$
a_o	10.68±0.06	−3.92±0.02	3.72±0.28	−0.49±0.30
a_1	−0.72±0.02	0.10±0.02	−0.17±0.10	−0.52±0.11
a_2	0.74±0.03	−0.56±0.03	1.75±0.16	−0.73±0.17
a_3	−0.47±0.04	0.10±0.03	−0.26±0.10	−0.20±0.11
n	9	9	13	13
R	0.999	0.999	0.986	0.979
s_o	0.06	0.04	0.28	0.31

For polar substituents bonded directly to the reaction center, the appearance of two extra effects can be expected [16, 17]. One of them is the repulsion of lone p-electron pairs from α-position. The other was

predicted by deviations from linearity between pK_a values for nitroalkanes and ΔH for the dehydrogenation of alkanes [4]. This effect is characteristic of Br, Cl, and CN, but not of F. Therefore, a conclusion about the resonance character of this effect must be drawn. So far as the groups mentioned are able to delocalize the charge without any steric hindrance, this effect must be separated from other resonance effects.

The repulsion scale of lone pairs ($E_{e\alpha}$) was determined from E* values and the conjugation scale (R) from pK_a values of dinitroalkanes [16]. Differences between experimental values and values calculated by Eq. (2) for substituents I, Br, Cl, F, and CN were analyzed by the equation

$$Y - Y(\varphi_\alpha, E_{s\alpha}, E_{s\beta}) = a_6 E_{e\alpha} + a_7 R \qquad (4)$$

In all cases for series XCH_2NO_2 and $XCH(NO_2)_2$, the statistical necessity for separating two contributions in the overall effect of substituents was confirmed.

Application of correlation analysis to the effects of polar substituents is illustrated by the examples listed in Table 3.

For polar substituents XCH_2, an additional contribution $a_5E_{e\beta}$, if existing, has always the sign opposite to the inductive one. Its absolute value is proportional to the charge density on the carbanionic reaction center. This contribution has a high value for the excitation process of nitronates

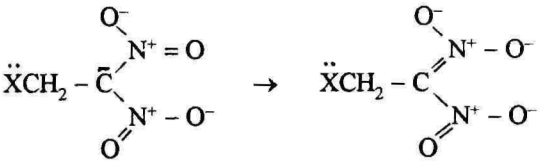

lower for the kinetic acidity of nitroalkanes

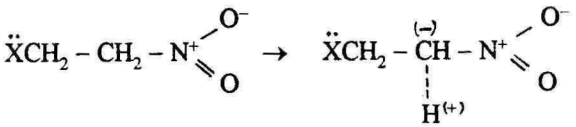

and unnoticeable for the equilibrium acidity of nitroalkanes

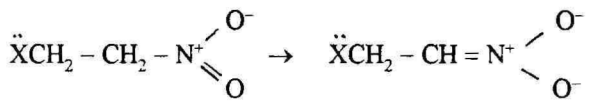

The contribution $a_6E_{e\alpha}$ of polar substituents bonded directly to the reaction center behaves exactly in the same way. Therefore, both of them are assumed to reflect the repulsion of lone pairs of electrons via the space.

Table 3. Values of Regression Coefficients of Eq. (3) and (4).

Parameter	$A(Y_e)$		$B(Y_k)$	
	Eq. (3)	Eq. (4)	Eq. (3)	Eq. (4)
a_4	−0.80±0.07	–	2.90±0.16	–
a_5	–	–	−0.56±0.27	–
a_6	–	0.86±0.04	–	−1.47±0.04
a_7	–	−0.70±0.02	–	0.86±0.05
n	6	5	22	4
s_0	0.16	0.17	0.20	0.27

An extra stabilizing effect of certain polar substituents bonded directly to the reaction center is confirmed. From Table 3 one can see that the separation of the total polar substituent effect of these group into two contributions must be considered reasonable from the statistical standpoint too. In this connection, the following facts are essential for all sets of interactions. First, the values of regression parameters a_i are independent of the set of substituents considered. This may be illustrated by comparing the correlation equation found in terms of the general multiparameter dependence for the equilibrium acidities of mono-nitroalkanes

$$pK_a' = (10.72 \pm 0.13) - (0.71 \pm 0.05)\varphi_\alpha + (0.74 \pm 0.07)E_{s\alpha} -$$
$$-(0.51 \pm 0.08)E_{s\beta} + (0.84 \pm 0.07)\sigma^* + (0.86 \pm 0.04)E_{e\alpha} - (0.70 \pm 0.03)R$$

with the values in Tables 2 and 3. Secondly, the dependence obtained by adding correlation equations for pK_a' and lg k' values describe the recombination rate values adequately in XCH_2NO_2 series as well as in $XCH(NO_2)_2$ series. A conclusion can be drawn that a marked redistribution of interactions is absent and thus the principle of independence and additivity of separate structural effects works.

By using the scales suggested fairly quantitative descriptions were obtained for the series studied. In this way, the necessity of taking into account all the respective properties of substituents is obvious for the understanding of the effect of structure on the kinetic and equilibrium acidity of carbon acids.

REFERENCES

1. A. I. Talvik, Organic Reactivity, (Tartu), **1966**, *2*, 35 (Russ.).
2. H. R. Timotheus, A. J. Talvik, Organic Reactivity, (Tartu), **1966**, *3*, 125 (Russ.).
3. A. J. Talvik, Organic Reactivity, (Tartu), **1972**, *9*, 233 (Russ.).
4. A. J. Talvik, V. A. Palm, Organic Reactivity, (Tartu), **1974**, *11*, 287.
5. A. Talvik, Organic Reactivity, (Tartu), **1978**, *15*, 91.
6. V. O. Pihl, V. G. Timotheus, A. E. Pihl, A. J. Talvik, Organic Reactivity, (Tartu), **1965**, *2*, 16 (Russ.).
7. A. J. Talvik, V. G. Timotheus, R. H. Timotheus, Organic Reactivity (Tartu), **1967**, *4*, 478 (Russ.).
8. A. J. Talvik, H. R. Timotheus, E. H. Loodmaa, V. G. Timotheus, T. I. Sarapuu, A. H. Laht, V. O. Kööbi, Organic Reactivity, (Tartu), **1971**, *8*, 409 (Russ.).
9. S. O. Hiidmaa, A. E. Pihl, A. J. Talvik, Organic Reactivity, (Tartu), **1966**, *3*, 62 (Russ.).
10. H. R. Timotheus, R. A. Tampere, R. J. Hiob, Organic Reactivity, (Tartu), **1971**, *8*, 109 (Russ.).
11. V. G. Timotheus, A. J. Talvik, Organic Reactivity, (Tartu), **1968**, *5*, 357 (Russ.).
12. A. Talvik, A. Pihl, H. Timotheus, A. Osa, J. Viira, V. Timotheus, Organic Reactivity, (Tartu), **1975**, *12*, 135.
13. Tables of Rate and Equilibrium Constants of Heterolytic Organic Reactions. 2 (1), Moscow, **1976**.

14. Tables of Rate and Equilibrium Constants of Heterolytic Organic Reactions. (Suppl.) 5 (1), Tartu, **1990**.
15. A. Talvik, Organic Reactivity, (Tartu), **1975**, *11*, 977.
16. A. Talvik, Organic Reactivity, (Tartu), **1977**, *14*, 187.
17. A. Talvik, A. Pihl, O. Parve, A. Haller, Organic Reactivity, (Tartu), **1978**, *15*, 559.

STRUKTUURI MÕJU KARBOHAPETE KINEETILISELE JA TERMODÜNAAMILISELE HAPPELISUSELE

A. Talvik

Resümee

Karbohapetena tuntakse süsivesinikke ja nende derivaate, mis dissotsieerudes moodustavad karbanioone. Struktuuri mõju nii dissotsiatsiooni kiirusele kui tasakaalule on väga muutuv, mistõttu selle uurimine on raske ja töömahukas. TÜ orgaanilise keemia kateedris on aastate kestel kasutatud karbohapete happelisuse selgitamiseks mitmesuguseid Gibbsi energia lineaarseid sõltuvusi. Eksperimentaalselt on uuritud happelisust ühendite seeriates XCH_2NO_2, $XCH(NO_2)COOC_2H_5$ ja $XCH(CN)_2$, kirjandusandmed on kogutud aastani 1990.

Alifaatsete ühendite korrelatsioonianalüüsis lähtutakse tavaliselt sõltuvusest $Y = f\,[\sigma^*, E_s]$. Estrite hüdrolüüsist defineeritud E_s skaala ei ole aga aatomite steerilise mõju skaalana piisavalt universaalne. Meie käsitlus steerilisest mõjust (vrdl. tekkeentalpia kaasaegse aditiivse skeemiga) jaotab summaarse efekti mitmeks komponendiks. Alküülasendatud karbohapete kineetilise ja termodünaamilise happelisuse kõige täpsema kirjelduse annab seos $Y = f_s\,[\varphi_\alpha, E_{s\alpha}, E_{s\beta}]$, kus kõik parameetrid arvestavad steerilist mõju. Elektronegatiivsete asendajate spetsiifiline mõju $Y_e = Y - f_s\,[\varphi_\alpha, E_{s\alpha}, E_{s\beta}]$ on samuti mitmeparameetriline: $Y_e = f_e\,[\sigma^*, R, E_{e\alpha}, E_{e\beta}]$. Lisaks tavapäraselt arvestatavale induktsioon- ja konjugatsioonmõjule (σ^* ja R skaalad) on oluline ka elektrostaatiline tõukumine ($E_{e\alpha}$ ja $E_{e\beta}$ skaalad). Tulemuste kooskõla dissotsiatsioonikiiruse, rekombinatsioonikiiruse ja tasakaalulise happelisuse jaoks näitab saadud seoste funktsionaalset iseloomu.

Vaevalt, et kasutatud mõjuskaalasid ja korrelatsioonivõrrandeid võib lugeda lõplikeks. Ometi näitavad meie tulemused kindlalt, et karbohapete kineetilise ja termodünaamilise happelisuse analüüsil ei saa piirduda korrelatsioonanalüüsi traditsiooniliste struktuurimõjudega.

SYNTHESIS OF 1,3-DIOLS

H. Timotheus
Institute of Organic Chemistry, University of Tartu

Abstract: The present paper reviews the synthetic methods for the preparation of 1,3-diols. The classification of the methods is based on the strategy of synthesis. The main attention is turned to the practical availability of the methods.

The synthesis of 1,3-diols has been the subject of investigation during 110 years. Systematic work in that region began about 100 years ago in Vienna (Lieben and his school) where substantial research was carried out up to World War I. Numerous methods discussed below were studied (the Claisen–Tishchenko reaction [1-12], the Tollens–Cannizzaro reaction [13-15], the reduction of aldols [16] and their reaction with organometallic compounds [17]). Later, the synthesis of 1,3-diols was advanced in many states (USA, Germany, France, Japan, the former USSR etc.). At present, the main interest is concentrated on the stereoselectivity of the methods, similarly to other regions of organic synthesis.

In the University of Tartu, the synthesis of 1,3-diols has been studied nearly 20 years (main problems are the aldol condensation and related reactions as well as the reduction of carbonyl and ester groups). For many 1,3-diols synthesized in the University of Tartu [18-30] the possibilities of manufacture have been investigated [31-36]. These diols are good extrahents of boron.

One of the most important applications of 1,3-diols is the extraction of boron compounds from aqueous solutions. It is essential both in analytical chemistry and in industry [19, 24, 27]. 1,3-Diols and their derivatives are widely used as polymer material plasticizers [37-40], aroma compounds in perfumery [41, 42] and the main components in cosmetic preparations [43], since they are nontoxic and noncarcinogenous [44, 45]. 1,3-Diols possess repellent properties for insects [46]. Their derivatives are used as liquid crystals [47, 48].

As mentioned above, stereochemistry has become the most important trend in synthesis. Unlike 1,2-diols, where two hydroxyl groups are usually introduced at the same time, and their addition to double bond is readily controlled, the synthesis of 1,3-diols is considerably more complicated. In many cases the forming of the carbon chain is combined with the reduction of carbonyl and related groups, and it is usually impossible to build up the whole structure of 1,3-diol by means of one-step synthesis. The reductions mentioned above usually represent the last steps in the synthesis strategy. Therefore, the number of stereo-selective reduction methods has considerably increased during the last 15 years, as these reductions involve complementary chiral centers.

The small number of reviews of the synthesis of 1,3-diols is somewhat surprising. General reviews have not been published; each existing paper considers only a narrow range of the structures of 1,3-diols and, inevitably, a rather small number of methods. So Ullmann's encyclopedia describes mainly 2,2-dialkyl-1,3-propanediols (from methyl to sec-butyl) [49], the review by Pihlaja and Ketola includes methyl-substituted 1,3-diols [50]. Similarly, Avots with co-workers has discussed the synthesis of 1,3-propanediol [51]. The synthesis of 2,2-dimethyl-1,3-propanediol (neopentyl glycol, one of the most important 1,3-diols in chemical industry) is the main topic of two reviews [38, 39]. Esafov with co-workers has described the 1,3-diols possessing at least one tertiary alcoholic hydroxyl [52]. The author of the present paper has reviewed some methods of the synthesis of diprimary 1,3-diols [53]. A more extensive review has been published by Kuchenbuch; besides simple structures some alicyclic 1,3-diols are described [40, 54].

During the last 15 years a number of reviews concerning stereo-selectivity in the synthesis of 1,3-diols and 1,3-polyol systems have been published [55-58]. New, often nontraditional ways of the synthesis of 1,3-diols are described in order to obtain high stereoselectivity (functionalizations of allyl alcohols, stereoselective reductions and alkylations, building up of long-chained 1,3-polyols etc.) [56].

The necessity (and possibility) of compiling a review which contains all properties (both physical and chemical) and methods of the synthesis for all 1,3-diols known at present is rather questionable. Firstly, the information concerning 1,3-diols is extraordinarily extensive (there is a great number of 1,3-diols containing several other functional groups). Secondly, most of 1,3-diols containing more than one chiral center in their molecule are not individual compounds but actually the mixtures of

stereoisomers. The exact composition of these mixtures and the properties of individual isomers must be the subject of further investigation. Probably, the methods of the separation of diastereomers will be available in the near future. Development is promising in this region [59].

We try to review the methods of the synthesis of 1,3-diols considering the convenience of the method and the availability of initial compounds, since many methods discussed below have been tested by us in practice. We do not pretend to the completeness of the data but try to characterize the most relevant routes and methods.

In order to systematize the possible structures of 1,3-diols we conceive them to be the derivatives of 1,3-propanediol:

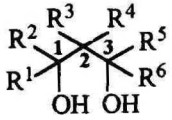

Some R may occur as alicycles, e.g. $R^1 + R^2$, $R^3 + R^4$, $R^1 + R^3$, and $R^1 + R^5$. The main structures of 1,3-diols are shown in Table 1.

Table 1. Main structures of 1,3-diols.

R at C^2 / R at C^1 and C^3	$R^3,R^4=H$	$R^4=H$	$R^3,R^4\neq H$
$R^1,R^2,R^5,R^6=H$	Ia	Ib	Ic
$R^2,R^5,R^6=H$	IIa $*C^1$	IIb $*C^1*C^2$	IIc $*C^1*C^2$
$R^5,R^6=H$	IIIa $*C^1$	III $*C^1*C^2$	IIIc $*C^1*C^2$
$R^2,R^6=H$	IVa $*C^1*C^3$	IVb $*C^1*C^2*C^3$	IVc $*C^1*C^2*C^3$
$R^6=H$	Va $*C^1*C^3$	Vb $*C^1*C^2*C^3$	Vc $*C^1*C^2*C^3$
$R^1,R^2,R^5,R^6\neq H$	VIa $*C^1*C^3$	VIb $*C^1*C^2*C^3$	VIc $*C^1*C^2*C^3$

Chiral centers are marked with an asterisk *, as usual.

One can see that chirality is quite important for 1,3-diols. There are only 3 structures without chirality; most of the structures have 2 or 3 chiral centers. Only the new chiral centres formed in the reaction will be shown below. The importance of several structures in practice is different. In general, simpler structures (carbon chain less branched at the hydroxyl group) are more important, e.g. IIa-c and IVa-c (particularly for the building up of 1,3-polyol systems). Vice versa, 1,3-diols possessing tertiary hydroxyl groups are relatively unstable. Both the elimination of water and the bond cleavage between tertiary and central carbon atoms may occur in the presence of strong acids or bases [52]. Moreover, in this case the formation of derivatives is sterically hindered.

It is reasonable to base the classification of methods on the retrospective strategy (the last or the last but one step of synthesis). In general, we do not view the problem of stereoselectivity, because it will be specially discussed, as mentioned above. We shall omit the syntheses of 1,3-diols via cleavage of the carbon chain because they are significant in quite special instances [50].

In most cases, if possible, R are marked as in Table 1 (R^1, R^2 at C^1; R^3, R^4 at C^2, and R^5, R^6 at C^3).

A. FORMATION OF CARBON CHAIN BEFORE LAST STEP

1. REDUCTIONS

They include the majority of the methods known at present.

1.1. β-HYDROXY CARBONYL COMPOUNDS

By means of these methods all structures of 1,3-diols, except VIa-c, are available. Therefore, it is useful to deal with the synthesis of β-hydroxy carbonyl compounds.

1.1.1. Synthesis of β-Hydroxy Carbonyl Compounds

1.1.1.1. Aldol Condensation

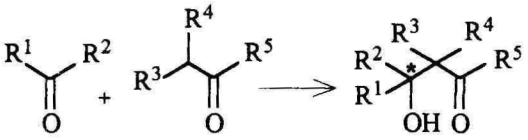

Doubtless, the aldol condensation is one of the most important methods to build up the carbon chain. It is well-known and a number of extensive monographs have been published [60, 61]. Recent works mainly consider new catalysts for increasing the yield of aldol and avoiding the formation of α, β-unsaturated carbonyl compound, e.g. alumina treated with alkali metal carbonates [62], ionites [63], transition metal thiocarbamates [64], naphthenates [65], etc. Non-catalyzed aldol condensation is also feasible if the methylene compound is Me_2CHCHO or another α-branched aldehyde. These methods require hard conditions (t°> 300° C, high pressure) [66, 67]. As we saw, stereoselectivity is one of the modern trends in aldol condensation whereby a new chiral center is generated. Good results are often obtained by means of several enolates (Li [69-72], Mg [70], Zn [70, 73], B [69, 71, 73, 74], Al [70], Si [69, 73], Sn [73], and particularly Ti [68, 69, 72, 73, 75-78]; see also [55-57]). At the same time, it is possible to lead the reaction to the kinetically controlled product (methyl or a less branched alkyl group as the carbanion center in ketone). The direction of the reaction towards aldol or an unsaturated carbonyl compound is conveniently controlled by a catalyst (e.g. Me_3SiCl/Et_3N or LiJ/Et_2O, respectively) [79].

In comparison with aldol condensation, the other ways to synthesize β-hydroxy carbonyl compounds are considerably less important and universal.

1.1.1.2. Addition of Water to α, β-Unsaturated Carbonyl Compounds

This method is rarely used. Perhaps the single convenient method to prepare α, β-unsaturated carbonyl compounds is the dehydration of aldols. However, it is much better to carry out aldol condensation in conditions which avoid the dehydration.

1.1.1.3. Reducing Ring Opening of α, β-Epoxy Carbonyl Compounds

The ring opening in α, β-epoxy carbonyl compounds has been actual for a long time, as these compounds are readily available from α, β-unsaturated carbonyl compounds [80-84] but mainly in order to get β-dicarbonyl compounds (see 1.4.1). Unfortunately, it is difficult to control the reaction [85-87]. Recently the reduction for the opening of the epoxy cycle has become important. By this method β-hydroxy carbonyl compounds are obtained with high yields and stereoselectivity (often higher than by aldol condensation). The reduction is carried out under radical reaction conditions; several reducing agents are used, e.g. Zn [88], Bu_3SnH [89, 90].

1.1.2. Reduction of β-Hydroxy Carbonyl Compounds by Means of Common Chemical and Catalytic Methods

The following reducing agents are often used: Na amalgam [16, 37], $LiAlH_4$ [91, 92], $NaBH_4$ [93], boranes [94, 95]. In the latest works high stereoselectivity is the main problem [92, 94]. The use of $NaBH_4$ allows us to carry out the reduction without the isolation of aldol. It is convenient and avoids the elimination of water; the yields are 80-90% [96].

High yields and stereoselectivities (99:1) are obtained by means of aldehydes as reducing agents in the presence of SmJ_2 [97].

Catalytic hydrogenation is often used in order to reduce the β-hydroxy carbonyl compounds if they have a relatively simple carbon chain. The usual catalyst is Raney Ni. If no dehydration takes place, the yields are >90% [37, 98, 99]. There are two methods among the reductions of β-hydroxy carbonyl compounds which are often carried out as one-pot syntheses, using aldehydes not only as the initial compounds for aldol condensation but also as the reducing agents.

1.1.3. Claisen-Tishchenko Reaction

In simple cases the general scheme is:

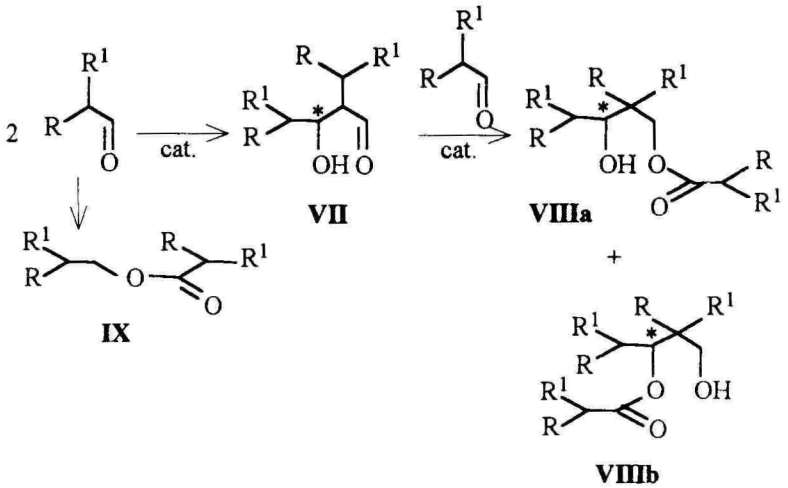

R may be H. The structures obtained here are II b or II c. A new chiral center is introduced in the first step and the chirality does not change latter. The scheme may be considered as the trimerization of the initial aldehyde. Two molecules of aldehyde react to give aldol VII which undergoes the Tishchenko reaction with the third aldehyde molecule. 1,3-Diol half-esters VIIIa and VIIIb are obtained. By the way, the existence of two half-esters has been firmly established, e.g. by means of GLC [100], but, probably, these half-esters are derived from two different diastereomers of 1,3-diol (not at all from the primary or secondary hydroxyl groups) [101]. Since the hydrolysis of the half-ester proceeds readily (though in some cases it is carried out separately), the Claisen-Tishchenko reaction is rather an one-pot synthesis. This reaction is advantageous if the initial aldehyde is cheap and available (two-thirds of the aldehyde form the carbon chain of the product, a third is expended on the reduction). The Claisen-Tishchenko reaction was studied already at the beginning of this century by Lieben and co-workers [1-12]. The later publications are rather sporadic; during the last 10 years interest in this region has greatly diminished.

Depending upon the conditions, the reaction may proceed in several competitive directions (besides the main one giving half-ester VIII). 1) reaction stays at the stage of aldol VII; if R^1 =H, α, β-unsaturated aldehyde is a possible product; 2) a simple ester IX, instead of aldol, is formed by the Tishchenko reaction. The probabilities of these directions are

determined by the catalyst, the solvent and the aldehyde structure. The right choice of the catalyst is perhaps the most important factor. One knows that the formation of aldol (or α,β-unsaturated aldehyde) is favoured by strong bases (alkali and alkaline earth metal hydroxides), the formation of a simple ester via the Tishchenko reaction is favoured by weak bases (Mg and Al alcoholates). Therefore, the proper catalyst must be of medium strength. In case of unbranched aldehydes, some complex alcoholates are effective, e.g. $Mg[Al(OEt)_4]_2$ (yields of half-ester 24-65%) [102, 103], $Mg[B(OMe)_4]_2$ (69-70%) [104], $Ca[B(OMe)_4]_2$ (51-61%) [104]. Several media (alcohols, ethers, benzene) are used. Unfortunately, these complex alcoholates are quite inconvenient to prepare. Among simple alcoholates $Ca(OEt)_2$ (yields of half-ester 40-50%) [103], alcoholates of Ti, Zr and Hf (>50%) [105] are satisfactory. These catalysts fail if the aldehydes are α-branched [102].

Phenolates are also used as catalysts [31, 100, 106, 107, 108]. Pochini and co-workers have studied the effect of Mg phenolates in benzene and in HMPT [100, 106, 107]. In HMPT $2,4,6\text{-}Me_3\text{-}C_6H_2OMgBr$ is effective (yields of half-ester > 90%), in benzene $(2,4,6\text{-}Me_3\text{-}C_6H_2O)_2Mg$ gives yields 63-80%. Some experiments of this series are performed without a solvent (the reaction medium is the initial aldehyde) but the yields are lower (49-58%). Li and Na phenolates are unsatisfactory as catalysts. In HMPT, PhOMgBr is also effective (yields of half-ester 72-92% for RCHO; R varies from methyl to octyl) [100]. This catalyst is somewhat uncomfortable to prepare (via RMgHal); moreover, HMPT is known as a cancer suspect agent. Using DMSO or DMFA instead of HMPT, the yields of half-ester are only a little lower (64-89%) [31, 108]. These methods also fail if the aldehydes are α-branched [108]. An interesting catalyst is $LiWO_2$ in THF; the yields are 38-65% for PrCHO and 38-50% for Me_2CHCHO [109].

Considerably stronger bases are necessary as catalysts for α-branched aldehydes. In most cases the aldehyde used here is Me_2CHCHO. These data are summarized in Table 2.

As one can see in Table 2, the reaction proceeds better in less polar media. Me(Et)CHCHO gives 1,3-diol (yield 59%) if the catalyst is KOH in EtOH; the hydrolysis of half-ester is carried out immediately in the reaction mixture [12].

Anhydrous K_2CO_3 without a solvent is a quite satisfactory catalyst for Me_2CHCHO; the reaction is slow (the equilibrium is achieved after 60 hours at 65° C, the synthesis is carried out in a closed vessel, the

yield of half-ester is 87%) [11]. Similar methods were earlier used in industry but at present their importance has diminished [49].

Table 2. Claisen-Tishchenko reaction in case of Me_2CHCHO.

Catalyst	Solvent	Yield of half-ester	Reference
KOH	H_2O	.....	5
KOH	EtOH	.....	5
$Ca(OH)_2$	H_2O	>20%	10
K_2CO_3	H_2O	34-41%	1,11
Na	Me_2CHCHO	.....	6
NaO(i-Bu)	i-BuOH	59%	110
NaO(t-Pent)	C_6H_6	83%*	111
NaOCO(i-Pr)	H_2O	29% (+11%)*	112
NaOAc	H_2O	25%	2

* - The yield of 1,3-diol is given.

In case of Me_2CHCH_2CHO, the Claisen-Tishchenko reaction has been studied in polar aprotic solvents using phenolates [108], and without a solvent, in the presence of K_2CO_3 as a catalyst [9, 11]. The yields of 1,3-diol are rather low (15-65% and 34%, respectvely). A further investigation is necessary.

If the cross Claisen-Tishchenko reaction is carried out between an unbranched aldehyde and Me_2CHCHO, the latter always appears as the methylene component in the aldol condensation step and the reducing agent in the Tishchenko reaction step [3, 4, 8].

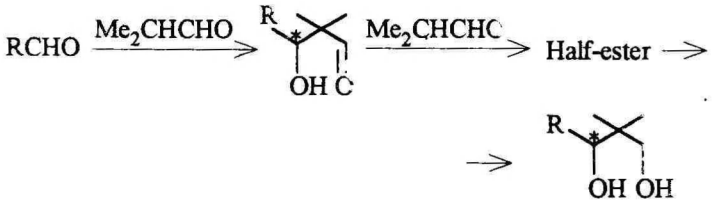

The structure IIc is formed. In this case the most effective catalyst is KOH (13,5% solution in 95% EtOH). The molar ratio RCHO :

Me_2CHCHO 1:2 is necessary. This method is a real one-pot synthesis, as in these conditions (room temperature or refluxing) half-ester is completely hydrolysed to 1,3-diol. R in the initial aldehyde is Me, Me_2CHCH_2 [4] and 4-i-Pr-C_6H_4 [8].

1.1.4. Tollens-Cannizzaro Reaction

The general scheme is:

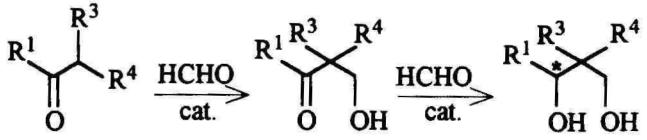

This method is well-known and has been considerably studied longer than 100 years [113]. Initial carbonyl compounds are several aldehydes and ketones having at least one H atom in α- position. The catalysts are alkali and alkaline earth metal oxides, and also anionites are used [114]. The reaction is usually carried out as an one-pot synthesis. Although the reaction proceeds easily and high yields are usual, there are some circumstances to be kept in view. The excess of HCHO is often used as it takes part in aldol condensation and, subsequently, in the reduction of aldol. Therefore all H atoms in α-position of the carbonyl compound are substituted by hydroxymethyl groups. Particularly in case of ketones the product is a polyol. The exact dosation of HCHO in order to guarantee the entering of a single hydroxymethyl group is possible but inconvenient. It excludes the one-pot conditions (the reduction of aldol must be carried out by a reducing agent other than HCHO). It is considerably simpler to dose HCHO for the substitution of all α-H atoms with hydroxymethyl groups while the carbonyl group remains unreduced [115]. This method is often used in industry because alkali metal formate (the product of the Cannizzaro reaction) is a useless ballast; vice versa, the catalytic hydrogenation of aldol gives no useless products [49]; an analogous situation is described in 1.1.3.

The only carbonyl compounds giving 1,3-diol without complications are α-branched aldehydes. The structure of the product is Ic (another possibility to get such a structure is the reduction of 2,2-dialkyl malonic esters, see 1.5.2). The only available α-branched aldehyde is Me_2CHCHO, therefore, some reviews discuss the synthesis of neopentyl

glycol, the product of the Tollens-Cannizzaro reaction in case of Me_2CHCHO as the initial aldehyde [38, 39]. In the Tollens-Cannizzaro reaction the key problem is the synthesis of α-branched aldehydes. Unfortunately, all these methods are rather inconvenient.

The oxidation of corresponding branched alcohols would be a relatively simple method; such alcohols are available, e.g. via the Grignard reaction:

$$RR^1CHMgBr \xrightarrow{HCHO} RR^1CHCH_2OH$$

or via the Guerbet reaction

$$2RCH_2CH_2OH \xrightarrow[Cu,\Delta]{} RC^*H(CH_2R)CH_2OH$$

Such a strategy of synthesis is too clumsy.

The most convenient method would be the alkylation of aldehydes. The methods known at present require the transformation of the aldehyde into a N derivative (Schiff's base, enamine), which is metallated by means of superbasic reagents and then alkylated [116-120].

A relatively convenient method would be the formylation of Grignard reagent [121]:

$$HCOOH \xrightarrow{EtMgBr} HCOOMgBr \xrightarrow{RMgBr} RCH(OMgBr)_2 \xrightarrow{H_2O} \longrightarrow RCHO$$

The preparation via the Darzens-Claisen condensation is also clumsy [122]:

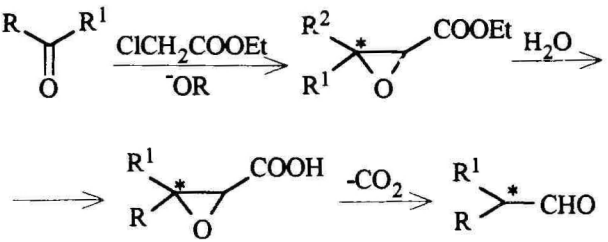

Some alicyclic α-branched aldehydes are available via the Diels-Alder reaction:

They take readily part in the Tollens-Cannizzaro reaction [53, 123]. Similar aldehydes have been synthesized from cyclolalkenes [124]:

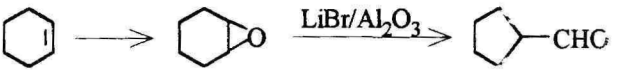

Oxo synthesis is rather inconvenient due to great number of several products; therefore, this method is mainly used in industry [125].

Probably the most promising method is the regioselective catalytic hydrogenation of α, β-unsaturated aldehydes prepared by aldol condensation [126]:

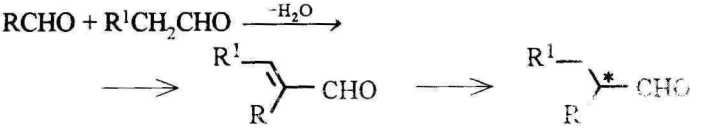

Often $R^1CH_2 = R$. The chemical reductions mostly fail in this case.

1.2. β-HYDROXY ESTERS

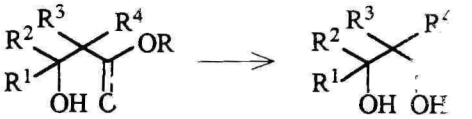

Structures IIIc or simpler are formed. No additional chiral center is generated.

7.2.1. Synthesis of β-Hydroxy Esters

7.2.1.1. *Reformatsky Reaction*

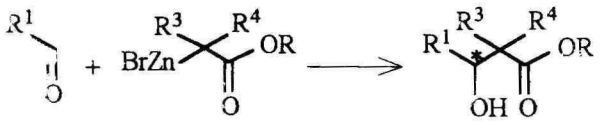

This well-known reaction is one of the best ways to obtain β-hydroxy esters [129-131].

7.2.1.2. *Reaction of Alkynyl Ethers with Aldehydes*

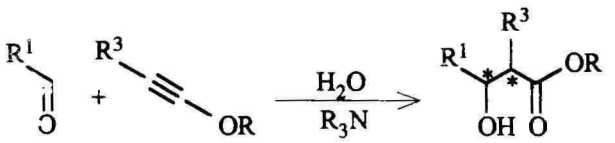

R^3 may be H; the yields are 30-60%. Yields are higher if R^1 and R^3 are small [132].

7.2.1.3. *Reducing Cleavage of α, β-Epoxy Acids*

The esters are available from β-hydroxy acids obtained as shown below:

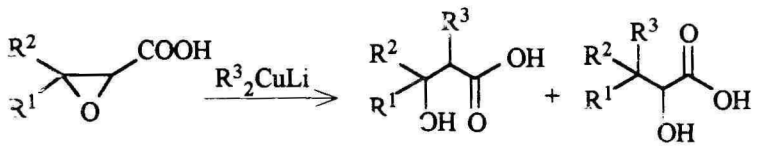

The reaction is regio- and stereoselective; if R^3 = Ar, α-hydroxy acid XI is the predominant product [133].

1.2.1.4. Claisen Rearrangement of β-Hydroxy Esters

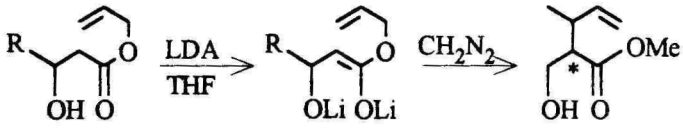

This method is smart but highly specific [134].

1.2.2. Reduction of β-Hydroxy Esters

$LiAlH_4$ is a good reducing agent [129]; probably the reducing agents used for simple esters are applicable (mild conditions are required in order to avoid dehydration), e.g. $NaBH_4$ in special conditions (diglyme + hν [135], $HSCH_2CH_2SH$ [136], H_2O + dioxane [137], excess of $NaBH_4$ in MeOH [138] , $AlCl_3$ etc. [139]), $LiBH_4$ and $Ca(BH_4)_2$ in ethers [140]. By the way, $LiAlH_4$ reduces also β-hydroxy acids (yields >90%) [130].

1.3. β -KETO ESTERS

The structures of products are IIc or simpler; often IIa as in 1.2. is obtained.

1.3.1. Synthesis of β-Keto Esters

1.3.1.1. Ester Condensation

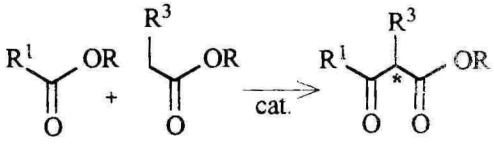

Often R^3 = H. Besides the well-known classical ester condensation [141] several other acylations are used, e.g.:

1)

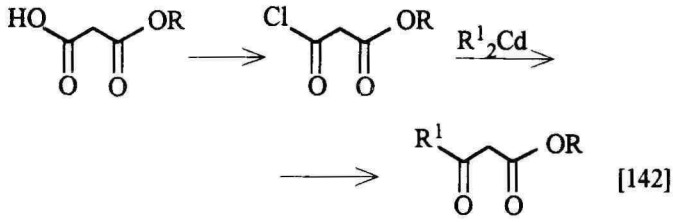

[142]

2)

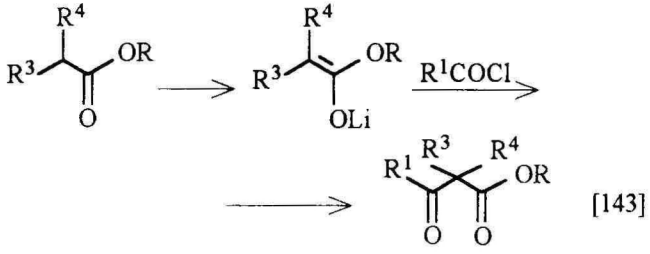

[143]

1.3.1.2. Rearrangement of α, β-Epoxy Esters

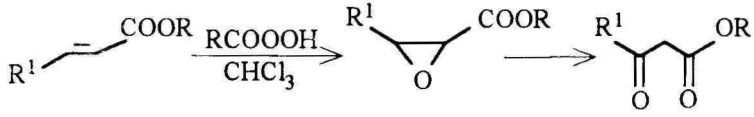

This method is very simple (the rearrangement epoxide → ketone proceeds immediately after epoxidation), but the reaction time is long (12 days) and the yields are rather low [144].

1.3.1.3. Alkylation of β-Keto Esters

Sometimes it is easier to alkylate the β-keto ester than to form the carbon chain directly via ester condensation. The alkylation of β-keto esters is a well-known method, similar to the alkylation of malonic esters (see 1.5.1); it is somewhat more difficult to carry out [145]. Nevertheless, using $(EtO)_2CO$ as a solvent, it is possible to introduce even one sec-butyl or two butyl groups into the β-keto ester [146].

1.3.2. Reduction of β-Keto Esters

Several complex hydrides are used, e.g. $LiAlH_4$ [147, 148], $LiBH_4$ in MeOH [149], $NaBH_4$ in EtOH [148], KBH_4 in MeOH [148]. In many cases it is possible to achieve high stereoselectivity and good yields (75-96%).

Sometimes a stepwise reduction of β-keto esters is useful. At first, the keto group is reduced by means of a mild reagent ($NaBH_4$) in order to avoid side reactions [147], or by means of a stereoselective reagent (R_3SiH) [150] if a new chiral center is generated. The reduction of the product (β-hydroxy ester) is simpler and proceeds without changes of chirality (see 1.2.). Therefore, traditional strong reducing agents work without complications [147].

Probably the use of $NaBH_4$ with additional reagents (see 1.2.2.) is possible; both keto and ester groups are reduced.

1.4. β-DICARBONYL COMPOUNDS

The initial compounds are mostly β-diketones:

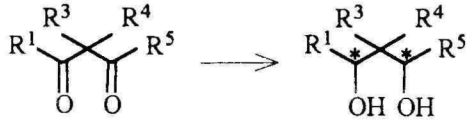

Structures obtained here are IVa-c. Often R^3, R^4 = H. There are only a few references about β-keto aldehydes and β-dialdehydes. A formylation of ketones with the subsequent reduction has been described [95]:

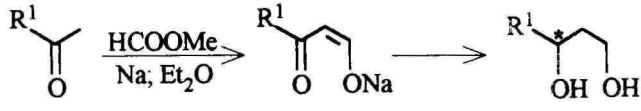

1.4.1. Synthesis of β-Diketones

1.4.1.1. Ester Condensation and Other Acylations

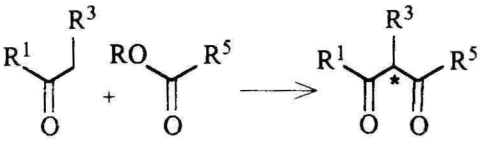

R^3 is often H. This method is similar to the method described in 1.3.1.1; the other initial compound is ketone. In order to influence regio-selectivity, the kinetically controlled enolate of ketone is prepared (see also 1.1.1.1). For this purpose, the bulky 2,4,6-Me_3-C_6H_2Li is used, or the trimethyl silyl ether of enolate is treated with MeLi. These methods are better than the use of LDA or BuLi [151]. In the latter case, the hydrazone of the initial ketone must be prepared [152]. Subsequently, the acylation with RCOCl is carried out as usual. A quite ingenious method to obtain β-diketone is also the acylation of vinyl acetate and the decomposition of the product [153]:

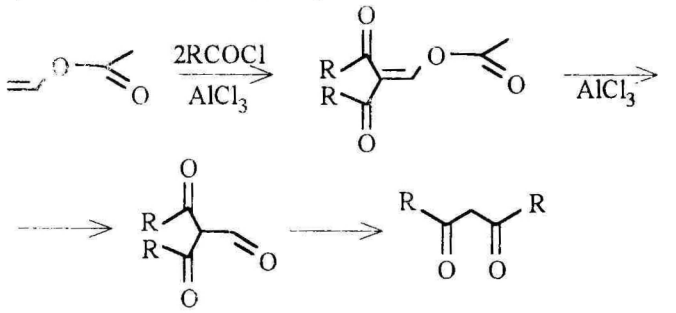

1.4.1.2. Synthesis of β-Diketones Via Chalcones

Ester condensation is sometimes an inconvenient way to prepare greater amounts of β-diketones (the use of stoichiometric quantities of solid alcoholate or NaH and highly dry media are required). Therefore, the method via chalcones is used [154]:

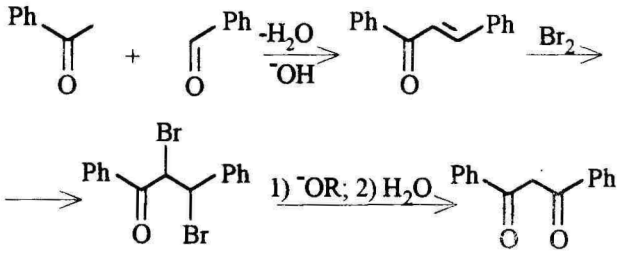

The yields in all steps are 90-95%, so that the total yield may be even higher than in case of ester condensation. Substituted benzaldehydes and acetophenones are also used in this method [155].

1.4.1.3. Cleavage of α, β-Epoxy Ketones

The cleavage of epoxy ring in α, β-epoxy ketones in order to prepare β-diketones has been studied for a long time [80-84] (see also 1.1.1.3). Depending on the reaction conditions, three products are obtained: β-diketone XII, α-diketone XIII and β-ketoaldehyde XIV (rearranged carbon chain) [86]:

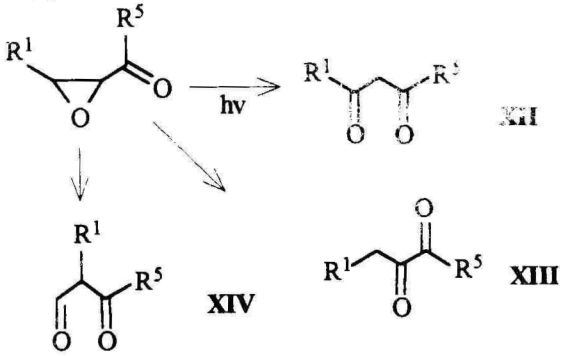

β-Diketone is obtained by the homolytic reaction (hν), the yield is 75% [85, 156].

1.4.1.4. Alkylation of β-Diketones

This reaction proceeds harder than in case of β-keto esters, as the probability of O-alkylation is considerable [145]. The O-alkylation may be prevented by means of R_4NF [157]. Therefore, the reaction of β-hydr-

oxy aldehydes (aldols) with organometallic compounds is sometimes a better method to obtain structures IVa-c (see B.1.1). The dialkylation of β-diketones is succeeded in the presence of Cu^{II} complexes [158].

1.4.2. Reduction of β-Diketones

$LiAlH_4$ or $LiAlH(Ot\text{-}Bu)_3$ in ethers or in CH_2Cl_2 are used. Stereoselectivity is achieved in the presence of $TiCl_4$ [159]. $LiAlH_4$ sometimes gives rather low yields, probably due to the strong enolization of β-diketones [50]. Using $NaBH_4$ in water - MeOH mixture, the separation of isomeric products (1,3-diols) is possible due to the different stability of their borate complexes [160]. The catalytic hydrogenation with Raney Ni is unsatisfactory (yield only 16%) [50].

1.5. MALONIC ESTERS

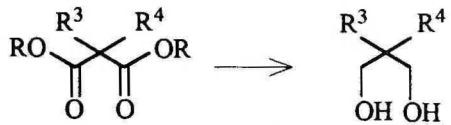

Structures Ia-c are obtained. By the way, structures Ic may be prepared via the Tollens-Cannizzaro reaction, but in many cases the dialkylation of malonic esters is considerably simpler and more reliable than the synthesis of α-branched aldehydes (see 1.1.4). In both cases the number of steps is equal. Both these methods allow us to synthesize cyclic diprimary 1,3-diols $(CH_2)_nC(CH_2OH)_2$.

1.5.1. Alkylation of Malonic Esters

Malonic esters are the most conventient C-H acids for alkylation and dialkylation. This alkylation is well-known and universal (usually by means of NaOH/EtOH and RHal), only the introduction of two bulky groups is difficult [145]. This method has been improved all the time to make it more convenient, particularly for dialkylation. So $i\text{-}Pr_2C(COOEt)_2$ is prepared using metallic Na in Et_2O (yield 40%) [161].

Both mono- and dialkylation are readily carried out in $(EtO)_2CO$ [146]. Alkylation by means of 1-alkenes is available in the presence of peroxides and oxides of Ag, Cu, Pb, Mn (yields 80 %) [162]. The presence of R_4NF is useful [157] similarly to the case of β-diketones. The use of DMFA as reaction medium avoids the preparation of absolute EtOH [157]. DMFA is also a convenient solvent for the alkylation via phase-transfer catalysis (e.g. K_2CO_3 or CaO as bases and $PhCH_2(Et)_3NCl$ as a catalyst; the yields are 21-90% for mono- and 30-80% for dialkylation) [163]. Secondary alkyls are considerably more difficult to introduce (yields 20-30%) [157, 163]. The introduction of tertiary alkyls is still more difficult. For tert-butyl the yield is only 7% [157] and increases to 29% when the reaction is carried out during two weeks [164]. Using electrophilic conditions (the presence of $AlCl_3$) the yield of 55% is available [165]. An indirect way has been used, including the Knoevenagel condensation of malonic ester with acetone and the subsequent reaction with the Grignard reagent to produce tert-butyl malonic ester (yield 60%) [165].

1.5.2. Reduction of Malonic Esters

$LiAlH_4$ is widely used here. The yields are various, often 90% [164, 166]. However, the quest for new reducing agents continues since the work with greater amounts of $LiAlH_4$ is somewhat uncomfortable. BH_3 Me_2S is also used [47, 48]. $NaBH_4$ in the presence of $AlCl_3$, $AlBr_3$, etc. seems to be a perspective reducing agent for malonic esters. If the synthesis is carried out in diglyme, safe and convenient conditions are guaranteed. The yields of 1,3-diols are rather good (60-90%) [32, 34-36, 140, 167]. The only lack of this method is a relatively slow hydrolysis of the reaction mixture.

The catalytic hydrogenation of malonic esters often proceeds poorly due to decomposition of the carbon chain and the reduction of ester group to methyl; the yields are lower than 40% [168].

2. HYDROLYSES

These methods are sometimes combined with reductions and have been partially discussed above (1.1.3.). Several hydrolyses of ethers, acetals etc. are used as auxiliary ways in the stereoselective synthesis of

1,3-diols and 1,3-polyol systems [55-57]; in this paper we do not discuss them.

The methods of hydrolysis are less important than reductions.

2.1. 1,3-DIOXANES

Since the Prins reaction is the main method for the synthesis of 1,3-dioxanes, it requires a more detailed discussion.

2.1.1. Prins Reaction

The reaction is apparently simple (the addition of aldehyde to alkene). 1,3-Dioxane (cyclic acetal) XV is formed:

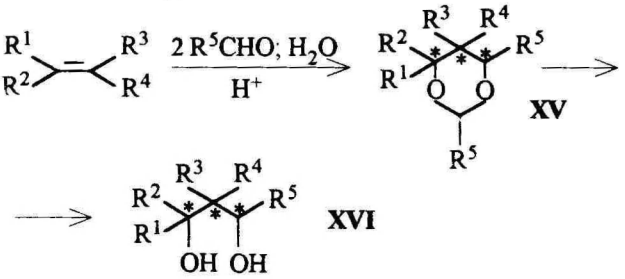

In principle, almost all structures of 1,3-diols, except VIa-c, are available in this reaction. The Prins reaction has been known longer than 75 years [169, 170], and some fundamental works have been published [171-175]. However, the course of the Prins reaction is rather complicated. A part of 1,3-dioxane XV is hydrolysed to 1,3-diol XVI already in the reaction mixture. If R^3 = H, there is an excellent possibility of water elimination. The allyl alcohol formed from XVI undergoes the Prins reaction as the initial alkene and gives with aldehyde new 1,3-dioxane, which will react further as described above. Moreover, the products may undergo several cyclizations and rearrangements. Often there are no dominant products in the reaction mixture.

It is usually impossible to carry out the complete hydrolysis of 1,3-dioxane in the reaction mixture, and a special hydrolysis (usually methanolysis) is necessary. Therefore, the Prins reaction is utilizable only in cases where the initial compounds are simple. In most cases the

aldehyde is HCHO, with 1-alkenes the yields of 1,3-dioxanes are 40-80% [171, 176]. Styrenes also give satisfactory yields [177, 178]. The reaction is sometimes carried out in the presence of carboxylic acids. In this case, instead of 1,3-dioxanes, the corresponding readily hydrolyzable 1,3-dicarboxylates are formed [177-180]. Ru^{III} salts are also used as catalysts [180].

At present the Prins reaction is rather seldom used for the preparative synthesis of 1,3-diols probably due to complicated regio- and stereo-selectivity (in dioxane XV 3 new chiral centers are formed) [172, 175], but it is useful in perfumery [41, 42].

In simple cases the Prins reaction is carried out as an one-pot synthesis (HCHO + C_4 - C_5 alkenes) [41, 176, 181].

2.1.2. Hydroformylation of Epoxides

This method is an interesting variant of oxo synthesis (see 1.1.4). Epoxides (readily available from alkenes) are treated with CO and H_2 in the presence of metal carbonyls as usual [125]. 1,3-Dioxanes, 1,3-diols and other products are obtained. At present this method is mainly used in industry due to a great number of products; hard conditions (high pressure) and scarce catalysts are necessary [51, 125].

2.1.3. Hydrolysis of 1,3-Dioxanes

As mentioned above, in most cases it is necessary to carry out the hydrolysis of 1,3-dioxane separately. The hydrolysis proceeds in acidic [42, 171], sometimes in alkaline medium [144] and is rather slow (7-12 hours refluxing). In the presence of $NaHSO_3$ the hydrolysis is substantially fastened (room temperature, some hours) and the yields are high [182].

2.2. OTHER ETHERS

An interesting method is the reaction of β-halogeno ketone with the Grignard reagent; the product (cyclic ether) is cleaved to give 1,3-diol [183]:

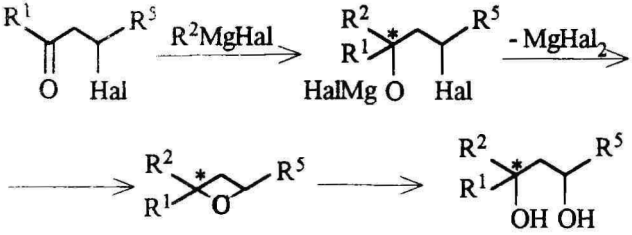

R^5 is often H. β-Halogeno ketones are prepared by the addition of HHal to α, β-unsaturated ketones (see also 2.3).

2.3. HALOGENO ALKANES AND ALKYL ACETATES

Kirchanov and co-workers have presented the following method:

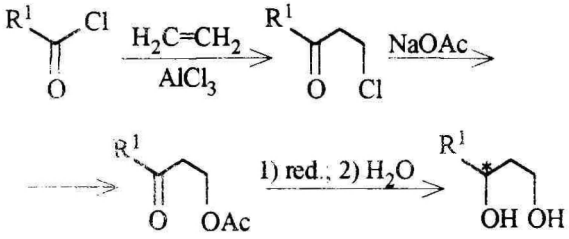

The yields in every step are 80-95%. The transformation Cl → OAc is necessary in order to avoid elimination and hydrogenolysis during the reduction; the latter is carried out by means of $NaBH_4$ or H_2/Raney Ni [184, 185].

2-Methyl-1,3-propanediol is also obtained via the hydrolysis of diacetate. The total scheme is [186]:

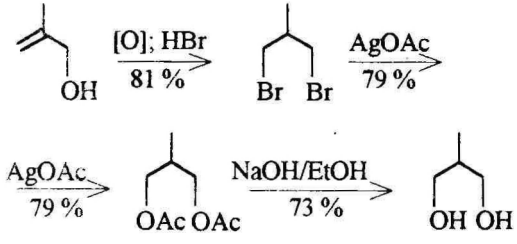

Diacetates of 1,3-diols are available using the addition of $CH_2(OAc)_2$ to alkene [187]:

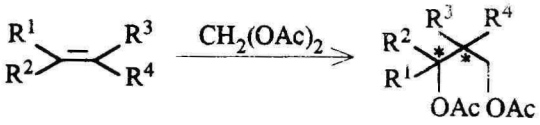

2.4. ALKYL BORATES

The addition of boranes to allyl alcohols with the consequent oxidation and hydrolysis is carried out:

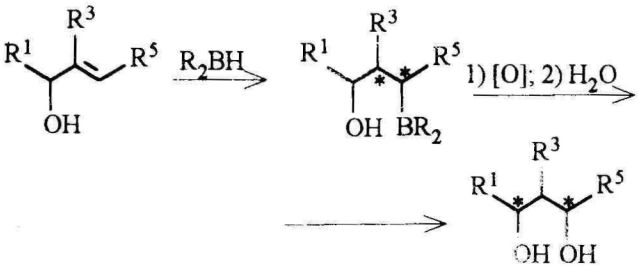

The sufficient regio- (>97%) and stereoselectivity (>9:1) is achieved [188-190]. Instead of allyl alcohols, alkenes [191] and alkynes [192] are also used. After the metallation into allyl and propargyl positions, respectively, a similar scheme to the one above is available (hydroboration, oxidation and hydrolysis) to give 1,3-diols (yields < 60%). In some cases 1,3-diols are obtained using the addition of $Hg(OAc)_2$ to conjugated (1,3) or methylene - separated (1,4) dienes [193].

B. FORMATION OF CARBON CHAIN IN LAST STEP

In most cases the addition of an organometallic compound to the carbonyl group takes place here. These methods may be divided into two groups: 1) organometallic compound carries out the reducing alkylation only (both functions have been previously fixed in positions 1 and 3); 2) the second function is introduced by means of an organometallic compound.

1. REDUCING ALKYLATIONS

The compounds considered in A.1 (reductions) are alkylated. The alkylating agent is always RMgHal. The study of these methods began already at the beginning of the century, but at present interest in this region has diminished. Most of these methods and corresponding 1,3-diols have been studied by Esafov and co-workers [37, 52, 195-208].

It stands to reason that the second mole of the organometallic compound is expended for all hydroxy compounds in order to form the corresponding alcoholate.

1.1. REDUCING ALKYLATION OF β-HYDROXY CARBONYL COMPOUNDS

The scheme is:

Almost all possible variants (some R may be H) have been investigated. These methods are particularly important for the synthesis of structures IIIa-c, Va-c and VIa-c; in the last case they are probably the only considerable possibilities of synthesis. The yields are 40-70%. The reaction is quite sensitive to steric effects. If R^5 and R^6 are isopropyl or other bulky groups, the yields are only 15-30% [201-203]. The 1,3-diols having at least one tertiary alcoholic hydroxyl decompose easily. In addition to dehydration, the carbon-carbon bond cleavage between tertiary and central C atom takes place [37, 52, 196, 197, 201, 202]. 1,3-Diols with secondary hydroxyls do not decompose in this manner [37]. By the way, the structure of the aldols synthesized by Esafov and co-workers where the methylene component is $MeCOCH_2R$, must be controlled thermodynamically not kinetically, contrary to Esafov's opinion. It has been checked by us in detail [209]. Consequently, the alkyl group at the central C atom remains in 1,3-diol achieved by means of RMgHal (structure IVb).

1.2. REDUCING ALKYLATION OF β-HYDROXY ESTERS

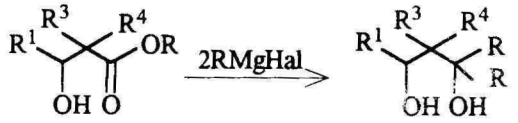

These methods have been studied by Pihlaja and Ketola (R^1 = Me, R^3, R^4 = H) [50]. The yields are 27–80%. Unlike the method described above, a new chiral center is not formed.

1.3. REDUCING ALKYLATION OF β-KETO ESTERS

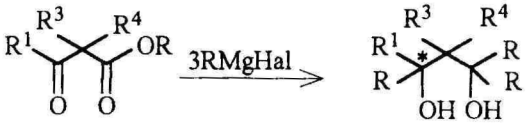

A new chiral center is formed. Esafov has shown that the Grignard reagent reacts poorly with β-keto esters, particularly if they have been alkylated [52].

1.4. REDUCING ALKYLATION OF β-DIKETONES

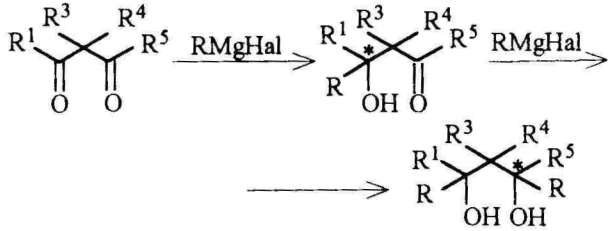

In this case two new chiral centers are formed. Michel and Canonne have studied this method [210]. Depending on the structure of β-diketones and RMgHal, several mixtures of isomers are formed (R^1, R^5 = Me; R^3, R^4 = H; R are alkyls, substituted phenyls and substituted benzyls).

By dosation of RMgHal, the immediate β-hydroxy ketone XVII is available [210]; it may be considered as an additional possibility of obtaining β-hydroxy carbonyl compounds (see A.1.1), but the value of it as a separate method is problematic.

1.5. REDUCING ALKYLATION OF MALONIC ESTERS

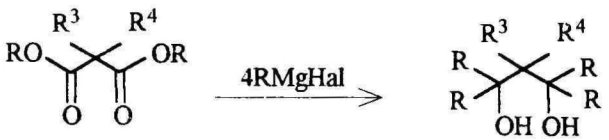

New chiral centers are not formed. This reaction proceeds only if R^3 and R^4 are small; the yields are low (20%). In other cases the reaction does not occur [52]. Probably, in this case it is useful to carry out the reaction by means of RLi or another sterically less hindered organometallic compound.

2. INTRODUCTION OF NEW FUNCTION INTO β-POSITION

The addition of several bifunctional organolithium compounds to the carbonyl group is used. The initial compounds are readily available; the yields of 1,3-diols are 50-80%. Some examples:

1)

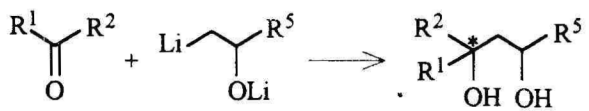

[211]

2)

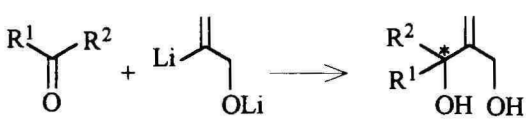

[212]

3)

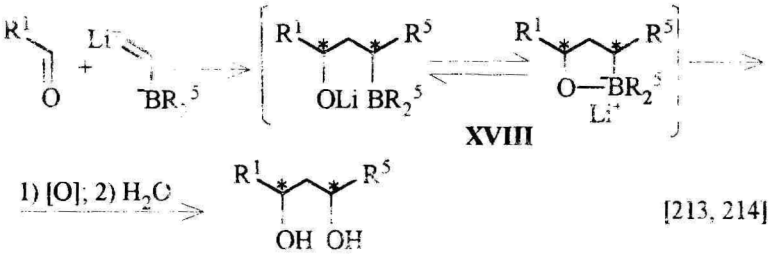

[213, 214]

In the last case the organoboron compound XVIII is oxidized and hydrolyzed as described in A.3. The stereoselectivity has been found to be unsatisfactory.

CONCLUSIONS

The increasing number of new stereoselective methods for the synthesis of 1,3-diols is fully intelligible. At the same time, a lot of older but perspective methods (often carried out as convenient one-pot syntheses, e.g. the Claisen–Tishchenko reaction) have been nearly forgotten; the stereochemistry of these reactions is almost unexplored. There is a wide range of research–the control of the stereoselectivity and the separation of stereoisomeric products of these reactions. In our opinion this thankworthy work will be done in the near future.

REFERENCES

1. M. Brauchbar, Monatsh., **1896**, *17*, 637-647.
2. M. Brauchbar, L. Kohn, Monatsh., **1898**, *19*, 16-55.
3. M. Lilienfeld, S. Tauss, Monatsh., **1898**, *19*, 61-76.
4. M. Lilienfeld, S. Tauss, Monatsh., **1898**, *19*, 76-89.
5. A. Franke, L. Kohn, Monatsh., **1898**, *19*, 354-375.
6. A. Lederer, Monatsh., **1901**, *22*, 536-544.
7. H. Rosinger, Monatsh., **1901**, *22*, 545-560.
8. F. Schubert, Monatsh., **1903**, *24*, 251-260.
9. M. Morgenstern, Monatsh., **1903**, *24*, 579-589.

10. P. Herrmann, Monatsh., **1904**, *25*, 188-196.
11. F. M. A. Kirchbaum, Monatsh., **1904**, *25*, 249-266.
12. V. Neustädter, Monatsh., **1906**, 27, 879-934.
13. A. Fischer, B. Winter, Monatsh., **1900**, *21*, 301-318.
14. A. Franke, Monatsh., **1913**, *34*, 1893-1913.
15. A. Franke, F. Sigmund, Monatsh., **1925**, *46*, 61-74.
16. W. Subak, Monatsh., **1903**, *24*, 167-173.
17. A. Franke, M. Kohn, Monatsh., **1906**, *27*, 1097-1128.
18. R. T. Ignash, E. M. Shvarts, P. I. Brusilovskii, H. R.-Ju. Timotheus, Trans. Latvian Acad. Sci. Chem. Ser., **1978**, 145-147 (Russ.)
19. R. T. Ignash, E. M. Shvarts, G. F. Guseva, Yu. I. Ostroushko, P. I. Brusilovskii, H. R. Timotheus, E. R. Mõttus, V All-Union Extraction Chemistry Conference, Novosibirsk, July 11-13, 1978. Theses. Novosibirsk, **1978**, p. 77 (Russ.).
20. R. T. Ignash, E. M. Shvarts, E. R. Mõttus, H. R.-Ju. Timotheus, Trans. Latvian Acad. Sci. Chem. Ser., **1979**, 7-10 (Russ.).
21. A. A. Bernane, E. M. Shvarts, H. R.-Ju. Timotheus, E. R. Mõttus, ibid, **1980**, 275-276 (Russ.).
22. R. T. Ignash, E. M. Shvarts, H. R.-Ju. Timotheus, E. R. Mõttus. ibid, **1981**, 614-617 (Russ.).
23. E. M. Shvarts, I. A. Kalve, H. R.-Yu. Timotheus, E. R. Mõttus, ibid, **1981**, 618-621 (Russ.).
24. A. E. Dzene, A. A. Bernane, E. M. Shvarts, H. R.-Yu. Timotheus. IV Analytical Chemistry Sci. Conference of Baltic Republics, Belorussian SSR and Kaliningrad Territory.Theses, Part I., Tallinn, **1982**, p. 73 (Russ.).
25. I. A. Kalve, E. M. Shvarts, H. R.-Yu. Timotheus, A. Ya. Käärd, Trans. Latvian Acad. Sci. Chem. Ser., **1982**, 605-608 (Russ.).
26. I. A. Kalve, E. M. Shvarts, H. R.-Yu. Timotheus, A. E. Dzene, ibid, **1984**, 172-174 (Russ.).
27. H. R.-Yu. Timotheus, T. H. Hansen. VI All-Union Conference on Chemistry and Technology of Inorganic Boron Compounds. Theses. Riga, P. Stuchka Univ., **1987**, p. 196 (Russ.).
28. E. M. Shvarts, I. A. Kalve, A. Ya. Putnin, H. R.-Yu. Timotheus, Trans. Latvian Acad. Sci. Chem. Ser., **1987** 471-476 (Russ.)
29. A. A. Bernane, E. M. Shvarts, H. R.-Yu. Timotheus, T. H. Hansen, ibid., **1987**, 48-51 (Russ.).
30. A. A. Bernane, E. M. Shvarts, H. R.-Yu. Timotheus, ibid. **1989**, 447-450 (Russ.).

31. H. R.-Yu. Timotheus, E. R. Mõttus, E. M. Shvarts, R. T. Ignash, P. I. Brusilovskii, USSR Invent. Cert. 709610; 21.09.1979.
32. H. R.-Yu. Timotheus, E. R. Mõttus, E. M. Shvarts, P. I. Brusilovskii, A. A. Bernane, USSR Invent. Cert. 1341174; 01.06.1987.
33. E. M. Shvarts, I. A. Kalve, H. R.-Yu. Timotheus, USSR Invent. Cert. 1415660; 08.04.1988.
34. H. R.-J. Timotheus, E. R. Mõttus, E. M. Shvarts, P. J. Brusilovskii, A. A. Bernane, Swiss Pat. CH66478A5; 29.07.1988.
35. H. R.-J. Timotheus, E. R. Mõttus, E. M. Svarc, P. E. Brusilovskij, A. A. Bernane, Wirtschaftspat. DDR 258916; 10.08.1988.
36. H. R.-J. Timotheus, E. R. Mõttus, E. M. Shvarts, P. J. Brusilovsky, A. A. Bernane, Brit. Pat. 2179937; 10.08.1988.
37. V. I. Esafov, V. I. Azarova, Sci. Repts. Ural Univ., **1969**, 83-92 (Russ.).
38. B. Cornils, H. Feichtinger, Chem.-Ztg., **1976**, *100*, 504-514.
39. P. Lappe, H. Springer, J. Weber, Chem.-Ztg., **1989**, *113*, 293-304.
40. J. Kuchenbuch, Kunststoff-Rundschau, **1958**, *5*, 337-343.
41. J. Kulesza, M. Druri, Riechstoffe, Aromen, Körperpflegemittel, **1969**, *19*, 157.
42. N. P. Solov'eva, T. M. Tsirkel, I. A. Terekhina, T. A. Rudolfi, S. A. Voytkevich, Chem. Heterocycl. Comp. (Russ.), **1971**, 1447-1450.
43. T. Yamamoto, T. Tatsumi, Jap. Pat. 5034650, 30.09.1976.
44. F. Stenback, P. Shubik, Toxicol. Appl. Pharmacol., **1974**, *30*, 7-13; C.A. **1975**, *82*, 26785 c.
45. J. W. Frankenfeld, D. L. Wright, U. S. Pat. 3970759; 20.07.1976.
46. R. Galun, Pyrethrum Post, **1975**, *13*, 2-4.
47. N. L. Sethofer, Fr.Pat., 2479252; 02.10.1981.
48. H. Sorkin, Fr .Pat., 2479824; 09.10.1981.
49. F. Merger, J. Paetsch, Ullmann's Encyclopedia of Industrial Chemistry. 5-th, Completely Revised Ed. Weinheim, Verlag Chemie, **1985**, V. A1, 307-310.
50. K. Pihlaja, M. Ketola, Acta chem. scand., **1969**, *23*, 715-726.
51. A. A. Avots, G. V. Glemite, Ya. R. Dzenitis, Trans. Latvian Acad. Sci. Chem. Ser., **1986**, 398-403 (Russ.).
52. V. I. Esafov, Sci. Works Ural State Univ. Org. Chem., I, **1971**, 172-206 (Russ.).
53. H. Timotheus, J. Riikoja, Acta et Comm. Univ. Tartuensis, **1982**, 616, 41-49 (Russ.).

54. J. Kuchenbuch, Kunststoff-Rundschau, **1958**, *5*, 398-403.
55. S. Masamune, W. Choy, Aldrichim. Acta, **1982**, *15*, 47-63.
56. T. Oishi, T. Nakata, Synthesis, **1990**, 635-645.
57. C. H. Heathcock, Aldrichim. Acta, **1990**, *23*, 99-111.
58. J. S. Panek, M. Yang, J. S. Solomon, J. Org. Chem., **1993**, *58*, 1003-1010.
59. U. Mäeorg, M. Karro, H. Timotheus, E. Loodmaa, Proc.Estonian Acad. Sci. Chem., **1987**, *36*, 181-185 (Russ.).
60. A. T. Nielsen, W. J. Houlihan, Org. Reactions, **1968**, *16*, 2-444.
61. R. Luft, Ann. de chim., 1959, 746-793.
62. A. J. Mulder, R. van Helden, Brit. Pat. 1458129; 08.12.1976.
63. F. Merger, R. Planz, E. Nebe, BRD Pat. 1643727; 04.03.1976.
64. H. Mimoun, Thao Do, I. Sérée de Roch., Fr.Pat. 2287434; 07.05.1976.
65. M. G. Katsnelson, S. Sh. Kagna, L. I. Nikitina, O. M. Oranskaya, I. V.Semenskaya, J. Org. Chem., (Russ.), **1986**, *22*, 1598-1603.
66. H. Pommer, H. Müller, G. Klotman, H.Köhl, H. Oberwien, BDR Pat. 1643751; 24.06.1976.
67. A. W. McCollum, H. J. Hagemeyer, Jr.U.S.Pat. 4017537; 12.04.1977.
68. G. Stork, G. A. Kraus, G. A. Garcia, J. Org. Chem., **1974**, *39*, 3459- 3460.
69. T. Mukaiyama, K. Narasaka, Chemistry (Jap.), **1977**, *32*, 576-579.
70. K. Narasaka, J. Synth. Org. Chem. Jap., **1979**, *37*, 307-319.
71. Li Yi, N. Paddon-Row, K. N. Houk, J. Org. Chem., **1990**, *55*, 481-493.
72. M. P. Bonner, E. R. Thornton, J. Am. Chem. Soc., **1991**, *113*, 1299-1308.
73. T. Mukaiyama, Pure & Applied Chem., **1983**, *55*, 1749-1758.
74. D. A. Evans, T. R. Taber, Tetrahedron Lett., **1980**, *21*, 4675-4678.
75. T. M. Reetz, R. Peter, Tetrahedron Lett., **1981**, *22*, 4691-4694.
76. M. Netz-Stormes, E. R. Thornton, Tetrahedron Lett., **1986**, 27, 897-900.
77. S. Shirodkar, M. Netz-Stormes, E. R. Thornton, Tetrahedron Lett., **1990**, *31*, 4699-4702.
78. M. Netz-Stormes, E. R. Thornton, J. Org. Chem., **1991**, *56*, 2489-2498.
79. R. K. Kelleher, M. A. McKervey, Pongsak Vibuljan, J. Chem. Soc. Chem. Comm., **1980**, 486-488.

80. E. Weitz, A. Scheffer, Ber., **1921**, *54*, 2327-2344.
81. S. Juliá, J. Masana, J. C. Vega, Angew. Chem., Int. Ed. Engl., **1980**, *19*, 929-931.
82. S. Juliá, J. Guixer, J. Masana, J. Rocas, S. Colonna, R. Annuciata, H. Molinari, J. Chem. Soc. Perkin Trans., I, **1982**, 1317-1324.
83. S. Colonna, H. Molinari, S. Banfi, S. Juliá, J. Masana, A. Alvarez, Tetrahedron, **1983**, *39*, 1635-1641.
84. K. D. R. Gupta, S. Naithani, Current Sci., **1989**, *58*, 1016-1018.
85. S. Bodforss, Ber., **1918**, *51*, 214-219.
86. E. Weitz, A. Scheffer, Ber., **1921**, *54*, 2344-2353.
87. E. Hasegawa, K. Ishiyama, H. Kashiwazaki, T. Horaguchi, T. Shimizu, Tetrahedron Lett., **1990**, *31*, 4045-4048.
88. B. Marsman, H. Wynberg, J. Org. Chem., **1979**, *44*, 2312-2314.
89. E. Hasegawa, K. Ishiyama, T. Horaguchi, T. Shimizu, J. Chem. Soc. Chem. Comm., **1990**, 550-552.
90. E. Hasegawa, K. Ishiyama, T. Kato, T. Horaguchi, T. Shimizu, S. Tanaka, Y. Yamashita, J. Org. Chem., **1992**, *57*, 5352-5359.
91. Y. Tamaru, Tetrahedron Lett., **1985**, *26*, 3207-3210.
92. Y. Mori, M. Kuhara, A. Takeuchi, M. Suzuki, Tetrahedron Lett., **1988**, 5419-5422.
93. A. I. Gren', V. V. Kuznetsov, H. U. Vil'ginskaya, D. E. Stepanov, Reagents and Special Pure Substances (Russ.), **1978**, *6*, 24-26.
94. D. A. Evans, A. H. Hoveyda, J. Org. Chem., **1990**, *55*, 5190-5192.
95. D. E. Pearson, J. D. Weaver, Org. Prep. Proceed. Int., **1978**, 29-32; C.A., **1978**, 89, 23870 k.
96. H.Timotheus, unpublished data.
97. D. A. Evans, A. H. Hoveyda, J. Am. Chem. Soc., **1990**, *112*, 6447-6449.
98. F. Merger, E. Miesen, F. J. Broecker, W. Schroeder, K. Baer, J. Paetsch, L. Hupfer, BRD Pat., 3027890; 04.03.1982.
99. J. Weber, P. Lappe, H. Springer, BRD Pat. 3403696; 08.08.1985.
100. A. Pochini, G. Salerno, R. Ungaro, Synthesis, **1975**, 164-165.
101. U. Mäeorg, unpublished data.
102. M. S. Kulpinski, F. F. Nord, J. Org. Chem., **1943**, *8*, 256-270.
103. F. J. Villani, F. F. Nord, J. Am. Chem. Soc., **1947**, *69*, 2605-2607.
104. G. Hesse, M. Maurer, Liebigs Ann., **1962**, *658*, 21-38.
105. N. Yoshino, H. Akutsu, J. Chem. Soc. Jap., Chem. and Ind. Chem., **1978**, 742-747.

106. G. Casnati, A. Pochini, G. Salerno, R. Ungaro, Tetrahedron Lett., **1974**, *15*, 959-962.
107. G. Casnati, A. Pochini, G. Salerno, R. Ungaro, J. Chem. Soc., Perkin Trans. I, **1975**, 1527-1531.
108. H. Timotheus, Acta et Comm. Univ. Tartuensis, **1982**, *616*, 33-40, (Russ.).
109. G. M. Villacorta, J. San Filippo, Jr., J. Org. Chem.,**1983**, *48*, 1151-1154.
110. U. Schwenk, A. Becker, Liebigs Ann., **1972**, *756*, 162-169.
111. E. Elkik, Bull. Soc. chim. Fr., **1959**, 933-939.
112. J. Weber, H.-D. Hahn, P. Lappe, F. Thönssen, H. Springer, BRD Pat. 3447029; 26.06.1986.
113. T. A. Geissmann, Org. Reactions, **1950**, *2*, 106-127 (Russ.).
114. M. Majchrzak, K. Terelak, M. Pers, Przem. chem., **1985**, *64*, 73-75.
115. E. Fourneau, E. Benoit, R. Firmenich, Bull. Soc. chim. Fr., **1930**, *47*, 858-900.
116. G. Stork, S. R. Dowd, J. Am. Chem. Soc., **1963**, 85, 2178-2183.
117. G. Stork, A. Brizzolani, H. Landesman, J. Szmuszkowicz, R. Terrell, J. Am. Chem. Soc., **1963**, *85*, 207-222.
118. T. Cuvigny, H. Normant, Synthesis, **1977**, 198-200.
119. A. I. Meyers, A. Nabeya, H. W. Adickes, I. R. Politzer, G. R. Malone, A. C. Kovelesky, R. L. Nolen, R. C. Portnoy, J. Org. Chem., **1973,** *38*, 36-56.
120. D. Savoia, C. Trombini, A. Umani-Ronchi, J. Org. Chem., **1978**, *43*, 2907-2910.
121. F. Sato, K. Oguro, H. Watanabe, M. Sato, Tetrahedron Lett., **1980**, *21*, 2869-2872.
122. M. S. Newman, B. J. Magerlein, Org. Reactions, **1951**, *5*, 319-346 (Russ.).
123. H. E. French, D. M. Gallagher, J. Am. Chem. Soc., **1942**, *64*, 1497- 1499.
124. H. Suga, H. Miyake, Synthesis, **1988**, 394-395.
125. B. K. Nefedov, Organic Syntheses Based on Carbon Monooxide. Moscow, Nauka, **1978**, 222 p. (Russ.).
126. B. V. Joffe (Ed.), Modern Methods in Organic Synthesis, Leningrad Univ., **1974**, 92-133 (Russ.).
127. R. L. Shriner, Org. Reactions, **1948**, *1*, 9-52 (Russ.).
128. A. Fürstner, Synthesis, **1989**, 571-590.
129. C. Schaal, Bull. Soc. chim. Fr., **1973**, 3083-3086.

130. F. F. Blicke, H. Raffelson, J. Am. Chem. Soc., **1952**, *74*, 1730-1733.
131. M. W. Rathke, A. Lindert, J. Org. Chem., **1970**, *35*, 3966-3967.
132. H. Vieregge, J. F. Arens, Rec. trav. chim., **1959**, *78*, 921-928.
133. J. M. Chong, K. B. Sharpless, Tetrahedron Lett., **1985**, *26*, 4683-4686.
134. M. J. Kurth, Yu Chan-Mo, Tetrahedron Lett., **1984**, *25*, 5003-5006.
135. Jung Hoon Choi, Dae Whong Kim, Sang Chul Shim, Tetrahedron, Lett., **1986**, *27*, 1157-1160.
136. W. C. Guida, E. E. Entreken, A. R. Guida, J. Org. Chem., **1984**, *49*, 3024-3026.
137. A. Bianco, P. Passacantilli, G. Righi, Synth. Comm., **1988**, *18*, 1765- 1771.
138. M. S. Brown, H. Rapoport, J. Org. Chem., **1963**, *28*, 3261-3263.
139. H. C. Brown, C. Subba Rao, J. Am. Chem. Soc., **1956**, 78, 2582-2588.
140. H. C. Brown, S. Narasimhan, Yong Moon Choi, J. Org. Chem., **1982**, 4702-4708.
141. C. R. Hauser, B. E. Hudson, Jr. Org. Reactions, **1948**, *1*, 345-398 (Russ).
142. E. v. Rudloff, Canad. J. Chem., **1958**, *36*, 486-491.
143. M. W. Rathke, J. Deitch, Tetrahedron Lett., **1971**, *31*, 2953-2956.
144. A. A. Ansari, F. Ahmad, S. M. Osman, Fette, Seifen, Anstrichmittel, **1977**, 79, 328-330.
145. A. C. Cope, H. L. Holmes, H. O. House, Org. Reactions, **1959**, *9*, 125-444 (Russ.).
146. V. H. Wallingford, M. A. Thorpe, A. H. Homeyer, J. Am. Chem. Soc., **1942**, *64*, 580-582.
147. A. C. Cope, G. W. Wood, J. Am. Chem. Soc.,**1957**, 79, 3885-3888.
148. G. R. Brown, A. J. Foubister, J. Chem. Soc., Chem. Comm., **1985**, 455-456.
149. K. Soai, H. Oyamada, Synthesis, **1984**, 605-607.
150. M. Fujita, T. Hiyama, J. Am. Chem. Soc., **1985**, *107*, 8294-8296.
151. A. K. Beck, M. S. Hoekstra, D. Seebach, Tetrahedron Lett., **1977**, *18*, 1187-1190.
152. D. Enders, P. Weuster, Tetrahedron Lett., **1978**, *19*, 2853-2856.
153. A. Sieglitz, O. Horn, Ber., **1954**, *84*, 607-618.
154. Org. Syntheses, **1949**, *1*, 186-188 (Russ.).

155. H. Timotheus, unpublished data.
156. V. T. Ramakrishnan, J. Kagan, J. Org. Chem., **1970**, *35*, 2898-2900.
157. J. H. Clark, J. M. Miller, J. Chem. Soc. Perkin I, **1977**, 1743-1745.
158. M. E. Lloris, J. Marquet, M. Moreno-Mañanas, Tetrahedron Lett., **1990**, *31*, 7489-7492.
159. J. Barluenga, J. G. Resa, B. Olano, S. Fustero, J. Org. Chem., **1987**, *52*, 1425-1428.
160. J. Dale, J. Chem. Soc., **1961**, 910-922.
161. F. C. B. Marshall, J. Chem. Soc., **1931**, 2336-2338.
162. M. Hájek, J. Málek, Synth. Comm., **1977**, 454-457.
163. N. N. Sukhanov, G. I. Rutman, A. G. Liakumovich, U. G. Ibatullin, USSR Invent.Sert. 536156; 15.06.1977.
164. H. F. van Woerden, Rec. trav. chim., **1963**, 82, 920-922.
165. C. A. Buehler, D. E. Pearson, Survey of Organic Syntheses II. Moscow, Mir, **1973**, p. 334 (Russ.).
166. W. G. Brown, Org. Reactions, **1953**, 6, 409-460 (Russ.).
167. W. Weissflog, H. Enzenberg, K. Agatha, K. Knabe, H. Zaschke, M. Schierhorn, K.-D. Scherf, W. Schäfer, DDR Pat. 242402; 28.01.1987.
168. R. Connor, H. Adkins, J. Am. Chem. Soc., **1932**, *54*, 4678-4690.
169. H. J. Prins, Chem. Weekbl., **1917**, *14*, 932-939; C. 1918 I 168.
170. H. J. Prins, Chem. Weekbl., **1919**, *16*, 1510-1526; C. 1920 I 424.
171. D. R. Adams, S. P. Bhatnagar, Synthesis, **1977**, 661-672.
172. H. Griengl, K. P. Geppert, Monatsh., **1976**, *107*, 421-431.
173. H. Griengl, K. P. Geppert, Monatsh., **1976**, *107*, 675-684.
174. H. Griengl, P. Nowak, Monatsh., **1977**, *108*, 407-416.
175. H. Griengl, P. Nowak, Monatsh., **1978**, *109*, 11-19.
176. M. G. Safarov, G. I. Rutman, A. G. Liakumovich, U. G. Ibatullin, USSR Invent.Sert. 536156; 15.06.1977.
177. R. W. Shortridge, J. Am. Chem. Soc., **1948**, *70*, 873-874.
178. L. Červený, A. Marhoul, M. Železny, V. Ružička, Chem. Prum., **1976**, *26*, 519-522.
179. J. J. S. Bajorek, R. Battaglia, G. Pratt, J. K. Sutherland, J. Chem. Soc. Perkin I, **1974**, 1243-1245.
180. J. T. Cazat, I. Tkatchenko, J.-R. Bernard, Fr. Pat. 2467189; 17.04.1981.
181. D. L. Rakhmankulov, E. A. Kantor, A. M. Syrkin, N. E. Maksimova, G. I. Rutman, I. M. Belgorodskii, E. M. Sire, USSR Invent. Sert. 573470; 27.10.1977.

182. D. L. Rakhmankulov, N. E. Maksimova, USSR Invent. Sert. 574431; 09.11.1977.
183. J.-C. Combret, M. Larcheveque, Y. Leroux, Bull. Soc. Chim. Fr. **1971**, 3501-3508.
184. A. A. Kirchanov, A. S. Zanina, I. L. Kotlyarevskii, E. M. Shvarts, Trans. Acad. Sci. USSR, **1981**, 909-911 (Russ.).
185. A. A. Kirchanov, I. L. Kotlyarevskii, A. S. Zanina, All-Union A. M. Butlerov Memorial Conf., Kazan. Sept. 15-18 1986. Theses, Kazan, **1986**, p. 133 (Russ.).
186. J. H. Brewster, J. Am. Chem. Soc., **1951**, *73*, 366-370.
187. J. Colonge, H. Robert, Bull. Soc. chim. Fr., **1960**, 463-466.
188. H. C. Brown, J. C. Chen, J. Org. Chem., **1981**, *46*, 3978-3988.
189. K. Sisido, M. Naruse, A. Saito, K. Utimoto, J. Org. Chem., **1972**, *37*, 733-738.
190. W. C. Still, J. C. Barrish, J. Am. Chem. Soc.,**1983**,*105*, 2487-2489.
191. J. Klein, A. Medlik, J. Am. Chem. Soc., **1971**, *93*, 6313-6314.
192. A. Medlik-Balan, J. Klein, Tetrahedron, **1980**, *36*, 299-304.
193. H. C. Brown, D. J. Geoghegan, Jr., J. T. Kurek, G. J. Lynch, Organometal. Chem. Synth., **1970**, *1*, 7-22.
194. S. Sabetay, J. Bleger, Bull. Soc. Chim. Fr., **1930**, 885-894.
195. V. I. Esafov, J. Gen. Chem. (Russ.), **1960**, 30, 3272-3275.
196. V. I. Esafov, L. P. Zhukova, ibid, **1962,** *32*, 2816-2819.
197. V. I. Esafov, ibid, **1963**, 33, 3755-3759.
198. V. I. Esafov, V. N. Dashko, E. M. Marek, ibid, **1964**, *34*, 4094-4096.
199. V. I. Esafov, E. M. Marek, Sci. Repts. Ural Univ., **1969**, 56-60 (Russ.).
200. V.I. Esafov, V.I. Azarova, J. Org. Chem., (Russ.), **1970**, 6, 678-680.
201. E. M. Marek, V. I. Esafov, V. P. Kachalkov, High School Repts. Chem. Engin., **1970**, *13*, 986-988 (Russ.).
202. V. I. Esafov, E. M. Marek, S. I. Kotlyarova, A. V. Malyarenko, N.V. Korzun, ibid, **1970**, *13*, 1144-1146.
203. V. I. Esafov, I. F. Utrobina, ibid, **1970**, *13*, 1154-1156.
204. V. I. Esafov, I. F. Utrobina, N. I. Kiskina, Yu. B. Tuganov, Chem Heterocycl. Comp., (Russ.), **1972**, 295-297.
205. V. I. Esafov, I. F. Utrobina, L. M. Lepikhina, E. M. Karpinskaya, High School Repts. Chem. and Chem. Engin., **1972**, *15*, 382-383 (Russ.).
206. V. I. Esafov, I. F. Utrobina, ibid, **1972**, 15, 456-457.
207. V. I. Esafov, A. A. Vshivkov, J. Org. Chem. (Russ.), **1973**, 9, 235-237

208. V. I. Esafov, A. A. Vshivkov, High School Repts. Chem. and Chem. Engin., **1976**, *19*, 224-225 (Russ.).
209. H. R. Timotheus, P. I. Pehk, U. J. Mäeorg, M. K. Karro, V. A. Eiber, J. Org. Chem., (Russ.), **1989**, 25, 2295-2301.
210. J. Michel, P. Canonne, Canad. J. Chem., **1971**, *49*, 4084-4095.
211. E. J. Corey, G. N. Widinger, J. Org. Chem., **1975**, *40*, 2975-2976.
212. J. Barluenga, J. F. Fananas, M. Yus, J. Org. Chem., **1979**, *44*, 4798-4801.
213. K. Utimoto, K. Uchida, H. Nozaki, Chem. Lett., **1974**, 1493-1496.
214. K. Utimoto, K. Uchida, H. Nozaki, Tetrahedron, **1977**, *33*, 1949-1952.

1,3-DIOOLIDE SÜNTEES

H. Timotheus

Resümee

Käesolevas töös on antud ülevaade 1,3-dioolide põhilistest sünteesimeetoditest süstematiseerituna sünteesi strateegia, eeskätt viimase ja eelviimase etapi järgi. 1,3-Dioole vaadeldakse 1,3-propaandiooli derivaatidena, kus iga süsinikuaatomi juures võib olla kuni 2 asendusrühma:

$$R^1R^2C(OH)CR^3R^4C(OH)R^5R^6$$

Kõik võimalikud 1,3-dioolide struktuurid on ära toodud tabelis 1, kus on ära näidatud ka kiraalsete tsentrite arv vastavates struktuurides. Sünteesimeetodid on jagatud 2 suurde rühma: 1) meetodid, millede viimases etapis toimub redutseerimine või hüdrolüüs; süsinikskelett ja enamasti ka funktsionaalsete rühmade asukohad on juba varem formeeritud; 2) meetodid, millede puhul süsinikskelett formeerub viimases etapis (sageli koos teise funktsionaalse rühmaga). Meetodite käsitlemisel on põhilisteks kriteeriumiteks võimalikud produktide struktuurid, meetodi kasutatavus ja lähteainete kättesaadavus. Paljude meetodite puhul on vaadeldud lähteainete sünteesi võimalusi ja lähteainete modifitseerimist (alküülimine).

Käsitletakse ka mitmesuguseid uusi, mittetraditsioonilisi 1,3-dioolide sünteesi meetodeid (allüülalkoholide funktsionaliseerimised, bifunktsio-

naalsete liitiumorgaaniliste ühendite kasutamine jt.), mida kasutatakse sageli suure stereoselektiivsuse saavutamiseks keerulisemate 1,3-polüoolsete süsteemide sünteesil. Stereoselektiivsuse probleeme käesolevas töös eraldi vaadeldud ei ole, kuna see nõuab käsitlemist omaette ülevaatena. Tähelepanu on juhitud asjaolule, et mitmed vanemad, kuid perspektiivsed ja põhjalikult läbiuurimata sünteesimeetodid 1,3-dioolide saamiseks on seoses järsult kasvanud huviga uute, stereoselektiivsete meetodite vastu teenimatult unustusse jäänud.

SEX ATTRACTANTS FOR SOME FOREST *LEPIDOPTEROUS* SPECIES

T. Rodima, N. Lissov*, M. Saar
Department of Chemistry, University of Tartu
*Tatarstan Forestry Experimental Station

Abstact: Mixtures of Z- and E-8-dodecenylacetate, Z- and E-9-dodecenyl-acetate and respective E-9 alcohol, E-10-dodecenylacetate, dodecylacetate as well as Z-9, E-11-tetradecadienylacetate were tested for their capacity of sex attracting forest pests such as *Rhyacionia duplana, Blastesthia turionella, Dioryctria abietella, Cydia coniferana, C. strobilella, Semasia ratzeburgiana* and *Petrova resinella*. Mass trapping of *B. turionella* and *C. coniferana* males to control the forest pest population was tested.

Earlier work on pheromone materials for forest pest monitoring in Tartu University has yielded preparations for bark beetle *Ips typographus L., I. duplicatus Sahlb. and for Lepidopterous Tortrix viridana L., Panolis flammea* Schiff. and *Rhyacionia buoliana* Den.-Schiff.

This paper is devoted to sex attractants for spruce and pine seed, cone and shoot pests. The blends of pheromone compounds were worked out by Tartu University chemists in cooperation with the research workers of the Tatarstan Forestry Experimental Station (Russia) in 1990-1993.

In 1990 and 1991 field tests were carried out in fifteen-year-old pine plantations near pine forests in the "Mari Chodra" National Park (Republic of Mari El, Russia). In 1992 and 1993 field tests were conducted out in nine-ten-year-old pine plantations of about 15 ha in Republic of Tatarstan (Russia). It is to be noted that there were also few spruce seed trees in the area. Autumn inspections of the plantations revealed some *Rhyacionia duplana* Hbn. (about 1%), *Blastesthia turionella* L. (about 3%), *Cydia coniferana* Sax. (about 3%) and some others pests (less than 1%) damage.

M. Toth has reported E-9-dodecylacetate [1] to be the sex pheromone for *R. duplana*. It is also a component of the pheromone for *B. turionel-*

la [2]. E-9-dodecylacetate and Z-9-dodecylacetate are the pheromone compounds for *Petrova resinella* L. [2]. E-8-dodecylacetate is a pheromone component for *Cydia strobilella* L. [3] and Z-9,E-11-tetradecadienylacetate is that for *Dioryctria abietella* F. [4,5]. In the field experiments in Tatarstan these species and *Semasia (Zeiraphera) ratzeburgiana* Sax. were caught in pheromone traps. The same species as well as *Cydia coniferana* Sax. were found in traps in the Mari El Republic. According to the pheromone list [1,3] and [2] the pheromone for *C. coniferana* is a mixture of E-8-dodecylacetate and E-10-dodecylacetate in relation of 9:1 or 1:1.

All components of the sex attractants were synthesized at the Laboratory of Organic Synthesis of Tartu University according to Schemes 1 and 2. Pheromone preparations were made by carrying the pheromones onto the inner surface of 17 mm long pieces of medical rubber tubes of 1,5x4 mm. The dispensers were placed on the sticky bottoms (143 cm^2) of laminated cartoon delta traps. The traps were hung in the trees at about 2m from the ground in the middle of April and kept there until the beginning of August. There were three replications for each preparation. The identification of species was made by one of us in cooperation with the research workers of the Leningrad Zoological Institute.

Some preliminary field experiments to test the pheromone preparations were also made in the Forest Institutes of Latvia, Lithuania, Ukraine and Moscow.

In 1990 and 1991 field experiments were made to control *B. turionella* and *C. coniferana* populations in pine plantations.

Scheme 1. [6]

$$HC \equiv CLi + Br(CH_2)_mOTHP \xrightarrow{liq.NH_3/THF} HC \equiv C(CH_2)_mOTHP$$

$$CH_3(CH_2)_2Br + LiC \equiv C(CH_2)_mOTHP \xrightarrow{liq.NH_3/THF}$$

$$\rightarrow CH_3(CH_2)_2C \equiv C(CH_2)_mOTHP \xrightarrow[2)[H].\ a)P_2Ni;\ b)LiAlH_4]{1)MeOH;\ H^+}$$

$$\rightarrow CH_3(CH_2)_2\ \overset{Z\ or\ E}{CH = CH}\ (CH_2)_mOH \xrightarrow{Ac_2O;\ Py}$$

$$\rightarrow CH_3(CH_2)_2\ \overset{Z\ or\ E}{CH = CH}\ (CH_2)_mOAc, \qquad \text{where } m = 6, 7, 8.$$

Scheme 2.

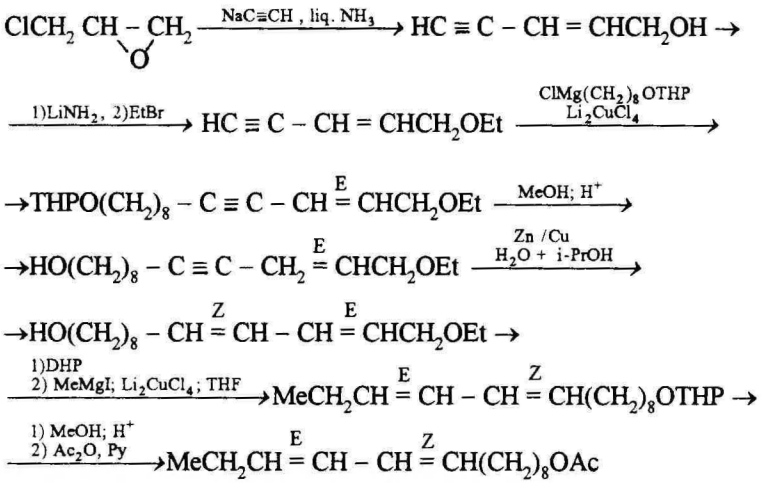

RESULTS AND DISCUSSION

Tables 1 and 2 present the catches of specimens and the composition of preparations tested in the field experiments.

R. duplana and *B. turionella* were attracted to all preparations containing blends of E-9-dodecenylacetate and E-9-dodecenylalcohol. The preparations that proved to be effective are presented in Table 1. *R. duplana* failed to demonstrate any preference to acetate/alcohol relations of 19:1, 9:1 or 4:1 or to the pheromone amount in the preparations (1 mg or 0.41 mg). Dodecylacetate in 0.1 to 2 mg quantities per dispenser seemed to have little effect on the capture of *R. duplana*, the 0.1 mg dose per dispenser somewhat reduced *B. turionella* capture. We think that preparations PB-81 and PB-91 A/2 can be effectively used to monitor *R. duplana* and *B. turionella*, as the flight of the former ends in the middle of May and that of the latter just begins at that time.

Dioryctria abietella v. pinetella Rodz. was attracted to blends of E-9-dodecenylacetate and Z-9-dodecenylacetate, and more stable and species specific were preparations PB - 181 and PB - 1810A. Contrary to expections, no specimens of the pest, we consider to be *D. abietella v.*

pinetella, were attracted to lures containing pure Z-9, E-11-tetradecadienylacetate (0.1–0.5 mg) or its blends with Z-9-tetradecenylacetate and/or dodecylacetate, except in the Ukraine, in 1991 where 3–5 specimens were found attracted to preparations D-10 and DA-50 (see Table 2 for compositions).

However, in the Mari National Park, the preparations containing Z-9, E-11-tetradecadienylacetate did attract *Cydia coniferana.* 0.1–0.9 mg of Z-9-tetradecenylacetate added to 0.9–0.1 mg of Z-9, E-11-tetradecadienylacetate did neither increase nor decrease the capture. Pure Z-9-tetradecenylacetate attracted about 60% of the capture of 0.5 mg dose of pure Z-9, E-11-tetradecadienylacetate In Tatarstan *C. coniferana* was not attracted to these compounds and the autumn inspection of plantation did not reveal any C. coniferana damage.

Semasia (Zeiraphera) ratzeburgiana Sax. was well attracted to traps baited with Z-8-dodecenylacetate.

The preparation effective in trapping. *Petrova resinella* L. in 1988, 1990 and 1992 was EA - 91 (see Table 2). The low captures of 1991 and 1993 can be explained by *P. resinella* being of two-year generation.

Some small catches of other species were occasionally noted, such as *Cydia pactolana* Zell., *Dioryctria mutatella* Fucks., *D. splendidella* H.-S. In Latvia some nontarget species, such as *Cnephasia alticolana* H.-S. (seria EA-preparations) and noctuid *Anaria cordigera* Thnbg (seria DA) were caught.

In 1990 and 1991, a mass trapping of *B. turionella* and *C. coniferana* males was carried out in the nine-to-ten-year-old pine plantations of the "Mari Chodra" National Park to control the pest population. Delta traps with 476 cm^2 of sticky bottom area were used. The traps were hung into the top portion of the tree crown. The exposition lasted fifty days. As seen in Table 3, the results are promising. However, to be used in major forest protection projects further, large-scale experiments are needed.

Table 1. Sex attractants for *R. duplana, B. turionella* and *D. abietella v. pinetella.*

Species	Preparations and compounds * (mg)					
	PB-81 12E9Ac 0.8 12E9OH 0.2	PB-81-2 12E9Ac 0.8 12E9OH 0.2 12Ac 0.3	PB-91A 12E9Ac 0.95 12E9Ac 0.95	PB-91A/2 12E9Ac 0.40 12E9OH 0.015	PB-181 12E9Ac 0.8 12Z9Ac 0.2	PB-181OA 12E9Ac 0.2 12Z9Ac 0.05 12Ac 0.2
	Number of specimens caught per trap per flight period					
R. duplana						
1991	51.3	–	–	–	–	–
1992	35.0	69	41	–	–	–
1993	67 ± 6.2	9 ± 1.4	47 ± 8.2	58 ± 9	–	22 ± 4.0
B. turionella						
1991	8.3	2.7	25.7	23.7	–	–
1992	13	19	28	–	2	4
1993	7 ± 0.9	7.9 ± 0.9	35 ± 6.0	12 ± 1.9	–	6 ± 1.1
D. abietella						
1991	–	–	–	–	9.0	25.7
1992	0	0	0	0	10	14
1993	0	0	0	0	–	9 ± 1.1

* The names of chemical compounds are encoded as follows: the first number indicates chain length, Z and E indicate the configuration of double bond(s) and the number following Z or E gives the position of double bond. Ac=acetate, OH= alcohol.

Table 2. Sex attractants for *C. Coniferana, C. strobilella, S. ratzeburgiana* and *P. resinella.*

Preparation and composition * (mg)			Species	No. of specimens caught per trap per flight period in			
				1990	1991	1992	1993
DA-10	14Z9E11Ac	0.1	*C. conifererana*	153±9	27.2		
DA-50	14Z9E11Ac	0.5	— " —	165±12	45.3		
CC-10	12E8Ac	0.1	*C. strobilella*			213	
	12E10Ac	0.1					
CC-171	12E8Ac	0.7	— " —			259	
	12E10Ac	0.3					
CC-191	12E8Ac	0.9	— " —				143±10
	12E10Ac	0.1					
CP-101	12Z8Ac	1.0	*S. ratzeburgiana*	52±7		88	42±4
CP-101/4	12Z8Ac	0.25	— " —				30±5
EA-61	12E9Ac	0.5	*P. resinella*	50±6		33	18±2
	12Z9Ac	0.5					
EA-91	12E9Ac	0.4	— " —	42±5		169	
	12Z9Ac	0.6					
EA-131	12E9Ac	0.3	— " —	42±5		31	
	12Z9Ac	0.7					
EA-161	12E9Ac	0.6	— " —			131	
	12Z9Ac	0.4					

*See the note at the end of Table 1.

Table 3. Effectivity of sex attractants in forest pests control

Species	Attractant composition*(mg)	No.of traps per ha	No. of moths caught per trap		% of damaged trees	
			1990	1991	1990	1991
Blastesthia turionella	12E9Ac 0.95	1	143	135	0.7	0.6
	12E9OH 0.05	2	120	117	0.3	0
	12Ac 1.0	3	99	61	0	0
		5	85	2	0	0
	Control	3	0	0	5.7	5.0
Cydia coniferana	14Z9E11Ac 0.1	1	864	397	0.3	0.4
		2	560	245	0	0
		3	318	160	0	0
		5	215	105	0	0
	Control	3	6	3	7.3	4.8

* see the note at the end of Table 1.

Acknowledgement. We thank Priit Vaher and his group for providing us with compounds used in this study.

REFERENCES

1. H. Arn, M. Toth, E. Priesner, "List of Sex Pheromones of Lepidoptera and Related Attractants" OILB-SROP, Paris, **1986**.
2. C. J. H. Booij, S. Voerman, J. Chem Ecol., **1984**, *10* (1), 135-144
3. 1990 year supplement to Ref.1.
4. C. Löfstedt, J. C. Van Der Pers, J. Löfqvist, B. C. Lanne, Ent. Exp and Appl., **1983**, *34*, 20-26.
5. C. Löfstedt, J. Löfqvist, A. Roques, Proc. Sec. Int. Cone and Seed Insects Working Party Conference, France, 3-5. sept. **1986**, pp. 1-9.
6. I. Gritchanov, P. Vaher, Proc. Acad. Sci. Estonia ser. Biol., **1989**, *38*, No. 3, 185-188.

MÕNINGATE METSA KAHJUSTAVATE LIBLIKATE SUGUATRAKTAKTIDEST

T. Rodima, N. Lissov*, M. Saar
Tartu Ülikool, *Tatarimaa Metsa Eksperimentaaljaam

Resümee

Käesolevas töös on esitatud katseandmed mõnede kuuse ja männi seemne-, käbi- ja võrsekahjurite suguatraktaktide-suguferomoonide kohta. Need on saadud 1990–1991 a. Mari El Vabariigi (Venemaa) rahvuspargis 15 aastastes männiistandikes ja 1992–1993 a. Tatarimaal (Venemaa) 9–10 aastastes männiistandikes läbi viidud katsetustel. Feromoonina toimivad ained on sünteesitud Tartu Ülikooli orgaanilise sünteesi laboris. Feromoonpreparaadid valmistati ainete segude immobiliseerimise teel 1.7 cm pikkustele meditsiinilise kummi voolikutükikeste sisepinnale. Kasutati kartongist prismakujulisi Atrakon A tüüpi püüniseid. Feromoonpreparaat asetati püünise põhjatahu liimistatud pinnale. Püüniste eksponeerimine kestis aprilli keskelt kuni augusti alguseni. Tehti kolm paralleelkatset. Püütud liblikate liigi määramisel kasutati Leningradi Zooloogia Instituudi teadlaste abi. Preparaatide koostis ja katsetulemused on koondatud tabelitesse 1 ja 2 (vt. inglisekeelne tekst)

Liikidele *Rhyacionia duplana* Hbn. ja *Blastesthia turionella* L. olid atraktiivseteks kõik preparaadid, mis sisaldasid E-9-dodetsenüülatsetaati ja E-9-dodetsenüülalkoholi. Läbi aastate stabiilsemaid preparaate PB-81 ja PB-91A/2 võiks soovitada nende liikide lendluse ja arvukuse järgmiseks silmas pidades asjaolu, et *R. duplana* lendlus lõpeb mai keskel ja *B. turionella* lendlus samal ajal just algab.

Liik, mis meie määramise järgi on *Dioryctria abietella v. pinetella* Rodz. lendas E-9-dodetsenülatsetaadi ja Z-9-dodetsenüülatsetaadi segule (stabiilsemad ja liigispetsiifilisemad preparaadid olid PB-181 ja PB-1810 A) ning ei lennanud preparaadile, mille koostises oli Z-9, E-11-tetradekadienüülatsetaat. Viimane aine on leitud liigi *D. abietella* F. näärmetest ja on osutanud talle atraktiivseks ka välikatsetustes [4, 5]. Mari Rahvuspargis läbi viidud katsetustes osutusid Z-9,E-11 tetradekadienüülatsetaati sisaldavad preparaadid atraktiivseteks liigile *Cydia coniferana* Sax. Viimatimainitule oli atraktiivne ka Z-9-tetradetsenüülatsetaat, mille lisamine dieensele komponendile aga ei suurendanud ega vähendanud püütud liblikate hulka. Kirjanduse [1,2,3] andmetel on *C. coniferana* feromooniks E-8-dodetsenüülatsetaadi ja E-10-dodetsenüülatsetaadi segu. Meil osutus selline segu atraktiivseks liigile *C. strobilella* L., kusjuures puhas E-8-dodetsenüülatsetaat seda liiki ei püüdnud. *Semasia ratzeburgiana* Sex. lendas hästi ühekomponentsele preparaadile (toimeaine Z-8-dodetsenüülatsetaat) ning liik *Petrova resinella* Z- ja E-9-dodetsenüülatsetaadi segule.

1990 ja 1991 a. viidi läbi välikatsetused liikide *B. turionella* ja *C. coniferana* arvukuse reguleerimiseks isaste vaakumi meetodil. Esialgsed tulemused osutusid lootustandvateks (vt. tabel 3).

PHOSPHORUS REMOVAL IN SOME SEWAGE PLANTS IN ESTONIA

A. Pruks, T. Tenno
Institute of Physical Chemistry, University of Tartu

Abstract: Phosphorus (P) removal in some sewage plants having basins with high energy density (HED) aerators operating with circulating flow and basins with conventional aeration operating in parallel was studied. The P content of activated sludges, phosphate release in anaerobic conditions, the alteration of P content during continuous aeration in laboratory and P removal effeciency in basins with conventional and HED aerators were studied. In some cases several features of the enhanced biological phosphorus removal (EBPR) process were observed, but in real conditions the established EBPR process does not take place. The reasons for these phenomena are discussed.

INTRODUCTION

Biological phosporus removal by activated sludge is noticeably cheaper than by the precipitation method which is widely used, as precipitation reagents are rather expensive. But in conventional biological sewage treatment plants phosporus removal is only 20-30 % and the method is not sufficient to meet the low effluent P concentrations required to prevent eutrophication [1, 2].

During the biological treatment stage, the only way to remove P is the uptake or precipitation by the produced biomass. In conventional biological treatment process, the P content of sludge is about 2% [2].

The P removal can be enhanced by introducing an anaerobic zone at the front end of the activated sludge process. In treatment plants with enhanced biological P removal polyphosphate-containing bacteria are enriched in the sludge [3]. The activated sludges of this kind have a high P content, up to 11% [4] and even 18% [5, 6].

In the biological sewage plants operating with HED aerators, the O_2 concentrations are very different in particular parts of basins and there are zones where the O_2 concentration is zero. This situation is

analogical to the main characteristic of the EBPR process - anaerobic/aerobic sequence of both waste water and sludge. There are some sewage plants in Estonia operating with HED aerators. P removal in such plants in Põlva and Viiratsi was investigated. Testing the hypothesis upon enhanced P removal in sewage plants operating with the above-mentioned aerators was the main purpose of this work.

EXPERIMENTAL

Activated sludges were obtained from the Põlva and Viiratsi sewage treatment plants. The Põlva sewage plant was fed with municipal wastewaters and dairy factory wastewaters. One basin with two HED aerators and seven basins with conventional (bottom) aeration were operating in this plant. The O_2 concentration in seven basins with conventional aeration near the outlet was different, 1.8-8.8 mg/l, in the basin with HED aerators the O_2 concentration was different in various parts of the basin, in the depth near the input there was not any detectable O_2. The pH in the basin with HED aerators was 6.7-6.8; in the other basins more than 7.1. In the Viiratsi sewage treatment plant, 3 basins with conventional aeration and 1 basin with two HED aerators were operating. Plant was fed with pig-breeding waste waters. The O_2 concentration in a large part of the basin with HED aerators was 0.1-0.2 mg/l.

For all determinations the activated sludges were centrifuged and washed with destilled water. For dry weight determination the sludge was dried at 100-105°C for 24 h. Total phosporus was quantified by the vanadomolybdophosphoric acid colorimetric method after persulfate digestion, according to APHA (1985) [7]. For the determination of phosphate release, the sludge was incubated for 24 h with 0,6M CH_3COONa solution, before incubation the suspension was gassed with Ar.

In laboratory the sludge was fed with a medium containing (in g/l) 0.32 NH_4Cl, 0.6 $MgSO_4 \cdot 7H_2O$, 0.07 $CaCl_2 \cdot 2H_2O$, 0.1 EDTA and 2 ml of trace metal solution containing 1.5 $FeCl_3 \cdot 6H_2O$, 0.15 H_3BO_4, 0.03 $CuSO_4 \cdot 5\ H_2O$, 0.03 KJ, 0.12 $MnCl_2 \cdot 4H_2O$, 0.06 $Na_2MoO_4 \cdot 2H_2O$, 0.12 $ZnSO_4 \cdot 7H_2O$, 0.15 $CoCl_2 \cdot 6H_2O$ [4] and 0.022 KH_2PO_4.

RESULTS

In general, the P content of activated sludge from the Põlva plant was relatively low and unstable in time, from 1.7 to 2.05 % P of dry weight. Such P content does not indicate any enhanced P removal. Mean P content of activated sludge from the basin with HED aerators was not higher than for sludges from other basins.

The P content of activated sludges from the Viiratsi sewage plant was higher and different in the basins with HED aerators and with conventional aeration. In the latter ones, the P content was on the average 2.35% and for the sludge from the basin with HED aerators 2.8%.

In spite of low P content in the sludges from the Põlva plant, the P release has been observed for all activated sludges in anaerobic conditions (Tab. 1.) Surprisingly, relative P release was higher for the Põlva activated sludges (16% to 20% of the whole P). P release from the Viiratsi activated sludges was 13% to 17%. This amount is obviously not in connection with polyphosphate accumulation, but with other kinds of P. Evidence for this is a remarkable P release without acetate and bubbling with Ar.

The efficiency of P removal in the Põlva plant fluctuates in time, but is similar enough for basins with conventional aeration and HED aerators. No connection between P removal efficiency and P content in activated sludges is detected. For example, P removal efficiency 64% for the basin with conventional aeration and 65% for the basin with HED aerators was detected simultaneously with the P contents of sludges 1.75% for the first and 1.7% for the second case, but the increase of the P content of sludge to 2.05% (conventional aeration) was detected at the same time with the decrease of P removal efficiency to 47%. P removal is to a considerable extent connected with influent P content. The decrease of influent P content has little influence upon effluent P content and, therefore, P removal decreases.

In laboratory, the activated sludges were aerated and fed with a medium containing P, as described above. The P content of the Põlva activated sludge increased to a negligible extent, but the P content of the Viiratsi activated sludge increased (in some days) to 4.6%. This indicates that the Viiratsi activated sludge can accumulate more P than in real conditions in the Viiratsi sewage plant.

Table 1.Activated sludge P content and phosphate release in anaerobic conditions

	Põlva plant		Viiratsi plant	
	HED aerators	Conventional aeration	HED aerators	Conventional aeration
P content (mg P/g dry weight)	17	17.5	28	23.5
Phosphate release (% of total P content)	16.3	19.8	13.5	16.4

DISCUSSION

The common characteristics of all EBPR processes are that the biomass passes through the anaerobic stage, preferentially while it is in contact with sewage organic substrate [8]. During this stage, the solution ortophosphate concentration increases. In the aerobic zone, the ortophosphate concentration decreases to a level lower than in the influent. The activated sludge P content correspondingly decreases in the anaerobic zone and increases in the aerobic zone. The phosphate release in the anaerobic zone is accompanied with the accumulation of poly-β-hydroxybuturate (PHB) [9] or poly-β-hydroxyvalerate (PHV) [10]. Suitable substrates for such accumulation are simple soluble organics, primarily acetate. The energy required for the storage of PHB or PHV is produced by decomposing polyphosphate from an intercellular store. Good P removal in the aerobic zone is obtained only if a sufficient P release in the anaerobic zone is observed [11, 12]. The required conditions are not only the absence of significant dissolved oxygen, but NO_3^- concentrations, too. Nevertheless, several authors have observed P release in the presence of nitrate, if there is any acetate in the solution. This means that the availability of acetate rather than the absence of nitrate allows polyphosphate organisms to release P. But the presence of nitrate disturbs anaerobic acetogenesis and acetate will not be formed. When all nitrates have been consumed by the denitrification process, facultative aerobic/anaerobic bacteria will switch over to fermentative metabolism [2].

Evidently, the presence of dissolved oxygen in the solution hinders P release. On the contrary, even small O_2 concentrations are sufficient to induce P uptake. However, in the San Antonio Rilling plant where the EBPR process was first observed [13], seems that the O_2 concentration in the first part of the plant was not zero. Obviously the conditions in the sludge flocks are not identical to these in the bulk solution [14]. When sludge organisms are brought together with sewage, O_2 is consumed very rapidly and in the flocks there can be anaerobic conditions, despite the O_2 presence in the solution.

The EBPR process establishes after some weeks of sludge cycling, during this time sludge is enriched with polyphosphate-containing bacteria. These are present in conventional activated sludges, too, but their quota is not high and the conditions are not suitable for polyphosphate accumulation. Alternating aerobic/anaerobic conditions are more suitable for polyphosphate-containing organisms, capable of accumulating carbon storage products (PHB/PHV) as a competitive tool. In spite of the presence of the aerobic zone in the first end of the HED basin in the Põlva sewage plant, no EBPR process was observed. Probably, one basin with HED aerators and the aerobic zone is not sufficient to enrich sludge with polyphosphate-containing bacteria, as there are seven basins with conventional aeration and activated sludge is common for all basins. The greater part of sludge circulates through basins with conventional aeration, and the anaerobic zone residence time compared to the aerobic zone residence time is short.

In the Viiratsi plant, the higher sludge P content and difference between basins with conventional aeration and basin with HED aerators indicates the accumulation of "superfluous" P. Although there are 3 basins with conventional aeration, and activated sludge is common for all basins, the area with low O_2 concentration is large. Probably there are anaerobic conditions in the sludge flocks, though there is a small amount of dissolved oxygen at measuring points in the bulk solution. As the P content by aeration in laboratory increases, it seems that the sludge retention time in the aerobic zone is not sufficient to achieve the maximum P content for this activated sludge. High O_2 concentrations in the basin with HED aerators are only in the aerators and near them. At the probe point near the outlet, there is low O_2 concentration. Understandably, the sequence of aerobic/anaerobic zones is important and in the Viiratsi plant it seems not to be favourable. It is essential that the anaerobic zone precedes the aerobic zone. In the Põlva plant, in the

basin with HED aerators this sequence exists, in the Viiratsi plant the location of zones and the strict anaerobic zone strech are indistinct.

It seems as if the Viiratsi activated sludge is capable of accumulating more P than practically in the plant. Unfortunately, the location of HED aerators does not make possible the formation of a large zone with high O_2 concentration at the last end of the basin, which can increase P removal. In the Põlva plant the higher importance of the basins with HED aerators can generate the EBPR process, as in the existing basin the necessary aerobic/anaerobic regime takes place.

CONCLUSIONS

Our conclusions from this study indicate that activated sludges capable of accumulating "superfluous" P can be extended in sewage plants with HED aerators. But in the Põlva sewage plant no EBPR process takes place. In the Viiratsi sewage plant some features of the EBPR process are revealed, but in real conditions the sludge does not accumulate the biggest possible amount of P for this sludge. Summarily, the Estonian sewage plants with HED aerators do not work under the real EBPR regime. Nevertheless, the Viiratsi plant sludge can accumulate more P than conventional activated sludge and if the aerobic/anaerobic zones are located more suitably, the EBPR process can take place. Unfortunately, to achieve such a location in the existing basin seems to be unrealizable without the rearrangement of aeration. But we suppose that in such type of basins as in Põlva, exploitation of basins with HED aerators only make it possible to achieve the occurrence of the EBPR process.

REFERENCES

1. J . Bever, A. Stein, H. Teichmann, Weitergehende Abwasserreinigung, R. Oldenbourg Verlag, München, Wien, **1993**, pp. 309-330.
2. M. T. Meganck, G. M. Faup, In D. L. Wise (Ed.), Biotreatment Systems, Vol. 3, CRC Press, Boca Raton, Florida, **1988**, pp. 111-203.
3. L. Buchan, Wat. Sci. Technol., **1983**, *15*, 87.
4. K. J. Appeldoorn, G. J. Kortsee, A. J. Zehnder, Wat. Res.,**1992**, *26*, 453.

5. M. C. Wetzel, R. E. Loewenthal, G. A. Ekama, G. v. R. Marais, Wat. Sth. Afr., **1988**, *14*, 81.
6. M. C. Wetzel, G. A. Ekama, R. E. Loewenthal, P. L. Dold, G. v. R. Marais, Wat. Sth. Afr., **1989**, *15*, 71.
7. APHA et al. Standard Methods for the Examination of Water and Wastewaters, 16th edition, Washington, **1985**, pp. 442-446.
8. J. L. Barnard, Water Wastes Eng., July, 1974, 33, August, **1974**, 41.
9. G. W. Fuhs, M. Chen, Microb. Ecol., **1975**, *2*, 119.
10. Y. Comeau, W. K. Oldham, K. J. Hall. In R. Ramadori (Ed.), Advances in Water Pollution Control: Biological Phosphate Removal from Wastewaters, Pergamon Press, Oxford, **1987**, pp. 39-55.
11. J. L. Barnard, Wat. Sth. Afr., **1976**, *2*, 136.
12. H. A. Nicholls, D. W. Osborn. J. Wat. Pollut. Control Fed., **1979**, *51*, 557.
13. D. Vacker, C. H. Connell, W. N. Wells, J. Wat. Pollut. Control Fed., **1967**, *39*, 750.
14. G. Schön, S. Geywitz, M. Mertens, Wat. Res., **1993**, *27*, 349.

FOSFORI ÄRASTAMINE MÕNINGATES EESTI HEITVEEPUHASTITES

A. Pruks, T. Tenno

Resümee

Käesolevas töös on uuritud fosfori ärastamist heitvetest Põlva ja Viiratsi biopuhastites, kus töötasid paralleelselt nii traditsioonilise aeratsiooniga kui ka kõrge energiatihedusega aeraatoritega varustatud basseinid, kus toimub intensiivne hapnikuga küllastamine suure läbivooluhulgaga aeraatorites. Kuna viimatimainitud aeraatorite puhul on väljaspool aeraatoreid lahustunud hapniku kontsentratsioon madal ja võib esineda anaeroobseid alasid, on sellistes puhastites võimalik kõrgendatud bioloogilise fosfori ärastamise (KBFÄ) mehhanismi esinemine. Vahelduvate anaeroobsete/aeroobsete tingimuste esinemisel aktiivmuda rikastub polüfosfaate akumuleerivate bakteritega, tõuseb muda fosforisisaldus ja fosfori ärastamise efektiivsus. Põlva puhastis

mingeid KBFÄ tunnuseid ei avastatud. Põhjuseks on ilmselt asjaolu, et kõrge energiatihedusega aeraatoritega varustatud basseini osatähtsus kogu süsteemis oli liialt väike (üks bassein kaheksast). Viiratsi puhastusseadmes seevastu vaatamata rangelt anaeroobsele tsoonile [illegible] esineb mõningaid KBFÄ mehhanismi iseloomustavaid tunnuseid. Viiratsi aktiivmuda fosforisisaldus on suhteliselt kõrge, kuigi madalam tavalt väiksem kui laboratooriumis sama muda aeroobsel saavutatud fosforisisaldus. Põhjuseks on ilmselt hästiaereeritava tsooni väike ulatus ja mittesobiv paiknemine. Seega hoolimata uurimuse [illegible] selgeltväljendunud KBFÄ mehhanismi mitte-esinemisest võiks teatud tingimustes kõrge energiatihedusega aeraatoritega puhastites siiski mehhanism siiski toimida.

RECOVERY OF SOME ORGANIC COMPOUNDS FROM VAPOUR SAMPLING CHARCOAL ADSORBENT

L. Saarinen, M. Reinik
Institute of Occupational Health, Helsinki,
Tartu Public Health Service

Abstract: In this work a convenient method for validating the recovery of solvent vapours from adsorbent materials is described. The method is applicable to both active and passive sampling systems, used by occupational health laboratories for the quantification of vaporous workplace pollution. The adsorption capacity of charcoal bed is different for various compounds and depends on the concentration of given substances in the gas phase. The bias caused by incomplete desorption is minimised by correcting the recovery found in the experiment by desorption efficiency.

INTRODUCTION

The general method used by many occupational health laboratories for the quantification of vaporous workplace pollution uses sampling on charcoal adsorbent, and the subsequent desorption with solvent for further gas chromatographic analysis. The problem, while using this method, arises from a poor recovery of some solvents from the adsorbent because of incomplete adsorption or desorption. In this work the recovery of some organic compounds was examined as a function of their amount adsorbed on charcoal bed. The theory on the adsorption of vapours applied in occupational hygiene monitoring is discussed. We also describe a convenient method which can be used to validate the recovery of vapours when sampled with adsorption materials. Our method is applicable to the studying of adsorption and desorption problems both for active and diffusive sampling systems. The advantage of this method to the study of failures of diffusive sampling is that there

is no need to know the sampling rates of diffusive samplers in this stage of the study.

Adsorption and desorption

Charcoal is a good adsorbent of sampling non-polar organic substances from the air; polar compounds are also adsorbed but problems arise in connection with desorption efficiency, i.e. the aliquot of an analyte desorbed from the adsorbent. By the term of recovery of adsorbed compound we mean the total yield of sampling, analysis and sample preparation, including desorption efficiency. Recovery is decreased by a low desorption efficiency, but also many other factors may interfere, such as adsorption capacity, humidity, temperature, stability of adsorbed compounds and time of storage [1]. Often the recovery depends on the amount of collected sample [2] and is different for a single component to the same component in a mixture [3, 4].

The adsorption capacity of charcoal depends on the structure of micropores of charcoal, i.e. pores with the diameter less than 2 nm. The surface area of the best sorts of coal is about 1000 m^2/g and, on average, 70-75 % of the surface contains micropores. The adsorption on the graphic-like (hydrophobic) part of charcoal is mainly governed by the van der Waals forces. The compounds capable of electron exchange can be adsorbed both on the hydrophobic part of the surface or on the surface oxides of charcoal. When water is present in the sampling environment in low concentrations, its molecules are mainly adsorbed on surface oxides. In that case, the water molecules act as secondary sites of adsorption. In the case of a high concentration of water present, capillary condensation takes place on the surface of charcoal. Condensed water makes it difficult to transport the molecules of organic compounds to the adsorption sites in the micropores, due to the fact that the adsorption capacity of charcoal is decreased [5].

In the desorption process, the adsorbed molecules have to be displaced from the surface of the adsorbent. There are two main methods of desorption mainly used in industrial hygiene: thermodesorption and desorption by extraction with a suitable solvent [6]. When charcoal is used for air sampling, deposition by a liquid solvent is used because counteractions of collected compounds may occur at high temperature needed for thermodesorption. Most frequently used solvent is carbon disulphide that is very effective in displacing non-polar molecules from

the hydrophobic part of charcoal [7]. In addition to that, the advantage of this solvent is also the giving of a low signal in the flame ionisation detector. However, carbon disulphide cannot interact with surface oxides, so the desorption of polar molecules is not complete. This shortcoming has been improved by adding a polar solvent to carbon disulphide [8]. Polar solvent increases the solvatation ability of carbon disulphide and, thereby, decreases intermolecular forces between polar molecules.

Currently, there are many techniques for determining the recovery and the desorption efficiency of compounds, using either static or dynamic approaches [9]. Usually, desorption efficiency is determined injecting a known amount of analyte or calibration stock solution directly a onto an unexposed adsorbent in the sampling device, allowing it to stand overnight, with a suitable solvent and analysing the solution by a gas chromatograph.

Another technique for the determination of desorption efficiency is the phase equilibrium method [10] which approaches the equilibrium from the direction opposite to other methods. The unexposed adsorbent is added into the standard solution. In a closed system, consisting of desorbent liquid and solid adsorbent, the analytes are believed to reach an equilibrium between solid and liquid phases.

A static method for determining the recovery of substances was used in this work: a known amount of analyte mixture was injected into a gas-tight vessel containing charcoal. This static system was left to stay until the liquid was vaporised and the equilibrium was obtained between gaseous and solid phases. Because the yield is also affected by interference between the components during adsorption, the measured parameter is a different parameter than only desorption efficiency

More exact results are obtained when gas mixture with a known concentration is driven through the layer of the adsorbent. This dynamic method matches exactly field air sampling conditions but requires a continuos system for the preparation of standard vapour mixtures. The accuracy and reproducibility of these methods depend on the way used for introducing the components to the adsorbent.

In case of the existence of such kind of equilibrium in it, it is possible to draw up a relation between desorption efficiency DE_i and the constant of equilibrium K_i:

$$1/DE_i = K_i M_S/M_l + 1$$

where M_S is mass of the sorbent and M_l mass of the solvent. The given equation connects desorption efficiency with the amount of the solvent and the sorbent. The value of *DE* obtained by this method is used for correcting the results of determinations of the solvent vapors content in the air.

EXPERIMENTAL

Materials

Commercially available analytical grade chemicals were used to prepare the mixture of ethanol, acetone, 2-propanol, ethyl acetate, 2-methyl-1-propanol, 1,1,1-trichloroethane, 4-methyl-2-pentanone, toluene and xylene. Commercially available charcoal was preconditioned in an oven at 100 °C for 2 hours.

Procedure

Granular activated carbon (150 mg) was placed in a gas-tight glass vessel (0.55 dm^3). The solvent mixture of ten components was injected into the vessel. The amount of each component varied from 0.1 μl per sample and the total amount of stock solution of these compounds varied from 1 to 50 μl in each examined charcoal bed. The relative humidity in the gas-tight vessels was maintained around 20 RH% by injecting 3 μl of water into each besides analytes. The test temperature was 20 ± 2 °C. The vessels with their contents were left to stand over-night, before taking samples into 5 ml carbon disulphide for desorption.

The standard solutions were prepared of the same stock solution which was used in the experiment with gas-tight vessels. From 1 to 5 μl of stock solution was mixed with 5 ml carbon disulphide.

Another set of samples called phase equilibrium set was prepared by adding 150 mg of unexposed charcoal into vials of standard solutions.

The GC analysis was performed on a gas chromatograph Hewlett-Packard model 5730A equipped with an autosampler Hewlett–Packard model 7671A.

RESULTS

The results of our experiment are given in tables 1, 2 and 3 illustrated in respective figures 1, 2 and 3 The recovery is given in percentage of expected value from standards of pure solution of components.

Table 1, figure 1. Recovery of vapours from adsorbent without correction.

Solvent	Recovery in percentage			
	Loading on charcoal bed (μl)			
	0.1	1	3	5
Ethanol	65	79	81	77
Acetone	93	97	95	85
2-Propanol	83	88	91	89
Hexane	94	101	101	99
Ethyl acetate	98	100	100	97
2-Methyl-1-propanol	77	90	93	91
1,1,1-Trichloroethane	100	101	100	97
4-Methyl-2-pentanone	94	99	99	97
Toluene	97	100	99	97
Xylene	96	100	99	97

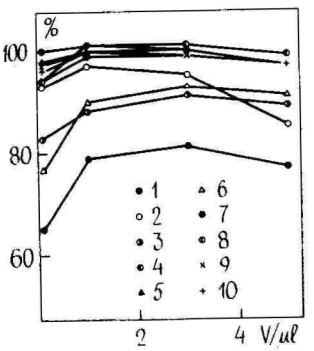

Table 2, figure 2 Desorption efficiency in phase equilibrium system.

Solvent	Desorption efficiency in percentage			
	Loading on charcoal bed (μl)			
	0.1	1	3	5
Ethanol	73	83	91	93
Acetone	93	94	200	99
2-Propanol	86	87	95	96
Hexane	106	98	103	102
Ethyl acetate	101	97	102	101
2-Methyl-1-propanol	87	91	96	96
1,1,1-Trichloroethane	107	101	103	100
4-Methyl-2-pentanone	101	98	101	99
Toluene	103	98	100	99
Xylene	104	98	100	99

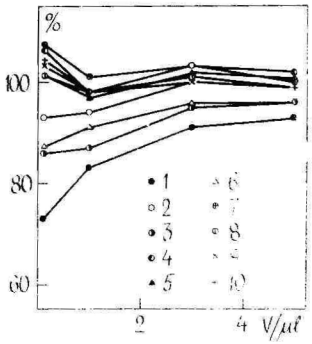

The recoveries for 10 components in the gas-tight vessel experiment are shown in figure 1. At loading levels higher than 1 μl of single analyte, the recoveries are around 100% for hexane, 1,1,1-trichloroethane, ethyl acetate, 4-methyl-2-pentanone, toluene and xylene. The more polar solvents ethanol, 2-propanol and 2-methyl-1-propanol have lower recoveries over the whole concentration area. At loading level 0.1 μl, all the compounds have decreased recoveries, compared to higher loading levels. The recoveries of acetone and ethanol have a maximum between 1 μl and 3 μl loading levels in this system because of poor desorption in small amounts and poor adsorption capacity at higher loading levels.

Table 3, figure 3. Recovery of vapours from adsorbent corrected with desorption efficiency.

Solvent	Recovery in percentage Loading on charcoal bed (μl)			
	0.1	1	3	5
Ethanol	89	95	90	83
Acetone	100	103	95	86
2-Propanol	97	101	96	93
Hexane	89	103	98	97
Ethyl acetate	97	102	98	96
2-Methyl-1-propanol	89	99	96	95
1,1,1-Trichloroethane	93	100	97	97
4-Methyl-2-pentanone	93	101	98	98
Toluene	94	102	99	98
Xylene	92	102	99	97

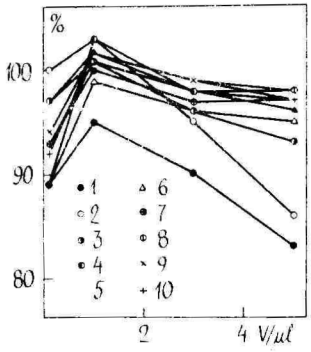

In figure 2 the desorption efficiencies in the phase equilibrium system are shown. The phase equilibrium method gives poor results for polar components ethanol, 1-propanol and 2-methyl-1-propanol. Desorption efficiencies over 100% occur due to the impurities of used charcoal.

In figure 3 it is seen that the recoveries for the given 10 components cannot be completely corrected by desorption efficiency based on phase equilibrium measurements. It is difficult to define the accurate correction coefficient for a small loading level because a strong and irrever-

sible adsorption. At higher loading levels of acetone and ethanol, the corrected recoveries are lower because of limited adsorption capacity of these polar compounds.

CONCLUSIONS

The adsorption and desorption phenomena are not reversible enough in our sampling and analysis system. The aliquot of an analyte released from the adsorbent during desorption is not a linear function of the amount of the adsorbed compound. The adsorption capacity of each analyte varies from compound to compound and is also dependant on gas phase concentrations and loading levels.

In our attempt to calibrate the measurement system, we minimised the bias caused by desorption with the simple phase equilibrium method. From a practical point of view, the desorption time is shorter than needed for obtaining equilibrium. In gas-tight vessel experiments it is possible to study the recoveries of the multicomponent system in different concentrations and ratios. The recovery is affected both by adsorption and desorption.

When validating the methods of gas and vapour sampling for official use, it is important to establish the quality classes for measurement systems where the total acceptable error is defined. Charcoal tubes can not be used for a sufficiently exact quantification of some compounds.

REFERENCES

1. R. G. Melcher, R. R. Langner, R. O. Kagel, Am. Ind. Hyg. Assoc. J., **1978**, *39*, 349.
2. J. C. Posner, J. R. Okenfuss, Am. Ind. Hyg. Assoc. J., **1981**, *42*, 643.
3. J. Rudling, Am. Ind. Hyg. Assoc. J., **1988**, *49*, 95.
4. R. L. Larkin, J. V. Crable, L. R. Catlett, M. J. Seymour, Am.Ind. Hyg. Assoc. J., **1977**, *38*, 543.
5. J. Rudling, E. Björkholm, Am. Ind. Hyg. Assoc. J., **1986**, *47*, 615.
6. S. Crisp, Ann.occup. Hyg., **1980**, *23*, 47.
7. NIOSH Manual of Analytical Methods. - U.S.Dept. of H.E.W., Public Health Service, Center of Disease Control, National Institute for Occupational Safety & Health, **1976**.

8. M. Fracchia, L. Pierce, R. Standley, Am. Ind. Hyg. Assoc.J., **1977**, *38*, 144.
9. J. Krajewski, J. Gromiec, M. Dobecki, Am. Ind. Hyg. Assoc.J., **1980**, *41*, 531.
10. R. A. Dommer, R. G. Melcher, Am. Ind. Hyg. Assoc. J., **1978**, *39*, 240.

MÕNINGATE ORGAANILISTE ÜHENDITE DESORPTSIOON AKTIIVSÕELT

L. Saarinen, M. Reinik

Resümee

Tööstusruumide õhus orgaaniliste lahustite aurude sisalduse määramiseks kasutatakse sageli proovi võtmist tahketele sorbentidele, järgnevat desorptsiooni sobiva solvendiga ja saadud lahuse gaaskromatograafilist analüüsi. Nimetatud meetodi kasutamisel tekivad probleemid mõningate ainete mittetäieliku adsorotsiooni ja desorptsiooniga. Artiklis on esitatud lihtne metoodika, mille abil saab määratavate komponentide leitud sisalduse kõrvalekallet tõelistest väärtustest vähendada viies arvutuslikult sisse parandusfaktori faasilise tasakaalu meetodil leitud desorptsiooni efektiivsuse näol. Antud parandus ei kompenseeri kõrgete ja madalate komponendi sisalduste juures ning eriti polaarsete ainete korral tekkinud viga täielikult. Seega tuleb antud meetod kasutamisel õhu saastuse määramisel eelnevalt teha kindlaks, kas see annab meile tulemuse lubatud vea piires.

ELEMENTAL COMPOSITION OF HISTORICAL GLAZES FROM ST. JOHN'S CHURCH OF TARTU

L. Piiri, L. Paama and T. Ilomets
Institute of Organic Chemistry, Institute of Chemical Physics,
University of Tartu

Abstract: Elemental composition of historical glazes were determined by sequential inductively coupled plasma-atomic emission spectrometry (ICP-AES), and by direct current plasma-atomic emission spectrometry (DCP-AES). The sample were taken from St. John's Church (Estonia, Tartu), built in the 13th-14th centuries. These analyses are important for the restoration works of the church.

The spectrochemical analysis of glaze materials of St. John's Church will give valuable information about the building, restoring and reconstruction of the church.

Several works have reported on the spectrochemical analysis of different ceramic materials by ICP-AES, DCP-AES and ICP-MS [1-3]. The need for a rapid and precise determination of the concentration of the major and minor constituents of glaze materials becomes more pressing. The multi-element analysis technique by ICP-AES and the matrix effects of easily ionizable elements in argon plasma were studied by L.Paama. The classical wet decomposition is a very time consuming sample preparation, but the fusion technique is an effective method for the sample preparation of ceramic materials [3, 6-7].

EXPERIMENTAL

Instrumentation

A sequential PU 7000 inductively coupled plasma atomic emission spectrometer was used for the measurements (Unicam Analytical Systems, Cambridge, England). The design of this spectrometer includes a 40.68 MHz free-running oscillator for driving the plasma, an Echelle

grating for the wavelength separation and a grid nebulizer for the sample aspiration. The spectrometer is equipped with a Gilson 221 Autosampler and is controlled by a Philips P 3230 computer. The results are printed out on a Philips NMS1461 printer.

Table 1. Operation parameters for sequential ICP-AES and DCP-AES.

	ICP-AES	DCP-AES
Plasma power	1.0 kW, 0.8 kW	approx 280 W
Coolant flow	13 (11 *) dm^3 min^{-1}	
Auxiliary flow	–	
Sample uptake	1.0 cm^3min^{-1}	2.0 cm^3min^{-1}
Nebulizer pressure	40 psi (280 kPa)	
Read delay	60 s	manual operation
Integration time	3 s	3 s
Number of Integrations	3	3

* was used for the determination of sodium

Table 2. Wavelengths used for various elements by sequential ICP-AES

Element/ Line	Wavelength nm	State	Stand.conc. range, mg dm^{-3}	DL mg dm^{-3}
Al 1	309.271	I	2.0 -100	0.12
Ca 2	396.847	II	1.0 - 10	0.04
Cu 1	324.754	I	1.0 - 10	0.03
Fe 2	259.940	II	1.0 - 10	0.09
Mg 1	279.553	II	1.0 - 10	0.03
Mn 2	259.373	II	1.0 - 10	0.02
Pb 3	280.199	I	2.0 -100	0.06
Si 1	251.611	I	2.0 -100	0.07
Zn 2	202.548	II	1.0 - 10	0.08
B 2	249.678	I	0.01- 10	0.03
Ti 1	334.941	II	0.01- 10	0.02
Na 2	589.592	I	1.0 - 50	0.14

I - atomic line, II - ionic line

Tin determination was performed with a SpectraSpan III B single-channel direct current plasma atomic emission spectrometer. A Czerny-

Turner type spectrometer with an Echelle grating is used in the optics module of the instrument. The reciprocal linear dispersion ranges from 0.062 nm/mm at 200 nm to 0.25 nm/mm at 800 nm. The d.c. argon plasma is formed by tungsten cathode and two graphite anodes in an inverted "Y" configuration. The constant current of 7 A and a voltage of 40 V are employed after the plasma is established. Argon of 99.99% purity was used as the plasma gas. The spectrometer was equipped with a Hewlett-Packard 85 microcomputer, for data processing and the emission signals were also registered with a Goetz 120E chart recorder. The ICP-AES and DCP-AES operation parameters and the measuring of wavelengths are summarized in Tables 1 and 2.

Reagents and Sample Decomposition

The stock solutions, containing 1000 mg·dm^{-3}of each element, were prepared using the following reagents (pro analysi, Merck): Al metal, $CaCO_3$, $Cu(NO_3)_2 \cdot 2H_2O$, Fe metal, Sn metal, $MgCl_2 \cdot 6H_2O$, $MnCl_2 \cdot 4H_2O$, $Pb(NO_3)_2$ and Zn metal. Commercial standard solution was used for silicon (Art. 19798, Merck). The calibration standards were prepared by serial dilution of the stock solution with water and concentrated nitric acid (Suprapur, Merck) was added to standard solutions (5% HNO_3 v/v). Pulverised samples were weighed (0.1±0.0002 g) into a platinum crucible, and 1 g of $Li_2B_4O_7$ 99pro analysi, Merck) was added. The sample was heated in a muffle furnace (Phoenix, Model Sigma 1) on 1100° C and kept for 30 min. The crucible was allowed to cool and put in a 250 cm^3 plastic beaker. The melt was dissolved in 150 cm^3 of 5% (v/v) HNO_3 (Suprapur, Merck), and the sample was transferred into a 250 cm^3 volumetric flask and diluted to the volume with water. Blanck samples were also prepared following the instructions described above.

For the determination of boron, the samples were fused with Na_2CO_3 and were heated in a furnace at 700° C for 30 min., at 800° C for 10 min. The melt was dissolved in 150 cm^3 5% (v/v HNO_3) and was transferred into a 250 cm^3 flask.

RESULTS AND DISCUSSION

Thirteen major and minor elements of the samples were determined by sequential ICP-AES. The lead emission line at 280.20 nm was used to find on optimum viewing position in the plasma for the determination of Si, Pb, Al, Fe, Ca, Mg, Cu, Mn and Zn. The boron emission line at 249.678 nm was used for the determination of boron. Sodium was determined at 589.592 nm and titanium at 334.941 nm. A direct currant plasma-atomic emission spectrometer was used for the determination of tin at 303.412.

The manufacturer of the instrument suggests that manganese ionic line Mn1 at 257.610 nm should be used as a general purpose element for the source peaking, i.e. for finding an optimum viewing position in the plasma [4]. However, when the source peaking with Mn was performed, very poor results were obtained for Al, Pb, Si, Zn and Fe in the sequential determination of the elements given in Table 2. When the source peaking with the lead emission line Pb3 at 280.199 nm was used, satisfactory results were obtained for Al, Ca, Cu, Fe, Mn, Mg, Pb, Si and Zn. The detection limits (3σ, blanks prepared as samples) were all in sub p.p.m. range (Table 2).

For the restoration of St. John's Church , the elemental composition of the glazes of the church has been studied in order to find out if it is possible to reproduce glazes and bricks with compositions very close to the original ones. For example, the colour of the glazes depends on the concentrations of copper, iron and manganese. The results obtained from the glazes are shown in Table 3. The last restoration of the church was in 1900. Some of the ceramic materials for restoration were made in Riga (Latvia) and Uhlensdorf (Germany).

The ICP-AES and DCP-AES proved to be suitable technique for the elemental analysis of the glazes and brick materials. The sample decomposition was conveniently made by fusion with lithium tetraborate and it was possible to measure directly both the main and minor elements of the samples. Chemical and spectral interferences were not encountered, and ionization interferences were negligible, although the samples contained high levels of aluminium, lead, lithium and silicon.

Table 3. Composition (%) of the glazes of St. John's Church

Element	Sample of glazes (%)									
	1G[a]		4G[b]		5G[b]		6G[c]		7G[c]	
	Element	Oxide	Element	Oxide	Element	Oxide	Element	Oxide	Element	Oxide
Pb	26.34	30.41	29.49	34.04	29.22	33.73	27.25	31.46	27.52	31.77
Si	15.01	32.11	17.36	37.14	17.39	37.20	16.52	35.34	18.02	38.55
Al	2.94	5.56	2.39	4.52	2.68	5.06	2.39	4.52	2.87	5.42
Fe	1.45	2.07	0.78	1.12	1.10	1.57	0.58	0.83	1.89	2.70
Mn	0.03	0.04	0.006	0.008	0.46	0.59	0.13	0.17	0.03	0.04
Cu	2.20	2.75	2.08	2.60	0.85	1.06	2.69	3.37	0.55	0.69
Mg	0.73	1.21	0.24	0.40	0.23	0.38	0.34	0.56	0.29	0.48
Ca	2.21	3.09	0.19	0.27	0.34	0.48	1.31	1.83	1.22	1 71
Zn	0.012	0.01	0.01	0.01	0.02	0.026	0.05	0.06	0.04	0.05
Ti	0.16	0.27	0.07	0.12	0.01	0.02	0.10	0.16	0.15	0.25
Na	0.20	0.27	0.22	0.30	–	–	0.41	0.55	0.69	0.93
Sn	0.05	0.07	1.20	1.53	–	–	0.09	0.11	0.06	0.08

Continued

Element	Sample of glazes (%)							
	8G[c]		9G[c]		10G[c]		10AG[a]	
	Element	Oxide	Element	Oxide	Element	Oxide	Element	Oxide
Pb	29.33	33.86	31.47	36.33	32.43	37.44	23.26	26.85
Si	16.85	36.05	16.48	35.26	15.87	33.95	18.35	39.26
Al	2.73	3.16	2.93	5.54	2.13	4.02	3.95	7.46
Fe	1.82	2.60	1.81	2.59	2.84	4.06	2.17	3.10
Mn	0.02	0.03	0.024	0.03	0.02	0.03	0.03	0.04
Cu	0.63	0.79	0.67	0.84	0.80	1.00	0.61	0.76
Mg	0.25	0.41	0.25	0.41	0.28	0.46	0.81	1.34
Ca	0.79	1.11	0.75	1 05	1.22	1.71	0.86	1.20
Zn	0.01	0.02	0.09	0.11	0.01	0.02	0.03	0.04
Ti	0.14	0.23	0.23	0.38	0.09	0.14	0.44	0.73
B	0.67	2.15	0.76	2.44	0.15	0.50	–	–
Na	0.82	1.11	0.99	1 33	0.32	0.43	0.02	0.04
Sr	0.07	0.09	0.07	0.09	0.14	0.18	0.07	0.09

[illegible]G, 4G, 5G, 6G, 7G, 8G, 9G, 10G and 10AG - samples of glazes

[illegible] - preparated in Tartu 1300-1700, [b] - preparated in Uhlensdorf in 1900, [c] - preparated in Riga 1900

REFERENCES

1. D. Pollmann, F. Leis, P. Tschöpel et al., ICP Information Newletter, **1994**, *19*, 259
2. L. Moenke-Blankenburg, T. Schumann and D. Günther. J. Anal. Atom. Spectrom., **1992**, *7*, 251.
3. J. Marshall, J. Carroll, J. S. Grighton et al., J. Anal. Atom. Spectrom. **1992**, *7*, 349R.
4. L. Paama, P. Perämäki and Lauri H. J. Lajunen. Acta et Comm. Univer. Tartuensis. Publications on Chemistry XXI. Tartu, **1993**, *966*, 146.
5. L. Paama, P. Perämäki and Lauri H. J. Lajunen. ICP Information Newsletter, **1994**, *19*, 149.
6. V. Carbonell, A. Sanz, H. Salvador et al., J. Anal. Atom. Spectrom., **1991**, *6*, 223.
7. P. Perämäki, L. H. J. Lajunen, L. Piiri and T. Ilomets. University of Oulu, Report Series in Chemistry, **1993**, *38*, 3.

TARTU JAANI KIRIKU AJALOOLISTE GLASUURIDE ELEMENDILINE KOOSTIS

L. Piiri, L. Paama, T. Ilomets

Resümee

Käesolevas töös uuriti Tartu Jaani kiriku ajaloolisi glasuure spektrokeemilise analüüsi meetodil. Analüüsi läbiviimiseks kasutati induktiivse plasma aatomemissioon spektromeetrit (ICP-AES) PU 7000 (Philips Cambridge. England) ja alalisvoolu gaasplasma aatomemissioon spektromeetrit (DCP-AES) Spectra Span III B (Beckman).

Glasuuride proovid võeti glasuuritud profiiltellistelt spetsiaalse kõvaulam-kaabitsaga. Vajalik kogus proovi lagundati loistamise teel liitiumtetraboraadiga. Boori määramiseks lagundati proovikaalutis loistamisel naatriumkarbonaadiga. ICP-AES meetodil määrati Pb, Al, Si, Fe, Mn, Ca, Mg, Zn, Cu, Ti, B, Na. Elementide avastamispiir analüüsitavates lahustes kõikus 0.02 kuni 0.14 mg/dm^3. Tina määramiseks glasuurides kasutati DCP-AES meetodit. Tina määrati laine-

pikkusel 303.42 nm. Tema avastamispiiriks plasmas on 0.02 mg/dm^3.

Tartu Jaani kirik on Põhja-Euroopa unikaalsemaid arhitektuuri- ja ajaloomälestusmärke. Ta ajalugu algab uuemate arheoloogiliste uuringute valguses juba enne eestlaste muistset vabadusvõitlust 13. saj. kahekümmendatel aastatel. Kirik muutus varemeiks 25 augustil 1944. a. II Maailmasõja lahingute käigus. Nüüd on asutud ta taastamisele. Kiriku restaureerimiseks on vajalikud paljud uuringud, nende hulgas ka eelmistel sajanditel kasutatud materjalide keemilise koostise kindlaksmääramine, millede hulka kuuluvad ka glasuurid ajavahemikus 13. kuni 20. sajand.

CHRONOPOTENTIOMETRIC STRIPPING ANALYSIS FOR DETERMINATION OF HEAVY METALS IN FOODSTUFFS

J. Ruut, V. Past
The Laboratory of Tartu Public Health Service
University of Tartu

Abstracts: The chronopotentiometric stripping analysis is used for the determination of heavy metals in foodstuffs and drinking water. The authors discuss problems connected with the analysis of a certain type of foodstuffs: bovine liver powder and milk powder.

INTRODUCTION

Chronopotentiometric stripping analysis (PSA) has been used for many years for the determination of heavy metals in several media [1]. However, its applications for the analysis of foodstuffs has been rather limited. We have used the method in our laboratory since 1991 [2].

EXPERIMENTAL

The PSA system consisted of a potentiostat PA3, a XY-recorder XY-4103 (both Laboratorni Pristroje, Prague), a TTA-80 titration assembly with a glassy carbon electrode F3500 as a working electrode, a reference saturated calomel electrode K4040, and an auxiliary Pt-electrode P1312 (all Radiometer, Copenhagen). The potential between the working and reference electrodes was amplified by a high-impedance input electrometer unit and transferred simultaneously to the recorder and an analogue-digital converter with the following signal processing in the computer memory. The system was controlled by a timer unit [3].

Dry ashing was used for the mineralization of foodstuffs. For this purpose, digestion apparatus producing a mixture of oxydative gases (NO_x, O_3, O_2) was applied.

Hydrochloric acid used as a supporting electrolyte and as a media for dissolving ashed organic matter, was prepared by molecular distilling

from a technical grade acid. The other reagents were of analytical grade. The liver powder sample was made of bovine liver. The sample was dried at 100°C and grinded to get a homogeneous powder. Milk powder sample was made in the Uelzen plant, Germany.

The working electrode was prepared by polishing its surface with 3 μm diamond powder, followed by coating in a mercury aqueous solution (0.05 g $Hg(NO_3)_2$ /l) in four 1-minute cycles at the plating potential −1.10 V. The potentials were determined against the saturated calomel electrode. The quality of the mercury layer was controlled visually.

Ashing was performed at the temperature range of 400...450° C, duration of the procedure was commonly 24 hours, the amount of the sample was 0.5.. 2 g of dry matter. Ashing residues were dissolved by boiling in 1 M hydrochloric acid during 10...15 minutes. As a result, a clear solution was obtained. The solution was transferred to an analytical cell, the volume was brought to 20 ml by using tridistilled water.

The working solution was electrolyzed in 4 minute cycles (plating potential −1.10 V), standard addition method was used to get stripping curves for cadmium and lead (stripping potential −0,70 V and −0,49 V respectively). 1 ml aliquote of the sample was taken for further determination of zinc, the solution was electrolyzed at −0.95 V in 2 minute cycles to determine the copper contents. The stripping potential of Cu was −0.3 V. After that, zinc determination was performed by using the aliquote sample, the plating potential was −1.30 V, the stripping potential was −1.1 V. 1 ml of $4 \cdot 10^{-4}$ M gallium(III)nitrate was added to prevent formation of the Zn-Cu intermetallic compound.

RESULTS AND DISCUSSION

Comparative tests were made using atomicabsorption spectrophotometry (AAS) at the Finnish Veterinary and Food Research Institute. Flame - AAS was used for Zn and Cu determination, graphite furnace techniques were used for Cd and Pb. In the liver powder and milk powder, the contents of Cd, Pb, Cu and Zn were determined by both methods.

By AAS, 0.196 mg/kg of Cd, 60.7 mg/kg of Cu and 297 mg/kg of Zn were found in the liver powder. Determination by PSA gave the following results 0.223 mg/kg [relative standard deviation of the mean value (RSD) 0.7%, at the confidence level (P) 0.95, the number of determinations (n) was 10], 82 mg/kg (RSD 0.06, P = 0.95, n = 10) and

308 mg/kg (RSD 0.07, P= 0.95, n = 10) for Cd, Cu and Zn, respectively.

For the milk powder, AAS gave 0.0002 mg/kg , 1.26 mg/kg and 29.9 mg/kg for Cd, Cu and Zn contents, respectively. The results obtained by PSA were as follows: Cd: < 10 μg/kg; Cu: 0.67 mg/kg (RSD 0.11, P = 0.95, n = 10); Zn: 30.2 mg/kg (RSD 0.13, P = 0.95, n = 10).

Thus, one can say that the reproducibility for the analysis results of Cd, Cu and Zn are, at least, satisfactory. The results of lead determination showed poor reproducibility. By AAS, 0.19 mg/kg of Pb was found in the liver powder. The results obtained by PSA show great variations in the lead contents after 24 hours of digestion: The lowest value was 0.196 mg/kg , the highest 1.22 mg/kg , altogether giving the mean value 0.639 mg/kg. At the same time, none of the standard deviations for single measurements exceeded 0.10 (4 standard additions were made). After 3 days of digestion of the liver powder samples, the mean value of the lead contents was 0.421 mg/kg (RSD 0.53, P = 0.95, n = 10). It seems that the extreme values found for 24-hour digestion were results of the incomplete destruction of organic matter and/or of the formation of electroactive compounds, which behave in the similar way lead does. Leakage of Pb from the glass walls of digestion vessel could also be suspected during long-time digestion, but, unfortunately, for comparative tests samples were mineralized separately in both places. In this case, the use of alternative digestion (wet ashing) must be considered.

In case of milk powder, flameless AAS yielded the result of 0.04 mg/kg for milk powder. Results for PSA sufficiently depended on the mineralization methods. While using nitrogen oxides and ozone during digestion, a somewhat unexpected result of 4.5 mg/kg was got for 1 g amount of a sample. Investigating the same samples by flame-AAS of the laboratory of Rakvere Meat Packing Factory, lead contents were found to be below the detection limit (< 1 mg/kg). While only air was used for digestion, the detected lead contents dropped sufficiently, the mean value of the lead contents obtained was 0.184 mg/kg (RSD 0.29, P = 0.95, n = 5). Prolongation of the mineralization time did not affect the results significantly.

A good reproducibility of results was obtained in the case of lead determination in unmineralized milk powder samples. Approximately 1 g of the sample was dissolved in tridistilled water. The resulting liquid was added to 15 ml of solution consisting of 10 ml 10 M HCl, 1 ml mercury(II)nitrate and ough to avoid the precipitation of milk proteins

and to extract lead from its organic complexes. Due to high concentration of chloride ions, well-reducing chloride s conducted in this way showed the lead contents 0.029 mg/kg (RSD 0.11, P = 0.95, n = 10). It means that the analysis of non-mineralized samples can be strongly recommended in addition to the dry ashing method.

One should mention that lead in milk powder has been a problematic item in Estonia. In the spring of 1994, the results of lead determinations in skimmed milk powder varied from 0.02 mg/kg to 3.5 mg/kg; electrochemical methods and AAS were used for the analyses. Consequently, a lot of work is to be done, considering this field of analysis: several methods of analysis and mineralization must be investigated to get correct results

On basis of analysis results brought, PSA could be considered as a useful tool for heavy metal analysis. However, certain problems may rise and should be taken into account, especially those connected with the mineralization procedures.

REFERENCES

1. D. Jagner, Anal. Chem., **1979**, *51*, 342
2. J. Ruut, International Symposia dediced to the memory of Prof. Theodor Lippmaa 1892-1992, II, Tartu, Estonia, September 3-7, 1992, 48
3. M. Miil, J. Ruut, V. Pihl, Acta et Comm. Univ. Tartuensis, Vol. 366, 116.

RASKMETALLIDE MÄÄRAMINE TOIDUAINETES INVERSIOONKRONOPOTENTSIOMEETRILISELT

J. Ruut, V. Pasi

Resümee

Töös on uuritud vooluta inversioonkronopotentsiomeetria kasutamist teatud liiki toiduainete analüüsil. Leiti, et kaadmiumi, vase ja tsingi määramisel on tulemused hästi kokkulangevad aatomabsorptsioonspektrofotomeetria kasutamisel saaduga. Plii määramisel saadud tulemused olid tunduvalt kõrgemad nendest, mis olid saadud AAS-i kasutades. Põhjuseks võib olla orgaanilise aine mittelagunemine ja/või elektroaktiivsete ainete teke mineraliseerimisel.

ANALYSIS OF NUTRIENTS

L. Reio
Swedish National Food Administration

Abstracts: Rapid methods for nutrient analysis are becoming more and more important to satisfy the needs of customers and producers. Analysis methods for determination of sugars, fatty acids, vitamins and protein contents are reflected in the article

DISCUSSION

Both the generally increased interest in nutritional problems and an ever increasing interest in retaining good health have gradually created a need for additional information as to the nutritive value of different foods. More and more people are becoming aware of possible health hazards of excessive intake of fats, sugars and certain food products. On the other hand, as prefabricated foods are getting more and more complicated in their composition, the questions of uniform quality and nutritive value become pertinent.

Food manufacturers need to monitor their production. Government institutions supervising the food products marketed in different countries need to know more about the contents of macro- and micronutrients in various products; very often in order to satisfy the consumer requests and investigate the public complaints. Fortification of foodstuffs with minerals and vitamins is still used in many countries. Infant food and special dietary foods are usually the most fortified products which need to be controlled regularly. In infant formulas are required vitamins A, D, E, C, B_6, B_{12}, thiamin, riboflavin, niacin, folacin, panthothenic acid and minerals calcium, phosphorus, magnesium, iron, iodine, copper. Vitamins K, biotin, choline, inositol and minerals zinc, manganese, sodium, potassium, chloride are recommended as additional nutrients.

Nutritional quality guidelines and nutrition labelling regulations have also accelerated an increased demand for the development of rapid

(more automatized) methods for assaying many nutrients. The total number of different analyses needed has increased considerably in the last decades.

With an increased labour cost, previously developed and comparatively time-consuming manual analytical chemical methods have gradually been replaced by a number of chromatographic methods, which have been more or less fully automatized. Food chemistry is essentially a separation chemistry, in addition to identification and quantitation problems. This progress of analytical techniques has been mainly possible by developing new efficient separation systems, high resolution resins, and column materials, devising pump systems, highly effective detector systems for gas, liquid and ion-exchange chromatography. Some examples are: UV-detection with variable wavelength, a fluorimetric detector, refractive index and conductometric detectors, and ICP-detectors for minerals. Different continuous-flow assay systems are usually accurate, precise and efficient; through computerization it is possible to control automatically many separation variables, such as temperature, pressure and the solvent/eluent gradient system, in the analysis of many food constituents.

Multicomponent determination began at the end of the fourties with the Stein-Moore amino acid separation procedure. This trend has continued to fatty acids, by using GLC in connection with capillary technique [1].

Automatized sugar analysis has always been a problem since sugars are hard to detect in UV. Derivatization was must for a long time when using GLC, several artefacts were produced depending on the derivatization reagents used. With the development of HPLC (High Pressure Liquid Chromatography), especially in connection with a refractive index detector, sugar analysis is no longer a problem. Sugars can be analyzed in water-solutions, without extraction and derivatization [2].

HPLC-system of analysis has also revolutionized the separation of fat-soluble vitamins. For the first time we have a reliable method, where several fat-soluble vitamins can be separated simultaneously. Years ago, vitamin E isomers were separated by GLC with difficulty. Water-soluble vitamins can also be separated by HPLC [3].

For protein determination the most frequently used procedure is the Kjeldahl method which has been fully automatized by using continuous digestors. The IR technique with double beam for liquids has been used for protein determination in milk for a long time. Measurements are

taken at 5.73 μm for fat (carbamyl ester linkage), at 6.46 μm for protein (amide group in peptide linkage) and at 9.6 μm for lactose (hydroxyl group). The double beam outfit is automatically corrected for strongly adsorbing water on these wavelengths [4].

For solid foodstuff preparations which can uniformly be ground and evenly displayed under the measuring field (cereals, milk powder), instruments working in near-infrared area are used. The sample is illuminated with six or more different wavelengths between 1.5...2.5 μm and the reflected light is detected. The signals are fed into a computer and compared against the standards fed earlier to the data system. This method enables to determine simultaneously the oil (fat), protein and/or moisture contents. Estimation of complex carbohydrates can also be performed. This method is rapid and seems to be suitable for the routine analysis of different grains. The procedure does not require the weighing of the sample which in a rapid analysis can be a time-limiting factor.

The method presented by Professor Kirsten, the Uppsala Agriculture Academy, applies automated elemental analysis equipment (Carlo Erba). Rapid analysis of CHNO/S in grain samples is performed without weighing the sample. The carbon content of grain seems to be fairly constant, and it can be used as an internal standard by the direct calculation of protein content on the basis of the carbon/nitrogen ratio. For the calculation of water contents, the carbon/oxygen ratio seems to be suitable; finally, the ratio carbon/sulphur provides an estimate for sulphur amino acids present [5].

Other unconventional methods can use neutron activation analysis whereby upon irradiation, ^{14}N isotope is formed with half life of 10 minutes. Emitted γ-rays from ^{14}N are then recorded. The analysis time with the use of computers is about 20 min with 1% precision for nitrogen determination. In addition, co-determination of P, K, Ca, Mg and Si is possible.

Proton activation technique leads to the formation of ^{14}O isotope from nitrogen which decays rapidly and radiation can be measured. Many methods are based on the well established ninhydrin reaction with amino acids. The blue colour is recorded spectrophotometrically. It is possible to compute the total amount of amino acids from single amino acid contents. This value with the correction of the loss of water by peptide linkage formation gives a good estimate of the total protein amount. One can avoid the risk of non-protein nitrogen compounds which may cause a higher protein value.

The use of ninhydrin methods usually enables to detect about 1 nanomole of the analyte. When higher sensitivity is used, a fluorescence detector must be used. The ninhydrin reagent is then replaced by *o*-phtalic aldehyde, and by fluorescence sensitivity around 10 picomoles can be reached.

The contents of amino acids such as lysine, methionine, and a few others, can indicate from which source the protein(s) has been derived from. Tryptophan is always lost in acid hydrolysis and in order to obtain an estimate for tryptophan, alkaline hydrolysis must be performed. This hydrolyzate can be analyzed once again and the estimations are of value when niacin equivalents are to be determined.

Acid hydrolysis is used in most cases of protein determinations, enzymatic hydrolysis is incomplete. No system of hydrolysis is perfect and therefore a limited destruction of amino acids is possible. In the presence of large amounts of carbohydrates, some racemization and other losses can take place. Large carbohydrate contents affect especially tryptophan in the acid medium, therefore alkaline hydrolysis is required. It leads, however, to the destruction of arginine, serine, threonine, cystine and cysteine at the cost of tryptophan which can be recovered.

Determinations of single amino acids, e.g. 3-methylhistidine as an estimate for "meat" in mixed meat products are also valuable. One can also mention the determination of proline and/or hydroxyproline in order to indirectly estimate the protein quality. High percentage of these amino acids, together with high glycine value, is indicative of the presence of a high content of connective tissue.

In order to estimate whether the protein is of animal or vegetable origin, some electrophoretic separations are applicable. However, it is difficult to draw conclusions of this problem, basing on amino acids patterns only.

All determinations of protein via nitrogen analysis are indirect estimations of crude protein. Chromatographic analysis enables to reveal and determine more and more non-protein nitrogen compounds. The amino acid analysis technique has given lower protein values for many foodstuffs than those found while using nitrogen analysis.

The widely accepted and used conversion factor 6.25 is based on the assumption that proteins (as mean value) contain 16% of nitrogen (6.25 x 16 = 100). In turn, it is based on the average nitrogen contents of all amino acids in protein and thus included in the protein composition. Tyrosine has 6.77% of nitrogen and represents the lowest value, while

the highest value is obtained with arginine which has 32.6% of nitrogen. Totally, approximately 20 protein amino acids occur in different proteins in different proportions.

Factor 6.25 applies generally to eggs, meat and fish; for almonds 5.18 is used. The following factors are in use: nuts 5.3, gelatin 5.5, wheat 5.7, soybeans 5.7. For oilseeds and cereals, the range is 5.20...5.75, for milk the factor is 6.38.

Investigations of mushrooms revealed that they contain a great number of nitrogen compounds other than amino acids and most likely here a conversion factor 2/3 × 6.25 is of a more realistic value.

From the nutritional point of view, the proper value for the total protein amount does not necessarily mean or guarantee that this protein is fully digestable. The total amino acid composition values are hereby helpful for evaluating the protein quality [6].

REFERENCES

1. D. V. McCalley, High Res. Chromat., **1989,** *12,* 465.
2. T. J. Bahowick, et al., Anal.Chem., **1992**, *64*, 255 R.
3. D. J. Anderson, et al., Anal.Chem., **1991**, *63,* 165 R.
4. C. L. Putzig, et al., Anal.Chem., **1992**, *64*, 270 R.
5. W. J. Kirsten, Anal. Chem., **1979**, *51,* 1173.
6. R. Sepp, Starch Stärke, **1979**, *31*, 57.

TOIDUAINETE ANALÜÜS

L. Reio

Resümee

Järjest suurenenud huvi toitumisprobleemide ja hea tervise säilitamise vastu on järk-järgult tekitanud vajaduse toiduainete toiteväärtuse ja lisandite määramiseks. Üha rohkem inimesi saab teadlikuks liigsest rasvade, süsivesikute ja mõnede toiduainete põhjustatud ohtudest tervisele. Teisest küljest, kuna eeltöödeldud toidud muutuvad koostiselt üha keerukamaks, muutub oluliseks nende ühtlane kvaliteet ja toiteväärtus.

Suhteliselt aeganõudvad keemilise analüüsi käsitsimeetodid on järkjärgult asendatud arvukate meetoditega, mis on rohkem või vähem automatiseeritud. Toidukeemia oluliseks osaks on lisaks kvalitatiivse ja kvantitatiivse analüüsi probleemidele ka erinevate ühendite lahutamine, mis on saanud võimalikuks tänu uute materjalide ja meetodite kasutuselevõtule.

Refraktomeetrilise detektori kasutuselevõtmine kõrgrõhuvedelikkromatograafias lihtsustas oluliselt suhkrute analüüsi, mida võib nüüd teha vesilahuses ekstraheerimise ja derivatiseerimiseta. Kõrgrõhuvedelik-kromatograafia on revolutsioneerinud ka rasvaslahustuvate vitamiinide analüüsi: esimest korda oli võimalik lahutada erinevaid vitamiine samaaegselt. On võimalik lahutada ka veeslahustuvaid vitamiine.

Proteiinide määramiseks on kasutusel mitmesugused automatiseeritud Kjeldahli meetodi modifikatsioonid. Tahkete toiduainete proteiinisisalduse analüüsiks kasutatakse ka infrapunast spektroskoopiat. Nii on võimalik üheaegselt määrata rasva, proteiini- ja niiskusesisaldus. Kasutusel on ka neutron- ja prootonaktivatsioonitehnikad. Paljud meetodid põhinevad ninhüdriini ja aminohapete vahelisele reaktsioonile. Üksikute aminohapete sisaldused summeeritakse; seejuures ei arvestata mitteproteiinset lämmastikku.

PROFESSOR LEMBITU REIO 70

Lembitu Reio was born in Tartu, on June 4th, 1924. He graduated from J. Westholm High School in Tallinn in 1943. In 1944 he escaped from Estonia to Sweden. From 1945 to 1972 he studied and worked in Departments of Physiological Chemistry and Metabolic Research of the Wenner-Gren Institute of Experimental Biology at Stockholm University, at the beginning as an assistant, and after defending his doctoral thesis in 1964, as an associate professor at the Institute of Biochemistry. Meanwhile, in 1960-1963 he worked as a research associate at Tulane University, Medical School in New Orleans, La., USA. In 1973-1990, L.Reio was a professor and head of laboratory of analytical chemistry at National Food Institute in Uppsala.

The work at Wenner-Gren Institute in 1945-1954 covers the following fields:

During his university years, L.Reio participated in constructing and building of two instruments, one for enrichment of stable ^{13}C, and the other for ^{15}N isotopes. It was the first apparatus of such kind in Europe, built according to the principles for separation published by Harold May. Its height was 11 metres and it ran through 3 floors. The device worked in 2 week periods without stopping.

The enriched $K^{13}CN$ and $^{15}NH_4NO_3$ were converted to suitable starting material for synthesizing products like glycine, alanine, aspartic acid, acetic acid, lactic acid, sugars etc. Mass-spectrometric analysis of these isotopes was introduced by L.Reio and his co-workers for the first time in Sweden in 1946/47.

In 1949, a radioactive ^{14}C-isotope from USA became available in the department, for the first time in Sweden. It was used to produce single-

and double-labelled compounds, such as $^{13}CH_3{}^{14}COOH$, which were used in the studies of biosynthesis of amino acids in microorganisms and yeasts, e.g., *Escherichia coli, Torulopsis utilis, Neurospora cressa, Aerobacter aerogenes, Rhodospirillum rubrum.*

For a great number of amino acids, L.Reio has established new synthesis pathways. Special attention was focused to biosynthesis of aromatic amino acids. He found that these aromatic structures were not polycondensates of acetic acid residues but were rather constructed from 3+4 carbon segments of sugar moieties.

Biosynthetic patterns for leucine, lysine, histidine, threonine showed to be different from what could have been expected from acetic acid entering the Krebs-Cycle of metabolism. Such data were unique and have been confirmed during next 10 years by other workers in this field.

In order to establish the distribution of isotopes in carbon atoms of amino acids, the protein was hydrolyzed, amino acids were separated and isolated in pure form in ca 100 mg quantities and submitted to chemical degradation. In many cases the single carbon atoms could be isolated as CO and their isotope content was determined. All degradation methods were new and worked out on microscale in the laboratory - some of these methods were used world-wide.

In 1948, after the synthesis of the vitamin Biotin was published by Du Vigneaud, this 12-step synthesis was repeated in order to explore its utility to yeast manufacturers.

Period between 1954-1964 was characterized by finding new methods for tracing aromatic compounds produced by moulds, mainly from different *Penicillium* moulds. L.Reio worked out a very elaborate paper chromatographic system with 6 solvent systems and 12 detection reagents in order to characterize the compounds. Characterization was performed on basis of distribution properties and colour reactions; he investigated approximately 900 compounds, with the main stress on phenol derivates. He created a computer-aided system and used it in order to find useful patterns. One of the presentations of this work was published in the first volume of "The Journal of Chromatography" in 1958 [1]. A multiple number of his articles has been published on in this journal [2].

1. L. Reio, J. Chromatog., **1958**, *1*, 338.
2. L. Reio, J. Chromatog., **1960**, *4*, 458.
   L. Reio, J. Chromatog., **1961**, *5*, 86.
   L. Reio, J. Chromatog., **1970**, *47*, 60.
   L. Reio, J. Chromatog., **1970**, *48*, 11.
   L. Reio, J. Chromatog., **1972**, *68*, 183.
   L. Reio, J. Chromatog., **1974**, *88*, 119.

In these series of cultivation of *Penicillium* moulds and isolation of some of the metabolic products, he detected orsellinic acid together with penicillic acid. This was the first time orsellinic acid was detected in *Penicillium Griseofulvum* and proved to be later one of the most important key-substances for biosynthesis of many aromatic compounds. Earlier, orsellinic acid had been known as a parent acid to many lichen acids of gyrophoric acid type,but had not been found in the mould cultures.

Penicillium Charlesii produced carolic and carlosic acids, with isotope techniques, the biosynthetic formation was established. For the first time also itaconic acid was isolated from this species.

During the period of 1960-1964, mainly in Tulane University, New Orleans, La USA, L.Reio introduced new methods to trace metabolic disturbances in case of mental diseases. Introduction of labelled ^{35}S-sulfate technique revealed that in cases of schizophrenia some sulfate acceptor compounds were predominantly present

Period of 1964-1972 at Stockholm University also involved teaching of advanced course in biochemistry - metabolism of proteins, fatty acids, sugars etc

In 1973-1990, his research activities involved vitamin research and analysis, improving and introducing new methods. The program involved biological methods (for vitamin D), microbiological methods (for riboflavin, pyridoxin, biotin, panthothenic acid, folic acid, vitamin B_{12}). Chemical methods for the rest of the vitamins. He improved analysis of fatty acids, especially separation of several trans-isomers and sterols Also he investigated alkaloids in potato products.

In the whole, L.Reio has published 95 articles.

Lembitu Reio has represented Sweden and National Food Administration as a delegate in several Codex Alimentarius Commissions' Sampling and Analysis in Budapest, Fats and Oils in London and Food Irradiation in Washington. In 1975 and 1982-1990, Lembitu Reio was a chairman of Swedish National Committee for Food Analysis. Lembitu Reio is also representing Sweden in FECS (Federation of European Chemical Societies) Working Party for Food Chemistry from 1986.

PROFESSOR LEMBITU REIO

Tuntud välis-eesti keemik Lembitu Reio on sündinud Tartus, 4. juunil 1924. a. 1943 aastal lõpetas ta Tallinnas J. Westholmi gümnaasiumi.

1944. a. lahkus ta Rootsi, 1945–1972 õppis ja töötas Stockholmi Ülikooli Wenner–Greni Eksperimentaalse Bioloogia Instituudi füsioloogilise keemia ja ainevahetuse osakondades, algul assistendina ja 1964. a. peale doktorikraadi kaitsmist Biokeemia Instituudi dotsendina.

1956. a. omistati L. Reiole Stockholmi Ülikooli filosoofiakandidaadi kraad keemias ja bioloogias. 1958. a. kaitses ta filosoofialitsentsiaadi kraadi Lundi Ülikoolis biokeemia ja analüütilise keemia erialal. Aastatel 1960–1963 töötas L. Reio Tulane'i Ülikoolis New Orleansis.

Wenner–Gren'i Instituudi perioodil 1945–1954 tegeles Lembitu Reio aparatuuri konstrueerimise ja ehitamisega ^{13}C ja ^{15}N isotoopide saamiseks. Sünteesitud $K^{13}CN$ ja $^{15}NH_4NO_3$ kasutati glütsiini, alaniini, aspargiinhappe, äädikhappe, piimhappe, suhkrute jm. sünteesi lähtematerjaliks.

1946/47 alustas Wenner-Greni Instituut esimesena Rootsis nende isotoopide mass-spektromeetrilist analüüsi. 1949. aastast alates kasutati Rootsis ^{14}C radioaktiivset isotoopi ühe ja kahe märgitud aatomiga ühendite sünteesiks, mida omakorda kasutati aminohapete biosünteesi uurimiseks.

L. Reio on tegelnud aromaatsete aminohapete biosünteesiga: uurinud isotoopide jaotust aminohapetes ja töötanud välja uued aminohapete keemilise degradeerimise meetodid. 1948. a. korrati instituudis vitamiin biotiini sünteesi. Töötati välja kromatograafiline meetod penitsiliini poolt toodetud aromaatsete ühendite määramiseks. Määrati hallituste poolt sünteesitud aromaatsete ühendite tekkeks olulisi vaheprodukte.

Tulani Ülikoolis 1960–1964 töötas Lembitu Reio välja uued meetodid metaboolsete kõrvalekaldumiste uurimiseks vaimuhaiguste korral, peamiselt ^{35}S isotoobi kasutamiseks fenoolsete ühendite sulfaatestrite määramisel.

1964–1972 tegeles Lembitu Reio biokeemia kursuse õpetamisega Stockholmi Ülikoolis, 1974–1991 pidas ta vitamiinide toime ja analüüsi alaseid loenguid Karolinska Instituudis. 1973–1990 töötas Lembitu Reio Uppsalas Rootsi Toiduainete Kontrolli Instituudis professorina ja keemia laboratooriumi juhatajana. Teadustöö hõlmas vitamiinide uurimise

ja analüüsi meetodite loomist ja täiustamist. Käesoleva ajani on ilmunud 95 teadusartiklit.

Lembitu Reio on esindanud Rootsi riiki ja Riigi Toiduametit mitmetes Codex Alimentarius komisjonides Budapestis, Londonis ja Washingtonis, aastatel 1975 ja 1982–1990 oli ta Rootsi Toiduainete Analüüsi Komitee esimees, 1986 aastast esindab ta Rootsit Euroopa Keemialiitude Föderatsiooni toiduainete keemia töögrupis.

Professor L. Reio on tihedates sidemetes Eesti, s. h. Tartu Ülikooli keemikutega. Ta on võtnud oma südameasjaks Eesti abistamise, eriti toiduainete kontrolli alal.

Käesoleval ajal on professor emeritus Lembitu Reio aktiivselt tegev Rootsi esindajana mitmetes rahvusvahelistes erialaorganisatsioonides.

K. Ilmoja
T. Tenno